

Bacterial Genome Plasticity and its Role for Adaptation
and Evolution of Asymptomatic Bacteriuria (ABU)
Escherichia coli Strains

(Über die Bedeutung der bakteriellen Genomplastizität
für die Adaptation und Evolution asymptomatischer
Bakteriurie (ABU) *Escherichia coli* Isolate)

Doctoral thesis for submission to a doctoral degree
at the Graduate School of Life Sciences,
Julius Maximilian University Würzburg,
Section: Infection and Immunity

submitted by

Jarosław Maciej Zdziarski

from

Góra, Poland

Würzburg, 2008

Submitted on:
office stamp

Members of the *Promotionskomitee*:

Chairperson:
to be completed by the office

Primary Supervisor: Prof. Dr. Dr. h. c. mult. Jörg Hacker

Supervisor (second): Prof. Catharina Svanborg

Supervisor (third): PD Dr.rer.nat. Ulrich Dobrindt

Day of Rigorosum:

Certificates were handed out on:

Erklärung

Gemäß § 4 Abs. 3 Ziff. 3, 5 und 8 der Promotionsordnung der Fakultät für Biologie der Bayerischen Julius-Maximilians-Universität Würzburg.

Ich versichere hiermit, dass ich die vorliegende Arbeit selbständig und nur unter Verwendung der angegebenen Quellen und Hilfsmittel verfasst habe.

Weiterhin versichere ich, dass die Dissertation bisher nicht in gleicher oder ähnlicher Form in einem anderen Prüfungsverfahren vorgelegen hat und ich bisher keine akademischen Grade erworben oder zu erwerben versucht habe.

Würzburg, im Juli 2008

(Jaroslaw Zdziarski)

Acknowledgement

This study was carried out at the Institute of Molecular Biology of Infectious Diseases at the University of Würzburg, Germany from September 15th, 2004 until May 31st, 2008. In this time period, many people helped me to accomplish my PhD dissertation.

First of all I am grateful to Prof. Jörg Hacker, who gave me the opportunity to join his group and for the whole support that allowed me to complete my PhD.

Secondly, I am very happy that Prof. Catharina Svanborg (Institute of Laboratory Medicine, Department of Microbiology, Immunology and Glycobiology, Lund University, Sweden) gave me the opportunity to stay in her laboratory and learn more about asymptomatic bacteriuria. By her extraordinary scientific input she made my work very interesting and ‘colourful’.

I kindly thank Prof. Björn Wullt (Department of Urology, Lund University Hospital, Sweden) for providing with consecutive re-isolates of strain 83972 and the corresponding patient data. Every scientific and non-scientific discussion, we had together, was just fantastic.

I would love to express my deepest gratitude to Dr. Ulrich Dobrindt who is a great supervisor. In the time of my PhD, he has helped me to develop scientific ideas and together we drilled into the depths of science. Despite his very tight schedule, we could go through all crazy things....and that he polished his polish...

Many thanks to all ‘Colis’ and ‘Staphis’, especially to Barbara Plaschke, whose experience and engagement significantly contributed to my work.

Torben – thanks for the “Zusammenfassung” and all that happy times.

In addition, to all ‘Lunds’ friends, especially Mattias Gustafsson, Bryndis Ragnarsdottir and Eva Ljunggren - thank you very much.

Special thanks to Hilde Merkert for many helpful advices and solving ‘unsolvable’ problems.

The German bureaucracy would be far more difficult without Elke Stahl, Claudia Borde and Wilma Samfass. Jozef handyman and his tools were also often needed in laboratory – thanks.

Lissi and Gabi from ‘die Küche’ – thank you very much and sorry for that ‘difficult material’ to be sometimes autoclaved.

Importantly, special thanks to my parents who gave me the opportunity to study and for the whole help – DZIEKUJE RODZICE!

And finally, thank you Kerstin for being there for me, and all support and love I have got from you!

– Danke schön – Thank you – Dziękuję –

TABLE OF CONTENT

1. SUMMARY	12
1. ZUSAMMENFASSUNG	14
2. INTRODUCTION.....	16
2.1. EPIDEMIOLOGY OF URINARY TRACT INFECTION	16
2.2. <i>ESCHERICHIA COLI</i> AS A PATHOGEN	18
2.2.1. <i>Virulence factors of uropathogenic E. coli</i>	20
Adhesins.....	20
Flagella	21
Toxins	21
Iron acquisition systems.....	22
O-, K-antigens and serum resistance.....	23
2.3. ASYMPTOMATIC BACTERIURIA (ABU).....	24
2.3.1. <i>UTI versus ABU</i>	24
2.3.2. <i>Escherichia coli strain 83972: a model ABU E. coli isolate</i>	24
2.4. MECHANISMS OF PATHOGEN RECOGNITION	26
2.5. NITRIC OXIDE - A HOST DEFENCE MECHANISM	27
2.6. GENOME PLASTICITY AND BACTERIAL EVOLUTION	28
2.7. BACTERIAL POPULATION DYNAMICS.....	30
2.8. AIMS OF THIS WORK.....	32
3. MATERIAL.....	33
3.1. STRAINS	33
3.2. PLASMIDS.....	34
3.3. OLIGONUCLEOTIDES.....	34
3.4. CHEMICALS AND ENZYMES	36
3.5. MEDIA, AGAR PLATES AND ANTIBIOTICS	37
3.5.1. <i>Media</i>	37
3.5.2. <i>Agar plates</i>	38
3.5.3. <i>Antibiotics</i>	38
3.5.4. <i>DNA Markers</i>	39
3.6. TECHNICAL EQUIPMENT	39
4. METHODS.....	42
4.1. WORKING WITH DNA.....	42
4.1.1. <i>Isolation of chromosomal DNA</i>	42
4.1.2. <i>Precipitation of DNA with alcohol</i>	42
4.1.3. <i>Determination of nucleic acid concentration and quality control</i>	43
4.1.4. <i>Polymerase chain reaction (PCR)</i>	43
Standard PCR.....	43
PCR with proof-reading polymerases.....	44
Box PCR	46
Triplex PCR	47
Multiplex PCR.....	47
Inverse PCR (IPCR).....	49
4.1.5. <i>Sequence analysis</i>	49
4.1.6. <i>Multi locus sequence typing (MLST)</i>	49
4.1.7. <i>Isolation of plasmids</i>	50
4.1.8. <i>Enzymatic digest of DNA with restriction nucleases</i>	51
4.1.9. <i>Horizontal gel electrophoresis</i>	51
4.1.10. <i>Plus Field Gel Electrophoresis (PFGE)</i>	52
4.1.11. <i>Restriction of high molecular weight DNA</i>	52
4.1.12. <i>Separation of restriction fragments by gel electrophoresis</i>	53
4.1.13. <i>Isolation of DNA fragments from agarose gels</i>	53
4.1.14. <i>Ligation of DNA fragments</i>	53
4.1.15. <i>Preparation of electrocompetent cells and electroporation</i>	54

Content

4.1.16 Gene inactivation by λ Red recombinase-mediated mutagenesis using linear DNA fragments	54
4.1.17. Southern Blot analysis	56
Vacuum blotting	56
Probe labelling (ECL™ Kit, Amersham Biosciences)	57
Hybridization and detection of the membrane	57
4.1.18. Comparative Genome Hybridization	58
Membrane Layout	58
Probes synthesis	58
Hybridization and detection	58
Quantification of hybridization signals	59
Data analysis	60
4.2. WORKING WITH RNA	61
4.2.1. Isolation of total RNA with RNAeasy Kit	61
4.2.2. Removal of contaminating DNA by DNase treatment and RNA cleanup	62
4.2.3. Reverse transcription (RT) for cDNA synthesis	62
4.2.4. Quantitative Real-Time PCR	63
4.2.5. Expression profiling using DNA arrays	64
Array Layout	64
RNA isolation and cDNA labelling	64
Array pre-hybridisation	65
Array hybridisation	66
Post-Hybridization washing	66
Scanning	67
Data analysis	67
4.3. 2D PROTEIN GEL ELECTROPHORESIS	68
4.3.1. Isolation of intracellular proteins and rehydration	68
4.3.2. Isolation of outer membrane proteins and rehydration	68
4.3.3. Determination of protein concentrations	69
4.3.4. Protein rehydration	69
4.3.5. Isoelectric focusing (IEF)	70
4.3.6. Equilibration	70
4.3.7. Second dimension - separation based on size	72
4.3.8. Proteins staining	73
4.3.9. Analysis of 2-D Gels with the Delta-2D® Software (Decodon)	73
4.3.10. Protein identification by MALDI-TOF-MS	73
4.4. ANALYSIS OF LIPOPOLYSACCHARIDES (LPS)	74
4.4.1. Isolation of LPS	74
4.4.2. Electrophoresis and staining with silver nitrate	74
4.5. PHENOTYPIC ASSAYS	76
4.5.1. Detection of type 1 fimbrial expression	76
4.5.2. Detection of F1C and P fimbrial expression	76
4.5.3. Detection of secreted α -hemolysin	77
4.5.4. Detection of biofilm forming abilities	77
In M63 defined media	77
In pooled, sterile human urine	77
4.6. CONTINUOUS CULTURE OF <i>E. COLI</i> IN MICROFERMENTERS	78
4.7. IN SILICO ANALYSIS	80
5. RESULTS	81
5.1. DIVERSITY OF CLINICAL ABU <i>E. COLI</i> ISOLATES	81
5.1.1. Analysis of relatedness of different ABU isolates	81
5.1.2. Comparative Genomic Hybridization (CGH)	83
5.1.3. Genomic fingerprints of different ABU isolates	85
5.1.4. Genome size of different ABU isolates	85
5.2. PHENOTYPIC VS. GENOTYPIC CHARACTERISTICS OF ABU <i>E. COLI</i> ISOLATES	87
5.2.1. Type 1 fimbriae	87
5.2.2. P fimbriae	89
5.2.3. F1C fimbriae	91

Content

5.2.4. Expression of α -hemolysin	92
5.2.5. LPS O side chain expression.....	92
5.2.6. Biofilm formation	93
5.2.7. Growth characteristics of ABU <i>E. coli</i> isolates.....	94
5.3. ADAPTIVE FLEXIBILITY AND GENOME PLASTICITY OF MODEL STRAIN 83972	95
5.3.1. Patient colonization.....	95
5.3.2. Patients' immune response upon colonization with strain 83972.....	96
5.3.3. Verification of the re-isolates	99
5.3.4. Genome structure of <i>in vivo</i> 83972 re-isolates.....	100
5.3.5. Phenotypes of different <i>in vivo</i> re-isolates	101
Motility.....	101
Growth characteristics	102
Competitiveness.....	103
Biofilm formation	104
5.3.6. Host independent growth of <i>E. coli</i> strain 83972	108
5.3.7. Genomic and phenotypic properties of ABU strain 83972 grown <i>in vitro</i>	110
Genetic structure of the <i>in vitro</i> 83972 re-isolates	110
Motility.....	112
Growth characteristics	112
Biofilm formation	113
5.4. TRANSCRIPTOME ANALYSIS OF 83872 RE-ISOLATES.....	115
5.4.1. Significant changes in the expression pattern.....	115
5.4.2. Individual adaptation of re-isolates	116
Transcriptome changes of <i>in vitro</i> re-isolate 4.9 relative to parent strain 83972.....	117
Transcriptome changes of <i>in vivo</i> re-isolate SR12 relative to parent strain 83972.....	118
Transcriptome changes of <i>in vivo</i> re-isolates KA25 and CK12 relative to parent strain 83972.....	119
5.4.3. Common adaptive patterns in re-isolates	120
5.4.4. Verification of microarray results by quantitative RT-PCR.....	122
5.5. CHANGES IN THE CYTOPLASMIC PROTEIN EXPRESSION OF THE 83972 RE-ISOLATES	125
5.5.1. Cytoplasmic proteome changes of <i>in vivo</i> re-isolate KA25 relative to parent strain 83972.....	126
5.5.2. Cytoplasmic proteome changes of <i>in vivo</i> re-isolate SR12 relative to parent strain 83972	128
5.5.3. Cytoplasmic proteome changes of <i>in vivo</i> re-isolate CK12 relative to parent strain 83972.....	130
5.6. OUTER MEMBRANE PROTEOME CHANGES OF THE <i>IN VIVO</i> RE-ISOLATES OF STRAIN 83972.	135
6. DISCUSSION.....	141
6.1. ASYMPTOMATIC BACTERIURIA IS CAUSED BY A HETEROGENEOUS GROUP OF <i>E. COLI</i> ISOLATES.....	141
6.2. IMPAIRED ABILITY OF ABU ISOLATES TO EXPRESS TYPICAL UPEC VIRULENCE FACTORS	142
6.3. GENOME REDUCTION AND EVOLUTION OF ST 73 ABU STRAINS.....	145
6.4. HOST IMMUNE RESPONSE DURING BACTERIAL COLONISATION.....	146
6.5. HOST-BACTERIUM INTERACTIONS	148
6.5.1. Bacterial variability and host response	148
6.5.2. Flagella expression / motility	151
6.5.3. Biofilm formation	152
6.5.4. Growth characteristics	153
6.6. METABOLIC ACTIVITY OF ABU ISOLATES.....	154
6.7. OUTER MEMBRANE PROTEIN PROFILE AND IRON UPTAKE	158
6.8. HOST DEFENCE-DRIVEN BACTERIAL GENE EXPRESSION	160
6.9. IMPLICATIONS AND OUTLOOK	164
7. REFERENCES	166
8. APPENDIX.....	178
8.1. LEGENDS TO FIGURES AND TABLES.....	178
8.2. EXPRESSION PROFILING DATA.....	181
8.3. CURRICULUM VITAE.....	195
8.4. PUBLICATIONS	196
8.5. ABBREVIATIONS	197

1. Summary

Asymptomatic bacteriuria (ABU) represents the long term bacterial colonization of the urinary tract, frequently caused by *Escherichia coli* (*E. coli*), without typical symptoms of a urinary tract infection (UTI). To investigate characteristics of ABU *E. coli* isolates in more detail, the geno- and phenotypes of eleven ABU isolates have been compared. Moreover, consecutive *in vivo* re-isolates of the model ABU strain 83972 were characterized with regard to transcriptomic, proteomic and genomic alterations upon long term *in vivo* persistence in the human bladder. Finally, the effect of the human host on bacterial adaptation/evolution was assessed by comparison of *in vitro* and *in vivo*-propagated strain 83972.

ABU isolates represent a heterologous group of organisms. The comparative analysis of different ABU isolates elucidated the remarkable genetic and phenotypic flexibility of *E. coli* isolates. These isolates could be allocated to all four major *E. coli* phylogenetic lineages as well as to different clonal groups. Accordingly, they differed markedly in genome content, i.e., the genome size as well as the presence of typical UPEC virulence-associated genes. Multi locus sequence typing suggested that certain ABU strains evolved from UPEC variants that are able to cause symptomatic UTI by genome reduction. Consequently, the high *E. coli* genome plasticity does not allow a generalized view on geno- and phenotypes of individual isolates within a clone. Reductive evolution by point mutations, DNA rearrangements and deletions resulted in inactivation of genes coding for several UPEC virulence factors, thus supporting the idea that a reduced bacterial activation of host mucosal inflammation promotes the ABU lifestyle of these *E. coli* isolates.

Gene regulation and genetic diversity are strategies which enable bacteria to live and survive under continuously changing environmental conditions. To study adaptational changes upon long term growth in the bladder, consecutive re-isolates of model ABU strain 83972 derived from a human colonisation study and from an *in vitro* long term cultivation experiment were analysed with regard to transcriptional changes and genome rearrangements. In this context, it could be demonstrated that *E. coli*, when exposed to different host backgrounds, is able to adapt its metabolic networks resulting in an individual bacterial colonisation strategy. Transcriptome and proteome analyses demonstrated distinct metabolic strategies of nutrients acquisition and energy production of tested *in vivo* re-isolates of strain 83972 that enabled

them to colonise their host. Utilisation of D-serine, deoxy- and ribonucleosides, pentose and glucuronate interconversions were main up-regulated pathways providing *in vivo* re-isolates with extra energy for efficient growth in the urinary bladder. Moreover, this study explored bacterial response networks to host defence mechanisms: The class III alcohol dehydrogenase AdhC, already proven to be involved in nitric oxide detoxification in pathogens like *Haemophilus influenzae*, was shown for the first time to be employed in defending *E. coli* against the host response during asymptomatic bacteriuria.

Consecutive *in vivo* and *in vitro* re-isolates of strain 83972 were also analysed regarding their genome structure. Several changes in the genome structure of consecutive re-isolates derived from the human colonisation study implied the importance of bacterial interactions with the host during bacterial microevolution. In contrast, the genome structure of re-isolates from the *in vitro* long term cultivation experiment, where strain 83972 has been propagated without host contact, was not affected. This suggests that exposure to the immune response promotes genome plasticity thus being a driving force for the development of the ABU lifestyle and evolution within the urinary tract.

1. Zusammenfassung

Asymptomatische Bakteriurie (ABU) stellt eine bakterielle Infektion der Harnblase über einen langen Zeitraum dar, die häufig von *Escherichia coli* hervorgerufen wird, ohne dass typische Symptome einer Harnwegsinfektion auftreten. Um die Charakteristika von ABU *E. coli* Isolaten genauer zu untersuchen, wurden die Geno- und Phänotypen von 11 ABU-Isolaten verglichen. Außerdem wurden in mehreren aufeinanderfolgenden *in vivo*-Reisolaten des Modell-ABU Stammes 83972 die Veränderungen im Transkriptom, Proteom und Genom während einer langfristigen Persistenz in der menschlichen Blase charakterisiert. Schließlich wurde der Effekt des menschlichen Wirtes auf die bakterielle Adaptation durch einen Vergleich von *in vitro*- mit *in vivo*-kultivierten Stämmen abgeschätzt.

ABU-Isolate stellt eine heterogene Gruppe von Organismen dar. Diese können den vier phylogenetischen Hauptgruppen von *E. coli* sowie unterschiedlichen klonalen Gruppen zugeordnet werden. Dementsprechend unterscheiden sie sich erheblich bezüglich der Zusammensetzung des Genomes, der Genomgröße und auch der Ausstattung mit UPEC-typischen Virulenz-assoziierten Genen. Multi-Lokus-Sequenz-Typisierung legt nahe, dass bestimmte ABU Stämme sich durch Genomreduktion aus UPEC Stämmen entwickelt haben, die eine Harnwegsinfektion mit charakteristischen Symptomen auslösen konnten. Folglich erlaubt die hohe Genomplastizität von *E. coli* keine generalisierte Betrachtung einzelner Isolate eines Klons. Genomreduktion über Punktmutationen, Genom-Reorganisation und Deletionen resultierte in der Inaktivierung einiger Gene, die für einige UPEC Virulenz-Faktoren kodieren. Dies stützt die Vorstellung, dass eine verminderte bakterielle Aktivierung der Entzündung der Wirtsschleimhaut den Lebensstil von ABU (bei diesen *E. coli*-)Isolaten fördert.

Genregulation und genetische Diversität sind Strategien, die es Bakterien ermöglichen unter sich fortlaufend ändernden Bedingungen zu leben bzw. zu überleben. Um die anpassungsbedingten Veränderungen bei einem langfristigen Wachstum in der Blase zu untersuchen, wurden aufeinanderfolgende Reisolatate, denen eine langfristige *in vivo*-Kolonisierung im menschlichen Wirt beziehungsweise eine *in vitro*-Kultivierung vorausgegangen ist, im Hinblick auf Veränderungen Genexpression und Genomorganisation analysiert. In diesem Zusammenhang konnte gezeigt werden, dass *E. coli* in der Lage ist, seine metabolischen Netzwerke verschiedenen Wachstumsbedingungen anzupassen und

individuelle bakterielle Kolonisierungsstrategien entwickeln kann. Transkriptom- und Proteom-Analysen zeigten verschiedene metabolische Strategien zur Nährstoffbeschaffung und Energieproduktion bei untersuchten *in vivo*-Reisolaten vom Stamm 83972, die es ihnen ermöglichen, den Wirt zu kolonisieren. Das Zurückgreifen auf D-Serin, Deoxy- und Ribonucleoside sowie die bidirektionale Umwandlung zwischen Pentose und Glucuronat waren hoch-regulierte Stoffwechselwege, die die *in vivo*-Reisolate mit zusätzlicher Energie für ein effizientes Wachstum in der Blase versorgen. Zudem wurden in dieser Studie die Netzwerke für eine Reaktion auf Abwehrmechanismen des Wirtes erforscht: Erstmals wurde hier die Rolle der Klasse-III-Alkoholdehydrogenase AdhC, bekannt durch ihre Bedeutung bei der Entgiftung von Stickstoffmonoxid, bei der Wirtsantwort während einer asymptomatischen Bakteriurie gezeigt.

Aufeinanderfolgende *in vivo*- und *in vitro*-Reisolate vom Stamm 83972 wurden ebenfalls bezüglich ihrer Genomstruktur analysiert. Einige Veränderungen in der Genomstruktur der aufeinanderfolgenden Reisolate, die von einer humanen Kolonisierungsstudie stammen, implizieren die Bedeutung einer Interaktion der Bakterien mit dem Wirt bei der Mikroevolution der Bakterien. Dagegen war die Genomstruktur von Reisolaten eines langfristigen *in vitro*-Kultivierungsexperiments, bei dem sich der Stamm 83972 ohne Wirtkontakt vermehrt hat, nicht von Veränderungen betroffen. Das legt nahe, dass die Immunantwort eine Genomplastizität fördert und somit eine treibende Kraft für den ABU Lebensstil und die Evolution im Harnwegstrakt ist.

2. Introduction

2.1. Epidemiology of urinary tract infection

Urinary tract infections (UTIs) are considered to be the most common bacterial infection in industrialized countries. About every third woman might have UTI episode(s) that require antimicrobial therapy by the age of 24 years, and 40 % to 50 % of women will experience at least one UTI during their lifetime (Foxman, 2002). It is estimated, however, that 20 % of all UTIs occur in men and rates are lower in young men and increase dramatically with increasing age (Griebing, 2005).

Patients with a normal genitourinary tract with no prior instrumentation are considered as “uncomplicated” (Stamm and Hooton, 1993). The majority of acute community-acquired, uncomplicated infections are caused by *Escherichia coli* (70 % to 90 %) or *Staphylococcus saprophyticus* (10 % to 15 %). *Klebsiella*, *Enterobacter*, and *Proteus* species and enterococci infrequently cause uncomplicated cystitis and pyelonephritis (Ronald, 2002). The reservoir for these bacteria is the human bowel flora and most infections result from bacteria introduced into the bladder via the urethra. Sexual activity significantly increases the frequency of uropathogen transmission and UTI incidence (Foxman *et al.*, 2002).

Specific subpopulations are more often prone to UTIs. This group includes infants, pregnant women, the elderly, patients with spinal cord injuries and/or catheters, patients with diabetes, or patients underlying urologic abnormalities (Foxman, 2002). An abnormal urinary tract may lead to colonisation with less virulent organisms that rarely cause disease in the anatomically or metabolically functional one. While in uncomplicated UTIs the most common causative pathogen is *Escherichia coli* (*E. coli*), the etiology of complicated UTI is more diverse and frequently polymicrobial in nature (Ronald, 2002). However, *E. coli* causes about 40 % of all nosocomial UTIs and represents one of the most frequently isolated nosocomial pathogen (Struelens *et al.*, 2004).

UTI can also be classified by the site of infection, as follows: infection of the bladder (cystitis) or the kidneys (pyelonephritis). Bacterial colonisation of the urinary tract is often accompanied by a wide spectrum of symptoms (symptomatic infection) like burning or pain

during urination, fever, cloudy or bloody urine and increased urination frequency (Shaikh *et al.*, 2007; Zorc *et al.*, 2005).

The presence of significant numbers of bacteria in the urine, however, might also not be associated with symptoms and is termed asymptomatic bacteriuria (ABU). ABU is probably the most common form of UTI with varying prevalence by age, gender, sexual activity and the presence of the genitourinary abnormalities (Table 1). ABU patients may carry more than 10^5 bacteria/ml of urine for years, but do not develop symptoms (Lindberg *et al.*, 1978). Asymptomatic bacteriuria is very common among elderly people with frequencies of colonisation ranging from 17 to 50 % in women and 6 to 34 % in men. However, 5% of young school girls will also be asymptotically colonized once until the age of 15 (Raz, 2003). Women with diabetes are reported to encounter ABU three-fold more often than non-diabetics (Nicolle *et al.*, 2006). In elderly patients with indwelling catheters draining in an open system, the incidence of bacteriuria is almost 100% and the vast majority of them are asymptomatic.

Table 1: Prevalence of asymptomatic bacteriuria in selected populations (Colgan *et al.*, 2006).

Population	Prevalence (%)
Healthy pre-menopausal women	1.0 to 5.0
Pregnant women	1.9 to 9.5
Post-menopausal women (50 to 70 years of age)	2.8 to 8.6
Patients with diabetes	
Women	9.0 to 27.0
Men	0.7 to 1.0
Older community-dwelling patients	
Women (older than 70 years)	> 15.0
Men	3.6 to 19.0
Older long-term care residents	
Women	25.0 to 50.0
Men	15.0 to 40.0
Patients with spinal cord injuries	
Intermittent catheter	23.0 to 89.0
Sphincterotomy and condom catheter	57.0
Patients undergoing hemodialysis	28.0
Patients with an indwelling catheter	
Short-term	9.0 to 23.0
Long-term	100

Escherichia coli is the most common organism isolated from patients with ABU, however, other species like *Pseudomonas aeruginosa*, *Enterococcus* spp., and group B streptococci are

reported (Colgan *et al.*, 2006). The microflora in patients with asymptomatic bacteriuria will be influenced by patient variables: healthy persons will likely be colonized by *E. coli*, whereas a nursing home resident with a catheter will most likely be colonized with a multi-drug-resistant polymicrobial flora (e.g., *P. aeruginosa*). Enterococci and Gram-negative bacteria are common in men (Warren *et al.*, 1982)

The treatment of asymptomatic bacteriuria is not always beneficial. Depending on the group of patients, if left untreated ABU protects from symptomatic infections (Hansson *et al.*, 1989a), and recurrences of bacteriuria after treatment occur in 50 % to 80 % of patients (Hansson *et al.*, 1989b). However, antibiotic treatment of ABU in pregnant women, patients prior to surgery and those with vesicoureteral reflux has been shown to be beneficial, if not necessary (Nicolle, 2006).

2.2. *Escherichia coli* as a pathogen

E. coli is a residential bacterium of the large intestine where it co-exists with the human host and both experience mutual benefits. However, there are several highly adapted clones that have acquired specific virulence attributes which confer an increased ability to colonize new niches and allows them to cause a broad spectrum of disease (Kaper *et al.*, 2004). A subset of *E. coli* is capable of causing enteric/diarrhoeal diseases and another subset causes extraintestinal diseases. Among the intestinal pathogens, there are six well-described pathotypes: enteropathogenic *E. coli* (EPEC), enterohaemorrhagic *E. coli* (EHEC), enterotoxigenic *E. coli* (ETEC), enteroaggregative *E. coli* (EAEC), enteroinvasive *E. coli* (EIEC) and diffusely adherent *E. coli* (DAEC) (Kaper *et al.*, 2004). The *E. coli* pathotypes implicated in extraintestinal infections have been called ExPEC (Russo and Johnson, 2000). UTIs are the most common extraintestinal *E. coli* infections and are caused by uropathogenic *E. coli* (UPEC).

Phylogenetic studies have shown that *E. coli* can be allocated to four main phylogenetic groups, designated ECOR (*E. coli* group of reference strains) group A, B1, B2 and D (Herzer *et al.*, 1990). Most strains responsible for UTI and other extraintestinal infections belong to ECOR group B2, or to a lesser extent, to group D, and they carry virulence determinants that are absent in ECOR group A and B1 strains (Johnson and Stell, 2000; Picard *et al.*, 1999). Most of the commensal strains belong to ECOR group A. The various pathotypes of *E. coli*

tend to be clonal and are characterized by shared O (lipopolysaccharide, LPS) and H (flagellar) antigens that define serogroups (O antigen only) or serotypes (O and H antigens) (Kaper *et al.*, 2004).

Pathogenic *E. coli* strains are often characterized by the presence of specific virulence traits that contribute to their pathogenic potential and characteristically are absent among commensal strains (Johnson, 1991; Johnson and Stell, 2000; Kaper *et al.*, 2004). Multiple studies on a number of UPEC strains implicate a variety of virulence and fitness factors that play an important role for urinary tract infection (Fig. 1). Generally, virulence and fitness factors can be grouped as adhesins, toxins and bacteriocins, iron acquisition systems, O-, K-antigens and serum resistance.

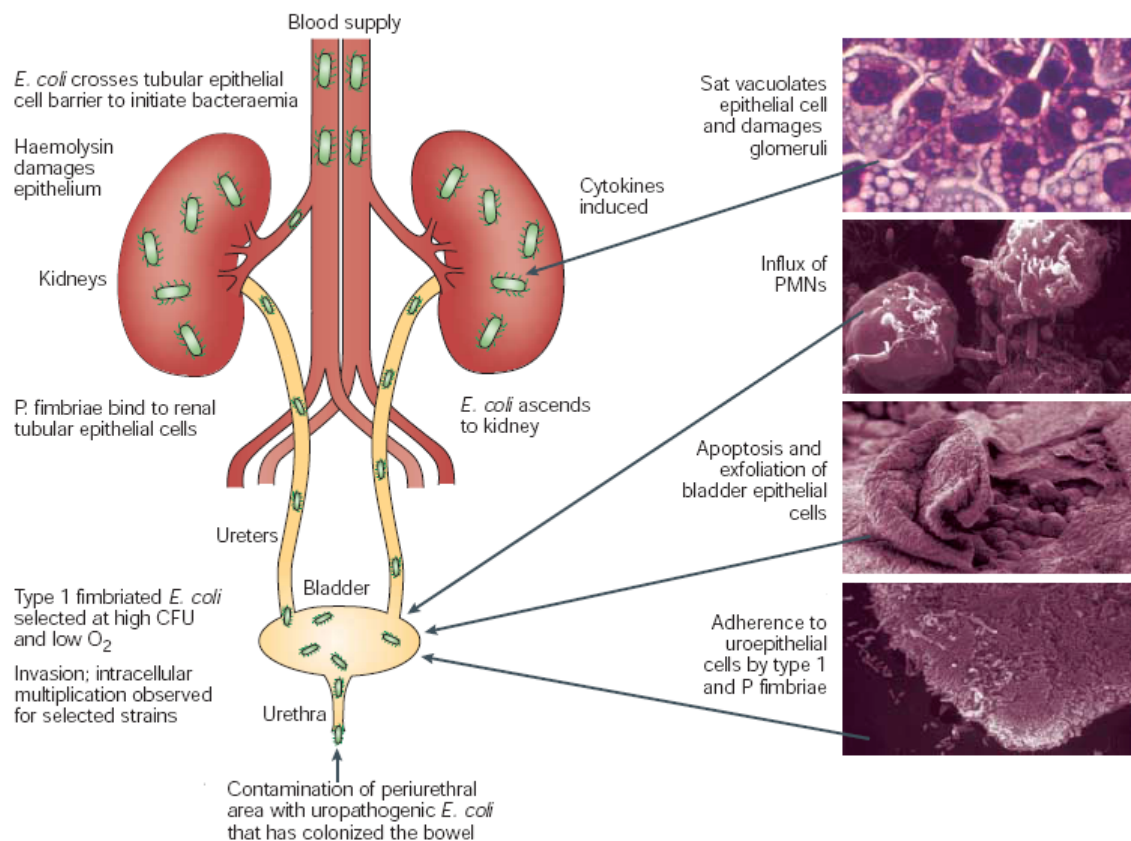


Fig. 1: Pathogenesis of urinary tract infection caused by uropathogenic *E. coli*. The figure shows the different stages of an ascending urinary tract infection and the involvement of particular virulence factors in that process (Kaper *et al.*, 2004).

2.2.1. Virulence factors of uropathogenic *E. coli*

Adhesins

Adherence factors facilitate the colonization of the urinary tract and promote *E. coli* colonization and persistence in the colon or vagina, which may serve as a reservoir for ascending infection in the urinary tract (Johnson, 1991). They include fimbrial (fimbriae, pili) and afimbrial adhesins. Various adhesins have been identified and studied. The P-, type 1, S-, and F1C fimbriae exhibit a composite structure, consisting of a rod-shaped shaft of 6-7 nm in diameter comprising over a thousand major and minor subunits (Sauer *et al.*, 2000). The adhesin is located at the very tip of the fimbriae, often connected with the shaft via the so-called adapter pilus (Schilling *et al.*, 2001). The adhesin and some other minor subunits are responsible for the specific binding to carbohydrate moieties on the surface of eukaryotic cells, therefore contributing to specific adherence (Johnson, 1991). The synthesis, export, correct folding and ordered assembly during fimbrial biogenesis occurs in a coordinated manner (Smyth *et al.*, 1996). The P-, S- and F1C-fimbriae are more exclusively associated with extraintestinal *E. coli* isolates and the tip of these adhesins recognizes carbohydrate moieties: Gal α (1-4)Gal, α -sialyl-2,3- β -galactose, and GalNAc β (1-4)Gal β , respectively (Johnson, 1991). P fimbriae are shown to induce strongly inflammatory response (Bergsten *et al.*, 2005; Wullt *et al.*, 2002).

Type 1 fimbriae are not only expressed by pathogenic strains, and there is no difference in *fim* gene frequency in more and less virulent strains in the urinary tract (Plos *et al.*, 1991). This fimbrial type mediates adhesion to mannose-containing oligosaccharides, e.g. on bladder epithelial cells. Type 1 fimbriae promote attachment and virulence in the murine urinary tract infection model (Hagberg *et al.*, 1983; Snyder *et al.*, 2004). The fimbriae have been shown to enhance bacterial survival, to stimulate mucosal inflammation and to promote bacterial invasion (Anderson *et al.*, 2003; Connell *et al.*, 2000). Allelic variation exists in *fimH*, the gene for the lectin subunit of type I fimbriae. Sokurenko *et al.* (1997) have shown that type 1 fimbriae with different *fimH* alleles vary in their ability to recognize various mannosides and only those capable of mediating high levels of adhesion via mono-mannosyl residues are more capable of mediating *E. coli* adhesion to uroepithelial cells. Therefore, it seems that certain variants of type 1 fimbriae may contribute more than others to *E. coli* urovirulence.

Most of the UPEC strains express curli fimbriae. It is suggested that these fimbriae play a role only in the early phase of infection (e.g., adherence to periurethral skin surface), since they are frequently expressed only at 30 °C (Olsen *et al.*, 1993). In the last years, isolates have been detected in which co-expression of curli fimbriae and cellulose occurs at 30 °C as well as at 37 °C (rdar morphotype), but the importance of this trait for the survival and colonization in the host organism remains unclear (Zogaj *et al.*, 2001).

Flagella

The bacterial flagellum is a long helical surface appendage composed of polymerized flagellin subunits encoded by *fliC*. Although it has never been proven, flagella-mediated motility has been hypothesized to play a role in the pathogenesis of UTI caused by UPEC (Emody *et al.*, 2003). Lane *et al.* (2005) demonstrated that flagella and flagellum mediated motility/chemotaxis may not be absolutely required but contributes to the fitness of bacterium and therefore significantly enhance colonisation of the urinary tract by UPEC. The same group later demonstrated that UPEC indeed utilize flagellin to ascend the upper urinary tract and *fliC* mutant bacteria were able to colonize the bladder but were significantly attenuated in the kidneys (Lane *et al.*, 2007). Flagella are also implicated in virulence of other *E. coli* pathotypes, by inducing interleukin 8 expression and Toll-like receptor 5 (TLR-5) activation upon adhesion of EPEC to epithelial cells *in vitro* (Giron *et al.*, 2002). Moreover, flagella have been shown to contribute to the virulence of other uropathogens, such as *Proteus mirabilis* (Mobley *et al.*, 1996).

Toxins

Toxins are prominent virulence factors of bacterial pathogens. Three toxins play a major role during UTI: the cytotoxic necrotizing factor 1 (CNF-1), the cytolethal distending toxin (CDT) and α -haemolysin.

The α -haemolysin is widely disseminated among pathogenic bacteria and widely distributed in UPEC as well as in EHEC isolates. The *hly* gene cluster encoding the toxin and the enzymes for its biosynthesis is located on PAIs or on plasmids. Secretion via the type I secretion pathway, a posttranslational maturation and the presence of a C-terminal calcium binding domain are characteristics of this pore-forming toxin (Johnson, 1991). α -hemolysin is able to lyse a broad range of host cells which probably contributes to inflammation, tissue injury, and impaired host defences (Cavalieri *et al.*, 1984).

CDT is a secreted protein which has the capacity to inhibit cellular proliferation by inducing an irreversible cell cycle block at the G2/M position (Comayras *et al.*, 1997). CDT is composed of three polypeptides (CdtA, B and C) which are all required for CDT activity. The direct role of the toxin in urinary tract infection, however, remains to be proven.

CNF-1 is widely distributed in extraintestinal pathogens and belongs to a toxin family which modifies Rho, a subfamily of small GTP-binding proteins that are regulators of the actin cytoskeleton (Aktories, 1997). The gene for CNF-1 is chromosomally located on different pathogenicity islands of UPEC (Blum *et al.*, 1994). Eukaryotic cells intoxicated with CNF-1 exhibit membrane ruffling, formation of focal adhesions and actin stress fibers and DNA replication in absence of cell division.

Iron acquisition systems

Iron is needed by all living cells. *E. coli* uses iron for oxygen transport and storage, DNA synthesis, electron transport, and metabolism of peroxides. Ferric iron is highly insoluble and almost all of this iron is complexed with host iron proteins. Part of the host response to infection is to further reduce the amount of iron available for the invading pathogen (Der Vartanian *et al.*, 1992). Pathogens are able to counter the iron restriction imposed by their hosts through the use of siderophores. Siderophores can compete with host iron-binding proteins and several siderophore-based transport systems are known to be required for effective host colonisation. The genes coding for the biosynthesis of such iron-uptake systems in *E. coli* may be located on plasmids or on the chromosome. The gene clusters encoding the enzymes for enterobactin (*ent*) and the ferric dicitrate transport system (*fec*) have a commonly conserved localization in the *E. coli* core genome. However the *fec* gene cluster has been identified to be PAI-encoded in *Shigella flexneri* (Luck *et al.*, 2001). The *iuc* operon coding for aerobactin is either located on plasmids (pColV) or on different genomic islands, whereas the yersiniabactin-encoding HPI (*fyu/irp*) is widely distributed among *Enterobacteriaceae* and shows a rather conserved chromosomal localization at the *asnT* gene. The *chu* system is a well-characterized haeme transport system that firstly has been found in the chromosome of EHEC O157:H7 strains (Torres and Payne, 1997). This system enables the bacteria to utilize iron directly from the haeme and is widely distributed among UPEC isolates (Wyckoff *et al.*, 1998). The *iro* gene cluster (coding for the enzymes required for salmochelin biosynthesis), firstly described for *Salmonella enterica* (Baumler *et al.*, 1996), is involved in the uptake of catecholate-type siderophore compounds. The *iro* genes are widely distributed among *E. coli*

isolates and can be chromosomally or plasmid-encoded (Dobrindt *et al.*, 2003). The ability for iron acquisition of bacteria might be advantageous for their survival in the urinary tract, therefore it is considered an important fitness trait.

O-, K-antigens and serum resistance

Lipopolysaccharide (LPS) is a key component of the outer membrane of Gram-negative bacteria. It comprises three distinct regions: Lipid A, the oligosaccharide core, and commonly a long-chain polysaccharide O antigen that causes a smooth phenotype (Amor *et al.*, 2000). Lipid A is the most conserved part of LPS. It is connected to the core part, which links it to the O repeating units. The O repeating units are highly polymorphic, and more than 190 serologically distinguished forms in *E. coli* are known today (Orskov *et al.*, 1977). Since LPS is located on the outer surface of bacterial cells, its expression is known to be responsible for many features of the cell surface of the Gram-negative bacteria, such as resistance to detergents, hydrophobic antibiotics, organic acids, serum complement factors, adherence to eukaryotic cells etc. (Barua *et al.*, 2002; Jacques, 1996; Svanborg-Eden *et al.*, 1987). It has been suggested that some of these characteristics, especially resistance to the bactericidal effect of the complement system, are dependent on the length of the O side chain (Porat *et al.*, 1992). LPS is believed to significantly contribute to virulence by protecting bacteria from the bactericidal effect of serum complement (Reeves, 1995).

Capsular polysaccharides, more than 80 types of which have been described for *E. coli*, are linear polymers of repeating carbohydrate subunits that sometimes also include a prominent amino acid or lipid component. They coat the cell, interfering with O-antigen detection and protecting the cell from host defence mechanisms (Johnson, 1991). Zingler *et al.* (1993) reported that the most frequent K antigens determined in 253 UPEC isolates are K1 and K5 (31 % and 35 % of the cases respectively); nevertheless more than 26 different K-antigens were identified. The high prevalence of these two capsular serogroups is not astonishing, since both capsular oligosaccharides mimic human antigens by being antigenically and structurally similar to carbohydrates present in human glycosphingolipids, thus preventing effective immune response against bacteria expressing them. The K1 capsule is present in all MENEK isolates and contributes to the ability to cross of the blood-brain barrier (Kim, 2002).

2.3. Asymptomatic bacteriuria (ABU)

2.3.1. UTI versus ABU

While much effort was taken to characterise isolates and the virulence traits of bacteria causing symptomatic urinary tract infections (Brzuszkiewicz *et al.*, 2006; Welch *et al.*, 2002), not much is known why patients with ABU do not develop symptoms. The organisms recovered in many cases belong to the same types of bacteria that cause cystitis, the most common being *E. coli* (Raz, 2003). However, little is yet known about the difference between symptomatic and asymptomatic UTI in terms of pathogenesis, natural history and risk factors. Hanson (1982) suggested that strains with decreased virulence may colonize the urine rather than cause asymptomatic infection. Hull *et al.* (1998) compared virulence factors of isolates from UTI and ABU with isolates from patients with a neuropathic bladder due to spinal cord and brain injury. This group reported that UTI isolates are more likely than ABU strains to be haemolytic and exhibit mannose-resistant hemagglutination of human erythrocytes. It has been also shown that adhesiveness to human urinary tract epithelial cells was high for *E. coli* strains isolated from patients with acute pyelonephritis and acute cystitis, and low for asymptomatic bacteriuria strains (Edén *et al.*, 1979). Taken together, it has been suggested that there might exist differences in the virulence between UTI and ABU isolates. However, the molecular basis for this is unknown.

2.3.2. *Escherichia coli* strain 83972: a model ABU *E. coli* isolate

Many uropathogenic *E. coli* isolates (e.g. strain 536, UTI89, CFT073, J96, NU14) are widely used as a model to investigate symptomatic UTIs. However, the only established prototypic ABU isolate is currently *E. coli* strain 83972. This strain has originally been isolated from a young Swedish girl, who carried it for at least three years without symptoms (Lindberg *et al.*, 1975). Isolate 83972 belongs to the phylogenetic lineage B2 of *E. coli* indicating a close relatedness to the UPEC strains, which cause symptomatic UTI. Moreover, it belongs to the same sequence type as UPEC strain CFT073 and commensal *E. coli* Nissle 1917 (Zdziarski *et al.*, 2008) (Fig. 2). The strain does not express classical UPEC virulence factors, but genotypic analysis has revealed that this *E. coli* possess a large number of virulence-associated genes (Dobrindt *et al.*, 2003). A recent genotypic analysis of selected pathogenicity factors of strain 83972 suggested that the loss of functional type 1, F1C, and P fimbriae was due to deletions or multiple point mutations (Klemm *et al.*, 2006; Roos *et al.*, 2006a).

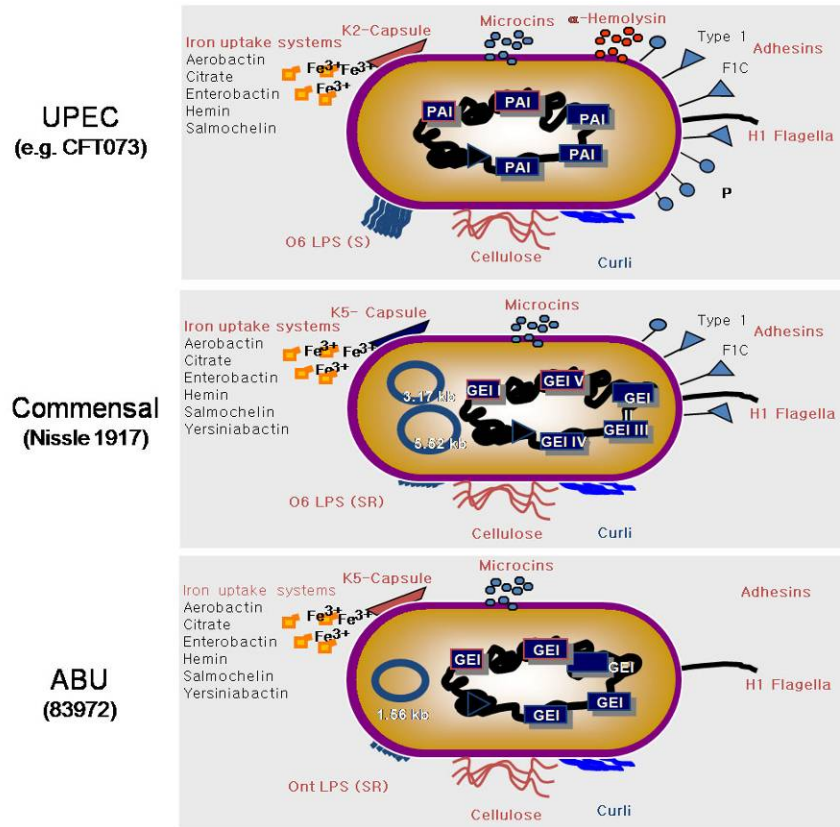


Fig. 2: Phenotypic comparison of *E. coli* strains CFT073, Nissle 1917 and 83972. All these strains belong to the same sequence type, ST 73 (Dobrindt, U.).

Strain 83972 has been successfully used as a prophylactic agent in patients with recurrent urinary tract infections (Andersson *et al.*, 1991; Sunden *et al.*, 2006). For this, the bladder of patients was deliberately colonised with a monoculture of *E. coli* 83972 and asymptomatic bacteriuria was established for up to three years (Wullt *et al.*, 1998). In these cases successful long-term colonisation with strain 83972 prevented the establishment of symptomatic UTI. Deliberate colonisation with this strain has also been shown to reduce the frequency of UTI in patients with a neurogenic bladder secondary to spinal cord injuries (Hull *et al.*, 2000). Interestingly, pre-incubation of catheters with strain 83972 has been reported to prevent colonisation by bacterial or fungal uropathogens (Darouiche *et al.*, 2001; Trautner *et al.*, 2003). In all these cases, a controlled asymptomatic bacteriuria with strain 83972 did not jeopardize the health of the patients and reduced the necessity of antibiotic treatment. Thus further scientific efforts are required to establish colonisation with strain 83972 as a potential prophylactic approach against symptomatic UTI in a routine manner. Such an approach certainly improves the quality of life of people suffering from chronic UTI infections and reduces occurrence of antibiotic resistance.

2.4. Mechanisms of pathogen recognition

The variation in urinary tract virulence reflects the ability of bacteria to trigger mucosal and systemic host responses. Through different molecular interactions bacteria may activate cellular responses, cause cell detachment, and invade or kill cells by apoptosis (Svanborg *et al.*, 2001). Attachment to the mucosa is an essential step in pathogen recognition that activates the host defence signalling pathways (Bergsten *et al.*, 2004). UPEC use type 1-, F1C- and P-fimbriae for epithelial cell adherence at different stages of the infection (Johnson, 1991; Mobley *et al.*, 1994; Wullt *et al.*, 2002).

Type 1- and P-fimbriated *E. coli* share the ability to activate epithelial cells, but they differ in receptor specificity. In case of P fimbriae, the receptors are glycosphingolipids with Gal α (1-4)Gal β receptor motifs, and the PapG tip adhesin binds to these oligosaccharide epitopes (Fischer *et al.*, 2006). Type 1 fimbriae bind to mannose-containing oligosaccharides on bladder epithelial cells (Svensson *et al.*, 1994). Host response to these two fimbriae is controlled by the Toll-like receptor 4 (TLR4), but different adaptor proteins are involved in the down-stream signalling (Fischer *et al.*, 2006).

LPS as a principal component of the Gram-negative cell surface (Yang *et al.*, 1999). Its recognition is mediated by CD14 that subsequently interacts with TLR4 (Beutler, 2000), followed by down-stream signalling. However, Samuelsson *et al.* (2004) demonstrated that CD14 is not expressed by the urinary tract epithelium. Therefore, the expression of fimbriae but not the presence of LPS-“coated” bacteria *per se* decides about the quantity of the host response (Svanborg *et al.*, 2006).

Down-stream signalling causes transcriptional activation and production of inflammatory mediators in the epithelial cell. As a result, chemotactic substances are secreted that include the chemokines IL 6 and IL 8 (Agace *et al.*, 1993a). A chemotactic gradient is created and, in response to the gradient, neutrophils leave the bloodstream, migrate through the tissues and cross the epithelial barrier into the lumen (Agace *et al.*, 1993b; Godaly *et al.*, 1997; Hang *et al.*, 1999). Neutrophils (PMNs) are phagocytes, capable of ingesting microorganisms or particles. They can internalise and kill many microbes by the formation of a phagosome into which reactive oxygen species and hydrolytic enzymes are secreted. Neutrophils have been shown to increase 43-fold expression of the inducible nitric oxide synthase (iNOS) during UTI when compared to non-infected controls (Wheeler *et al.*, 1997). As a consequence, the

nitric oxide concentration in the urine during UTI is increased 30 to 50 times (Lundberg *et al.*, 1996).

2.5. Nitric oxide - a host defence mechanism

Nitric oxide (NO) at concentrations of approximately 10^{-7} M controls blood pressure in mammals and is a messenger in the central and peripheral nervous system (Fang, 2004). In addition to its natural physiological function, NO is a defence molecule against microbial infections (Bang *et al.*, 2006; Bogdan, 2001; Coban and Durupinar, 2003; Fang and Vazquez-Torres, 2002). Nitric oxide is potentially reactive because of the physical instability of oxygen- or nitrogen-based unpaired electrons in their orbits, which leads to a number of deleterious pathological consequences *in vivo* (Akaike, 2001). NO, being a lipophilic radical, diffuses across cell membranes and through the cytoplasm. Sustained NO generation by macrophages inhibits at higher concentrations key enzymes including terminal oxidases and other haem-containing enzymes that bind dioxygen, and Fe-S centres in enzymes such as aconitase. Toxic effects may also arise from reactions involving nitrosation or the peroxynitrate, formed from the reaction of NO with a superoxide anion (Hughes, 1999). These products may store NO or exert toxic effects while their formation may initiate redox or conformational changes (Poole, 2005).

One particularly important effect of NO in the biological systems is its ability to cause genomic alterations (Sakai *et al.*, 2006; Weiss, 2006; Wink *et al.*, 1991). When DNA is exposed *in vitro* to HNO_2 or to NO, the exocyclic amines of the nucleobases form unstable N-nitroso (-N-N = O) derivatives that lead to deamination. Thus, adenine is deaminated to hypoxanthine, guanine is deaminated to xanthine, and cytosine is deaminated to uracil (Shapiro and Pohl, 1968). The deaminated products pair with different bases than their aminated counterparts. Therefore, they almost always produce mutations during subsequent replication. Nitrosation of cellular secondary amines and amides produces alkylating agents that cause mutagenic lesions at many sites in DNA (Victorin, 1994). Other DNA lesions include interstrand and intrastrand cross-links, protein-DNA cross-links, the formation of oxanine from guanine (Suzuki *et al.*, 2000), and DNA replication block, which leads to base substitutions and single-base frameshifts involving translesion DNA synthesis (Sakai *et al.*, 2006).

NO and its congeners exert toxic effects, and microbes have evolved a number of mechanisms for coping with these reactive nitrogen species and their derivatives. Enteric bacteria, such as *E. coli* and *Salmonella enterica* serovar Typhimurium, use two major mechanisms to detoxify NO, the flavohemoglobin Hmp and the flavorubredoxin NorV (Poole *et al.*, 1996; Poole, 2005). The flavohemoglobin detoxifies NO by an O₂-dependent denitrosylase mechanism, producing NO₃⁻ under aerobic or microaerobic conditions or by the slower O₂-independent reduction of NO to N₂O (Poole, 2005). The flavorubredoxin NorV along with its cognate reductase, NorW, however, catalyzes the reductive detoxification of NO only under microaerobic or anaerobic conditions (Gardner *et al.*, 2002). The periplasmic cytochrome *c* nitrate reductase NrfA, which reduces NO₂⁻ to NH₃, may also be able to directly reduce NO (Poock *et al.*, 2002).

NO in the living cell interacts with biomolecules within its immediate environment and forms other reactive nitrogen species (RNS), such as S-nitrosoglutathione (GSNO) and nitrosothiols through interactions with glutathione (GSH) and thiols, respectively (Kidd *et al.*, 2007). The GSH-dependent formaldehyde dehydrogenase AdhC is conserved from man to bacteria and has GSNO reductase activity (Liu *et al.*, 2001), which can limit levels of S-nitrosoglutathione during nitrosative stress. Recently, it has been shown that AdhC is required for the defence against nitrosative stress in *Haemophilus influenzae* (Kidd *et al.*, 2007), however, its function in *Salmonella enterica* serovar Typhimurium remains unclear (Bang *et al.*, 2006).

2.6. Genome plasticity and bacterial evolution

Genome evolution is a continuous process that comprises long-term ‘macroevolution’ which over millions of years leads to the development of new species, and a short-term ‘microevolution’ that alters already existing species/pathotypes enabling them to colonize new environmental niches (Ziebuhr *et al.*, 1999). However, continuously changing environmental conditions force bacteria to start adaptive process. Along regulatory responses that act at the expression level, microorganisms must have evolved strategies allowing the generation of genetic diversity (Arber, 1993). Point mutations, recombination between homologous DNA sites, and the action of transposable genetic elements are major mechanisms by which genome flexibility is achieved (Fig. 3). The capture and spread of genes by horizontal gene transfer involving plasmids, phages and other mobile elements also

contribute to this process. Finally, the clustering of genes on large genomic island and their mobilization enables bacteria to gain or lose huge amounts of DNA involved in adaptation to distinct ecological niches (Ziebuhr *et al.*, 1999).

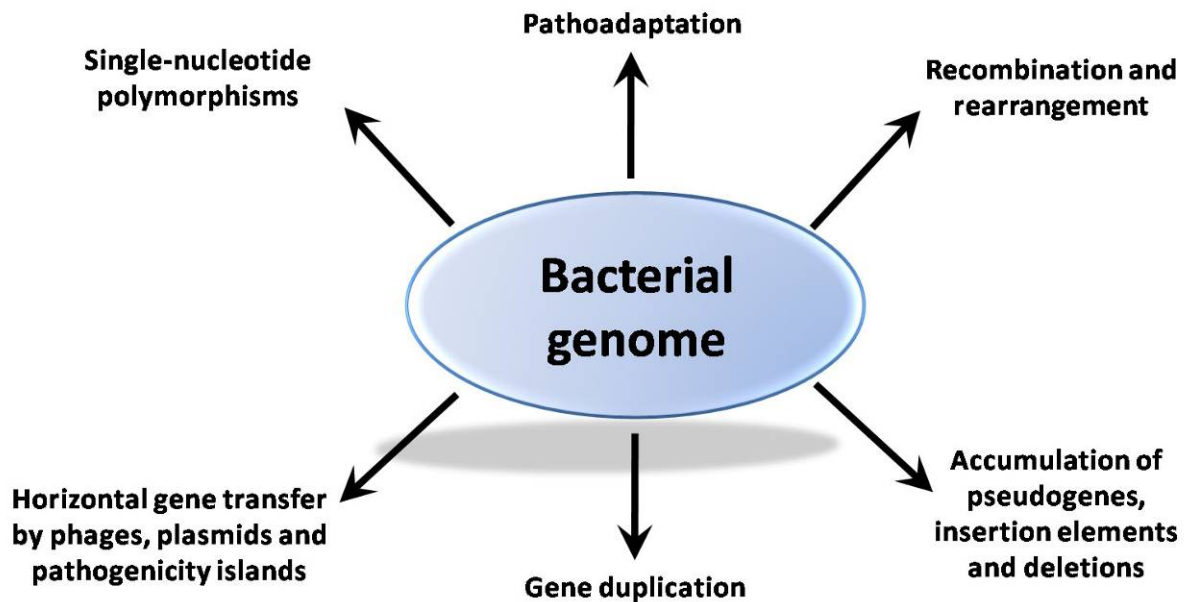


Fig. 3.: Bacterial genome plasticity. There are three main forces that shape bacterial genomes: gene acquisition, gene loss and gene variation. All three can occur in a single bacterium. Some of the changes that result from the interplay of these forces are shown.

E. coli migrating from the large intestine, its natural reservoir, to the urinary tract have to face challenging new conditions, incl. different growth rates, nutrient limitation, host response, and urodynamics in the bladder. Successful colonisation of this niche requires bacterial adaptation to these conditions. Therefore genome alterations in combination with selective pressure will contribute to that process.

Point mutations are considered as driving forces in a slow evolutionary process. During replication, point mutations can be generated by slipped-strand mispairing, resulting in expression or non-expression of particular genes (Leathart and Gally, 1998). Regulatory genes which control coordinated gene expression under changing environmental conditions have also been found to be subject to point mutations and small deletions (Hengge-Aronis, 1999). Some mutations, so called ‘pathoadaptive’ mutations, enable single bacterial clones to become more pathogenic without the acquisition of additional genes. This mechanism is

based on random mutagenesis which offers the bacterium a strong advantage under a selective pressure (Sokurenko *et al.*, 1999). In addition to the modification of structural and regulatory genes, point mutations also contribute to the development of bacterial resistance to antibiotics (Musser, 1995).

The generation of large deletions of the bacterial chromosome represents another major principle of genome plasticity. Excisions are frequently observed in *Streptomyces* spp., where large deletions comprising up to 800 kb of DNA occur (Birch *et al.*, 1991). Recently it has been shown for the ABU strain 83972 that an internal deletion of 4.2 kb DNA stretch resulted in inactivation of type 1 fimbriae (Klemm *et al.*, 2006).

Bacterial insertion sequence (IS) elements are small mobile DNA units encoding only for features necessary for their own mobilization and mediate mutations and DNA rearrangements in bacteria (Mahillon and Chandler, 1998). IS elements can be regarded as repetitive DNA sequences, randomly distributed on the bacterial chromosome that have the capacity to cause inactivation of genes by random and in some cases also by site-specific transposition. In addition to simple transposition, IS elements also give rise to complex DNA rearrangements including deletions, inversions, gene amplifications and the fusion of two DNA molecules by co-integrate formation (Arber, 1993).

Another way of genome rearrangements is acquisition or loss of particular regions on the bacterial chromosome, termed 'pathogenicity islands' (PAI) (Hacker *et al.*, 1997; Hacker and Kaper, 2000). Similarly, there are DNA regions that do not contain virulence-associated genes, but nevertheless contribute to the fitness of the bacterium. These so-called genomic islands (GEIs) encode for additional traits that may be beneficial for the bacteria under certain growth conditions (Hacker and Carniel, 2001). Genomic islands represent (formerly) mobile DNA elements and are considered to have been acquired by horizontal gene transfer, thereby contributing to the evolutionary potential of bacteria (Dobrindt *et al.*, 2003; Hacker *et al.*, 2003).

2.7. Bacterial population dynamics

Biologists have long been interested in the observation of the dynamics of evolutionary changes. Charles Darwin remarked: "in looking for the gradations by which an organ in any

species has been perfected, we ought to look exclusively to its lineal ancestors; but this is scarcely ever possible, and we are forced in each case to look to species of the same group, that is to the collateral descendants from the same original parent-form” (Darwin, 1872). However, Darwin could only use a comparative approach by necessity, evolution nowadays can be assessed in action. Beyond simply observing evolution in nature, some biologists sought to carry out experiments that ran for many generations, with controls and replication, to test hypotheses about the evolutionary process. In this context, microbial evolution experiments have received increasing attention.

Richard Lenski captures microbial evolution in a conceptually simple approach: Populations are established from single clones, then propagated in a controlled and reproducible environment for many generations. A sample of the ancestral population is stored indefinitely (for example, frozen at $-80\text{ }^{\circ}\text{C}$), as are samples from various time points in the experiment. After a population has been propagated for some time, the ancestral and derived genotypes can be compared with respect to any genetic or phenotypic properties of interest, which provides information on the dynamics of the evolutionary process and the extent of evolutionary change. Importantly, adaptation can be quantified by measuring changes in fitness in the experimental environment, in which fitness reflects the propensity to leave descendants (Lenski *et al.*, 1991).

The very extensive work of Lenski and colleagues resulted in many interesting conclusions. One feature that was seen, is that fitness gains are initially rapid but tend to decelerate over time (Cooper and Lenski, 2000; de Visser and Lenski, 2002; Lenski *et al.*, 1991). In a 10,000 generations experiment with 12 *Escherichia coli* populations, the morphology (cell size) and average fitness (measured in competition with the ancestor) evolved rapidly for the first 2,000 generations and were nearly static for the last 5,000 generations (Lenski and Travisano, 1994). Such dynamics indicate that populations, after being placed in a new environment, are evolving from a region of low fitness towards an adaptive peak or plateau. Evolutionary adaptation in experimental microbial populations typically occurs through the substitution of relatively few mutations that confer large benefits, as opposed to countless mutations with small benefits (Rozen *et al.*, 2002). 12 replicate bacterial populations, although founded by the same clone, and evolving in identical environments, diverged from one another in their relative fitness, morphological features and performance in other environments (Korona *et al.*, 1994; Lenski *et al.*, 1991).

These experimental conditions, however, are very distinct to those in the urinary tract. The inflow of urine into the bladder (Coolsaet *et al.*, 1980) rather resembles a continuous than a batch bacterial culture. Moreover, intra-individual differences of patients are very prominent (Rezzi *et al.*, 2007). Similar to a ‘natural experiment’ that involves the colonization of several neighbouring islands by the same ancestor species demonstrated that subtle environmental differences promoted divergence (Darwin, 1872), the urinary tract of individual patients might be considered as the “Galapagos archipelago” for the evolution of ABU *E. coli* strains.

2.8. Aims of this work

The role of multiple virulence-associated factors of uropathogenic *E. coli* involved in the development of symptomatic and chronic UTI has been elucidated so far, but only little information was available on characteristics of ABU isolates. Therefore one aim of this study was the detailed characterisation of clinical ABU isolates. The geno- and phenotypic diversity and relatedness of ABU isolates should be assessed using comparative genome hybridisation, pulsed-field gel electrophoresis and multi locus sequence typing. Moreover, virulence and fitness factors of this group of organisms should be further characterised and compared to those of UPEC and non-pathogenic *E. coli* strains.

Another aim was the assessment of bacterial adaptation and microevolution in the urinary tract using ABU strain 83972 as a model. Consecutive re-isolates of this strain derived from a deliberate human colonisation study and *in vitro* continuous culture should be analysed with regard to phenotypic and genomic alterations. *In vitro* transcriptome and proteome analysis should be performed to assess bacterial adaptation upon prolonged growth of strain 83972 in the urinary bladder.

3. Material

3.1. Strains

All bacterial strains used in this study and their relevant genotype are listed in (Table 2).

Table 2: Bacterial strains used in this study

Strain	Relevant properties	Reference
UPEC 536	clinical isolate from pyelonephritis; O6:K15:H31	(Berger <i>et al.</i> , 1982)
CFT073	clinical isolate from pyelonephritis, O6:K2:H7	(Mobley <i>et al.</i> , 1990)
<i>E. coli</i> MG1655	F-, λ -, <i>ilvG</i> , <i>rfb-50 rph-1</i>	(Blattner <i>et al.</i> , 1997)
Nissle 1917	Probiotic <i>Escherichia coli</i> strain, O6:K5:H7	(Nissle, 1918)
83972	Asymptomatic bacteriuria isolate	(Lindberg and Winberg, 1976)
83972 <i>cat</i>	Cm ^R	This study
ABU5	Asymptomatic bacteriuria isolate	(Svanborg C, Lund)
ABU20	Asymptomatic bacteriuria isolate	(Svanborg C, Lund)
ABU21	Asymptomatic bacteriuria isolate	(Svanborg C, Lund)
ABU27	Asymptomatic bacteriuria isolate	(Svanborg C, Lund)
ABU37	Asymptomatic bacteriuria isolate	(Svanborg C, Lund)
ABU38	Asymptomatic bacteriuria isolate	(Svanborg C, Lund)
ABU57	Asymptomatic bacteriuria isolate	(Svanborg C, Lund)
ABU62	Asymptomatic bacteriuria isolate	(Svanborg C, Lund)
ABU64	Asymptomatic bacteriuria isolate	(Svanborg C, Lund)
KA22	83972 strain derivate – human colonization study	(Wullt B, Lund)
KA25	83972 strain derivate – human colonization study	(Wullt B, Lund)
IJ15	83972 strain derivate – human colonization study	(Wullt B, Lund)
SN16	83972 strain derivate – human colonization study	(Wullt B, Lund)
SN25	83972 strain derivate – human colonization study	(Wullt B, Lund)
CK3	83972 strain derivate – human colonization study	(Wullt B, Lund)
CK6	83972 strain derivate – human colonization study	(Wullt B, Lund)
CK9	83972 strain derivate – human colonization study	(Wullt B, Lund)
CK12	83972 strain derivate – human colonization study	(Wullt B, Lund)
SR3	83972 strain derivate – human colonization study	(Wullt B, Lund)
SR6	83972 strain derivate – human colonization study	(Wullt B, Lund)
SR12	83972 strain derivate – human colonization study	(Wullt B, Lund)
POS6	83972 strain derivate – human colonization study	(Wullt B, Lund)
POS9	83972 strain derivate – human colonization study	(Wullt B, Lund)
POS12	83972 strain derivate – human colonization study	(Wullt B, Lund)
POS18	83972 strain derivate – human colonization study	(Wullt B, Lund)
83972_1.1 – 83972_1.16 ^a	83972 strain derivates – continuous culture in LB + NO	This study
83972_2.1 – 83972_2.16 ^a	83972 strain derivates – continuous culture in urine + NO	This study
83972_3.1 – 83972_3.16 ^a	83972 strain derivates – continuous culture in LB	This study
83972_4.1 – 83972_4.16 ^a	83972 strain derivates – continuous culture in urine	This study

a) Sixteen independent re-isolates numbered from 1 to 16

3.2. Plasmids

All plasmids used during this study are listed in (Table 3).

Table 3: Plasmids used in this study.

Plasmid	Relevant properties	Reference
pKD46	<i>repA101</i> (ts), <i>araBp-gam-bet-exo</i> (λ red recombinase under the control of <i>araB</i> promoter), Ap ^R (<i>bla</i>)	(Datsenko and Wanner, 2000)
pKD3	<i>oriRγ</i> , Ap ^R , <i>cat</i> -gene flanked by FRT sites	(Datsenko and Wanner, 2000)
pKD4	<i>oriRγ</i> , Ap ^R , <i>npt</i> -gene flanked by FRT sites	(Datsenko and Wanner, 2000)
pCP20	Yeast Flp recombinase gene (FLP, <i>aka exo</i>) ts- <i>rep</i> , Ap ^R , Cm ^R	(Datsenko and Wanner, 2000)

3.3. Oligonucleotides

All oligonucleotides used for PCR, RT-PCR, gene disruption using the λ Red-based method (Datsenko and Wanner, 2000) were purchased from Sigma-Genosys (Steinheim, Germany). The sequences and the application of all oligonucleotides are listed in (Table 4).

Table 4: Oligonucleotides used in this study.

Primer	Primer sequence (5' - 3')	Target gene	Product size	Application
papOP1f	cctccatcatgctgttcag	<i>pap</i> operon		<i>pap</i> operon sequencing
papSQ1	gggaacatggcgcatca	<i>pap</i> operon		<i>pap</i> operon sequencing
papSQ2	aagtcggtattgccggtgc	<i>pap</i> operon		<i>pap</i> operon sequencing
papSQ3	agaaggtgctttctcagcagttgc	<i>pap</i> operon		<i>pap</i> operon sequencing
papSQ4	tgccctgcaataccattgacgggt	<i>pap</i> operon		<i>pap</i> operon sequencing
papSQ5	tggcatgatggtcagtgctgc	<i>pap</i> operon		<i>pap</i> operon sequencing
papSQ6	tcaggacctggacagttcagttcg	<i>pap</i> operon		<i>pap</i> operon sequencing
papSQ7	aaactggcggactggaaca	<i>pap</i> operon		<i>pap</i> operon sequencing
papSQ8	aatgtccggtggaacacgtc	<i>pap</i> operon		<i>pap</i> operon sequencing
papOP1f	cctccatcatgctgttcag	<i>pap</i> operon		<i>pap</i> operon sequencing
papSQ10	aagtcagcgggtgggtatcgt	<i>pap</i> operon		<i>pap</i> operon sequencing
papSQ12	tgcaattctgcccggaaaac	<i>pap</i> operon		<i>pap</i> operon sequencing
papKf	gatgataaaaagcacaggcgct	<i>pap</i> operon		<i>pap</i> operon sequencing
papSQ13	gaccctgaccttaagggaacg	<i>pap</i> operon		<i>pap</i> operon sequencing
KM_papE-f	gaggaaaactgattattcctgc	<i>pap</i> operon		<i>pap</i> operon sequencing
papEF multi	gcaacagcaacgctggtgcatcat	<i>pap</i> operon		<i>pap</i> operon sequencing
papSQ15	tggttacagagtgacagcaggtctg	<i>pap</i> operon		<i>pap</i> operon sequencing
papG AlleleIII-f	ggcctgcaatggatttacctgg	<i>pap</i> operon		<i>pap</i> operon sequencing
papG AlleleIII-r	ccaccaaatgaccatgccagac	<i>pap</i> operon		<i>pap</i> operon sequencing
papSQ16b	tctggcatggtcatttggtgg	<i>pap</i> operon		<i>pap</i> operon sequencing
papG rev OP	tcatgagcagcgttgctgaacc	<i>pap</i> operon		<i>pap</i> operon sequencing
focOP1f	tcagtgaagcatgcccacaaactg	<i>foc</i> operon		<i>foc</i> operon sequencing
focSQ2	attaaggcagccctgtaggtgg	<i>foc</i> operon		<i>foc</i> operon sequencing
focSQ3	tgatgacagatacgggtgtcgt	<i>foc</i> operon		<i>foc</i> operon sequencing
focSQ4	ggctgttttatccatgcccgggtg	<i>foc</i> operon		<i>foc</i> operon sequencing
focSQ5	ggaaggcaaatggacaggtatgg	<i>foc</i> operon		<i>foc</i> operon sequencing

Material

focSQ6	ccgggtaaattagagttcaccctg	<i>foc</i> operon		<i>foc</i> operon sequencing
sfaF3.2	gttcagctacaggcaccga	<i>foc</i> operon		<i>foc</i> operon sequencing
focSQ8	gtatgcaccgacaattcacggt	<i>foc</i> operon		<i>foc</i> operon sequencing
focOP1r	agttcagggaccagctgatgctc	<i>foc</i> operon		<i>foc</i> operon sequencing
focOP2f	tcaacgttgatctgagtgggcagc	<i>foc</i> operon		<i>foc</i> operon sequencing
focSQ10	aggtgcatctgatacgcgca	<i>foc</i> operon		<i>foc</i> operon sequencing
focSQ11	ggcaatgttcaggataaacctgc	<i>foc</i> operon		<i>foc</i> operon sequencing
sfaG3.1	cattctctgcatgctggc	<i>foc</i> operon		<i>foc</i> operon sequencing
focSQ12	tgatagcagccaacagcacctc	<i>foc</i> operon		<i>foc</i> operon sequencing
focSQ13	cagaatgaagatgcctctggctcag	<i>foc</i> operon		<i>foc</i> operon sequencing
focSQ14	taggcagctctctgtgagctctg	<i>foc</i> operon		<i>foc</i> operon sequencing
focSQ15	ttcagaagtgacactccgga	<i>foc</i> operon		<i>foc</i> operon sequencing
focSQ16	cgatgtttaccggatgactgatgc	<i>foc</i> operon		<i>foc</i> operon sequencing
focOP2r	aatcgggtgcgctgtcgatca	<i>foc</i> operon		<i>foc</i> operon sequencing
hlyC for	gcatgtatcctggctctgg	<i>hly</i> operon	331	<i>hly</i> operon detection
hlyC rev	caccctgatggctctgaat	<i>hly</i> operon	331	<i>hly</i> operon detection
hlyA for	cggtacttggtggcgatg	<i>hly</i> operon	338	<i>hly</i> operon detection
hlyA rev	tcaccgcatagagctgggt	<i>hly</i> operon	338	<i>hly</i> operon detection
hlyB for	ctggttacgtcgtcaggtg	<i>hly</i> operon	322	<i>hly</i> operon detection
hlyB rev	gcgcatgatgacatgctcc	<i>hly</i> operon	322	<i>hly</i> operon detection
hlyD for	tcgctcaaggacaacgcga	<i>hly</i> operon	336	<i>hly</i> operon detection
hlyD rev	ctttccggactgactctcc	<i>hly</i> operon	336	<i>hly</i> operon detection
hly for	ctgggatcgtactgtatgag	<i>hly</i> operon	7990	<i>hly</i> operon amplification
hly rev	ccctgactcagactcacagc	<i>hly</i> operon	7990	<i>hly</i> operon amplification
hlySQ1	actacagtctgcaaagcaatcctc	<i>hly</i> operon		<i>hly</i> operon sequencing
hlySQ2	agctaatcaaccaactcgtggac	<i>hly</i> operon		<i>hly</i> operon sequencing
hlySQ3	gatggtgacagtttactgtctgc	<i>hly</i> operon		<i>hly</i> operon sequencing
hlySQ3.5	gcaatgtttgaacatgctgccag	<i>hly</i> operon		<i>hly</i> operon sequencing
hlySQ4	tccagaagcaagtcttgacca	<i>hly</i> operon		<i>hly</i> operon sequencing
hlySQ5	cagatctgcttgatggcgga	<i>hly</i> operon		<i>hly</i> operon sequencing
hlySQ6	gcagttgcccgaatgcca	<i>hly</i> operon		<i>hly</i> operon sequencing
hlySQ7	ctgttaccgggaaactggca	<i>hly</i> operon		<i>hly</i> operon sequencing
hlySQ8	tctggtggaatcagtcacg	<i>hly</i> operon		<i>hly</i> operon sequencing
hlySQ9	tcggtatcaaatctgagcaggtc	<i>hly</i> operon		<i>hly</i> operon sequencing
hlySQ10	gaatatcagctgtcacgcagc	<i>hly</i> operon		<i>hly</i> operon sequencing
fimH All for	atgaaacgagttattaccct	<i>fimH</i>	525	<i>fimH</i> sequencing
fimH All rev	cacatcattattggcgtaaatat	<i>fimH</i>	525	<i>fimH</i> sequencing
KM-fimB-f	aataccgggctcatgctg	<i>fim</i> operon	339	<i>fim</i> operon detection
KM-fimB-r	gaatctccagtgacaaccg	<i>fim</i> operon	339	<i>fim</i> operon detection
KM-fimE-f	atgcagggcgtgtgttacg	<i>fim</i> operon	390	<i>fim</i> operon detection
KM-fimE-r	gttcataaccacaagcatgcc t	<i>fim</i> operon	390	<i>fim</i> operon detection
KM-fimA-f	ggctctggctgatactacac	<i>fim</i> operon	437	<i>fim</i> operon detection
KM-fimA-r	ccggttgcaaaataacgcgc	<i>fim</i> operon	437	<i>fim</i> operon detection
KM-fimI-f	caatgtttgctctggccgg	<i>fim</i> operon	386	<i>fim</i> operon detection
KM-fimI-r	gccgtttccagttgtctgg	<i>fim</i> operon	386	<i>fim</i> operon detection
KM-fimC-f	aatggtggtgcccggacg	<i>fim</i> operon	445	<i>fim</i> operon detection
KM-fimC-r	gag aat tcg cgc tac gac g	<i>fim</i> operon	445	<i>fim</i> operon detection
KM-fimD-f	gaatctgctggcgatgatg	<i>fim</i> operon	442	<i>fim</i> operon detection
KM-fimD-r	catcgaaaatatcgccctgag	<i>fim</i> operon	442	<i>fim</i> operon detection
KM-fimF-f	gcacgattactatccgcgg	<i>fim</i> operon	397	<i>fim</i> operon detection
KM-fimF-r	ctgtgtcgccattagccg	<i>fim</i> operon	397	<i>fim</i> operon detection
KM-fimG-f	atgaaatggtgcaaactgtggg	<i>fim</i> operon	434	<i>fim</i> operon detection
KM-fimG-r	caatgctctgacctgtaacgg	<i>fim</i> operon	434	<i>fim</i> operon detection
KM-fimH-f	gggctgctcggtgaaatgc	<i>fim</i> operon	445	<i>fim</i> operon detection
KM-fimH-r	catcgctgttatagttgttgctc	<i>fim</i> operon	445	<i>fim</i> operon detection
fecR for	gcttagcacggcaccagct	<i>fecR</i>		Inverse PCR
fecI for	tcaccggttgccgatagtg	<i>fecI</i>		Inverse PCR
Del 2 for	ttctggcatgtgctggctcag			Inverse PCR
Del 3 for	tgctaaatcacgtcagcgct			Inverse PCR
Del 4 for	gtcttcgggtgaacgcactctg			Inverse PCR

Material

Del 4 rev	aaaggctcaggtcggatacc			Inverse PCR
Box	ctacggcaaggcgacgctga			Box PCR
16SRNA_for	aactgagacacggtccagact	<i>rrnB</i>	330	qRT-PCR
16SRNA_rev	ttaacgctgcaccctccgt	<i>rrnB</i>	330	qRT-PCR
frmA_for	tcaaacctggcgaccatgtg	<i>frmA</i>	268	qRT-PCR
frmA_rev	agcaggcagacgtgttcatg	<i>frmA</i>	268	qRT-PCR
hmpA_for	ggcaatatctcggcgtctgg	<i>hmp</i>	220	qRT-PCR
hmpA_rev	actggtgtgtcatctgcgac	<i>hmp</i>	220	qRT-PCR
tar_for	agtggcaactggcggttacc	<i>tar</i>	205	qRT-PCR
tar_rev	cgttgcatatgtgaaacgctctg	<i>tar</i>	205	qRT-PCR
metR_for	tgccatagatgccaatagctg	<i>metR</i>	232	qRT-PCR
metR_rev	tcagggtgtaacaccagacg	<i>metR</i>	232	qRT-PCR
iutA_for	accatgatggagttgaggctg	<i>iutA</i>	222	qRT-PCR
iutA_rev	catgatgtccagccgattgg	<i>iutA</i>	222	qRT-PCR
yeiC_for	gcgcaactaatcaatccgggtg	<i>yeiC</i>	215	qRT-PCR
yeiC_rev	ctaaggttgcaatccgcgac	<i>yeiC</i>	215	qRT-PCR
ABU_marker_for	tcttatccgcatgctgagagc	<i>fim</i>		83972 specific
ABU_marker_rev	tgacctgtgcagtaccacgag	<i>fim</i>		83972 specific
pABU_for	acatagatccctcatgcccgtg	pABU		83972 specific
pABU_rev	cgtcgggtgttacagcagatgg	pABU		83972 specific

3.4. Chemicals and enzymes

All chemicals and enzymes used in this study were purchased from the following companies: New England Biolabs (Frankfurt am Main), Invitrogen (Karlsruhe), MBI Fermentas (St. Leon-Roth), Roche Diagnostics (Mannheim), Gibco BRL (Eggenstein), Dianova (Hamburg), Difco (Augsburg), Merck (Darmstadt), Oxoid (Wesel), GE Healthcare/Amersham Biosciences (Freiburg), Roth (Karlsruhe), Serva and Sigma-Aldrich (Taufkirchen), Axxora (Lörrach). Radionucleotides were purchased from GE Healthcare/Amersham Biosciences (Freiburg).

The following commercial kits were used:

- Plasmid Mini and Midi kit, QIAGEN (Hilden)
- PCR purification kit, QIAGEN (Hilden)
- Gel extraction kit, QIAGEN (Hilden)
- RNeasy kit, QIAGEN (Hilden)
- ABI Prism BigDye Terminator Cycle Sequencing Ready Reaction kit, Applied Biosystems (Foster City, USA)
- ECLTM Direct Acid Labeling and Detection System, and ECLTM advance system, GE Healthcare/Amersham Biosciences (Freiburg)
- Roti-Nanoquant, Roth (Karlsruhe)
- OpArray Hybridization Buffer Kit, Operon (Cologne)

3.5. Media, agar plates and antibiotics

All media were autoclaved for 20 min at 120 °C, if not stated otherwise. Supplements for media and plates were sterile filtered through a 0.22 µm pore filter and added after cooling down the media to <50 °C.

3.5.1. Media

LB medium (Luria-Bertani): (Sambrook, 1989)

10 g	Tryptone from casein	
5 g	Yeast extract	
5 g	NaCl	ad 1 l dH ₂ O

M63 minimal medium:

1 x M63 media

Ingredient	stock	final concentration	for 800ml
M63 salts	5x	1x	160 ml
FeSO ₄	1 ‰	0.001 ‰	800 µl
MgSO ₄	10 ‰	10 ‰	800 µl
Thiamin	0.2%	0.5 ‰	2 ml
Glucose	20 ‰	0.4 ‰	16 ml
Casamino acids	10 ‰	1 ‰	80 ml
KOH	10 M	pH 7	5.2 ml

5 x M63 salts

(NH ₄) ₂ SO ₄	15 mM	8 g
KH ₂ PO ₄	100 mM	54.4 g
ad up to 800 ml ddH ₂ O and autoclave		

FeSO ₄	1 mg / 1 ml in H ₂ O and sterile filtration
MgSO ₄	10 g / 100 ml in H ₂ O and autoclaving
Thiamin	20 mg / 10 ml in H ₂ O and sterile filtration
Glucose	20 g / 100 ml in H ₂ O and autoclaving
Casamino acids	10g / 100 ml in H ₂ O and autoclaving
KOH	10 M in H ₂ O and autoclaving

Urine

Human urine was collected at least from 10 healthy male and female volunteers, pooled and sterilized by filtration. Sterile urine was stored at 4 °C not longer than one week.

3.5.2. Agar plates

LB agar plates:

LB medium + 1.5 % (w/v) agar (Difco Laboratories, Detroit, USA)

Motility agar plates

LB medium + 0.3 % (w/v) agar

Blood agar plates:

LB plates containing 5 % (v/v) washed sheep erythrocytes

Congo Red agar plates:

1 l autoclaved LB agar without salt

1 ml 0.4 mg ml⁻¹ Congo Red dye solution

1 ml 0.2 mg ml⁻¹ Coomassie brilliant blue R-250

Dye solutions were stirred for 1h at 50 °C before sterile filtration

MacConkey agar plates:

BBLTM MacConkey Agar, Beckton Dickinson

3.5.3. Antibiotics

When appropriate, media and plates were supplemented with the antibiotics listed in the Table 5, in the indicated concentrations. Stock solutions were sterile filtered and stored at -20 °C until usage.

Table 5: Antibiotic substances used in this study.

Antibiotic	Stock concentration	Solvent	Working concentration
Chloramphenicol (Cm)	50 mg ml ⁻¹	EtOH	20 µg ml ⁻¹
Ampicillin (Ap)	100 mg ml ⁻¹	dH ₂ O	100 µg ml ⁻¹
Kanamycin (Km)	50 mg ml ⁻¹	dH ₂ O	50 µg ml ⁻¹
Streptomycin	20 mg ml ⁻¹	dH ₂ O	20 µg ml ⁻¹

3.5.4. DNA Markers

To determine the size of DNA fragments in agarose gels, the “Generuler™” 1-kb DNA ladder, purchased from MBI Fermentas, was used (Fig. 4A), whereas in PFGE the Lambda Ladder PFG Marker from New England BioLabs was used (Fig. 4B).

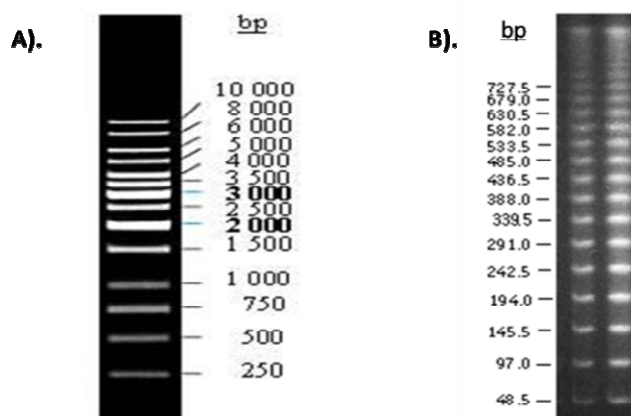


Fig. 4: DNA markers used for electrophoresis: (A) Generuler 1-kb DNA ladder (Fermentas); (B) Lambda Ladder PFG Marker (BioLabs)

3.6. Technical Equipment

2D-Electrophoresis chamber	Ettan DALT six, Amersham Biosciences
Autoclaves	Integra Bioscience, H+P Varoclav
Balances	IL-180, Chyo Balance Corp
	Kern 470
	Ohaus Navigator
Bioanalyzer	Agilent Technologies, 2100expert
Centrifuges	Beckmann J2-HC® JA10 and JA20 rotors

Material

	Beckmann L-70 Ultracentrifuge
	Heraeus Sepatech Megafuge1.OR
	Heraeus Sepatech Biofuge 13R
	Hettich Mikro20
Clean bench	NUAIRE, Class II, type A/B3
Documentation	BioRad GelDoc2000 + MultiAnalyst Software V1.1
Electrophoresis systems	BioRad
Electroporator	Gene Pulser, BioRad
Hybridization oven	HybAid Mini 10
FastPrep	FastPrep-24 MP™
Isoelectric Focussing	MultiPhor, Amersham Biosciences
Incubators	Memmert Tv40b (30 °C, 43 °C)
	Heraeus B5050E (37 °C)
Magnetic stirrer	Heidolf MR3001K
MALDI-TOF-MS	Proteome-Analyzer 4700, Applied Biosystems
Microarray scanner	GenePix 4000B, Molecular Devices
Microarray hybridization chamber	Scienion
Micropipettes	Eppendorf Research 0.5-10 µl, 1000 µl
	Gilson pipetman 20 µl, 200 µl
Microwave AEG	Micromat
Power supplies	BioRad Power Pac 300
PCR-Thermocycler	Biometra T3
pH-meter	WTW pH 525
Photometer	Pharmacia Biotech Ultrospec 3000
	Thermo Scientific NanoDrop™ 1000
Phosphoimager	Amersham Biosciences, Typhoon 4600
Real Time PCR Thermocycler	Bio Rad, MyiQ
Scanner	HP ScanJet IIcx
Shakers	Bühler TH30 SM-30 (37°C, 150 rpm)
	Innova 4300, New Brunswick Scientific (37°C, 220 rpm)
	Innova 4230, New Brunswick Scientific (30°C, 220 rpm)
Speedvac	Savant SC110
Thermoblocks	Liebisch
Vacuum Blotter	Pharmacia + LKD Vacu Gene Pump

Material

Vaccum pump	Univac Uniequipe
Videoprinter	Mitsubishi Hitachi, Cybertech Cb1
Vortexer	Vortex-Genie 2 TM Scientific Industries
UV-Crosslinker	BioRad
Waterbath	GFL 1083, Memmert

4. Methods

4.1. Working with DNA

4.1.1. Isolation of chromosomal DNA

Bacteria from 1 ml an overnight culture were harvested by centrifugation for 4 min at maximum speed in a table centrifuge. After washing with 1 ml TNE buffer, cells were centrifuged for 4 min and resuspended in 270 μ l TNE-X buffer. 30 μ l lysozyme (5 mg ml⁻¹) were added and samples were incubated for 20 min at 37 °C. Afterwards, 15 μ l proteinase K (20 mg ml⁻¹) were added and further incubated up to 2 h at 65 °C until the solution became clear. The genomic DNA was precipitated by addition of 0.05 vol 5 M NaCl (15 μ l) and 500 μ l ice-cold ethanol. After short incubation on ice DNA was collected by centrifugation for 15 min. After washing two times with 1 ml 70% (v/v) ethanol, DNA pellets were air-dried and redissolved in 100 μ l 100 dH₂O (Clermont *et al.*, 2000b).

TNE	
10 mM	Tris
10 mM	NaCl
10 mM	EDTA

TNE-X	
TNE + 1 % Triton X-100	

4.1.2. Precipitation of DNA with alcohol

DNA was either precipitated with ethanol or isopropanol. In the first case, 0.1 vol 3 M Na-acetate (pH 4.8) were added to the sample prior to the addition of 2.5 vol ice-cold 100 % (v/v) ethanol. For the precipitation with isopropanol, 0.7 vol were used. Samples were incubated at -80 °C before centrifugation (13,000 rpm, 4 °C, >20 min). The DNA pellet was washed with 70 % (v/v) ethanol, air-dried and resuspended in dH₂O.

4.1.3. Determination of nucleic acid concentration and quality control

Nucleic acid concentrations were determined either using a standard spectrophotometer in quartz cuvettes with a diameter of 1 cm or using a NanoDrop® instrument where cuvettes were not needed. In both cases, absorption at 260 nm of 1.0 corresponds to 50 µg ml⁻¹ double stranded DNA or 40 µg ml⁻¹ RNA. The purity of the preparations was determined by measurement of the absorption of the sample. DNA and RNA were considered sufficiently pure when the ratio A260 / A280 was higher than 1.8 or 2.0, respectively. Additionally, RNA integrity was determined by capillary electrophoresis using an Agilent 2100 Bioanalyzer instrument.

4.1.4. Polymerase chain reaction (PCR)

This method allows the exponential amplification of DNA regions *in vitro* by using a heat stable DNA polymerase from *Thermus aquaticus* (*Taq*). This way, even small amounts of template DNA can be amplified to high copy numbers and easily visualized.

Standard PCR

For routine PCR amplification, *Taq* DNA polymerase kits of different suppliers (QIAGEN, Sigma, Invitrogen, Roche) were used. Usually the reaction was performed in a final volume of 20 µl.

Mix for one sample:

2 µl	10 x reaction buffer
2 µl	20 mM dNTP mix
0.6 µl	25 mM MgCl ₂
1 µl	10 pM primer solution 1
1 µl	10 pM primer solution 2
1 µl	100 ng µl ⁻¹ template DNA or boiled cells
0.05 µl	<i>Taq</i> DNA polymerase
12.35 µl	dH ₂ O

For the Sigma Red *Taq* polymerase kit, both primers and template DNA were added to 8.6 µl dH₂O and 10 µl 2x Red *Taq* ready mix (see the manufacturer's instructions).

The thermal cycling profile was designed according to the elongation temperature (depending on the supplier), annealing temperature of the individual primers and the length of the expected amplification product:

Initial denaturation	2 min	95 °C	
1. Denaturation	45 s	95 °C	} 25 – 35 cycles
2. Annealing	45 s	54 – 60 °C	
3. Elongation	1 min / 1kb	72 °C	
Final elongation	10 min	72 °C	

PCR with proof-reading polymerases

Either for site directed mutagenesis using PCR products or for sequencing, a different polymerase with 3' → 5' proof-reading activity was used in order to prevent misincorporations during extension. The composition of a typical PCR mix is given below.

Mix for one sample (DAP Goldstar polymerase; Eurogentec):

5 µl	10 x Opti buffer
5 µl	20 mM dNTP mix
3.5 µl	50 mM MgCl ₂
1 µl	10 pM primer solution 1
1 µl	10 pM primer solution 2
1 µl	100 ng µl ⁻¹ template DNA
0.5 µl	DAP Goldstar polymerase
xxx µl	dH ₂ O

50 µl	

Followed by thermal cycling profile:

Initial denaturation	2 min	95 °C	
1. Denaturation	45 s	95 °C	} 25 – 35 cycles
2. Annealing	45 s	54 – 60 °C	
3. Elongation	1 min / 1kb	72 °C	
Final elongation	10 min	72 °C	

Mix for one sample (Phusion; Finnzymes):

10 µl	5 x HF or GC buffer
1 µl	20 mM dNTP mix
1.5 µl	50 mM MgCl ₂ (optional)
1 µl	10 pM primer solution 1
1 µl	10 pM primer solution 2
1 µl	100 ng µl ⁻¹ template DNA
0.5 µl	Phusion polymerase
xxx µl	dH ₂ O

50 µl	

Followed by thermal cycling profile:

Initial denaturation	30 s	98 °C	
1. Denaturation	10 s	98 °C	} 25 – 35 cycles
2. Annealing	30 s	45 – 72 °C	
3. Elongation	30 s / 1kb	72 °C	
Final elongation	10 min	72 °C	

Box PCR

The Box PCR is a PCR-based DNA fingerprinting technique for identification and discrimination of bacterial strains. Repetitive intergenic sequence elements are amplified and this results in a strain-specific DNA band pattern (fingerprint), what allows a direct strain to strain comparison. PCR products obtained by amplification with Box A1 primer were separated by 1.5 % agarose gel electrophoresis for 2 h at 140 mA.

Mix for one sample:

2 µl	10 x reaction buffer
1 µl	20 mM dNTP mix
0.8 µl	25 mM MgCl ₂
0.2 µl	100 pM Box A1 primer
4 µl	5 x Q solution
1 µl	100 ng µl ⁻¹ template DNA or boiled cells
1 µl	<i>Taq</i> DNA polymerase
10 µl	dH ₂ O

Followed by thermal cycling profile:

Initial denaturation	6 min	95 °C	} 35 cycles
1. Denaturation	1 min	94 °C	
2. Annealing	1 min	53 °C	
3. Elongation	8 min	72 °C	
Final elongation	16 min	72 °C	

Triplex PCR

The affiliation of *E. coli* isolates to the four main phylogenetic groups (ECOR A, B1, B2, and D) was based on triplex PCR (Clermont *et al.*, 2000a). In a single PCR reaction two genes (*chuA* and *yjaA*) and an anonymous DNA fragment (TspE4.C2) were amplified (standard PCR assay) and separated by 1 % agarose gel electrophoresis. ECOR group determination was done as shown in Fig. 5.

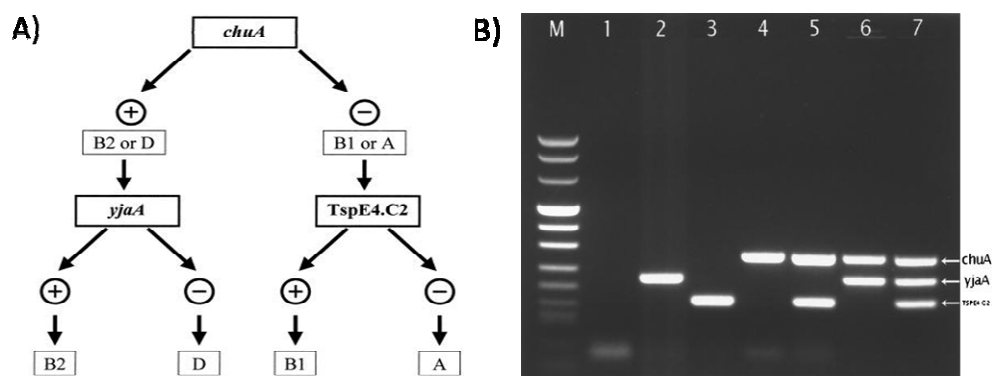


Fig. 5: A) Triplex PCR profiles specific for the four *E. coli* phylogenetic groups. Each combination of *chuA* and *yjaA* gene and DNA fragment TSPE4.C2 amplification allowed the determination of the phylogenetic group of a given strain; B) Lanes 1 and 2, ECOR group A; lane 3, ECOR group B1; lanes 4 and 5, ECOR group D; lanes 6 and 7, group ECOR B2. Lane M, DNA size marker.

Multiplex PCR

In order to detect fitness- and virulence associated genes of extraintestinal pathogenic *E. coli*, a multiplex PCR was used (Johnson and Stell, 2000). For this, 29 primer pairs according to their respective PCR product size were sorted in five pools (Fig. 6). After electrophoresis in a 2 % agarose gel, each of the PCR products was represented by a single DNA band.

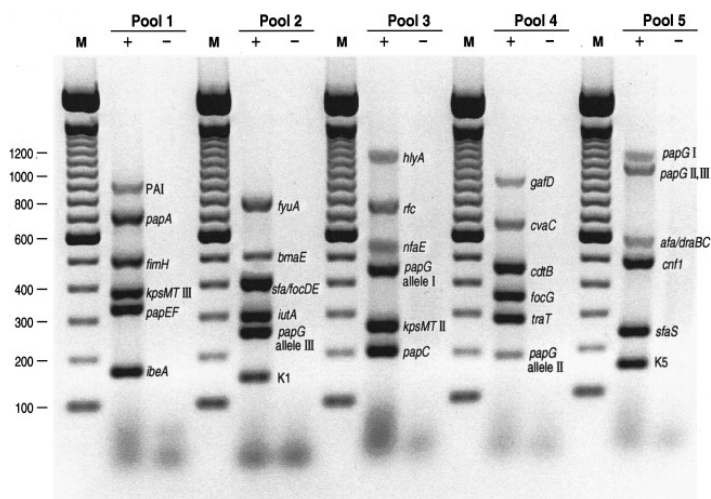


Fig. 6: Agarose gel showing PCR products from the multiplex virulence factor-PCR assay, as amplified simultaneously in 5 separate reactions using primer pools 1–5. M, molecular weight standard; +, positive control DNA; –, negative control DNA (Johnson and Stell, 2000).

Mix for one pool:

2 µl	10 x reaction buffer
2 µl	20 mM dNTP mix
1.5 µl	25 mM MgCl ₂
2.5 µl	10 pM primer mix
1 µl	boiled bacterial cells
0.5 µl	<i>Taq</i> DNA polymerase
11.5 µl	dH ₂ O

Followed by the thermal cycling profile:

Initial denaturation	5 min	95 °C	} 30 cycles
1. Denaturation	30 s	94 °C	
2. Annealing	45 s	63 °C	
3. Elongation	3 min	72 °C	
Final elongation	10 min	72 °C	

Inverse PCR (IPCR)

In order to amplify unknown DNA with the help of a small region of known DNA sequence, an inverse PCR was carried out. Amplification by IPCR of unknown DNA regions flanking a particular gene requires a previous digestion of genomic DNA and identification of the corresponding restriction fragment which contains a part of the known sequence as well as unknown flanking sequences by Southern hybridization. The size of the required fragment should not exceed 1 – 3 kb to facilitate amplification by PCR. Genomic DNA was then digested with the chosen restriction enzymes. The sample was diluted and the restriction fragments were ligated in order to obtain circular DNA fragments. PCR amplification was performed with primers complementary to the ones used for probe generation, using the circularized genomic DNA fragments as a template.

4.1.5. Sequence analysis

The nucleotide sequences of genomic DNA or plasmid constructs were determined using fluorescent dye terminators (ABI prism BigDye terminator kit, Applied Biosystems). The sequencing-PCR mix for one sample was:

30 ng	PCR product (or: 0.5 µg plasmid DNA)	
1.5 µl	10 pM primer	
2 µl	5 x buffer (kit component)	
2 µl	premix (kit component)	ad 10 µl ABI-H ₂ O

The thermal cycling profile for the PCR reaction was: 40 cycles of denaturation at 96 °C for 30 s, annealing at 60 °C for 15 s, and extension at 60 °C for 4 min, followed by final extension at 60 °C for 2 min. Sequencing products were purified by ethanol precipitation and analyzed in a ABI prism sequencer (Perkin Elmer).

4.1.6. Multi locus sequence typing (MLST)

The allocation of the isolates to different clonal lineages was done as stated on the following [website:](http://web.mpiibberlin.mpg.de/mlst/dbs/Ecoli/documents/primersColi_html)
http://web.mpiibberlin.mpg.de/mlst/dbs/Ecoli/documents/primersColi_html. Briefly,

seven house-keeping genes of being typed *E. coli* strain were amplified. The PCR reaction contained 50 ng of chromosomal DNA, 20 pmol of each primer, 200 μ mol (10 μ l of a 2 mM solution) of the dNTPs, 10 μ l of 10x PCR buffer, 5 units of proof-reading Taq polymerase and water to 100 μ l. The thermal profile was as follows: 2 min at 95 °C, 30 cycles of 1 min at 95 °C, 1 min at annealing temp, 2 min at 72 °C followed by 5 min at 72 °C. Resulted PCR products were purified and subjected to sequencing.

<i>adk</i>	adenylate kinase
<i>fumC</i>	fumarate hydratase
<i>gyrB</i>	DNA gyrase
<i>icd</i>	isocitrate/isopropylmalate dehydrogenase
<i>mdh</i>	malate dehydrogenase
<i>purA</i>	adenylosuccinate dehydrogenase
<i>recA</i>	ATP/GTP binding motif

Sequences were analyzed using Vector NTI™ software. Sequence types (STs) were assigned using the *E. coli* MLST database hosted at the Max-Planck-Institute for Infection Biology (Berlin).

4.1.7. Isolation of plasmids

While using the QIAGEN Plasmid Midi and Mini Kit, bacteria were collected from 100 ml over night cultures by centrifugation (6,000 rpm, 4 °C, 15 min) and resuspended in 4 ml buffer P1, according to the manufacturer's recommendations. After 5 min incubation at room temperature, 4 ml buffer P2 was added for lysis of the cells. After clearing of the suspension, 4 ml neutralization buffer P3 was added and samples were incubated for 10 min on ice. Cell debris and genomic DNA was removed by centrifugation (11,000 rpm, 4 °C, 30 min). Plasmid DNA containing supernatant was loaded on equilibrated columns by gravity flow. Columns were washed with buffer QC. Subsequently, plasmid DNA was eluted with 3.5 ml buffer QF and precipitated by addition of 0.7 vol isopropanol. After centrifugation (13,000 rpm, 4 °C, 20 min), DNA pellets were washed with 70 % (v/v) ethanol, air-dried and resuspended in water.

Plasmid isolation using the QIAspin mini kit were performed in a similar way with some modifications: bacteria were harvested from 1-10 ml over night cultures, buffer N3

containing guanidine hydrochloride was used for neutralization, and plasmid DNA was purified from the supernatant by using small spin columns, which were centrifuged at 13,000 rpm for 1 min DNA was eluted in a small volume of dH₂O and directly used for further experiments.

4.1.8. Enzymatic digest of DNA with restriction nucleases

The DNA was dissolved in dH₂O and mixed with 0.2 vol 10 x reaction buffer and 1 U of restriction enzyme per 1 µg of DNA. The final volume of the sample was 15 µl for plasmid DNA and 50 µl for genomic DNA. The reaction mixture was incubated 37 °C depending of the specific requirements of the enzyme (stated by supplier). Plasmid DNA was digested for one to two hours and genomic DNA at least for 3 hours, eventually overnight. When appropriate, the reaction mix was stopped by heat inactivation (20 min at 65 °C).

4.1.9. Horizontal gel electrophoresis

For routine analytical and preparative separation of DNA fragments, horizontal gel electrophoresis was performed using agarose gels under non-denaturing conditions. Depending on the size of the DNA fragments to be separated, the agarose concentration varied between 1 and 2 % (w/v) in running buffer (1 × TAE). In order to have a visible running front and to prevent diffusion of the DNA, 0.2 vol loading dye was added to the samples before loading. The electrophoresis was carried out at a voltage in the range between 16-120 V. The gels were stained in an ethidium bromide solution (10 mg ml⁻¹), washed with water and photographed under a UV-transilluminator.

50x TAE buffer:

2 M Tris
6 % (v/v) acetic acid (99.7 %)
50 mM EDTA (pH 8.0)
ad 1 l dH₂O

6x loading dye:

0.25 % Bromophenol blue
0.25 % Xylenecyanol FF
15 % Ficoll (Type 400, Pharmacia)
30 % Glycerol
ad 50 ml dH₂O

4.1.10. Plus Field Gel Electrophoresis (PFGE)

Isolation of high molecular weight genomic DNA

Bacteria were grown overnight in 10 ml LB medium at 37 °C, then 4 ml of the culture were harvested by centrifugation and the pellet was washed two times with SE buffer. After resuspending the cells in 1 ml SE, OD₆₀₀ was measured (100 µl cells + 900 µl SE buffer). When necessary, the optical density had to be adjusted in the range between 0.6 and 0.7. LGT agarose (2 %) was prepared and cooled to 45-50 °C. 900 µl of the bacterial suspension were mixed with 900 µl agarose and poured into appropriate moulds by pipetting. After solidifying, agarose blocks were cut in pieces with approximately identical size (0.5 × 0.3 × 0.1 cm), and then incubated in 5 ml NDS solution (freshly supplemented with 2 mg/ml proteinase K) overnight at 50 °C with agitation. For the complete removal of the proteinase K, the blocks were washed at least four times for 2 h with TE buffer. So prepared agarose blocks with immobilized DNA were stored at 4 °C in TE buffer for at least one week before they could be used for restriction.

SE buffer:	TE buffer:
75 mM NaCl	10 mM Tris-HCl, pH 7.5
25 mM EDTA, pH 7.5	1 mM EDTA, pH 7.5
NDS buffer:	LGT buffer:
1 % N-laurylsarcosine	10 mM Tris-HCl, pH 7.5
500 mM EDTA, pH 9.5	10 mM MgCl ₂
2 mg/ml proteinase K	0.1 mM EDTA, pH 7.5

4.1.11. Restriction of high molecular weight DNA

LGT agarose blocks containing the high molecular weight DNA were transferred into a new Eppendorf tube. Blocks were pre-incubated 1 h at 50 °C in 1 ml 1 × NEB buffer. Restriction was carried out for 3 h at 37 °C in an 150 µl overall reaction mixture containing 1 x restriction buffer and 30 U restriction enzyme, when recommended with addition of BSA.

10 × NEB buffer:
50 mM NaCl
10 mM Tris-HCl
10 mM MgCl
1 mM DTT

4.1.12. Separation of restriction fragments by gel electrophoresis

High molecular weight DNA was separated on an 0.8 % (*I-CeuI*) and 1 % (*XbaI*, *AvrI*) (w/v) agarose gel (1 × TBE buffer with 1 mM urea) by horizontal electrophoresis. The gels were run for 21-24 h with pulse periods of 0.5-50 s. After staining in an ethidium bromide solution (10 g/ml), the gels were photographed on UV-transilluminator.

4.1.13. Isolation of DNA fragments from agarose gels

DNA was purified from agarose gels using the QIAquick Gel Extraction Kit (QIAGEN). Agarose pieces containing the DNA fragment of interest were cut out of the gel and subsequently melt for 10 min at 50 °C in QG buffer (supplied by the manufacturer). The DNA was separated from the rest of the solution by applying the mixture to QIAquick spin columns followed by centrifugation for 1 min. Columns were washed with 750 µl PE buffer (supplemented with ethanol). Residual PE buffer was removed by centrifugation (2 x 1 min). Finally, DNA was by eluted from the column with 20-50 µl sterile dH₂O.

4.1.14. Ligation of DNA fragments

Linearized vector and insert DNA after restriction digest can be ligated either due to the presence of sticky ends or by blunt-end ligation. The modifying enzyme for ligation process was a T4-DNA ligase (New England Biolabs). Best efficiencies were obtained using an insert/vector ratio of 3/1. Reactions were performed over night at 16 °C in a final volume of 15 µl containing 1.5 µl 10 x ligation buffer and 50 U T4 ligase.

4.1.15. Preparation of electrocompetent cells and electroporation

50 ml LB medium were inoculated with 500 μ l bacterial overnight culture and grown until OD₆₀₀ of 0.6-0.8. The cells were collected by centrifugation for 10 min at 2,000 \times g at 4 °C. The pellet was left on ice for 30 min and then washed with 50 ml ice-cold dH₂O. After the second centrifugation step in the same conditions, pellet was resuspended in 25 ml 10 % (v/v) glycerol, centrifuged again and finally resuspended in 600 μ l of 10 % (v/v) glycerol. Cells were stored as 40 μ l aliquots at -80 °C. For electroporation, one aliquot was thawed on ice and mixed with ~ 0.5 μ g DNA. The mixture was applied into a “Gene pulser” cuvette (BioRad) with a distance between the electrodes of 0.1 cm and incubated for 10 min on ice. Cells were electroporated using a Gene pulser transfection apparatus (BioRad) at the following conditions: 2.5 kV, 25 μ F, and 600 Ω for linear fragments or 200 Ω for plasmids. Immediately after electroporation, 1 ml LB medium was added to the cuvettes. The mixture was transferred into a new tube and incubated at 37 °C (or 30 °C for temperature-sensitive plasmids) for 1 h before the cells were plated on selective agar.

4.1.16 Gene inactivation by λ Red recombinase-mediated mutagenesis using linear DNA fragments

The construction of the mutants was performed using linear DNA for recombination, as described by Datsenko and Wanner (Datsenko and Wanner, 2000). This method relies on the replacement of a chromosomal sequence with an antibiotic marker that is generated by PCR using primers with homology extensions to the flanking regions of the target sequence. Recombination is mediated by the Red recombinase derived from the λ phage. This recombination system consists of three genes (γ , β , *exo*), which encode the phage recombinases and an inhibitor of the host RecBCD exonuclease V, which normally mediates degradation of linear DNA in the cell. A schematic overview of the procedure is depicted in Fig. 7.

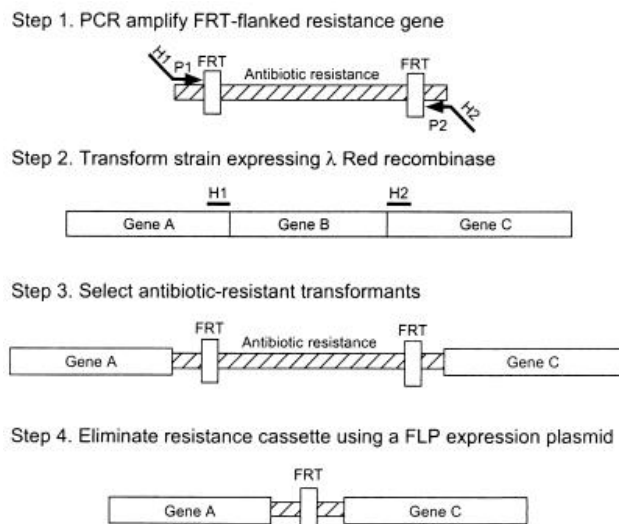


Fig. 7: Strategy for inactivation of chromosomal genes using PCR products (Datsenko and Wanner, 2000).

Meanwhile, bacterial cells were first transformed with the pKD46 helper plasmid by electroporation. Transformants were selected at 30 °C on agar plates containing 100 µg ml⁻¹ ampicillin. Of these transformants, electrocompetent cells were prepared from 50 ml LB cultures supplemented with ampicillin and 3 ml of a 0.1 M arabinose solution to induce the Red recombinase on the helper plasmid. 40 µl competent cells were transformed with 5 µl of the linear PCR fragment by electroporation. After the addition of 1 ml LB medium to the cuvette, cells were allowed to recover by incubation for 2 h at 30 °C with aeration. In contrast to normal electroporation, the cultures were then taken out of the incubator and left standing on the bench top over night at room temperature. On the next morning, cells were spun down, resuspended in 300 µl LB medium and distributed onto three agar plates supplemented with the appropriate antibiotic (Cm or Km, respectively). Transformants with confirmed allelic exchange were also re-streaked onto ampicillin-containing agar plates at 37 °C to confirm loss of the temperature-sensitive helper plasmid pKD46.

The antibiotic marker could be removed with the help of the FLP recombinase (encoded on plasmid pCP20), which mediates recombination between the two FRT sites flanking the antibiotic cassette, thus leaving behind a complete deletion of the open reading frame. Electroporation was performed as described in section 4.1.15. Transformants were first selected on ampicillin-containing agar plates at 30 °C, and then re-streaked onto LB agar

plates with no antibiotic. These plates were incubated at 37 °C in order to induce the loss of the second helper plasmid pCP20. The deletion mutants now could be used to introduce a second or third mutation by starting the whole procedure from the beginning. All mutations were confirmed by both PCR and Southern hybridization.

4.1.17. Southern Blot analysis

Vacuum blotting

For Southern blot analysis, 10 µg chromosomal DNA were restricted with an appropriate endonuclease, harboring 1 to 5-kb DNA fragments containing the target gene. The DNA fragments were separated by horizontal gel electrophoresis. Meanwhile, a nylon membrane (Nytran Super Charge; pore size 0.45 µm; Schleicher&Schuell, Dassel, Germany) of appropriate size was shortly preincubated in dH₂O and then soaked for 10 min in 20 × SSC. Afterwards, DNA was transferred from the agarose gel to the membrane using a vacuum blotter (Amersham-Pharmacia) by applying a 50 mbar vacuum. The following solutions were applied on the surface of the agarose gel during the blotting procedure:

Depurination solution (0.25 N HCl)	8 min
Denaturation solution (0.5 N NaOH; 1.5 M NaCl)	8 min
Neutralization solution (0.5 M Tris-HCl, pH 7.5; 1.5M NaCl)	8 min
20 × SSC (0.3 M Na-citrate, pH 7.0; 3 M NaCl)	>50min

After DNA transfer, the nylon membrane was incubated for 1 min in 0.4 N NaOH and 1 min in 0.25 M Tris-HCl, pH 7.5 for neutralization. The membrane was then shortly dried and the DNA was crosslinked to the membrane by exposure to UV light.

Probe labelling (ECLTM Kit, Amersham Biosciences)

For labelling of DNA probes, the ECLTM-Kit (enhanced chemoluminescence) was used. The binding of a DNA probe to the complementary sequence on the nylon membrane was detected by chemoluminescence. Positively charged horseradish peroxidase molecules were mixed with the negatively charged DNA probe. Addition of glutaraldehyde covalently linked the horseradish peroxidase molecules with the DNA probes. Reduction of H₂O₂ by the peroxidase requires the oxidation of luminol which results in light emission, which can be detected by suitable light-sensitive films, e.g. the Hyperfilm ECL. For labeling of the probe, 100 ng DNA per ml hybridization buffer in a final volume of 10 µl in dH₂O were denatured for 10 min at 90 °C and cooled for 5 min on ice. Subsequently, 10 µl labelling reagent and 10 µl glutaraldehyde were added. The mixture was incubated for 10 min at 37 °C and then added to the hybridization reaction.

Hybridization and detection of the membrane

Hybridization of the membrane was carried out over night at 42 °C in hybridization solution (10-15 ml), after the nylon membrane had been pre-incubated at 42 °C in the hybridization solution for 1 h. The next day, the membrane was washed twice for 20 min at 55 °C with wash solution I and two times for 10 min at RT with wash solution II. The membrane was placed on Whatman paper to remove the rest of the wash solution, and then incubated for 5 min in 5-10 ml detection solution I and detection solution II provided with the kit and mixed immediately (1:1) before application to the membrane. The membrane was superficially dried on Whatman paper and packed in saran wrap avoiding air bubbles on the top surface of the membrane. Chemoluminescence was detected by exposure of the membrane to Hyperfilm ECL. The exposure time depended on the signal intensity.

Wash solution 1: 0.5 × SSC; 0.4 % (w/v) SDS

Wash solution 2: 2 × SSC

4.1.18. Comparative Genome Hybridization

Membrane Layout

For genomes comparison, an *E. coli* K12-specific array (Panorama *E. coli* gene arrays from Sigma-Genosys, Cambridge, United Kingdom) and the *E. coli* “pathoarray” (Dobrindt *et al.*, 2003) were used in combination. Therefore, by using both types of arrays, it was possible to estimate and compare the genomic content of different ABU strains.

Probes synthesis

2 µg of total genomic DNA (see section 4.1.1.) was used as a template for direct incorporation of [³³P]-dATP (Amersham Pharmacia, Freiburg, Germany) by a randomly primed polymerization reaction using 0.75 µg random hexamer primers (New England Biolabs, Frankfurt (Main), Germany) and 10 U Klenow fragment of the DNA polymerase I (New England Biolabs) according to manufacturer’s recommendations. Unincorporated nucleotides were removed with Microspin S 200 HR spin columns (Amersham Pharmacia). Incorporation rates of labelled nucleotides were determined by measuring radioactivity of the cDNA in the eluate (equals incorporated radionucleotides) and of the radioactivity retained in the column (equals unincorporated radionucleotides).

$$\text{Incorporation rate} = \frac{\text{radioactive count (eluate)}}{\text{radioactive count (column + eluate)}} \times 100 \%$$

The obtained value can be used as a marker for the quality of reverse transcription and should be > 50 %.

Hybridization and detection

Hybridization of the labelled DNA to the membranes was performed as recommended in the technical protocol for the Panorama *E. coli* K-12 array (Sigma Genosys). After 10 min denaturation at 93 °C in hybridization buffer, labelled DNA was added to the pre-hybridized membranes and incubated for 16 h at 65 °C in a hybridization oven.

Membranes were washed three times for 3 min in washing solution at room temperature, followed by three additional washing steps for 20 min at 65 °C. After washing, the membranes were sealed in plastic film and exposed to a PhosphoImager screen (Molecular Dynamics) for 48 h. Membranes could be re-used up to 10 times after stripping (see Panorama-Array manual).

Hybridization buffer:

5 x SSPE

2 % SDS

1 x Denhardt's reagent

100 µg ml⁻¹ sonicated, denatured salmon testes DNA

Washing solution:

0.5 x SSPE

0.2 % SDS

20 x SSPE:

3.6 M NaCl

0.2 M NaH₂(PO₄); pH 7.7

20 mM EDTA

100 x Denhardt's reagent:

% Ficoll (MW 400,000)

2 % polyvinylpyrrolidone

2 % BSA

Quantification of hybridization signals

Exposed PhosphoImager screens were scanned on a Typhoon 8600 variable mode imager (Molecular Dynamics) at 50 µm resolution. Spot intensities were measured with the ArrayVision software (Imaging Research, St. Catharines, Canada) using the overall spot normalization function of the program (Table 6).

Table 6: Parameters of the ArrayVision pre-set protocols (Wizard) used for reading intensity values.

Parameter	<i>E. coli</i> K-12 array	<i>E. coli</i> pathoarray
Array type	Radio-isotopic array	Radio-isotopic array
Analysis type	Detection	Detection
# of arrays	4	4
# of extra channels	1	1
Measure type	MTM density	MTM density
Array organization (spots)	3 levels (18432 total spots)	2 levels (1536 total spots)
Level 1 (Spots)	4 x 4	4 x 4
Level 2 (Spot groups)	16 x 24	8 x 12
Level 3 (sub-arrays)	3 x 1	-
Spot shape	Circle	Circle
Start position	Defined	Not defined
Alignment	Not aligned	Not aligned
Labels	Custom	Custom
Replication	On	On
Background	Corners between spots (average)	Corners between spots (average)
Reference	All spots	All spots
Segmentation:	Off	Off
Anchors:	None	None

Data analysis

For each strain three independent hybridizations were performed. Mean values were calculated from the duplicate spots of the each gene in all three arrays. The mean of the normalized intensity values of the duplicate spots of each gene was used for further analysis. To avoid extreme intensity ratios for genes close to or below the detection limit, signal intensity values corresponding to a signal to noise (S/N) ratio <1.0 were scaled up to a value corresponding to an S/N ratio=1.0. ORFs were recorded as lacking/not detectable if the S/N ratio was below 1.0 in at least two of the three hybridization experiments. In addition, *E. coli* K-12 strain MG1655-specific ORFs were recorded as lacking/not detectable if the ratio of the individual S/N ratios of the analyzed strain and that of the reference strain MG1655 was <0.3 in at least two of three experiments. The missing/not detectable ORFs were then aligned with their chromosomal location to determine the number and the size of chromosomal regions absent in the different *E. coli* strain. In addition, the fact that the ORFs are arranged on the DNA macroarrays without regard to their chromosomal localization minimizes the record of false negative spots, at least with respect to regions consisting of more than one gene, because the probability

that two adjacent ORFs would be recorded as absent due to hybridization artifacts is very low. Multiple positive signals for single genes were verified by PCR.

Hierarchical cluster analysis of the hybridization data was performed with the CLUSTER software (Eisen *et al.*, 1998) based on the presence or absence of genes. Red and black denote the presence or absence of ORFs, respectively. The output was displayed with the software TREEVIEW (Eisen *et al.*, 1998).

4.2. Working with RNA

For RNA work, special care had to be taken in order to prevent contamination of the samples with exogenous RNases. Gloves were worn throughout the whole experiment and RNase free pipette tips and reaction tubes were used. For all buffers and solutions, water was pre-treated over night with 0.1 % (v/v) diethylpyrocarbonate (DEPC) at 37 °C and autoclaved twice to remove remaining DEPC.

4.2.1. Isolation of total RNA with RNeasy Kit

RNA was isolated using the RNeasy Mini kit (QIAGEN) according to the supplied protocol. All subsequent steps of the RNeasy protocol were performed at room temperature. For RNA isolation bacteria were grown at 37 °C in 125 ml of pooled human urine until the optical density OD₆₀₀ reached 0.15. For RNA isolation from Luria Broth (LB) cultures, bacteria were grown without agitation at 37 °C in 25 ml until the OD₆₀₀ reached 0.6. 50 ml of the urine culture and 4 ml of the LB culture were taken and centrifuged at 6000 rpm for 5 min. The supernatant was removed and pellets were resuspended in 20 ml (urine culture) and 4 ml (LB culture) of PBS and RNeasy Protect Qiagen 1:1 (v/v), respectively. Samples were incubated at room temperature (RT) for 5 min and centrifuged at 6000 rpm for 10 min. Bacterial pellets were either stored at -80 °C or bacterial RNA was immediately isolated. In the second case, bacterial pellets were resuspended thoroughly in 100 µl of lysozyme-containing TE buffer (50 mg/ml) and incubated at 37 °C for 5 s with vortexing every 2 min. The following steps of the protocol are consistent with those of the protocol supplied with the RNeasy Mini kit.

4.2.2. Removal of contaminating DNA by DNase treatment and RNA cleanup

Contaminating DNA was removed from total RNA preparations by DNase I digestion. 15 µg RNA in a final volume of 85 µl were mixed with 10 µl 10 x DNase I buffer and 10 µl RNase-free DNase I (New England Biolabs). Samples were incubated for 1 h at 37 °C, followed by RNA cleanup using the RNeasy Mini kit (QIAGEN). According to the manufacturer's instructions, 350 µl RLT buffer supplemented with 10 µl β-mercaptoethanol and 250 µl 100 % (v/v) ethanol were added to the DNase-treated RNA samples, before loading them onto the purification columns. After brief centrifugation, the columns were transferred to fresh collection tubes and washed twice with 500 µl RPE buffer. Finally, RNA was eluted from the column in 30 µl nuclease-free water.

As a control for successful DNA removal, 2 µl of the DNase-treated RNA or 1 µl DNA as positive control were used as a template in a PCR reaction with primers binding within the coding sequence of the *fimA* gene. The DNase digest was considered as complete if no product could be amplified from the RNA samples.

4.2.3. Reverse transcription (RT) for cDNA synthesis

For cDNA synthesis, the Superscript III reverse transcription kit (Invitrogen) was used. 2 µg of total RNA in a final volume of 10 µl were mixed with 1 µg of random hexamer primers (Amersham Biosciences). Primer annealing was carried out at 65 °C for 5 min. After 5 min cooling, 9 µl of a reverse transcription mixture were added to the samples. The composition of the RT-mix for 1 sample was:

- 1 µl 25 mM deoxynucleotide mix
- 1 µl 0.1 M dithiothreitol (DTT; kit component)
- 4 µl 5 x first strand buffer (kit component)
- 1 µl 40 U µl⁻¹ RNase OUT recombinant RNase inhibitor (Invitrogen)
- 1 µl 200 U µl⁻¹ Superscript III reverse transcriptase (kit component)

cDNA synthesis was performed at 52 °C for 60 min, followed by heat inactivation of the transcriptase at 70 °C for 15 min.

4.2.4. Quantitative Real-Time PCR

To evaluate expression of single genes, a quantitative Real-Time PCR (qRT-PCR) approach was used. This method employs polymerase chain reaction to amplify gene transcripts in presence of the SYBR Green I dye (BioRad). This fluorescent dye intercalates into double stranded DNA and emits signals collected by the optical camera within the MyiQ cycler (BioRad). The number of cycles needed to reach a certain fluorescent signal threshold (CT) was used to calculate transcript levels. Primers for selected genes were designed using the FastPCR software (Ruslan Kalendar, Institute for Biotechnology, University of Helsinki, Finland) with the following parameters: product length range from 190 to 300 nt; annealing temperature 57 - 59 °C. Before their use for expression profiling, the different primer pairs were checked for amplification efficiency with pooled cDNA from different experiments. Only primer pairs with an amplification efficiency of at least 90 % were used. For copy number estimation, cDNA samples derived from the reverse transcription reaction were 100-fold diluted in dH₂O and the reaction mix was prepared (for one reaction) as follows:

12.0 µl	cDNA
12.5 µl	SYBR Green Mix 2 ×
0.25 µl	Primer 1 (10 µmol)
0.25 µl	Primer 2 (10 µmol)

With following thermal cycling profile:

3 min 95 °C
30 s 95 °C
30 s 60 °C – 40 cycles
20 s 72 °C
30 s 95 °C – 57 °C (melting curve)

All PCR reactions were done in triplicates in three independent experiments. To be able to compare transcript levels from different RNA preparations, the *rrnB* gene encoding for 16 S RNA was used as an internal control.

4.2.5. Expression profiling using DNA arrays

Expression profiling is a technique to study the relative amounts of all transcripts at a given time of sample collection, thereby allowing to monitor the expression level of every single gene detectable by the array.

Array Layout

For expression profiling oligonucleotide glass microarrays (Operon Biotechnologies, Inc.) were used. A single Operon *E. coli* Custom 55156017 array contains 10816 longmer oligonucleotide probes covering the complete genomes of six *Escherichia coli* strains (6 genomes and four plasmids). The number of open reading frames (ORFs) or genes represented is as follows: 4269 ORFs of non-pathogenic *E. coli* K-12 strain MG1655, 5306 ORFs of enterohemorrhagic *E. coli* O157:H7 strain EDL933, 5251 ORFs of enterohemorrhagic *E. coli* O157:H7 strain Sakai, 5366 ORFs of uropathogenic *E. coli* strain CFT073, 322 ORFs of uropathogenic *E. coli* strain 536, 448 ORFs of uropathogenic *E. coli* strain UTI89, 3 genes of EHEC plasmid OSAK1, 10 genes of EHEC plasmid pO157_Sakai, 97 genes of EHEC plasmid pO157_EDL933 and genes of UPEC plasmid pUTI89. In addition, the array comprises also a number of positive and negative controls. Each probe contains an amino linker at the 5' end. Probes are spotted as single spots in 32 blogs (4 columns, 8 rows), each blog with 18 columns x 19 rows.

RNA isolation and cDNA labelling

Total RNA was prepared from mid-log phase cultures grown in urine at 37 °C followed by DNase treatment, as described in section 4.2.2. All procedures involving fluorescent dyes had to be done quickly and by avoiding exposure to light because of photosensitivity. All solutions were prepared with DEPC-treated water. All experiments were done in triplicates including the overnight culture.

Reverse transcription was performed using SuperScript IIITM reverse transcriptase (Invitrogen) and the fluorescently labelled nucleotides Cy3- and Cy5-dCTP (Amersham Pharmacia, Freiburg, Germany). For primer annealing, 10 µg total RNA were mixed with 1 µg of hexamer oligos in a total volume of 15 µl. The annealing mix was heated for 10 minutes at 70 °C, then cooled down to room temperature for 5 min followed by brief centrifugation. In the meantime, the reaction mix was prepared:

<u>Reaction mix:</u>	<u>1 reaction</u>
5x first strand buffer	8 μ l
0.1x DTT	4 μ l
Nucleotide mastermix	4 μ l
RNaseOut	1 μ l
SuperScript III TM (200 U/ μ l)	1 μ l
RNase free H ₂ O	4 μ l

Then, 22 μ l of the reaction mix was pipetted into a small PCR reaction tube together with 15 μ l annealing mix and 4 μ l Cy3- or Cy5-dCTP (1 mM) was added. The total mix 41 μ l was incubated for 1h at 46 °C in the thermoblock of a thermocycler. After 25 min, another 1 μ l of SuperScript IIITM reverse transcriptase (200 U/ μ l) was added. The reaction was stopped by addition of 5 μ l EDTA (500 mM) and to hydrolyze RNA, 10 μ l NaOH (1 M) was added, followed by incubation at 65 °C for 15 min. The reaction mixture was cooled down to room temperature and 25 μ l Tris-HCl (1M, pH 7.5) was added.

Labelled targets were purified using the Qiaquick PCR Purification Kit (Qiagen) according to the manufacturer's instructions with minor changes: Briefly, 5 volumes of PB buffer were added, the sample applied to column and centrifuged at max speed for 30 s. The column was then washed with 700 μ l PE buffer and dried by centrifugation. cDNA was eluted in 30 μ l dH₂O. Of this, 1 μ l was taken for quality control and quantification using the NanoDrop photometer. The remaining cDNA was dried using a vaccum centrifuge. The cDNA pellet was resuspended in 2 μ l dH₂O.

Array pre-hybridisation

Arrays were cleaned by compressed air from dust particles and pre-hybridised in pre-warmed OPArray Pre-Hyb solution at 42 °C for 1 h. During that time Wash Solution 1 was prepared by diluting OpArray Wash B 1:40 (v/v) with chromatography grade H₂O. Arrays were washed for 5 min at 20-25 °C and immediately transferred to a box with sterile H₂O, rinsed for 30 seconds. This step was repeated twice. The slides were dried in Falcon tubes with a hole in the bottom by centrifugation at 1200 rpm for 10 min. Residual liquid was removed by compressed air.

Array hybridisation

The hybridization chamber was rinsed with sterile dH₂O and dried thoroughly. In the four corners of the chamber, 15 µl of sterile dH₂O were added in order to keep the humidity during hybridisation time. The OpArray was placed into the chamber with the DNA side up (barcode side up) and the spotted area was covered with a LifterSlip. Cy5- and Cy3-labelled targets were mixed with 36 µl of OpArray Hyb Buffer, denatured at 65 °C for 5 min and then applied slowly to one end of the LifterSlip in order to disperse across the OpArray surface. The hybridization chamber was closed and the arrays were incubated in a water bath at 42 °C for 14-16 hours.

Post-Hybridization washing

For Post-Hybridization washing following solutions were used:

Wash Solution 2:

50 ml OpArray Wash A

25 ml OpArray Wash B

Bring Wash Solution 2 final volume to 500 ml with sterile dH₂O

Wash Solution 3:

50 ml OpArray Wash A

Bring Wash Solution 3 final volume to 500 ml with sterile dH₂O

Wash Solution 4:

5 ml OpArray Wash A

Bring Wash Solution 4 final volume to 500 ml with sterile dH₂O

After hybridisation was completed, arrays were washed in pre-warmed Wash Solution 2 at 42 °C for 10 min, transferred to Wash Solution 3 and shaken for another 10 min at RT. Subsequently, arrays were washed twice in Wash Solution 4 at RT for 5 min. Alike in the pre-

hybridisation step, drying was done by centrifugation of the array in Falcon tubes for 10 min and then the arrays were immediately scanned.

Scanning

Hybridised and washed slides were scanned using a GenePix Model 4000B Microarray Scanner (Axon Instruments Inc., Union City, CA 94587, USA) with a resolution of 5 μm pixel size. The excitation frequencies of the two lasers were 532 nm and 635 nm. The gain settings for the photomultiplier tubes were adjusted to use the entire dynamic range of the instrument and to get comparable fluorescence yields in both channels. Images of Cy3 and Cy5 signals were recorded as 2 layer 16bit TIFF files and analysed using the GenePix Pro 6.0 software.

Data analysis

For each experiment, at least three independent hybridizations were performed, one with a dye switch. After removal of bad quality spots (if less than 70 % of foreground pixels were below background intensity plus 2 standard deviations in both channels or if the signal to noise ratio were below 3 in both channels or if the difference between ratio of medians and regression ratio exceeded 20 % in one of the channels) the remaining intensities were saved as gpr output data files. For statistical validation and further analysis the Acuity 4.0 (Molecular Devices, USA) software was used. For all data, the local background was subtracted from the intensity values of each spot on the array and normalized by both linear ratio-based methods and non-linear lowess including print-tip groups. For statistical significance, one sample t-test was applied and the resulting data set was exported to Microsoft Excel. Hierarchical clustering of genes for visualisation of expression patterns was performed with the CLUSTER software (Eisen *et al.*, 1998). The output was displayed with the software TREEVIEW (Eisen *et al.*, 1998).

For data analysis, a cut-off value of 1.7 was used although the commonly used threshold value is twofold (DeRisi *et al.*, 1997; Wildsmith and Elcock, 2001). Several studies have shown that a lower cut-off ranging from 1.4 to 1.74 can be used reliably if the results are reproducible in more replicates (Perez-Amador *et al.*, 2001).

4.3. 2D protein gel electrophoresis

4.3.1. Isolation of intracellular proteins and rehydration

Bacteria were grown at 37 °C without agitation in 400 ml of pooled human urine until OD₆₀₀ = 0.2 and harvested by centrifugation (10,000 X g, 10 min, 4°C). Pellets were washed three times with decreasing volumes of TE buffer (1 x 50 ml TE, 1 x 25 ml TE, 1 x 10 ml TE) and were then resuspended in 700 µl TE buffer. Cell lysis was done using the FastPrep (MP™) device twice for 30 s at 5.5 x g with an incubation on ice for 1 min in between, followed by a two-step centrifugation for 10 min at 13,000 rpm at 4 °C. The supernatant was each time transferred into a fresh Eppendorf tube. The isolated intracellular proteins were frozen at -80 °C or used immediately for 2D gel electrophoresis.

300 µg of proteins were passively rehydrated on 17-cm, pH 4 to 7 immobilized pH gradient strips (Amersham Biosciences) in 330 µl of rehydration buffer in a total volume of 350 µl. When needed, the vacuum centrifuge was used to increase the protein concentration of the samples.

Rehydration Buffer:

0.76 g	1.5 M Thiourea
2.4 g	8 M Urea
50 mg	1 % 3-[(3-Cholamidopropyl)dimethylammonio]-1 propansulfonat (CHAPS)
50 mg	12.9 mM DTT
26 µl	0.04 % Pharmalyte™ 3-10 for IEF
<u>xxx ml</u>	<u>H₂O</u>
5 ml	

4.3.2. Isolation of outer membrane proteins and rehydration

Bacteria were grown in 800 ml of pooled human urine at 37 °C in 2 l flasks, without agitation until OD₆₀₀ = 0.2 and harvested by centrifugation (10,000 x g, 10 min, 4 °C). Pellets were washed and resuspended in 10 ml of 10 mM HEPES, pH 7.0, containing 250 U of benzoic acid ultrapur nucleic acid (Sigma) and 400 µl of 25x complete EDTA-free protease inhibitor stock solution (Roche, # 11873580001). Following four passages through the chilled French

pressure cell at 15,000 psm, lysates were centrifuged (6000 x g, 10 min, 4 °C) to remove unbroken cells and cell debris, the supernatants were diluted to 60 ml with 0.1 M carbonate buffer, pH 11, and incubated with stirring at 4 °C for 1 h. Carbonate-insoluble membranes were collected by ultracentrifugation (120,000 x g for 1 h at 4 °C). The resulting outer membrane pellet was rinsed with 10 mM HEPES, pH 7.0 and solubilized in 800 µl rehydration solution I at room temperature for 30-60 min. Soluble OMPs were quantified using the Roti® Nanoquant solution (Roth) and either immediately used for 2D gel electrophoresis or stored at -80°C.

4.3.3. Determination of protein concentrations

Protein concentrations were determined using the Roti-Nanoquant solution (Roth) following the manufacturer's instructions. 200 µl protein samples were mixed with 800 µl 1 x assay solution, and absorbance was measured at 590 nm and 450 nm. Protein concentrations were then calculated using the following formula (based on a bovine serum albumin (BSA) calibration curve):

$$\mu\text{g protein} = \frac{A_{590\text{nm}} / A_{450\text{nm}} - 0.4475}{0.1132}$$

4.3.4. Protein rehydration

17-cm, pH 4 to 7 immobilized pH gradient strips (Amersham Biosciences) were passively rehydrated overnight with 300 µg of outer membrane proteins in 315 µl rehydration solution-I and 35µl rehydration solution-II .

Rehydration solution-I:

1.52 g 1,5 M Thiourea

4.8 g 8 M Urea

xxx ml H₂O

10 ml

Rehydration solution-II (10X):

50 mg	1% 3-[(3-Cholamidopropyl)dimethylammonio]-1 propansulfonat (CHAPS)
50 mg	12.9 mM DTT
26 µl	0.04% Pharmalyte™ 3-10 for IEF
474 µl	H ₂ O

4.3.5. Isoelectric focusing (IEF)

During this step proteins were separated according to their isoelectric points (pI). The pI is the pH at which a protein will not migrate in an electric field and is determined by the charged groups in the protein. Proteins can carry positive, negative or no charge depending on their local pH, and for every protein there is a specific pH at which its net charge is zero; this is their isoelectric point. pI's generally fall in the range of 3 to 12, with most being between 4 to 7. When a protein is placed in a medium with a pH gradient and subjected to an electric field, it will initially move towards the electrode with the opposite charge. During migration through the pH gradient, the protein will pick up or lose protons. As it migrates, the net charge and the mobility will decrease and the protein will slow down. Eventually the protein will arrive at the point in the pH gradient which is equal to its pI. Here, it will be uncharged and hence stop migration. If the protein should happen to diffuse to a region outside its pI it will pick up a charge and hence move back to the position where its charge is neutral. In this way proteins are focused into sharp bands.

Rehydrated IPG strips were placed with the plus mark to the anode in a Protean IEF Multiphor cell. On both ends of the strips connecting papers soaked with water were placed. The IPG strips were placed in cover oil. Isoelectric focussing was performed with a 500-V linear ramp for 1 h, a 1000-V linear ramp for 1 h, and a 3500-V rapid ramp for 22 h. During the run, the connecting papers were exchanged 3 to 4 times in order to improve protein separation.

4.3.6. Equilibration

An equilibration step is necessary to saturate the IPG strip with SDS buffer system before the second dimension separation. Equilibration is a multi-step process to ensure that the proteins are suitable for SDS-PAGE analysis. This ensures that the strip has the correct pH suitable for

subsequent analysis and preserves the fully denatured state of the protein. Glycerol ensures that the proteins are adequately transferred from the first to the second dimension and reduces electroendosmosis in the buffer upon application of the electrical field. Electroendosmosis is the movement of buffer within the IPG (immobilized pH gradient) strip and is due to the fixed charge associated with the ampholytes present in the strip. Electroendosmosis can interfere with protein transfer from the IPG strip to the second dimension. A second equilibration alkylates any thiol groups in the protein preventing their reoxidation. Reoxidation can result in protein smears within the gel. It also alkylates any remaining DTT to prevent smears of proteins and other artefacts which may occur during protein staining within the gel.

Prior to separation in a second-dimension, the immobilized pH gradient strips were subsequently equilibrated in 50 ml equilibration buffer-I and 50 ml equilibration buffer-II each time for 25 min under gentle agitation.

Preparation of equilibration buffers:

Basic buffer composition (100 ml):

3.3 ml	1.5 M Tris-HCL pH 8.8
36 g	6 M Urea
30 ml	30 % Glycerol (87 %)
4.0 g	4 % SDS
xxx	H ₂ O

The solution can be stored in aliquots in 50 ml Falcon tubes at -20 °C.

Equilibration buffer-I:

300 mg	38.9 mM DTT
50 ml	Basic buffer

Equilibration buffer-II:

2.25 g	24.3 mM iodacetamid
a few crystals	Bromophenol blue
50 ml	Basic buffer

4.3.7. Second dimension - separation based on size

Proteins were subsequently separated on the basis of their molecular mass using sodium dodecyl sulphate polyacrylamide gel electrophoresis (SDS-PAGE). SDS binds to most proteins in a constant fashion (about 1.4 grams of SDS per gram of protein) and also masks any charge of the protein by forming large anionic complexes. SDS also disrupts any hydrogen bonds, blocks many hydrophobic interactions and partially unfolds the protein molecules minimising differences based on secondary or tertiary structure. Proteins move through the gel towards the anode during electrophoresis. The rate at which they move is inversely proportional to their molecular mass.

Equilibrated IPG stripes with proteins resolved in the first dimension were applied to a second dimension gel and covered by 1 % agarose in 2 x electrophoresis buffer avoiding air bubbles. The lower electrophoresis unit was filled in with 1 x electrophoresis buffer and the upper unit with 2 x electrophoresis buffer. Second dimension separation was performed overnight at 6 - 12 Watt (400 V, 300 mA).

Polyacrylamide gel 12.5 % (6 gels, 400 ml)

66 ml	H ₂ O
162 ml	Acrylamide A 30 %
68 ml	Acrylamide B 2 %
100 ml	1.5 M Tris-HCl pH 8.8
4 ml	10 % SDS
1 ml	10 % Ammonium persulfate (APS)
200 µl	N,N,N',N'-tetramethyldiamin (TEMED)

10 x Electrophoresis Buffer (1 l)

30.3 g	Tris
144 g	Glycin
10 g	SDS
xxx	H ₂ O

4.3.8. Proteins staining

After the second dimension, the gels were fixed by incubation for 1 to 2 h in fixing solution followed by washing in dH₂O (2 x 10 min). Afterwards, the gels were incubated for 24 h in a Coomassie staining solution. On the next day, gels were washed 3 x 1 h in dH₂O, wrapped in a plastic sleeve and scanned.

Coomassie staining solution (B1131 G250 Brilliant Blue, Sigma)

150 ml	H ₂ O
100 g	10 % Ammonium sulphate
100 ml	10 % H ₃ PO ₄ (85 %)
1.2 g	0.12 % G250 Brilliant Blue
200 ml	20 % EtOH (100 %)
550 ml	H ₂ O

Fixation Solution (2 l)

800 ml	40 % Ethanol (100 %)
400 ml	20 % Acetic Acid (100 %)
800 ml	H ₂ O

4.3.9. Analysis of 2-D Gels with the Delta-2D® Software (Decodon)

The image analysis was performed with the Delta-2D® Software (<http://www.decodon.com>), which is based on dual-channel image system. Before, gels were scanned and saved as a gray scale TIFF image. An overlay of two wrapped 2-D gels was visualized by either green, red or yellow false colour code representing proteins expressed in the wild type, the mutant, or in both strains, respectively. In addition, a statistical analysis was performed based on spot intensities from at least 3 gel replicates.

4.3.10. Protein identification by MALDI-TOF-MS

In order to identify proteins separated during the 2-D electrophoresis, gels were washed in dH₂O for 1 h followed by spot excision. Gel pieces with a diameter not bigger than 2 mm

from different parts of the spot were subjected to MALDI-TOF-MS (Matrix-Assisted Laser Desorption-Ionization – Time Of Flight Mass Spectrometer) at the Institute for Microbiology and Molecular Biology of the University of Greifswald. Proteins were digested with trypsin, mixed with a matrix solution and allowed to co-crystallise on a target plate. Laser-pulsed voltage was applied to the target plate to accelerate the ionised sample towards a time-of-flight mass analyser. This peptide mass fingerprint was used to search databases to identify the protein.

4.4. Analysis of lipopolysaccharides (LPS)

4.4.1. Isolation of LPS

For analysis of the LPS composition, cells from an agar plate or pellets of liquid cultures were used. After weight measurement, the cells were resuspended in an adequate amount of water so that the concentration was 1 mg cells per 30 µl suspension. 30 µl samples (i.e. 1 mg cells) were mixed with 10 µl 4 x SDS-sample buffer and incubated at 100 °C for 10 min. After brief cooling, 20 µl 1 x SDS-sample buffer supplemented with 100 µg proteinase K were added to the samples, which then were incubated at 60 °C for 1 h for removal of proteins. 30 µl of the LPS preparations were used for electrophoresis.

4.4.2. Electrophoresis and staining with silver nitrate

Separation of the LPS components was performed by denaturing polyacrylamide gelelectrophoresis (Tsai and Frasch, 1982). The acrylamide gel consists of two parts: a lower part mediating the separation, and an upper part, which is used for concentration of the sample in a single running front after entering the gel. 15 % separation gels were used in a format of 20 x 20 cm, and electrophoresis was carried out over night at 8 mA at room temperature. The gel composition was:

15 % Separation gel:	15 ml 30 % acrylamide:bis-acrylamide (37.5:1)
	5 ml 1.5 M Tris-HCl, pH 8.8
	10 ml dH ₂ O
	300 µl 10 % (w/v) SDS
	250 µl 10 % (w/v) Ammonium persulfate (APS)
	8 µl TEMED

5 % Collecting gel:	1.96 ml 30 % Acrylamide:bis-acrylamide (37.5:1)
	2.8 ml 0.5 M Tris-HCl, pH 6.8
	4.6 ml dH ₂ O
	112 µl 10 % (w/v) SDS
	32 µl 10 % (w/v) APS
	16 µl TEMED
10 x Running buffer:	30 g Tris
	144 g Glycine
	10 g solid SDS
	ad 1 l dH ₂ O
4 x SDS-loading buffer:	2.5 ml 1 M Tris-HCl, pH 6.8
	4 ml 50 % (v/v) glycerol
	0.8 g solid SDS
	0.1 ml β-mercaptoethanol
	0.02 g Bromophenol blue
	ad 10 ml dH ₂ O

After electrophoresis, the polyacrylamide gels were stained with AgNO₃. All used devices were carefully washed with double-distilled water, and gloves were worn throughout the experiment. The gels were fixed over night in 100 ml 1 × fixation solution. The next day, the solution was replaced by 100 ml 1 × periodate solution and the gels were incubated for 5 min in for oxidation. Subsequently, the gels were washed three times for 30 min with dH₂O, and then incubated for 10 min in silver nitrate solution. After three more washes for 10 min with H₂O, gels were developed in developing solution preheated to 60 °C. As soon as the intensity of the appearing bands was satisfying, the reaction was stopped by incubation in 50 M EDTA solution for 10 min.

2 × fixation solution:	250 ml	Isopropanol
	70 ml	Acetic acid
	ad 500 ml in	dH ₂ O

Periodate solution:	0.87 g	Na-m-periodate (NaIO ₄)
	100 ml	1 × fixation solution
Silver nitrate solution:	1.4 ml	1 M NaOH
	1 ml	NH ₃ (33 %)
	70 ml	dH ₂ O
	1.25 ml	20 % (w/v) AgNO ₃
Developing solution:	100 ml	2.5 % (w/v) Na ₂ CO ₃
	27 µl	Formaldehyde (40%)

4.5. Phenotypic assays

4.5.1. Detection of type 1 fimbrial expression

Overnight cultures of the strains to be tested and of a positive (*E. coli* strain Nissle 1917) and of a negative (*E. coli* strain AAEC189) control were grown. The mannose-dependent yeast agglutination assay was carried out by mixing 10 µl of the different bacterial overnight cultures with 10 µl yeast cell suspension (1 mg/ml *Saccharomyces cerevisiae* cells diluted in 0.9 % (w/v) NaCl, with or without 2 % (w/v) mannose) on microscope slides (75:25:1 mm). The slides were kept on ice until the aggregation of yeast and bacterial cells was observed in absence of mannose.

4.5.2. Detection of F1C and P fimbrial expression

Overnight cultures of the strains to be tested and of a positive (*E. coli* strain Nissle 1917) and of a negative (*E. coli* strain AAEC189) control were grown. For the immunoagglutination assay, a polyclonal α-F1C or P fimbriae rabbit antibody was used (provided by Dr. S. Kahn, Würzburg), that was diluted 1:1000 in 1 × PBS. The immunoagglutination assay was carried out by mixing 10 µl of the bacterial overnight culture with 10 µl of the α-F1C or P fimbriae antibody solution on microscope slides (75:25:1 mm) and incubation on ice until the aggregation of the bacterial cells was clearly observed.

4.5.3. Detection of secreted α -hemolysin

To test hemolytic activity, cells from *E. coli* colonies were spread onto sheep blood agar plates (Oxoid) with a toothpick and incubated overnight at 37 °C. Lysis of the blood cells by α -hemolysin was detected by formation of clear halos around the colonies after incubation.

4.5.4. Detection of biofilm forming abilities

Biofilm formation was assessed in a microtiter plate assay modified after O'Toole and Kolter (1998). Bacteria were grown overnight in pooled human urine or M63 medium at 37 °C with agitation.

In M63 defined media

On the next morning, 158 μ l fresh minimal medium were distributed in a microtiter plate (8 wells per strain) and inoculated with 1.6 μ l of the overnight cultures. 96 well plates were incubated statically at 37 °C for 24 h. Subsequently, were carefully washed twice with 1 x PBS and dried for 1 h at 80 °C. Biofilm was stained with 0.1 % crystal violet for 10 min. Staining solution was discarded and plates were rinsed twice with 1 x PBS. To quantitate the biofilm formation, wells were destained with 180 μ l destaining solution (80 % ethanol / 20 % acetone) for 10 min. Remaining biofilm was dissolved by pipetting the solution up and down several times, before diluting the solution 10 times in dH₂O and measuring absorbance at 570 nm.

In pooled, sterile human urine

To assess the biofilm forming ability in human urine, 24-well flat bottom polystyrene plates (# 83.1836 SARSTEDT, Sarstedt Tissue) were used. In each well 1.5 ml sterile urine was inoculated with 15 μ l bacterial overnight culture. The plates were incubated statically at 37 °C for 24 h. Washing and staining procedure as described above.

4.6. Continuous culture of *E. coli* in microfermenters

Long term *in vitro* bacterial culture was established in order to propagate bacteria over 2000 generations (Fig. 8; Fig. 9). Bacteria were grown under four different culture conditions:

1. LB
2. LB + Nitric Oxide
3. Urine
4. Urine + Nitric Oxide

Single microfermenters in a form of glass tube with an air and media inflow and a media outflow were placed in a water bath at 37 °C. Fresh media was pumped in by a peristaltic pump from a media tank with the velocity of 500 ml per 24 h. Fresh solutions of nitric oxide containing media (25 mM DETA NO_nate, Cayman Chemical, US) were supplied every second day because of the 58 h DETA NO_nate half-life. Bacterial colonization of the fresh media reservoir was prevented by placing a hydrophilic filter in front of the each fermenter. Aeration of the culture was achieved by using an aquarium bubbler. Media and air inflow enhanced media outflow which was collected in an autoclavable tank. All elements were assembled and sterilized by autoclaving. Two days before inoculation, the microfermenter setup was tested for any leakage and potential contamination. Inoculation was performed by injection of 100 µl bacterial overnight culture into each of the microfermenters through a rubber gasket in the fermenter's screw lid. Sampling was done weekly and bacteria were stored in glycerol stock cultures at –80 °C. At each sampling time point, bacteria were plated on McConkey and Congo Red agar plates in order to assess the culture homogeneity. Moreover, the number of bacteria in the culture was assessed by counting colony forming units on agar plates and by OD₆₀₀ measurements. Spontaneous mutator phenotype formation was monitored by plating bacteria on a streptomycin agar plates (100 µg/ml).

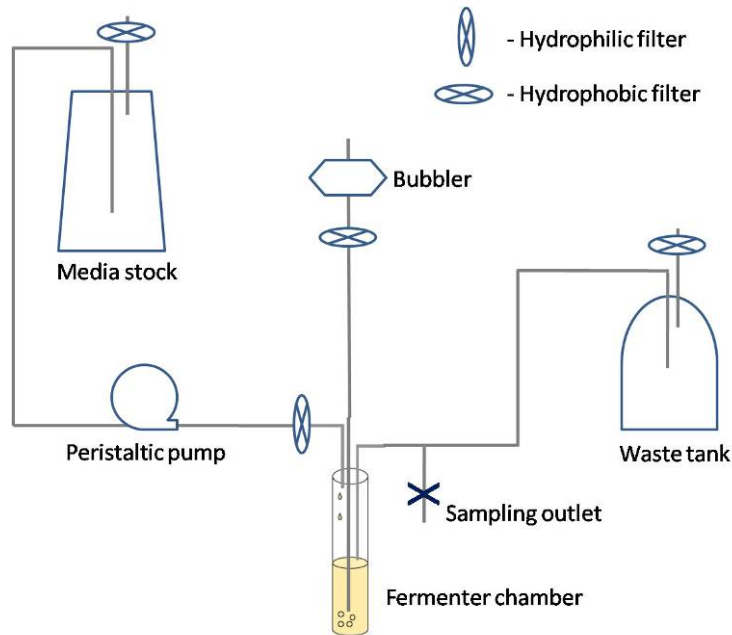


Fig. 8: Schematic construction of the single flow culture unit. Fresh media was pumped by a peristaltic pump into the microfermenter via hydrophilic filter. Media and air inflow forced media outflow to the waste container.

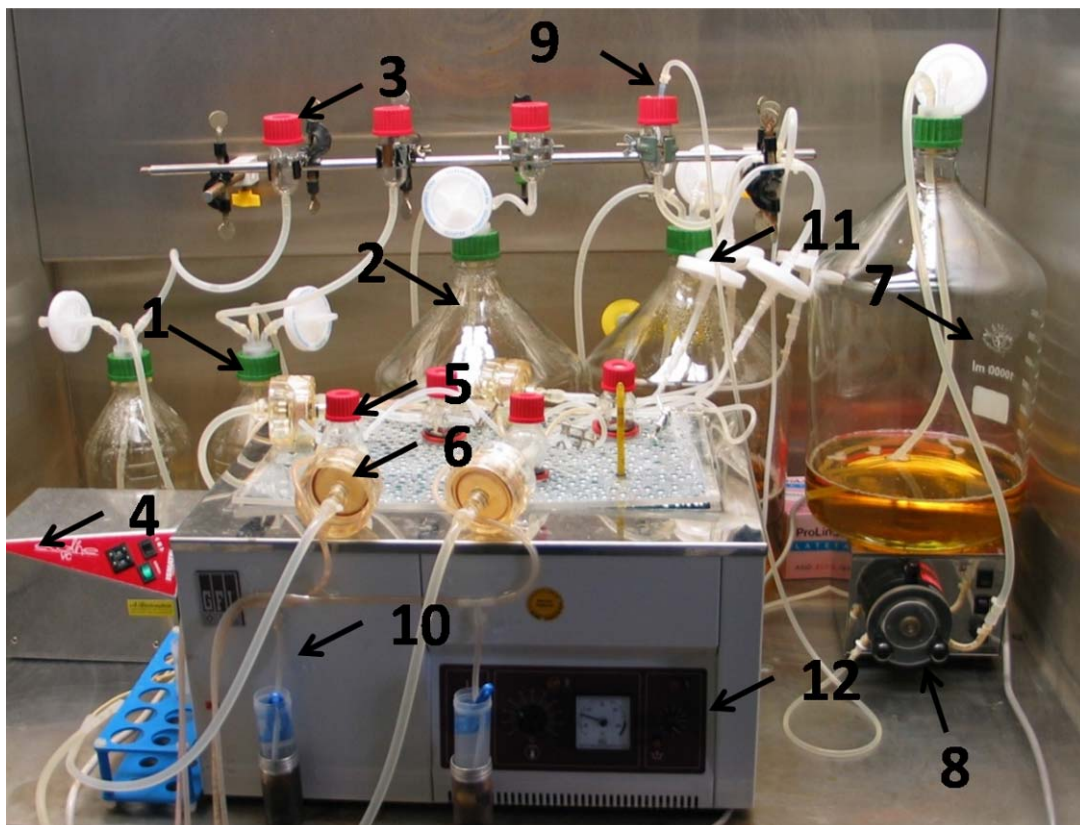


Fig. 9: Four-chamber microfermenter setup. 1) LB + NO fresh media reservoir; 2) LB fresh media reservoir; 3) Fresh media loading system with a rubber gasket; 4) multi-channel peristaltic pump; 5) single fermenter chamber with a rubber gasket on the top for inoculation; 6) hydrophilic filter to prevent bacterial colonization; 7) fresh media loading reservoir; 8) fresh media loading peristaltic pump; 9) syringe needle for sterile media transfer; 10) sampling system, tubing kept always in ethanol 11) hydrophobic filters for culture aeration system

4.7. In silico analysis

For standard sequence comparison and similarity searches, the Basic Local Alignment Search Tool (BLAST) at the National Centre for Biotechnology Information (NCBI) homepage was used. For alignments of nucleotide and amino acid sequences, the BioEdit sequence alignment editor V7.0.1 and VectorNTI V7.0 was used. Genome comparison was performed using the Artemis Comparison Tool (ACT) Release 4 of the Sanger Institute.

5. Results

5.1. Diversity of clinical ABU *E. coli* isolates

The aim of this part of the study was the comparative geno- and phenotypic analysis of eleven ABU isolates to characterize in detail a larger group of strains of this pathotype and to extend the knowledge on the underlying molecular mechanisms of the ABU lifestyle.

5.1.1. Analysis of relatedness of different ABU isolates

Affiliation to the main *E. coli* phylogenetic lineages revealed that seven of the ABU strains tested belonged to ECOR groups B2 and D which typically include ExPEC isolates. Four isolates, however, represented members of the ECOR groups A and B1 (Table 7). For isolates of the latter phylogenetic groups, it is rather uncommon to be associated with extraintestinal infections.

A more detailed analysis of the phylogenetic relationships by MLST further corroborated the finding that the ABU strains belong to multiple different phylogenetic lineages (Table 7). Among the strains of the same ECOR group, different non-related clonal groups have been observed. Interestingly, the majority of ABU isolates of ECOR group B2 belongs to the sequence type (ST) 73 which also comprises the well-characterized UPEC O6 isolate CFT073 as well as the non-pathogenic fecal O6 isolate Nissle 1917. The STs 12 and 405 to which also ABU isolates have been allocated, comprise extraintestinal pathogenic as well as non-pathogenic isolates of ECOR group B2 and D, respectively. So far, only non-pathogenic strains belonging to ECOR group B1 have been described for ST 53.

Table 7: Genotypic characterization of asymptomatic bacteriuria *E. coli* strains by comparative genomic hybridization

	ABU Strain										
	57	21	38	62	20	27	37	83972	63	64	5
No. of <i>E. coli</i> strain MG1655 genes (n=4290) detected	3798 (88.5 %)	3670 (85.5 %)	3588 (83.6 %)	3919 (91.4 %)	3853 (89.8 %)	3796 (88.5 %)	3796 (88.5 %)	3925 (91.5 %)	3804 (88.7 %)	3866 (90.1 %)	3813 (88.9 %)
No. of ExPEC genes (n=274) detected	21 (7.7 %)	10 (3.6 %)	8 (2.9 %)	67 (24.5 %)	132 (48.2 %)	102 (37.2 %)	111 (40.5 %)	134 (48.9 %)	136 (49.6 %)	140 (51.1 %)	52 (19 %)
No. of IPEC genes (n=101) detected	2 (2 %)	1 (1 %)	2 (2 %)	3 (3 %)	5 (5 %)	3 (3 %)	4 (4 %)	6 (6 %)	2 (2 %)	4 (4 %)	18 (18 %)
ECOR group ^{a)}	A	B1	B1	B1	B2	B2	B2	B2	B2	B2	D
Sequence Type ^{b)}	554	553	553	53	73	73	73	73	555	12	405

^{a)} Affiliation to the main phylogenetic lineages of *E. coli* was performed according to (Johnson and Stell, 2000).

^{b)} Multi locus sequence typing (MLST) was performed as described on the following website (http://web.mpiib-berlin.mpg.de/mlst/dbs/Ecoli/documents/primersColi_html).

5.1.2. Comparative Genomic Hybridization (CGH)

In order to compare the genetic diversity of the different ABU *E. coli* isolates, the genome content was assessed by comparative genomic hybridization using an *E. coli* K-12 strain MG1655-specific array as well as the *E. coli* pathoarray. The results obtained from the K-12 array assesses the common genomic content with non-pathogenic strain MG1655, whereas the "E. coli pathoarray" detects many virulence determinants and island-associated genes present in different ABU genomes.

The CGH results demonstrated a considerable genetic diversity among the eleven ABU isolates tested (Fig. 10; Table 7). On average, 12.9 % of the translatable ORFs present in K-12 strain MG1655 were not detectable in the individual isolates. Based on the functional classification of the GenProtEC database of the chromosomally encoded genes and proteins of *E. coli* K-12 (<http://genprotec.mbl.edu>), the majority of these missing ORFs in every strain can be functionally grouped as coding for hypothetical, unclassified or unknown gene products.

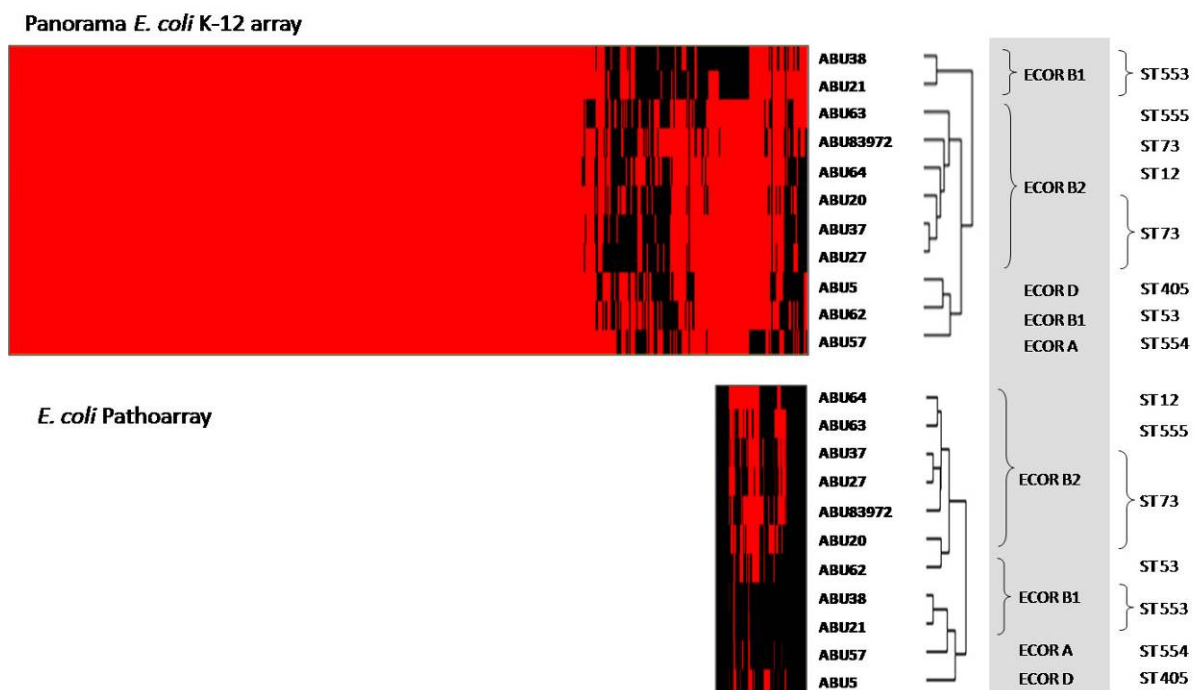


Fig. 10: Analysis of the genome content of ABU *E. coli* isolates. Red and black denote the presence and absence of genes, detected by comparative genomic hybridization respectively. The dendrogram shows the estimated relationships of the different strains obtained by hierarchical cluster analysis of the hybridization signals. The individual STs and major phylogenetic groups of the ABU isolates are indicated.

The eleven *E. coli* isolates also exhibited a great diversity in ORFs which represent mobile genetic elements or code for structural components of the cell. The alterations were found to be scattered over the entire *E. coli* MG1655 chromosome. However, prophages of strain MG1655 represent chromosomal variation "hot spots". The individual isolates could be subgrouped according to their CGH barcodes into certain clusters which generally correlate with the main phylogenetic lineage of the individual isolates.

Isolates of the ECOR groups A and B1 harboured markedly less ExPEC-associated genes (on average 9.7 % of the detectable ExPEC genes) than strains that belong to the ECOR groups B2 and D (on average 42.1 % of the detectable ExPEC genes), i.e. those phylogenetic groups that typically comprise extraintestinal pathogenic *E. coli*. Typical virulence-associated marker genes of intestinal pathogenic *E. coli* (IPEC) were usually only detected in very low amounts (on average 4.5 % of the detectable IPEC genes). The CGH results of the *E. coli* pathoarray were partially confirmed by PCR allowing the detection of typical ExPEC-associated and virulence-associated determinants coding for, e.g. different adhesins, toxins, the polyketide colibactin, siderophores, capsules (Table 7). Whereas the *fimH* gene coding for the adhesin of type 1 fimbriae was detectable in all strains tested, genes of the P- and S/F1C fimbriae-encoding gene clusters are only present in ABU isolates of ECOR group B2. The screening for toxin-, siderophore system- and group II capsule-encoding determinants resulted in similar findings.

These data indicate that ABU isolates differ considerably in their genome content with regard to the presence of virulence-associated genes of uropathogenic *E. coli*. The virulence-associated gene content of about two thirds of the ABU strains analyzed resembles that of typical UPEC, whereas in one third of the ABU isolates only a small amount of such determinants exists.

5.1.3. Genomic fingerprints of different ABU isolates

To further extend the genotypic comparison, the genome structure of the ABU strains was compared by PFGE and rep-PCR. Although the genetic fingerprints of individual isolates belonging to the same ST were very similar (Fig. 11A), the analysis of genomic *Xba*I restriction fragment patterns by PFGE indicated that members of the same ST differed considerably in their genome content and –structure (Fig. 11B).

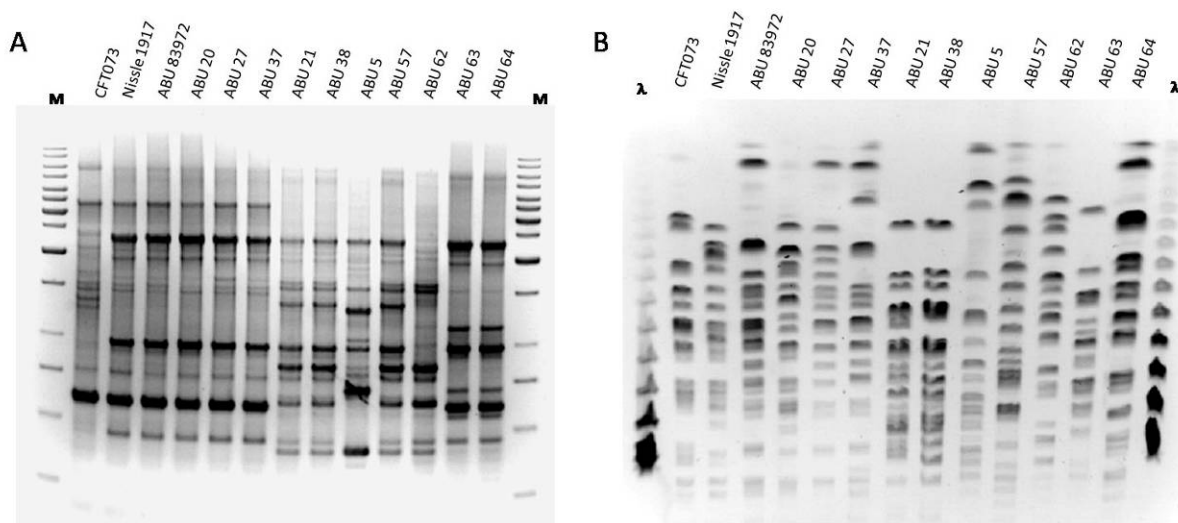


Fig. 11: Genomic fingerprints of asymptomatic bacteriuria *E. coli* isolates. The similarity of the genome structure was assessed by **A)** Box PCR and **B)** PFGE following *Xba*I digestion.

These results demonstrate that ABU isolates do not represent a specialized bacterial clone, but, instead, are a diverse group of strains that evolved independently from different ancestors of different evolutionary *E. coli* lineages.

5.1.4. Genome size of different ABU isolates

The assessment of the genome size by analysis of genomic I-*Ceu*I restriction fragment patterns by PFGE demonstrated that marked genome size differences exist even among strains of the same ST (Fig. 12; Table 8).

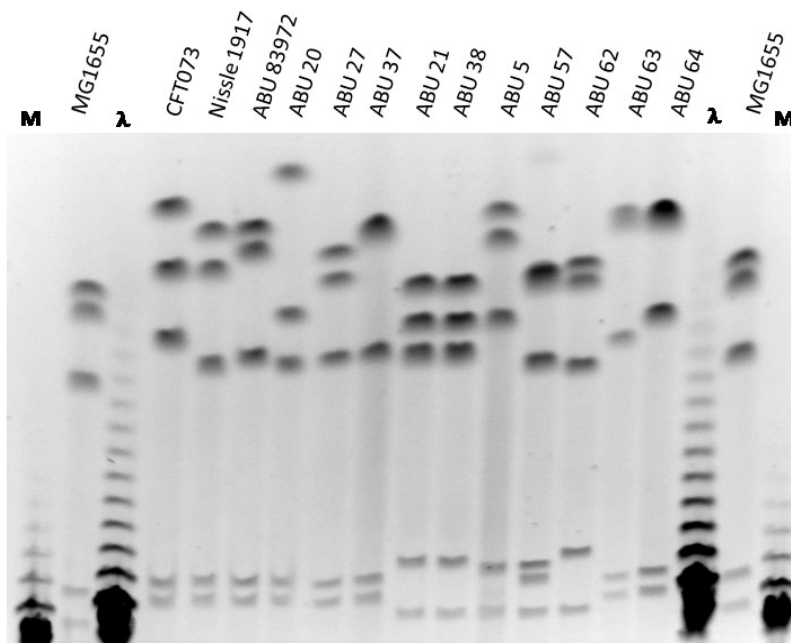


Fig. 12: Assessment of the genome size of asymptomatic bacteriuria *E. coli* isolates by PFGE following I-CeuI digestion.

The genome sizes of ABU isolates of the ECOR groups A and B1 more closely resembled that of non-pathogenic *E. coli* K-12 strain MG1655 which belongs to ECOR group A as well. In contrast, those of members of the ECOR group B2 and D were generally larger than that of strain MG1655. However, the genome sizes of ABU isolates belonging to ST73 were, with one exception, always smaller than that of UPEC strain CFT073 which causes symptomatic UTI.

Table 8: Genome size of ABU *E. coli* isolates

ABU Strain	57	21	38	62	20	27	37	83972	63	64	5
Genome size [Mb]	4.2	4.7	4.7	4.7	5.3	4.9	5.1	4.9	5.1	5.1	5.1
ECOR group	A	B1	B1	B1	B2	B2	B2	B2	B2	B2	D

These data demonstrate that ABU isolates differ in genome size and differences exist even among isolates of the same ST. As compared to UPEC strain CFT073, ABU isolates of the same sequence type have a reduced genome size.

5.2. Phenotypic vs. genotypic characteristics of ABU *E. coli* isolates

The carriage of virulence determinants and the ability to express them by different ABU *E. coli* isolates was compared. A number of phenotypic tests were performed in combination with polymerase chain reactions where genetic determinants were investigated in more detail.

5.2.1. Type 1 fimbriae

The expression of type 1 fimbriae was tested by yeast agglutination in the presence or absence of mannose. Surprisingly, only four out of eleven tested strains were able to express functional type 1 fimbriae, however, GCH revealed presence of *fimH* in all of these isolates. Therefore, the completeness of the *fim* gene cluster was investigated by PCR-based screening for each individual gene of the *fim* determinant (*fimB* to *fimH*). Accordingly, the complete gene cluster could be detected in strains 5, 20, 57, 62, 63 and 64. The absence of functional type 1 fimbriae in spite of the presence of the complete *fim* determinant in strains 5 and 57 suggested that these determinants have been inactivated by point mutations. In case of strains 27 and 37, a large 4,253-bp deletion within the *fim* gene cluster was observed which is also present in strain 83972. Due to this internal deletion including the *fimEAICD* genes, a truncated *fimB* gene is fused with a truncated *fimD* gene probably by recombination between a 7-bp DNA motif GGCGTTT present in both genes. Moreover, in strains 21 and 38, a 29,349-bp deletion of large parts of the KpLE2 phage element and the *fim* operon could be detected. In these strains, most likely insertion sequence (IS) element-mediated deletion was responsible for the loss of a chromosomal region ranging from a non-functional copy of IS1 upstream of *fecI* to *fimG* (Fig. 13). The 29-kb chromosomal region has been replaced by a 1,347-bp DNA stretch which represents a non-functional allele of an IS element, ISEhe3, frequently found, e.g. in *Shigella flexneri*.

Consequently, the *fim* determinant of the ABU strains tested represents a heterogeneous genomic region which is frequently subjected to point mutations and deletions which cause inactivation of this gene cluster.

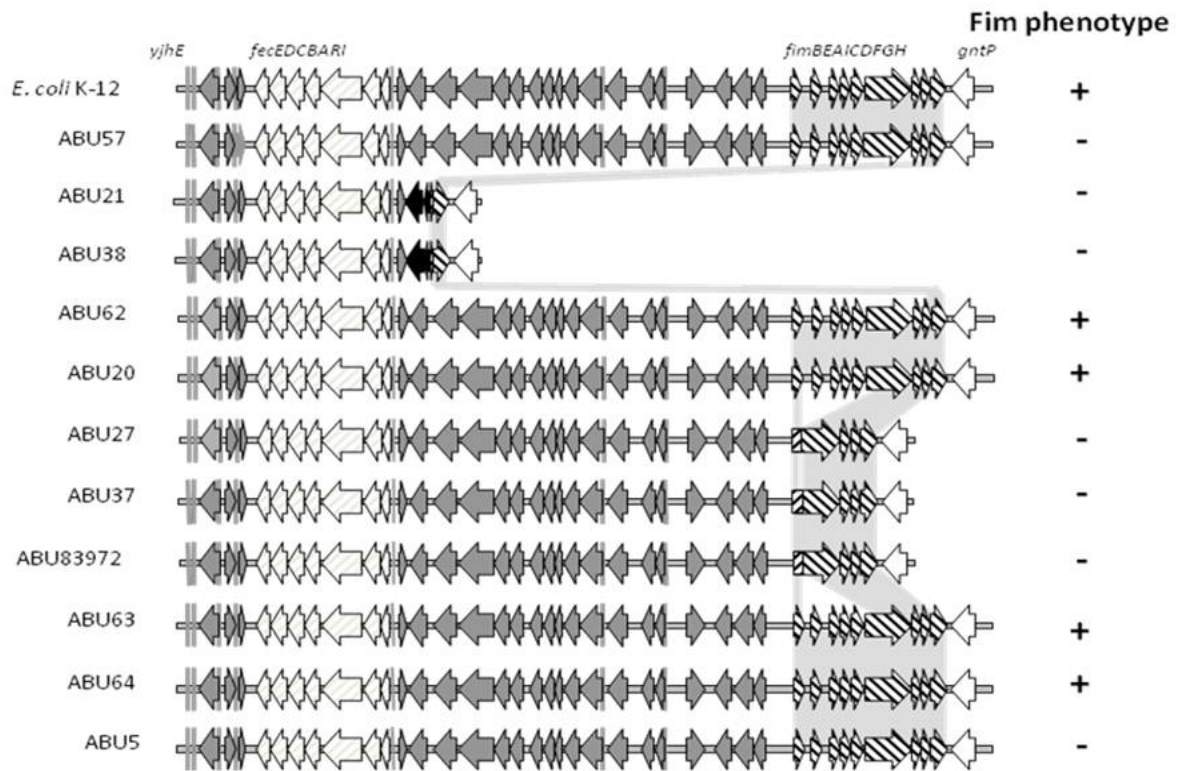


Fig. 13: Genetic structure of the *fim* determinant and adjacent KpLE2 phage-like chromosomal region in asymptomatic bacteriuria *E. coli* isolates. The scheme is based on the *E. coli* K-12 chromosome. Genes of the *fim* determinant are indicated by hatched arrows, ORFs of the KpLE2 prophage are indicated by filled grey arrows. Dotted arrows represent the *fec* determinant located within KpLE2. The ORF A and non-functional ORF B of ISEhe3-like element that replaces large regions of KpLE2 in ABU strains 21 and 38 are indicated by black arrows.

Moreover, analysis of the *fimH* allelic variation indicated that differences regarding the FimH amino acid sequence were visible between isolates of distinct phylogenetic groups (Fig. 14). Strains of ECOR groups A and B1 differed from those of groups B2 and D in the presence of valine at position 27 instead of alanine. The ABU isolates that belong to ECOR group B2 exhibit the highest number of amino acid exchanges relative to FimH of *E. coli* K-12 strain MG1655. Interestingly, marked differences in the FimH amino acid sequence were even observed among the closely related B2 strains of ST73.

ECOR group	Strain	ST	AA
ECOR B1	A	K12	3
	A	ABU57	554
	B1	ABU21	553
	B1	ABU38	553
	B1	ABU62	53
	B2	EcN	73
	B2	ABU20	73
	B2	ABU27	73
	B2	ABU37	73
	B2	ABU83972	73
	B2	CFT073	73
	B2	ABU63	555
	B2	ABU64	12
	D	ABU5	405
consensus			
<p>Sequence alignment for ECOR B1 (ST553):</p> <p>3 CKTANGTAIPIGGGSANVYVNLAPVNVGQNLVVDLSTQIFCHNDYPETITDYVTLQRGS</p> <p>3 CKTANGTAIPIGGGSANVYVNLAPVNVGQNLVVDLSTQIFCHNDYPETITDYVTLQRGS</p> <p>3 CKTANGTAIPIGGGSANVYVNLAPVNVGQNLVVDLSTQIFCHNDYPETITDYVTLQRGS</p> <p>3 CKTANGTAIPIGGGSANVYVNLAPVNVGQNLVVDLSTQIFCHNDYPETITDYVTLQRGS</p> <p>3 CKTANGTAIPIGGGSANVYVNLAPVNVGQNLVVDLSTQIFCHNDYPETITDYVTLQRGS</p> <p>3 CKTANGTAIPIGGGSANVYVNLAPVNVGQNLVVDLSTQIFCHNDYPETITDYVTLQRGS</p> <p>3 CKTANGTAIPIGGGSANVYVNLAPVNVGQNLVVDLSTQIFCHNDYPETITDYVTLQRGS</p> <p>3 CKTANGTAIPIGGGSANVYVNLAPVNVGQNLVVDLSTQIFCHNDYPETITDYVTLQRGS</p> <p>3 CKTANGTAIPIGGGSANVYVNLAPVNVGQNLVVDLSTQIFCHNDYPETITDYVTLQRGS</p> <p>3 CKTANGTAIPIGGGSANVYVNLAPVNVGQNLVVDLSTQIFCHNDYPETITDYVTLQRGS</p> <p>3 CKTANGTAIPIGGGSANVYVNLAPVNVGQNLVVDLSTQIFCHNDYPETITDYVTLQRGS</p> <p>3 CKTANGTAIPIGGGSANVYVNLAPVNVGQNLVVDLSTQIFCHNDYPETITDYVTLQRGS</p> <p>3 CKTANGTAIPIGGGSANVYVNLAPVNVGQNLVVDLSTQIFCHNDYPETITDYVTLQRGS</p> <p>3 CKTANGTAIPIGGGSANVYVNLAPVNVGQNLVVDLSTQIFCHNDYPETITDYVTLQRGS</p>			
ECOR B2	A	K12	63
	A	ABU57	554
	B1	ABU21	553
	B1	ABU38	553
	B1	ABU62	53
	B2	EcN	73
	B2	ABU20	73
	B2	ABU27	73
	B2	ABU37	73
	B2	ABU83972	73
	B2	CFT073	73
	B2	ABU63	555
	B2	ABU64	12
	D	ABU5	405
consensus			
<p>Sequence alignment for ECOR B2 (ST73):</p> <p>63 AYGGVLSNFSGTVKYSGSSYPFPTTSETPRVVYNSRTDKPWPVALYLT PVSSAGGVAIKA</p> <p>63 AYGGVLSNFSGTVKYSGSSYPFPTTSETPRVVYNSRTDKPWPVALYLT PVSSAGGVAIKA</p> <p>63 AYGGVLSNFSGTVKYSGSSYPFPTTSETPRVVYNSRTDKPWPVALYLT PVSSAGGVAIKA</p> <p>63 AYGGVLSNFSGTVKYSGSSYPFPTTSETPRVVYNSRTDKPWPVALYLT PVSSAGGVAIKA</p> <p>63 AYGGVLSNFSGTVKYSGSSYPFPTTSETPRVVYNSRTDKPWPVALYLT PVSSAGGVAIKA</p> <p>63 AYGGVLSNFSGTVKYSGSSYPFPTTSETPRVVYNSRTDKPWPVALYLT PVSSAGGVAIKA</p> <p>63 AYGGVLSNFSGTVKYSGSSYPFPTTSETPRVVYNSRTDKPWPVALYLT PVSSAGGVAIKA</p> <p>63 AYGGVLSNFSGTVKYSGSSYPFPTTSETPRVVYNSRTDKPWPVALYLT PVSSAGGVAIKA</p> <p>63 AYGGVLSNFSGTVKYSGSSYPFPTTSETPRVVYNSRTDKPWPVALYLT PVSSAGGVAIKA</p> <p>63 AYGGVLSNFSGTVKYSGSSYPFPTTSETPRVVYNSRTDKPWPVALYLT PVSSAGGVAIKA</p> <p>63 AYGGVLSNFSGTVKYSGSSYPFPTTSETPRVVYNSRTDKPWPVALYLT PVSSAGGVAIKA</p> <p>63 AYGGVLSNFSGTVKYSGSSYPFPTTSETPRVVYNSRTDKPWPVALYLT PVSSAGGVAIKA</p> <p>63 AYGGVLSNFSGTVKYSGSSYPFPTTSETPRVVYNSRTDKPWPVALYLT PVSSAGGVAIKA</p> <p>63 AYGGVLSNFSGTVKYSGSSYPFPTTSETPRVVYNSRTDKPWPVALYLT PVSSAGGVAIKA</p> <p>63 AYGGVLSNFSGTVKYSGSSYPFPTTSETPRVVYNSRTDKPWPVALYLT PVSSAGGVAIKA</p>			

Fig. 14: Allelic variation of the FimH type 1 fimbrial adhesins among asymptomatic bacteriuria *E. coli* isolates. The allocation of the individual strains to the main phylogenetic lineages and clonal groups has been indicated.

5.2.2. P fimbriae

To further extend the knowledge about fimbriae expression of the ABU strains, the expression of P fimbriae was tested. PCR screening resulted in five strains positive for the *pap* fimbrial determinant whereas agglutination with P-fimbriae-specific antibodies was positive only for ABU strain 64. Sequence analysis and comparison of the *pap* operons of ABU strains 27, 37 63 and 83972 showed that these strains harbour the identical *papG* allele which codes for a non-functional P fimbrial adhesin.

Table 9: Geno- and phenotypic characterization of selected virulence traits of asymptomatic bacteriuria *E. coli* strains

Strain	α -Hemolysin		Type 1 fimbriae	P fimbriae			F1C fimbriae		Mo- tility [mm]	Colicins /Micro- cins	Aero- bactin	LPS	Other detected virulence-associated genes ^{b)}
	<i>hly</i>	Hly	<i>fim</i>	Fim	<i>pap</i>	Pap	<i>foc</i>	F1C					
ABU57	-	-	<i>fimBEAICDFGH+</i>	-	-	-	-	-	0	+	-	rough	<i>fyuA, iutA, kpsMT(II)</i>
ABU21	-	-	<i>fimH+</i>	-	-	-	-	-	13	+	-	smooth ^a	-
ABU38	-	-	<i>fimH+</i>	-	-	-	-	-	9	+	-	smooth ^a	-
ABU62	-	-	<i>fimBEAICDFGH+</i>	+	-	-	-	-	24	-	-	smooth ^a	<i>iutA</i>
ABU20	+	+	<i>fimBEAICDFGH+</i>	+	-	-	+	+	5	+	-	rough	<i>cnf1, clbA-Q, fyuA, iroN-B, kpsMT(II), malX</i>
ABU27	+	-	<i>fimB':':DFGH+</i>	-	+	-	+	-	42	-	-	rough	<i>cnf1, clbA-Q, fyuA, iroN-B, malX</i>
ABU37	+	+	<i>fimB':':DFGH+</i>	-	+	-	+	+	0	-	-	rough	<i>cnf1, clbA-Q, fyuA, iroN-B, kpsMT(II), malX</i>
ABU83972	+	-	<i>fimB':':DFGH+</i>	-	+	-	+	-	9	-	+	rough	<i>cnf1, clbA-Q, fyuA, iutA, iroN-B, kpsMT(II), malX</i>
ABU63	+	+	<i>fimBEAICDFGH+</i>	+	+	-	-	-	42	-	-	smooth	<i>cnf1, fyuA, kpsMT(II), ibeA, malX</i>
ABU64	+	+	<i>fimBEAICDFGH+</i>	+	+	+	+	+	42	-	-	smooth	<i>cnf1, clbA-Q, fyuA, iroN-B, kpsMT(II), rfc, malX</i>
ABU5	-	-	<i>fimBEAICDFGH+</i>	-	-	-	-	-	0	+	-	rough	<i>afa/draBC, fyuA, kpsMT(II), traT, malX</i>

^{a)} The O side chains are shorter than those of smooth UPEC strain 536 (Fig. 17).

^{b)} The screening for the ExPEC virulence-associated genes was performed using a multiplex PCR describes before (Dobrindt *et al.*, 2001). The screening for the colibactin polyketide determinant and for the salmochelin determinant was performed as described previously (Nougayrède *et al.*, 2006; Sunden *et al.*, 2006).

5.2.3. F1C fimbriae

The same approach was used to analyze functionality of F1C fimbriae where agglutination with antibodies specific for F1C fimbriae was positive only for isolates 20, 27 and 64. However, PCR-based detection of the F1C fimbriae-encoding gene cluster was also positive for strain 27 and 83972. Similarly, these three strains also differed in their ability to express functional F1C fimbriae. Comparison of the DNA sequence of the encoding *foc* determinant in these strains (Fig. 15) demonstrated that the A to T transition at the *focD* nucleotide position 1415 results in exchange of glutamine 472 against a leucine residue in the *FocD* fimbrial usher of the latter two strains. Mutation of this amino acid alone results in a non-functional *FocD* usher protein (Table 10).

Strain	AA		
FocD_ABU27	421	YRAFNLGVGKNNMGWLGAVSLDATRANARLPDESRRHDGLSYRFLYNKSLTETGTNIQLIGY	480
FocD_ABU83972		YRAFNLGVGKNNMGWLGAVSLDATRANARLPDESRRHDGLSYRFLYNKSLTETGTNIQLIGY	
FocD_ABU37		YRAFNLGVGKNNMGWLGAVSLDATRANARLPDESRRHDGQSYRFLYNKSLTETGTNIQLIGY	
FocD_EcN		YRAFNLGVGKNNMGWLGAVSLDATRANARLPDESRRHDGQSYRFLYNKSLTETGTNIQLIGY	
FocD_CFT073		YRAFNLGVGKNNMGWLGAVSLDATRANARLPDESRRHDGQSYRFLYNKSLTETGTNIQLIGY	
SfaF_536		YRAFNLGVGKNNMGWLGAVSLDATRANARLPDESRYDGQSYRFLYNKSLTETGTNIQLIGY	
SfaF_UTI89		YRAFNLGMGKNNMGWLGAVSLDATRANARLPDESRRHDGQSYRFLYNKSLTETGTNIQLIGY	
FocD_AD110		YRAFNLGVGKNNMGWLGAVSLDATRANARLPDESRRHDGQSYRFLYNKSLTETGTNIQLIGY	
FimD_O157_H7		YRAFNFGIGKNNMGALGALSVDMTQANSTLPDDSQHDGQSVRFLYNKSLNESGTNIQLVGY	
FimD_K12		YRAFNFGIGKNNMGALGALSVDMTQANSTLPDDSQHDGQSVRFLYNKSLNESGTNIQLVGY	
FimD_CFT073		YRAFNFGIGKNNMGALGALSVDMTQANSTLPDDSQHDGQSVRFLYNKSLNESGTNIQLVGY	
		*****-:-***** ***-:-* *-**:- ***-:-:** * *****_-:-*****-:-**	

Fig. 15 Amino acid alignment of FocD, SfaF and FimD fimbrial ushers. The conserved Gln472 residue of FocD has been indicated in red. EcN, *E. coli* Nissle 1917.

Table 10: Identification of the Gln472 → Leu substitution critical for FocD function

Strain	FocD amino acid substitution	Functional F1C fimbriae
CFT073	Gln 472, Ala 889	+
Nissle 1917	Gln 472, Ala 889	+
ABU27	Leu 472, Val 889	-
ABU37	Gln 472, Val 889	+
ABU83972	Leu 472, Val 889	-

5.2.4. Expression of α -hemolysin

The ability to express α -hemolysin was checked by plating bacteria on sheep blood agar plates. Only strains 20, 37, 63 and 64 were able to lyse erythrocytes, however, strains 27 and 83972 harboured all genes of the *hly* gene cluster. Nucleotide sequence comparison of the *hly* operon of the closely related strains ABU27, ABU37 and ABU83972 revealed that the non-hemolytic phenotype of strains 27 and 83972 relative to ABU37 is due to an A→T transition at the *hlyA* nucleotide position 416 thus resulting in a premature stop codon and thus a truncated HlyA toxin gene product (Fig. 16).

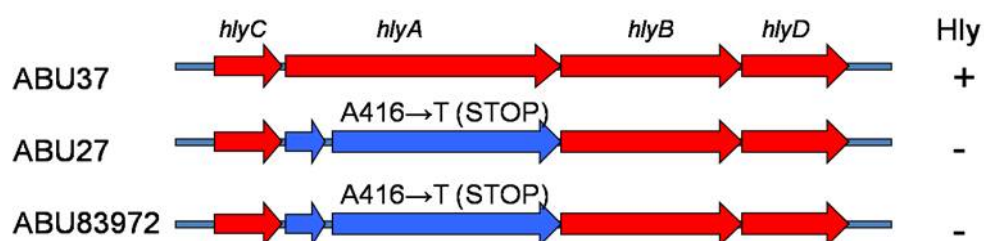


Fig. 16: Inactivation of the *hly* determinant in strains 27 and 83972

5.2.5. LPS O side chain expression

The ABU isolates exhibited considerable diversity with regard to LPS O side chain expression (Fig. 17): strains that belong to ECOR group B2 either expressed long chain LPS or no side chains. Interestingly, all ST73 isolates tested exhibited a rough LPS phenotype. The O side chain length of the three isolates that belong to ECOR group B1 was shorter than that of smooth strains expressing long O side chains. ABU isolate 5 (ECOR group D) and 57 (ECOR group A) did not express O side chains.

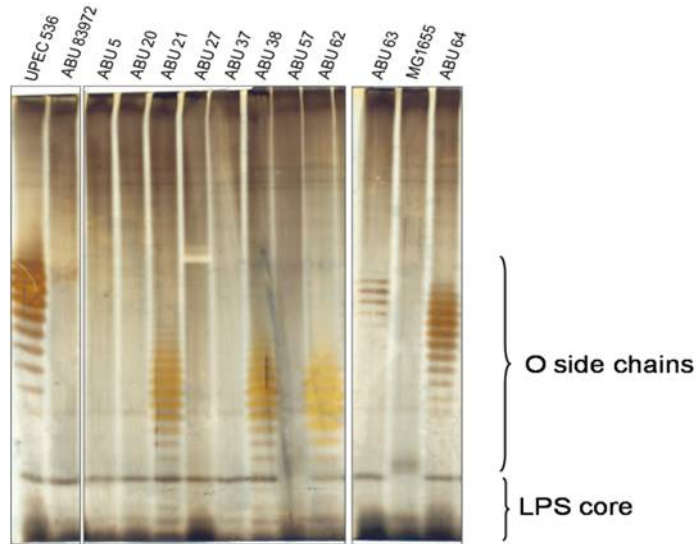


Fig. 17: Analysis of the LPS phenotype among asymptomatic bacteriuria *E. coli* isolates

5.2.6. Biofilm formation

The ABU isolates differed markedly with regard to their ability to form biofilms (Fig. 18). Even among strains of the same sequence type, i.e. the strains of ST73, more than threefold differences were observed in their biofilm formation.

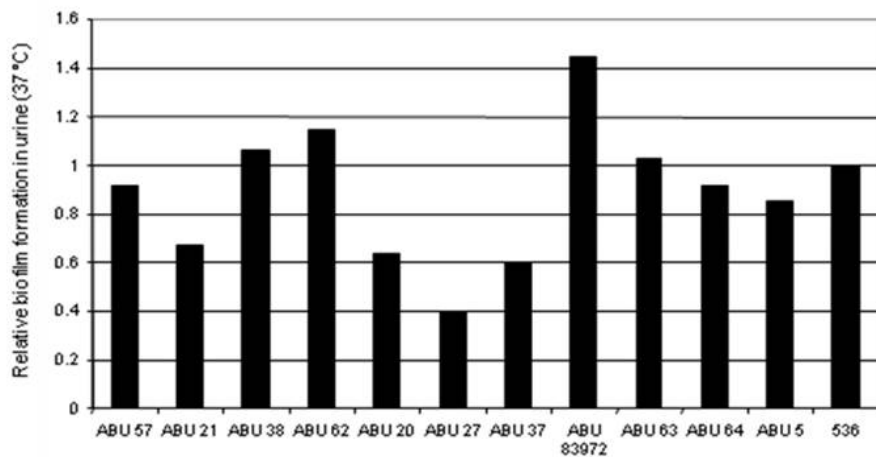


Fig. 18: Analysis of biofilm formation of asymptomatic bacteriuria *E. coli* isolates in urine. The ability to form biofilms was compared to that of uropathogenic *E. coli* strain 536 that causes symptomatic urinary tract infections.

5.2.7. Growth characteristics of ABU *E. coli* isolates

In order to characterize ABU isolates in terms of growth properties, the bacteria were grown statically at 37 °C in pooled human urine. As a control UPEC strains CFT073, 536, NU14 and J96, as well as non-pathogenic K-12 strain MG1655 were grown under the same conditions. With respect to growth rate and their final optical density, all ABU strains grew well in urine (Fig. 19). The isolates 83972, 20, 21, 37 and 62, however, grew better in the early exponential phase than isolates that belong to ECOR group A or D. The ABU model strain 83972 grows as fast as other tested UPEC strains except strain NU14 which grew rather like the *E. coli* K-12 strain MG1655.

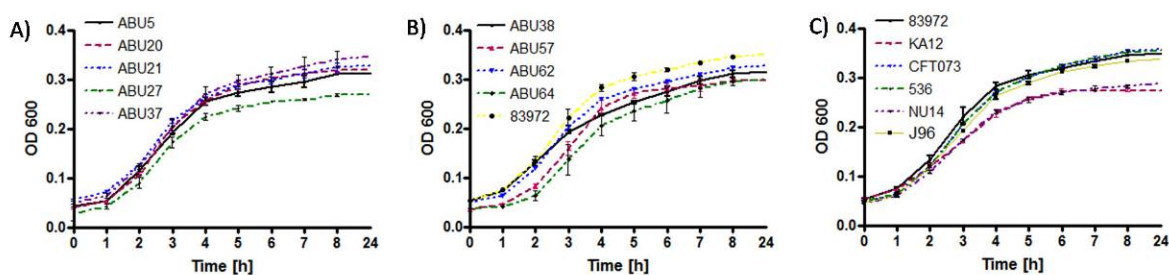


Fig. 19: Growth characteristics of *E. coli* isolates in pooled human urine at 37 °C: A, B) ABU *E. coli* isolates; C) UPEC strains, K-12 strain MG1655 and ABU strain 83972.

Taken together, a number of phenotypic tests revealed significant differences among investigated isolates with regard to expression of virulence factors. ABU strains often carried virulence determinants on the chromosome but did not express them. DNA amplification and sequencing led to the discovery that in many cases loss of the function was due to point mutations or IS mediated DNA deletions. Regarding LPS expression, no common pattern could be observed, and finally, all ABU isolates grew very well in urine.

5.3. Adaptive flexibility and genome plasticity of model strain 83972

ABU strain 83972 has been successfully used in a medical treatment pilot study (2004-2006) for bladder colonization of patients suffering from recurrent urinary tract infections due to various bladder dysfunctions (Sunden *et al.*, 2006). Access to consecutive re-isolates of strain 83972 from different patients allowed us to study bacterial adaptation in response to host colonization. Microbial genome rearrangements and changes in the global gene expression profiles of the individual re-isolates were analyzed and correlated to host response.

5.3.1. Patient colonization

In the Department of Urology of the Lund University hospital (Sweden), the patients participating in the pilot study of deliberate bladder colonization with ABU strain 83972 were treated with appropriate antibiotics to sterilize their urinary bladder. After an antibiotic-free interval, the patients were catheterized and the bladder was emptied. Thirty millilitres of *E. coli* strain 83972 (10^5 colony-forming units (CFU)/ml) were instilled in the bladder and the catheter was removed. This procedure was repeated on the next 2 days. According to individual study protocols, subsequent urine samples were taken to assess host response parameters: interleukin 6 (IL 6) and interleukin 8 (IL 8) levels, numbers of polymorphonuclear cells (PMN), and to prove the success or failure of the colonization procedure. Urine samples have been obtained from the patients in monthly intervals and bacterial samples were stored in agar stamps at room temperature. Several re-isolates of strain 83972 from different time points were subjected to phenotypic and genotypic characterisation.

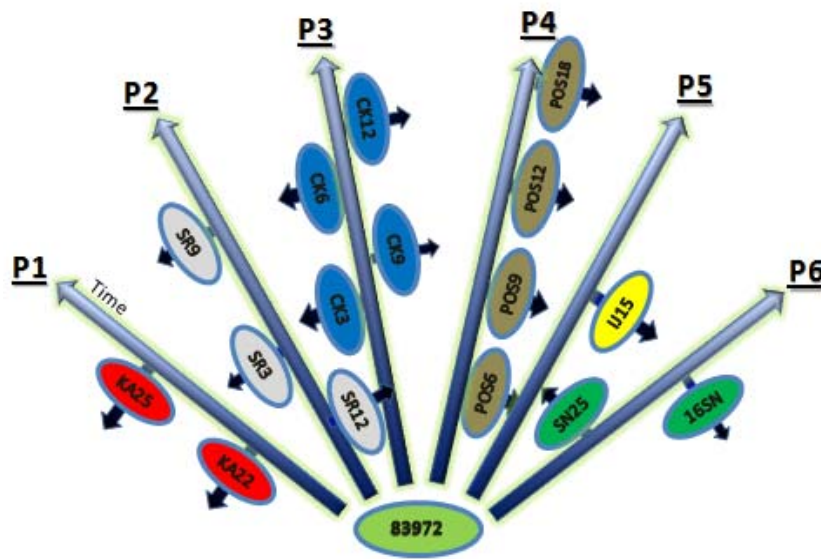


Fig. 20: Schematic representation of the experimental design. Patients P1 to P6 were colonized with ABU strain 83972. Blue arrows illustrate the time of colonization. Re-isolates were collected at different time points. Re-isolates obtained from different inoculations of the same patient are represented on opposite sides of an arrow.

5.3.2. Patients' immune response upon colonization with strain 83972

The colonized patients, four males and two females, differed with respect to their host immune response towards bacterial colonization of the bladder. The mean of IL 8 expression in the strongest “responder” KA was more than 8-fold higher than in patient SR and 6-fold higher in patient SN (Fig. 21). While IL 8 expression was very diverse among colonized patients, their IL 6 expression did not differ drastically. In patient IJ, however, the IL 6 expression was more than 2-fold lower compared to that of the other patients. Noteworthy, in some patients only low IL 6 levels were detected in their urine, while their IL 8 expression was very high. The influx of PMNs into the bladder could be correlated with IL 8 expression, except for patient CK (Fig. 21; Fig. 22).

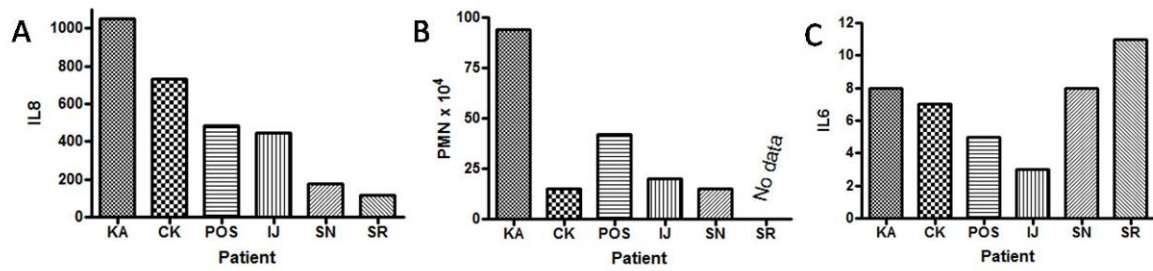


Fig. 21: Mean of host response parameters in urine samples collected from patients during the time of colonization with strain 83972: **A)** IL 8 expression; **B)** PMNs influx into the bladder; **C)** IL 6 expression. These data were kindly provided by Dr. B. Wullt, Lund.

To access the dynamics of host response upon asymptomatic bladder colonization by strain 83972, the levels of IL 8 and PMN influx in the bladder at each sampling time point were compared (Fig. 22). Only patients KA and POS were permanently colonized by 83972 during the duration of the colonization study, whereas in patients SR, CK, IJ and SN the bladder was cleared once from strain 83972 so that they had to be re-colonized. Interestingly, the deviation of the IL 8 expression from the mean value in the first group of patients was very low and less than 2-fold and 4-fold for KA and POS respectively. In contrast, a 10- and 16-fold increase in IL 8 expression was followed by rapid bacterial clearance in patients IJ and SN, respectively. In patient CK, bacterial colonization of the bladder was lost already after a 3.5-fold IL 8 induction, however, the bacteria were lost about one month after that event.

Moreover, in patient SR a 3.8-fold induction of IL 8 (after 3 months) did not result in immediate bacterial clearance. However, bacteria were lost after eight months of bladder colonization and the host response at that time point was at the mean level.

Results

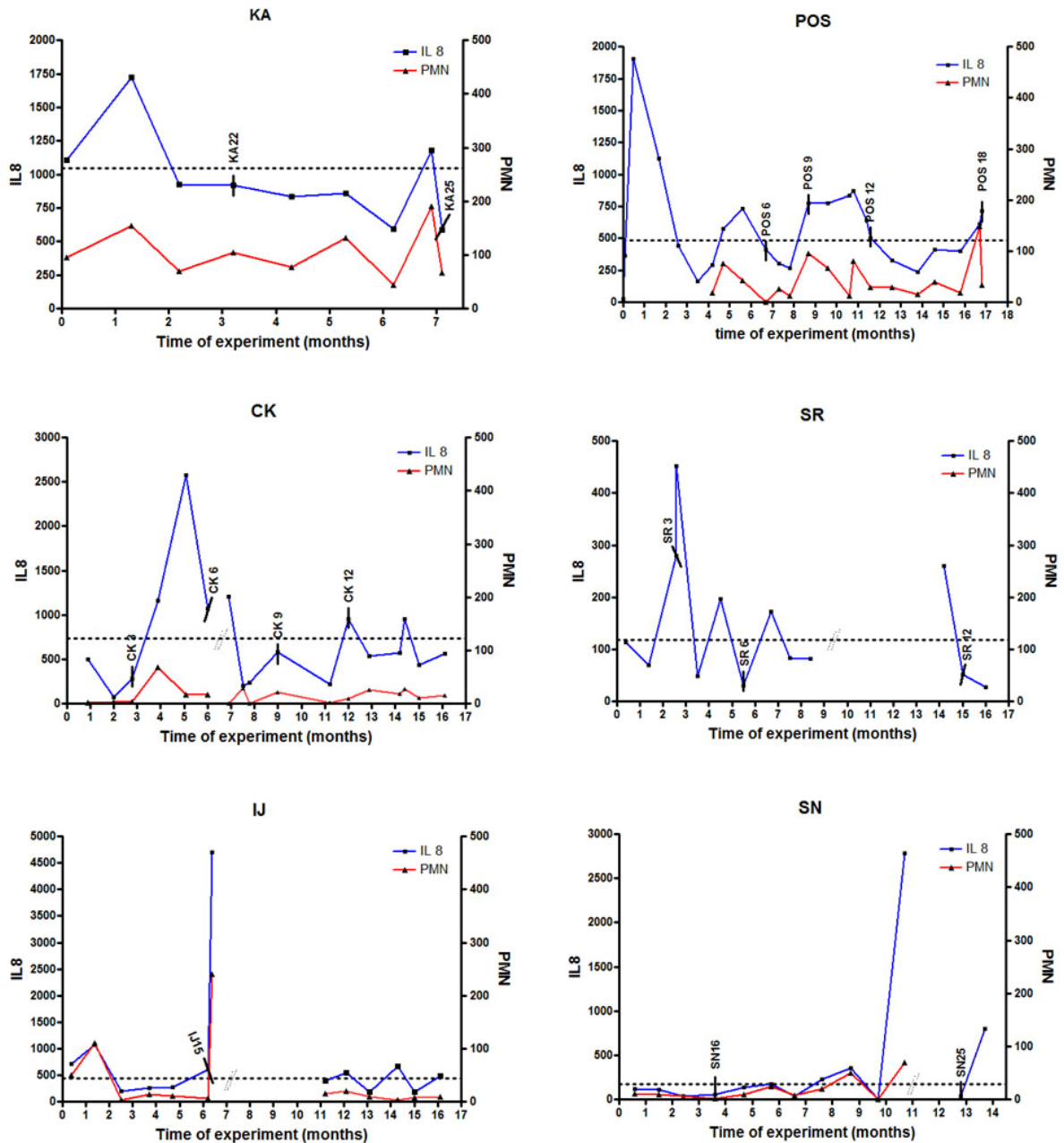


Fig. 22: Levels of IL 8 and PMNs at each sampling time point. Black bars indicates time points corresponding to all investigated re-isolates, dotted double lines show bacteria clearance from the bladder. Single dotted line across the graph shows the mean of IL 8 expression. These data were kindly provided by Dr. B. Wullt, Lund.

Taken together, the individual host response described as PMN influx into the bladder, IL6 and IL8 production differed from patient to patient. At different time points of the colonization experiment, the levels of the response parameters were different. An increase in IL 8 expression generally correlated with an increase in PMN influx into the bladder. In a certain group of patients bacterial clearance was a direct follow up of increased host response.

5.3.3. Verification of the re-isolates

Bacteria recovered from the patient's urine samples were confirmed to be derivatives of strain 83972 by means of PCR. Two genetic markers specific for the *E. coli* strain 83972 were amplified: a DNA fragment covering a 4.7-kb deletion in the *fim* gene cluster (Fig. 23) and a fragment of a cryptic plasmid specific for strain 83972.

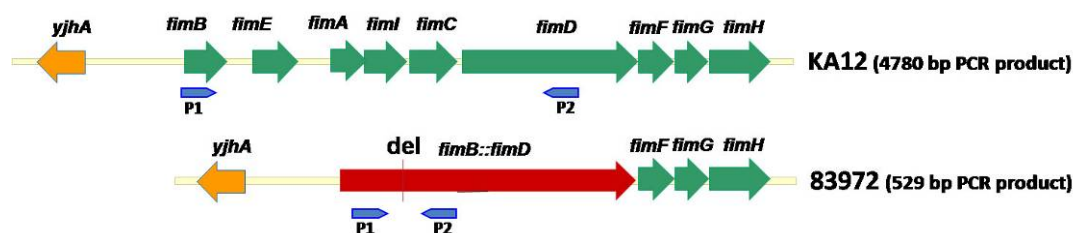


Fig. 23: Genetic organization of the *fim* loci in *E. coli* K-12 and *E. coli* 83972. P1 and P2 - primers used for PCR amplification.

The two designed primer pairs did not result in amplification of a PCR product with several prototypic non-pathogenic and pathogenic *E. coli* strains. Accordingly, these primer pairs were confirmed to be specific for strain 83972. In contrast, all tested patient re-isolates were positive for both *E. coli* 83972-specific genetic markers (Fig. 24) thus proving that they indeed represent derivatives of strain 83972.

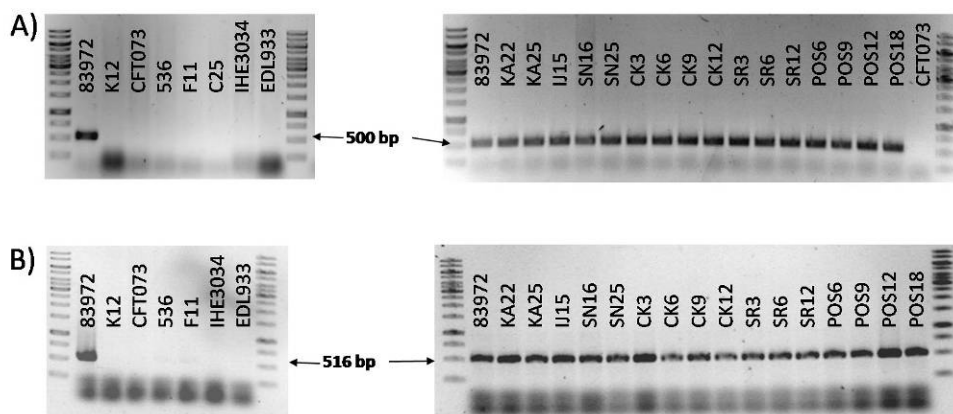


Fig. 24: Verification of the patient re-isolates of *E. coli* strain 83972. **A)** PCR amplification of a 4.7-kb internal deletion region of the *fim* operon; **B)** PCR amplification of a DNA region of the cryptic plasmid found in strain 83972.

5.3.4. Genome structure of *in vivo* 83972 re-isolates

Changes in the genome structure were assessed by PFGE following digestion with the endonucleases *XbaI* and *AvrII*, respectively (Fig. 25A and B). Depending on the enzyme used, different changes in the restriction pattern could be observed. Although most of the re-isolates exhibited the same DNA fingerprint as their parent strain 83972, significant changes in the genomic restriction pattern could be observed in five out of 16 re-isolates. Upon digestion with *XbaI*, the strains IJ15 and SR6 resulted in similar changes of their restriction pattern indicating that similar rearrangements occurred in these strains. Only strain CK12 showed differences in the restriction pattern relative to that of strain 83972 upon digestion with *XbaI* and *AvrII*. Interestingly, in none of the re-isolates from patient POS modifications of the restriction pattern could be observed, although the latest re-isolate, POS18, colonized the bladder for 536 days. In contrast, strain SR12 exhibited significant changes in the PFGE pattern already after 54 days of bladder colonization.

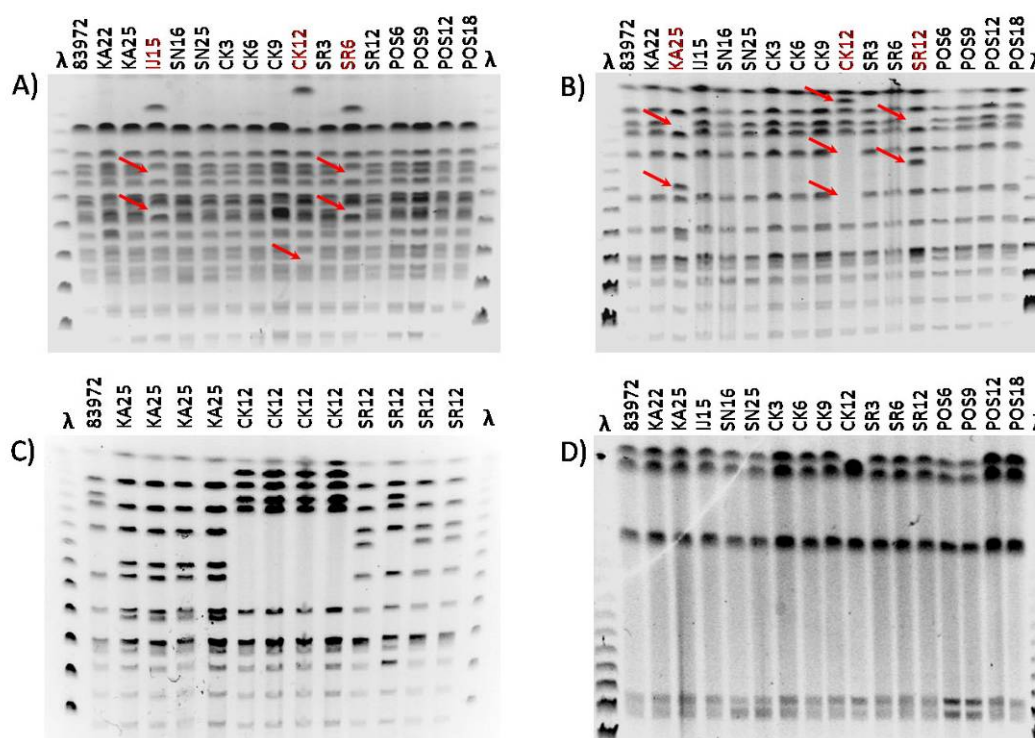


Fig. 25 Genomic fingerprints of *in vivo* re-isolates of strain 83972 from different human patients. Representative consecutive re-isolates from the same patient are indicated by an identical letter code. The numbers indicate the order of sampling time points. The genome structure was assessed by PFGE following: **A)** *XbaI* digestion; **B)** *AvrII* digestion; **C)** Comparison of the genome structure of different clones from the same urine samples by PFGE following *AvrII* digestion; **D)** Assessment of the genome size of *in vivo* re-isolates of strain 83972 by PFGE following *I-CeuI* digestion. Changes in the restriction pattern are indicated by red arrows.

Moreover, the analysis of the genomic I-*CeuI* restriction fragments by PFGE demonstrated that strain CK12 is the only re-isolate with a reduced genome size compared to strain 83972 (Fig. 25D).

In order to roughly assess the complexity of the *E. coli* 83972 population colonizing the bladder, different colonies from the same urine samples were subjected to PFGE following digestion with *AvrII* (Fig. 25C). It turned out, that all three tested re-isolates represented at least a major fraction of the bacterial population in the bladder of their hosts. While all four independent colonies tested from the urine sample KA25 and CK12 exhibited a uniform restriction pattern, one colony from the SR12 sample had the same restriction pattern as the parent strain 83972, the other three colonies had an identical DNA fingerprint that differed from that of strain 83972.

Taken together, genomic alternations of *in vivo* re-isolates were accessed. Five out of 16 re-isolates of strain 83972 showed changed genome structure as accessed by PFGE. Moreover, bacterial complexity in the bladder was low and in most cases analyzed re-isolate represented a major fraction of the bacterial population in the urine sample.

5.3.5. Phenotypes of different *in vivo* re-isolates

Motility

As the first test, re-isolates were stabbed on urine swarm agar plates to assess their motility (Fig. 26). The parent strain 83972 exhibited a very low motility, however, was not completely non-motile when compared to strain 536 Δ *fli* used as a negative control. A number of re-isolates showed a similar low motility. However, the strains IJ15, SN16, SN25, CK6, SR6 and SR12 exhibited higher motility than the strain 83972 (Table 11) and also differed among each other. Moreover, strains POS6 and POS9 were less motile than strain 83972, comparable to strain 536 Δ *fli*. These data demonstrate that strain 83972 is capable of modulating the swarming ability in response to the growth environment.

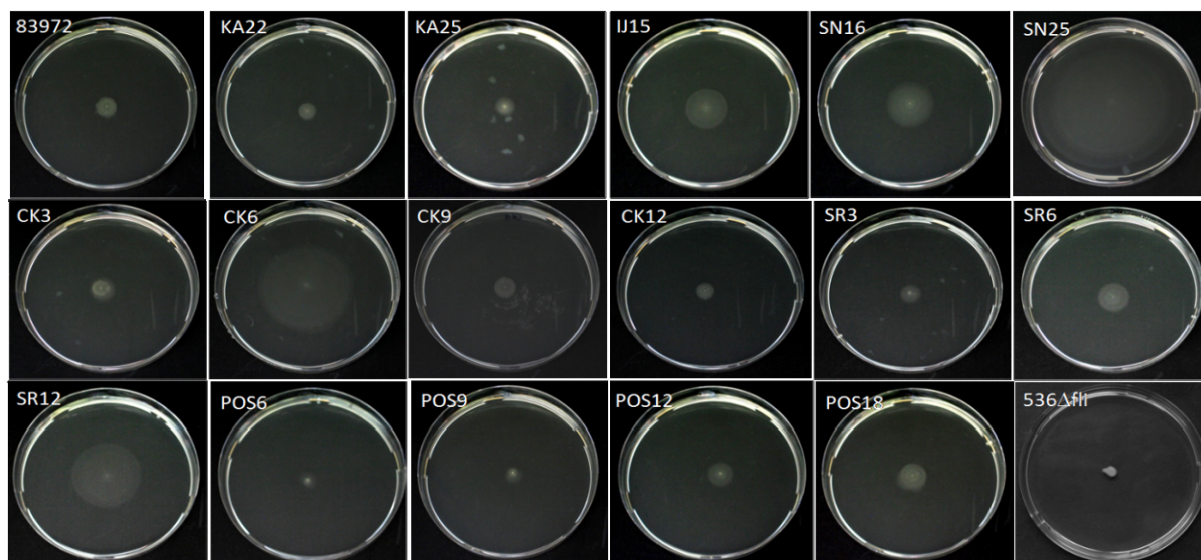


Fig. 26: Motility of *in vivo* re-isolates of strain 83972 on urine soft agar plates incubated overnight at 37 °C.

Growth characteristics

The growth characteristics of the re-isolates *in vitro* were assessed in pooled human urine as well as in LB medium and compared to those of strain 83972 (Fig. 27; Table 11). Generally, almost all re-isolates did not reach the same final bacterial number and had lower growth rates in the urine compared with the parent strain. Only growth of strains CK3, CK9 and CK12 was similar to that of *E. coli* 83972. The most significant decrease in growth was observed in case of isolates from patient POS. Interestingly, only the re-isolate SN16 grew better than strain 83972.

Bacterial growth in Luria broth resulted in similar results relative to growth in urine where most of the re-isolates grew worse with respect to growth rate and optical density reached compared to the parent strain (Table 11). Re-isolates of patient SR, however, grew as well as parent strain 83972 in LB medium (data not shown). However, the differences were most prominent for re-isolates of patients KA, IJ and POS.

These data may indicate a possible correlation between the growth characteristics of re-isolates and the immune response of their specific host. In general, re-isolates from patients with a stronger host response grew more slowly than re-isolates from patients with weaker host response. However, bacterial growth characteristics as well as host response are very complex phenomena and differ from patient to patient.

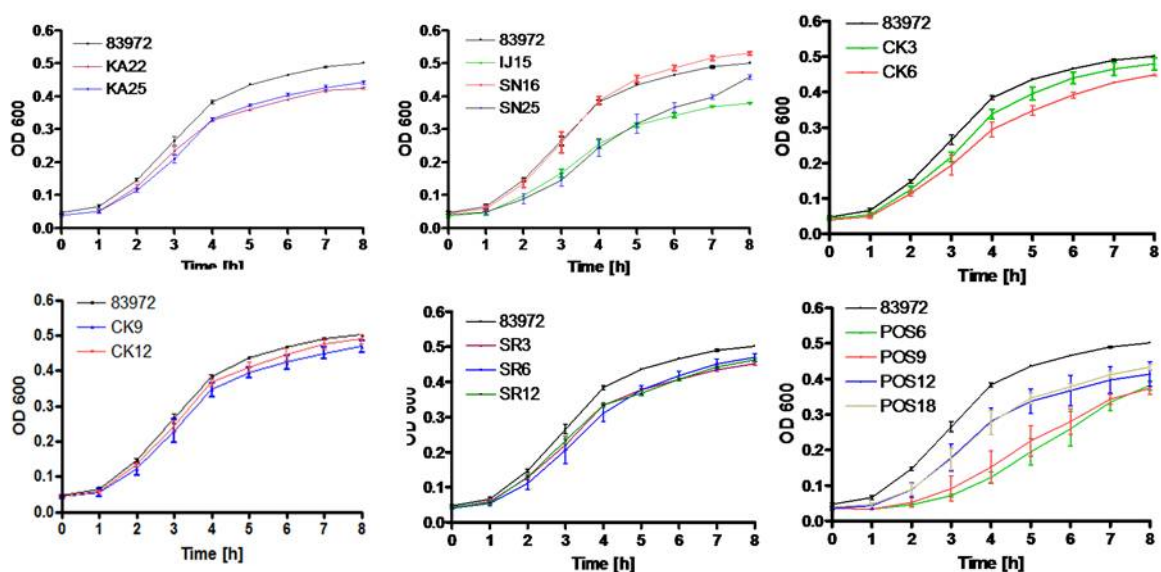


Fig. 27: Growth characteristics of *in vivo* re-isolates of strain 83972 and their parent strain in pooled human urine.

Competitiveness

To test whether the re-isolates differ with respect to competitiveness in urine from their parent strain, *E. coli* strain 83872 was tagged with a chloramphenicol resistance cassette. Using the λ Red-mediated integration of linear DNA fragments into the bacterial chromosome (Datsenko and Wanner, 2000), the *cat* cassette was integrated into the bacteriophage λ chromosomal attachment site of strain 83972.

For growth competition experiments, identical bacterial numbers of strain 83972 $_{cat}$ and one re-isolate were mixed and grown for 72 h in pooled human urine. At different time points (6, 24, 48 and 72 hours), the ratio of the parent strain 83972 $_{cat}$ and the re-isolate was determined by counting colony forming units (CFUs) on LB agar plates supplemented with chloramphenicol and LB plates, respectively. The results of the growth competition experiments with the different re-isolates are shown in Fig. 28.

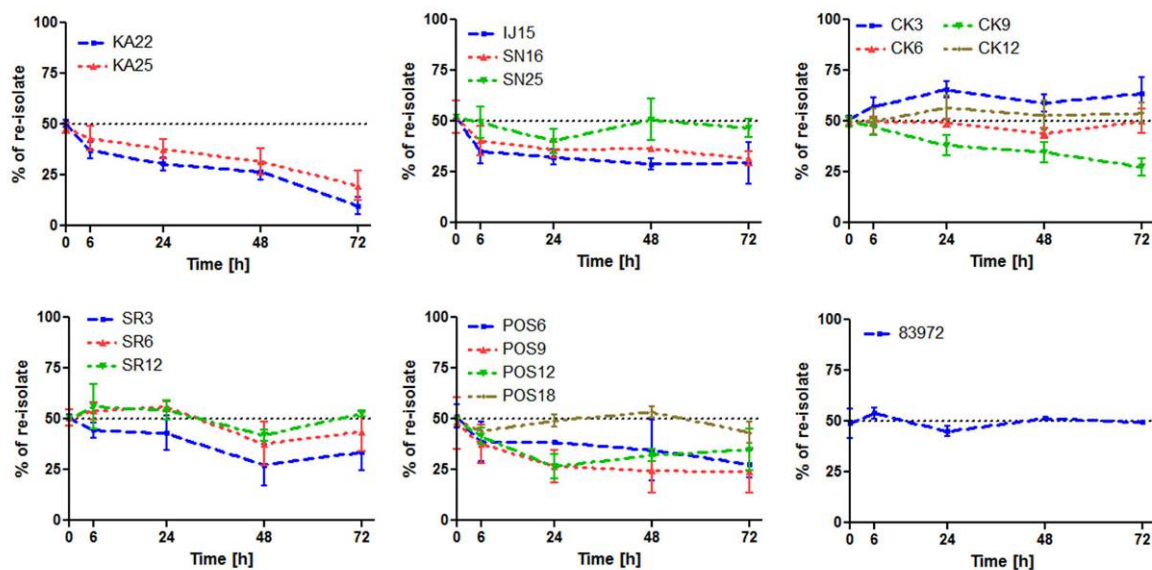


Fig. 28: Competitiveness in urine of *in vivo* re-isolates of *E. coli* 83972 against their parent strain derivative 83972*cat*. All experiments were performed in triplicates. The last graph shows the control experiment where the parent strain and its chloramphenicol-resistant variant 83972*cat* have been co-cultured.

In a control experiment, the parent strain 83972 was co-cultured with its chloramphenicol-resistant derivative 83972*cat* which did not show any difference in competitiveness thus confirming that the introduction of the *cat* cassette had no negative effect on the growth rate. However, the re-isolates co-cultured in urine with strain 83972*cat* exhibited differences in their competitiveness. The most striking difference was observed for the re-isolates KA22 and KA25 which represented only 25 % or less of the total culture after 72 h of growth. Similarly, the fraction of re-isolates IJ15 and SN16 already decreased significantly after 6 h of co-cultivation with strain 83972*cat*. With exception of strain SN16, this could be correlated with the reduced growth of these strains relative to their parent strain (Fig. 27). Most of the re-isolates from patient POS as well as strain CK9 were also outcompeted to a different extend by the strain 83972*cat*. Generally, re-isolates which were shown to be less competitive were also characterized by slower growth rates in urine relative to the parent strain.

Biofilm formation

It has been published that increased biofilm formation is characteristic for ABU isolates and that this trait may be important for colonization of the urinary tract (Hancock *et al.*, 2007). Consequently, re-isolates obtained from the human colonization study were investigated for their biofilm forming ability. For that purpose, bacteria were grown in microtiter plates in pooled human urine, as well as in M63 minimal medium, and the biofilm formation was

compared to that of strain 83972 (section 4.5.4.). In addition, UPEC strain 536 and non-pathogenic laboratory K-12 strain MG1655 were included as positive and negative controls, respectively (Fig. 29).

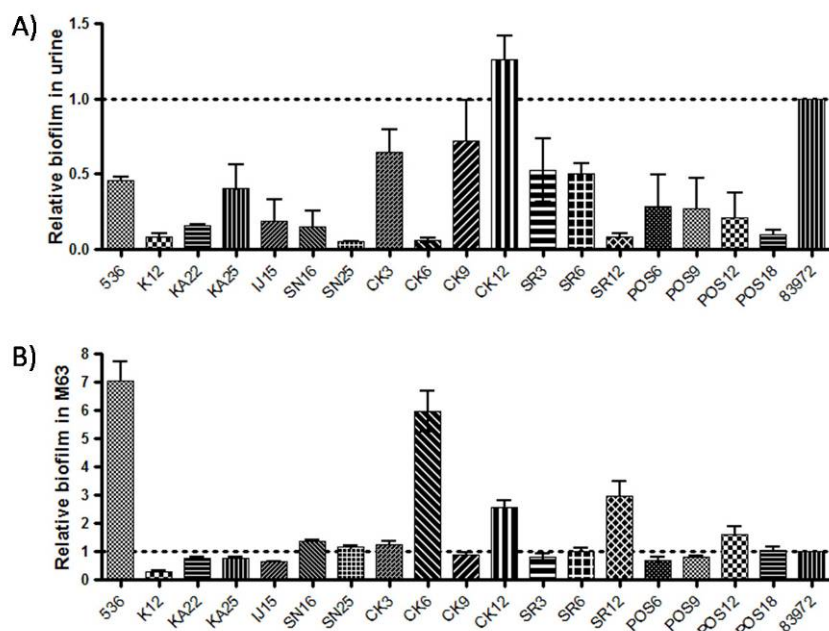


Fig. 29: Analysis of biofilm formation of *in vivo* re-isolates of ABU strain 83972 at 37 °C. **A)** Biofilm formation in pooled human urine; **B)** Biofilm formation in M63 media. Biofilm formation of the strains tested was normalized to that of parent strain 83972.

Surprisingly, except for strain CK12, all re-isolates formed poorly biofilm in urine when compared to strain 83972. Moreover, the ability to form biofilms of re-isolates SN25, CK6, SR12 and POS18 was as low as or less than that of non-pathogenic K-12 strain MG1655. The ability to form biofilms of the other seven re-isolates (KA25, CK3, SR3, SR6, POS6, POS9, POS12) was comparable to that of UPEC strain 536. In general, most of the tested re-isolates were not able to form as good biofilm as the ancestor strain 83972. In contrast, the biofilm assays in M63 minimal medium showed very distinct results. Except for strains CK6, CK12 and SR12, biofilm formation of the re-isolates was comparable to that of their parent strain 83972. Re-isolate CK6 formed nearly as much biofilm as strain 536, which was 7-fold higher than that of strain 83972.

In general, biofilm formation could be correlated with the swarming ability (Fig. 26). Strains with increased motility formed less biofilm than strains exhibiting low motility. The results of the phenotypic characterization of the *in vivo* re-isolates of strain 83972 are summarized in Table 10.

Table 11: Geno- and phenotypic characterization of *in vivo* re-isolates of ABU strain 83972. Arrows up and down indicate better or worse than ABU83972, respectively; = no difference

Re-isolate	Date of isolation	Duration of bladder colonization [days]	IL6 level in urine [pg/ml]	IL8 level in urine [ng/ml]	No. of PMNs in urine x 10 ⁴ /ml	<i>Xba</i> I	<i>Sfi</i> I	<i>Avr</i> II	Genome size	Motilit	Growth (UR)	Growth (LB)	Competitiveness(UR)	Biofilm (UR)	Biofilm (M63)
KA 22	2/22/2005	130	9	833	78				=	=	↓	↓	↓	↓	↓
KA 25	5/17/2005	214	6	586	66			+	=	=	↓	↓	↓	↓	↓
IJ 15	8/9/2004	185	2	604	7	+	+		=	↑	↓	↓	↓	↓	↓
SN 16	1/17/2005	108	2.8	59	2				=	↑	↑	↑	↓	↓	=
SN 25	10/17/2005	24	2.8	41	nd				=	↑	↓	↓	=	↓	=
CK 3	12/16/2004	83	2.8	287	3				=	=	=	↓	↑	↓	=
CK 6	3/23/2005	180	17	1069	16,7				=	↑	↓	↓	=	↓	↑
CK 9	6/23/2005	63	5	586	22				=	=	=	↓	↓	↓	=
CK 12	9/23/2005	155	13	952	10	+	+	+	↓	=	=	=	=	↑	↑
SR 3	2/3/2005	77	21	278	13				=	=	↓	=	↓	↓	=
SR 6	4/5/2005	138	7	30	3	+	+		=	↑	↓	=	=	↓	=
SR 12	11/1/2005	54	10	245	21			+	=	↑	↓	=	=	↓	↑
POS 6	12/2/2004	168	4	731	43				=	↓	↓	↓	↓	↓	↓
POS 9	3/4/2005	260	7	774	96				=	↓	↓	↓	↓	↓	=
POS 12	6/3/2005	351	9	505	29				=	=	↓	↓	↓	↓	=
POS 18	12/5/2005	536	nd	nd	nd				=	=	↓	↓	=	↓	=

Differences in the restriction pattern are indicated by “+”. An increase or decrease of the traits tested relative to ABU strain 83972 is indicated by corresponding arrows; no differences between re-isolate and parent strain are indicated by “=”.

Taken together, these data demonstrate differences in phenotypes of strain 83972 *in vivo* re-isolates. Consequently, growth characteristics were affected and almost all re-isolates did not reach the same final bacterial number and had lower growth rates in the urine. Generally, re-isolates that were characterized by slower growth rates in urine, were shown to be less competitive relative to the parent strain. These data also demonstrate that strain 83972 is capable of modulating the swarming ability in response to the growth environment. Furthermore, most of the tested re-isolates were not able to form as good biofilm as the parent strain 83972 and this phenotype could be correlated with the swarming ability.

5.3.6. Host independent growth of *E. coli* strain 83972

Bacterial growth is modulated by several environmental factors like competition for nutrients, niche-specific conditions, or host response. In order to identify host factors that affect bacterial growth and adaptation, an *in vitro* continuous culture system was designed in which cultures of strain 83972 could be propagated for more than 2000 generations without an impact of host factors. Consecutive *in vitro* re-isolates of strain 83972 were taken once a week and characterized with regard to their pheno- and genotypic properties.

Strain 83972 was grown in LB medium and pooled human urine with and without addition of nitric oxide (NO). Under all four conditions, strain 83972 grew very well (Fig. 30) and the growth rates were comparable in cultures with and without NO. However, for cultures in LB medium with and without addition of NO the optical density and number of CFU tended to rise with time of the experiment. Also, in all four microfermenters the OD₆₀₀ and CFU slightly varied, what could be due to sampling errors. Nevertheless, an increase in OD₆₀₀ always corresponded to an increase in CFU.

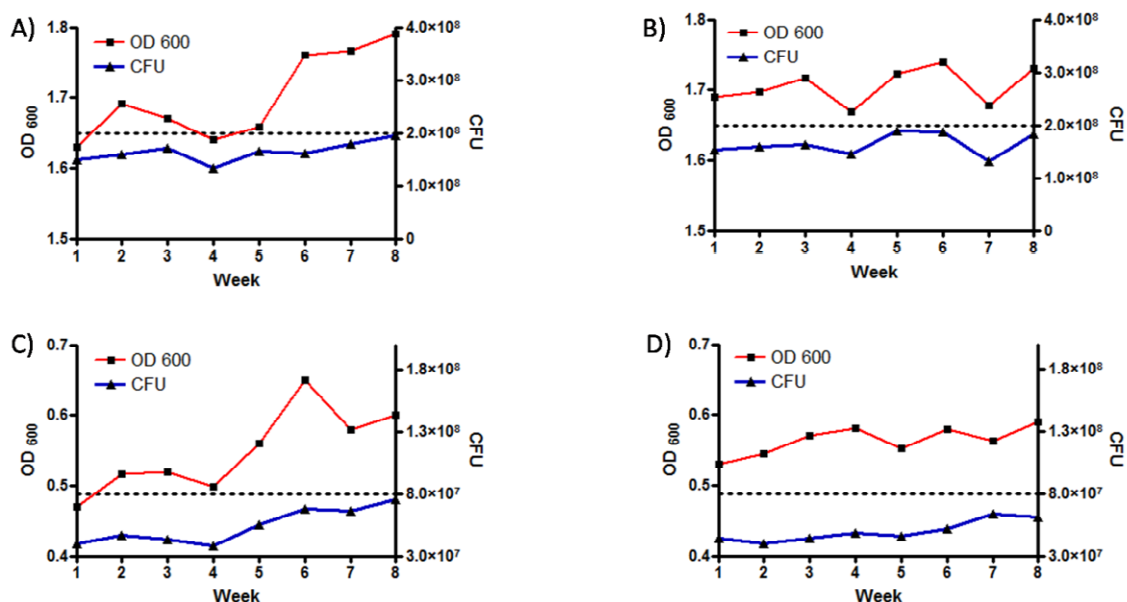


Fig. 30: Growth dynamics of *E. coli* strain 83972 during continuous culture experiments in LB medium + NO A), urine + NO B), LB medium C) and urine D).

At each sampling time point, bacteria were tested for spontaneous occurrence of resistance against streptomycin in order to monitor the occurrence of mutator phenotypes. Only three

resistant isolates were found, however, at different sampling points. Interestingly, all of the resistant clones were obtained from the urine + NO culture, after 1, 2 and 6 weeks of cultivation.

Moreover, biofilm formation of strain 83972 differed under these four growth conditions (Fig. 31). The addition of exogenous nitric oxide significantly decreased biofilm formation without affecting bacterial growth (Fig. 30). Scanning electron microscopy indicated that the drastic differences could be due to extracellular matrix production. Comparing samples from the urine cultures with and without nitric oxide indicated that the biofilm structure without exposure to nitric oxide is more homogenous and less densely packed with crystals and extracellular matrix (Fig. 31 B and D).

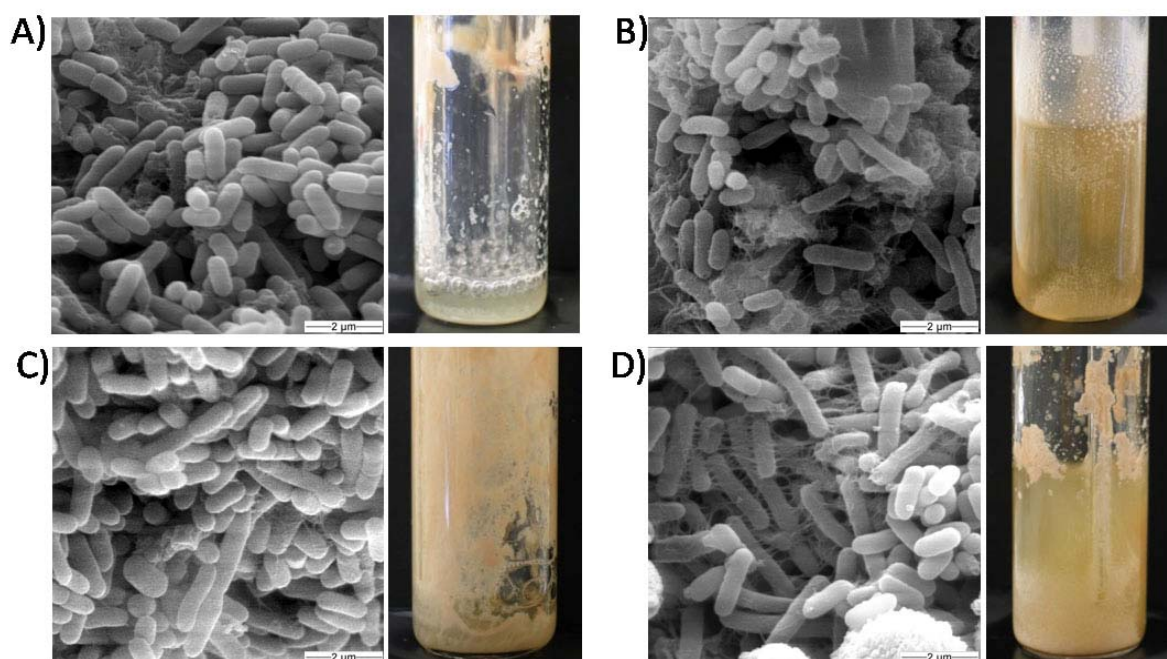


Fig. 31: Biofilm formation of ABU strain 83972 in continuous cultures in LB medium + NO **A**), urine + NO **B**), LB medium **C**) and urine **D**). In each section of the figure: left – scanning electron micrograph of the biofilm architecture; right – overview of biofilm formation in the corresponding microfermenter.

Taken together, an *in vitro* continuous culture system was designed in which strain 83972 was successfully propagated for more than 2000 generations and later on compared to those re-isolates obtained from patient colonisation study.

5.3.7. Genomic and phenotypic properties of ABU strain 83972 grown *in vitro*

In order to characterise genotypic and phenotypic properties of the strain 83972 after long term *in vitro* continuous culture, single *in vitro* re-isolates were defined. For this purpose, 17 independent colonies from every microfermenter were picked at the last sampling event after more than 2000 generations. Every colony was subsequently grown overnight in the same medium in which it has been propagated before. Bacteria from these cultures which represented an individual 83972 *in vitro* re-isolate were stored in glycerol stocks at -80 °C for later experiments.

Genetic structure of the in vitro 83972 re-isolates

According to restriction pattern determined by pulsed-field gel electrophoresis following digestion with *Xba*I or *Avr*II, the genetic structure of all *in vitro* re-isolates was not altered and was identical to that of strain 83972 used for initial inoculation of the fermenters (Fig. 32). This discovery is in contrast to the results obtained for the genome structure of *in vivo* *E. coli* 83972 re-isolates where multiple genome rearrangements were described even after less generations of growth in the human bladder (Fig. 25).

Interestingly, even the addition of mutagenic nitric oxide did not result in genomic alterations in *E. coli* strain 83972. The fact that growth in the human bladder induced genomic alterations detectable by PFGE, but not *in vitro* culture in pooled human urine, indicates that specific conditions exist within the human urinary tract which are driving forces of bacterial genome plasticity.

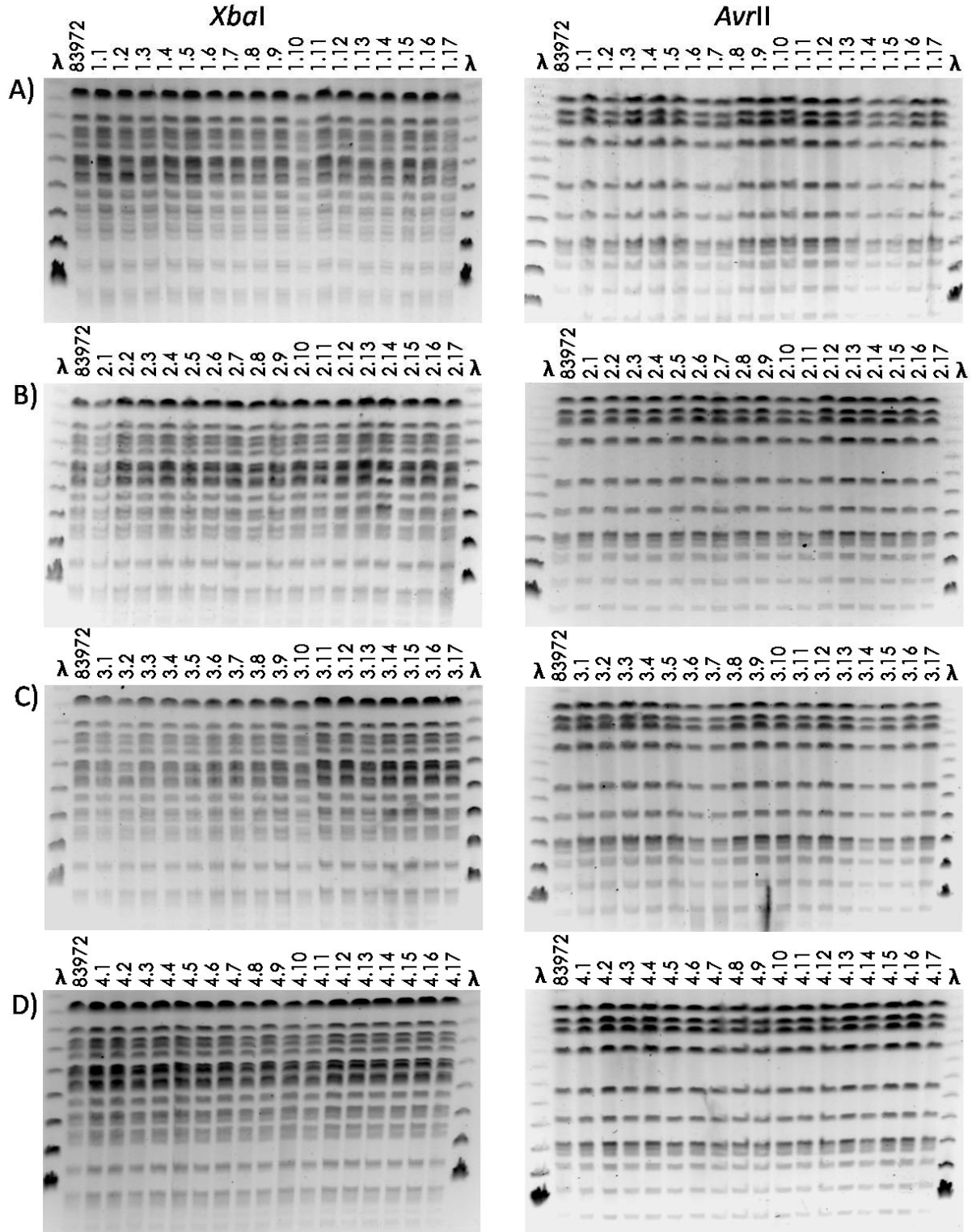


Fig. 32: Comparison of the genome structure of *in vitro* re-isolates of *E. coli* strain 83972 by PFGE following restriction with *XbaI* (left column) and *AvrII* (right column). 17 independent colonies were picked after more than 2000 generations in continuous cultures in LB medium + NO A), urine + NO B), LB medium C) and urine D).

Motility

As already described before (section 5.3.5.), *E. coli* strain 83972 is able to modulate the expression of flagella. The comparison of motility of *in vitro* re-isolates corroborated these results. In general, growth in Luria broth resulted more frequently in the occurrence of isolates with a changed motility relative to the parent strain 83972 than growth in urine. Interestingly, increased motility was only observed among urine culture isolates. In LB + NO culture, 1/3 of bacterial isolates showed decrease in motility, whereas in LB without NO culture already 2/3 isolates were non-motile. Similarly, in the urine cultures, the addition of NO decreased double the number of non-motile 83972 isolates (Table 12). Interestingly, in LB and urine cultures without addition of NO, decrease in motility could be correlated with increased whole culture population biofilm formation (Fig. 31).

Table 12: Motility of *in vitro* 83972 re-isolates on urine soft agar plates.

Re-isolate	LB + NO	UR + NO	LB - NO	UR - NO
1	0.0 ^a	4.0	8.3	3.3 ^a
2	2.7 ^a	9.3	0.0 ^a	7.0
3	6.0	6.7	2.3 ^a	3.3 ^a
4	5.3	7.3	11.0	12.7
5	4.7	6.7	2.0 ^a	10.3
6	6.3	7.3	2.0 ^a	8.0
7	2.0 ^a	3.3 ^a	2.0 ^a	12.0
8	6.3	14.0 ^b	0.0 ^a	6.0
9	0.0 ^a	6.0	9.0	11.3
10	3.0 ^a	2.0 ^a	13.7	3.0 ^a
11	3.0 ^a	5.3	0.0 ^a	26.3 ^b
12	5.0	6.3	0.0 ^a	3.0 ^a
13	7.0	8.7	0.0 ^a	22.7 ^b
14	5.0	6.7	0.0 ^a	22.0 ^b
15	6.7	23.3 ^b	0.0 ^a	11.3
16	5.3	6.3	0.0 ^a	3.0 ^a
17	8.0	29.0 ^b	0.0 ^a	6.0
83972	9.0	9.0	9.0	9.0

Motility was measured as the diameter [mm] of the swarming zone on the agar plate.

^{a)} less motile than the wild type strain 83972

^{b)} more motile than the wild type strain 83972

Growth characteristics

In addition, the growth characteristics of the *in vitro* re-isolates were tested in pooled human urine. In general, growth of all tested *in vitro* re-isolates did not differ markedly from those of their parent strain 83972 (Fig. 33). Nevertheless, most of the re-isolates from urine cultures

exhibited a slightly increased growth rate. Differences in the growth rates of re-isolates from LB cultures were always in range of the standard deviation.

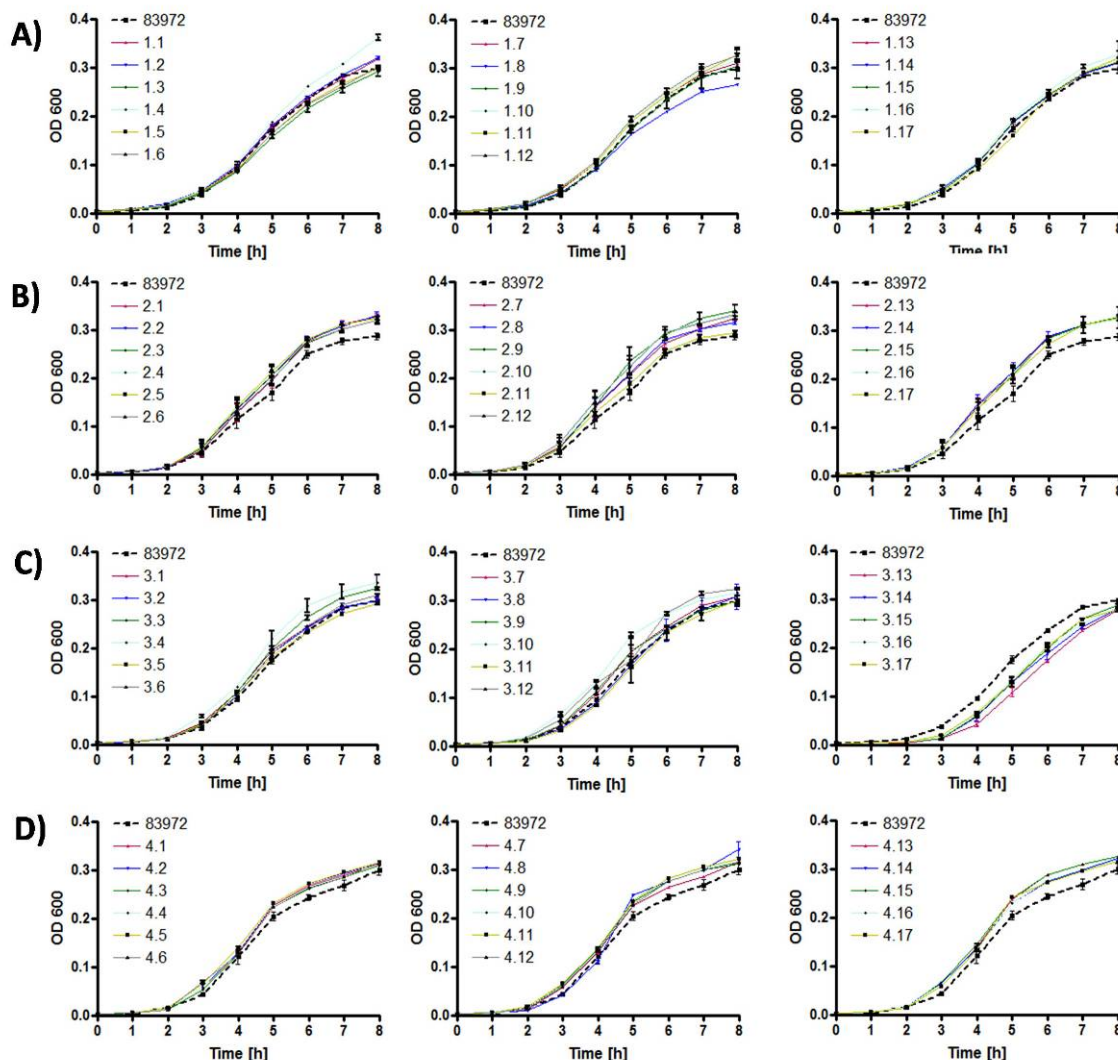


Fig. 33: Growth characteristics of *in vitro* re-isolates of strain 83972 and their parent strain in pooled human urine at 37 °C. 17 independent re-isolates were selected after more than 2000 generations in continuous cultures in LB medium + NO **A)**, urine + NO **B)**, LB medium **C)** and urine **D)**.

Biofilm formation

Similarly, the comparison of biofilm formation by the *in vitro* re-isolates resulted in a very few significant differences when compared to that of parent strain 83972 (Fig. 32). If biofilm formation of the *in vitro* re-isolates was altered relative to strain 83972, increased biofilm formation was observed mainly for isolates from LB cultures. Noteworthy, this observation is

in striking contrast to the results seen with the *in vivo* re-isolates (Fig. 26), which exhibited a remarkable decrease in biofilm formation.

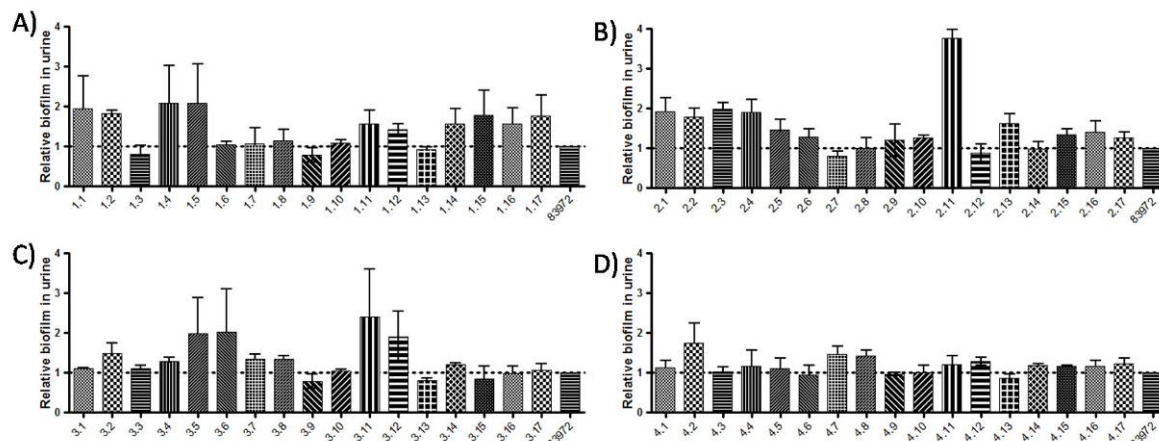


Fig. 34: Analysis of biofilm formation of *in vitro* re-isolates of ABU strain 83972 in pooled human urine at 37 °C. 17 independent re-isolates were selected after more than 2000 generations in continuous cultures in LB medium + NO **A**), urine + NO **B**), LB medium **C**) and urine **D**). Biofilm formation of the strains tested was normalized to that of parent strain 83972.

Taken together, genotypic and phenotypic properties of the strain 83972 after long term *in vitro* continuous culture were assessed. Consequently, the restriction pattern determined by pulsed-field gel electrophoresis revealed that the genetic structure of all *in vitro* re-isolates was not altered and was identical to that of strain 83972. This is in contrast to the finding that the genome structure of *in vivo* *E. coli* 83972 re-isolates, even after less generations of growth in the human bladder, was affected in multiple re-isolates. The growth characteristics of the *in vitro* re-isolates tested in pooled human urine did not differ markedly from those of their parent strain 83972. Similarly, the comparison of biofilm formation by the *in vitro* re-isolates resulted in a very few significant differences when compared to that of parent strain 83972. These observations are in striking contrast to the results seen with the *in vivo* re-isolates.

5.4. Transcriptome analysis of 83872 re-isolates

Multiple pheno- and genotypic experiments uncovered striking differences among *in vivo* 83972 re-isolates. In contrast, *in vitro* re-isolates exhibited fewer alterations. To evaluate changes on the transcriptional level, microarray experiments were performed. The transcriptome of parent strain 83972 was compared with those of the *in vivo* re-isolates SR12, CK12, KA25 and one randomly chosen *in vitro* re-isolate 4.9 upon growth in pooled human urine. RNA was extracted from the mid-logarithmic growth phase followed by reverse transcription using fluorescent labelled nucleotides. The resulting cDNA was hybridized to an oligonucleotide DNA microarray (OPERON). For each re-isolate three independent competitive hybridisations were performed.

5.4.1. Significant changes in the expression pattern

The statistical analysis using t-test showed a significant reproducibility of the triplicate hybridisations (Table 13). All changes in the expression patterns of the re-isolates must be due to prolonged growth either in the human bladder or in the continuous *in vitro* culture and could be still detectable after *in vitro* growth in pooled human urine. Exception for strain SR12, the vast majority of significantly affected genes in the other re-isolates were down-regulated when compared to the parent strain 83972 (Table 13). Interestingly, in all *in vivo* re-isolates the number of significantly affected genes was on average four-fold higher than in the *in vitro*-grown strain.

Table 13: Total number of de-regulated genes in the *in vivo* and *in vitro* re-isolates of ABU strain 83972.

	SR12	CK12	KA25	4.9
p < 0.05	2960	2630	2944	2065
up-regulated	170 (60 %)	35 (21 %)	35 (20 %)	6 (12 %)
down-regulated	109 (40 %)	131 (79 %)	135 (80 %)	43 (88 %)
Total ^a	279	166	170	49

^aNumber of significantly up- and down-regulated genes

De-regulated genes were allocated to different functional categories (Fig. 35). The distribution of down-regulated genes among the re-isolates was very diverse, however, strains CK12 and KA25 exhibited a certain similarity in the expression pattern of de-regulated genes. Strain SR12 differed not only in the total number of down-regulated but also in the high number of up-regulated genes, from which the vast majority could be grouped as coding for hypothetical

proteins, carbon and energy metabolism, and motility proteins. The high energy consumption due to flagella expression may be one reason for the increased expression of many genes involved in transport and energy production.

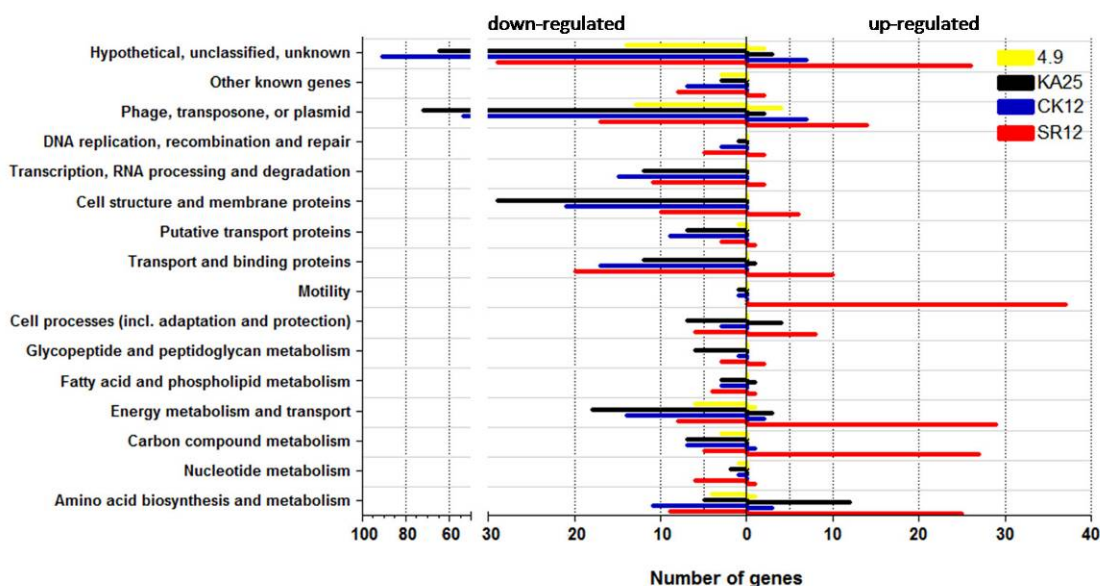


Fig. 35: Functional grouping of the de-regulated genes in *in vivo* and *in vitro* re-isolates of ABU strain 83972 upon *in vitro* growth in pooled human urine.

Apart from genes coding for hypothetical proteins and genes with unknown function, the second largest group of genes comprises those related to mobile elements like phages, transposons and plasmids (Fig. 35).

5.4.2. Individual adaptation of re-isolates

Hierarchical cluster analysis of all the genes affected as determined by microarray hybridisation demonstrated remarkable differences among the investigated re-isolates. The cluster analysis grouped together genes with the same expression pattern and resulted in six subclusters, of which the first two subclusters represent groups of differently up-regulated genes in the re-isolates. The last four subclusters pinpoint genes which are only down-regulated in the individual strain (Fig. 36).

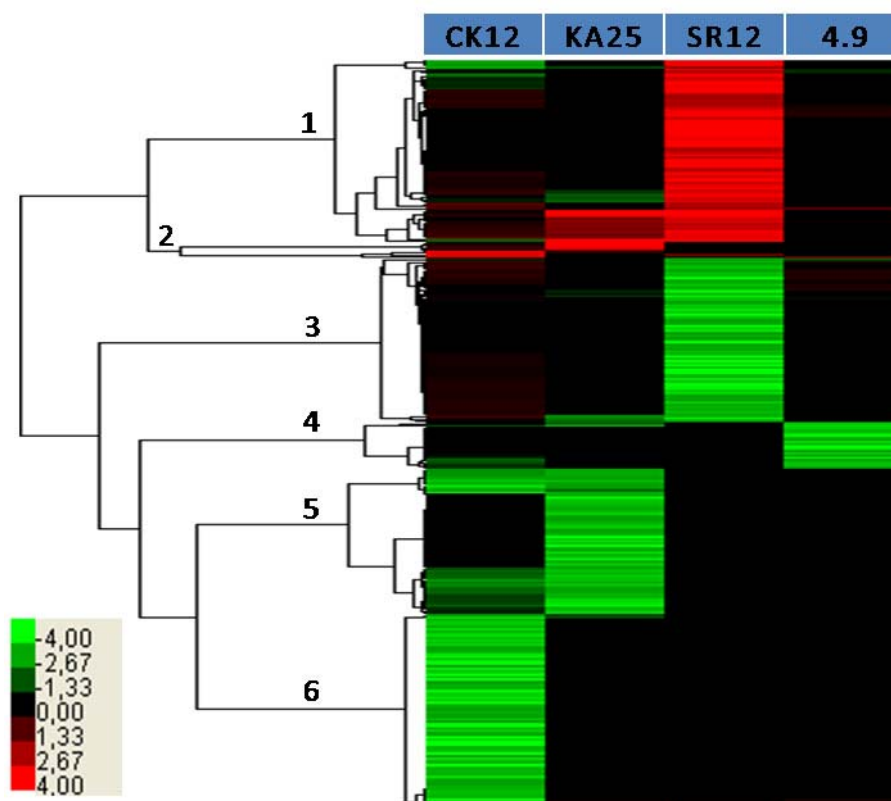


Fig. 36: Hierarchical cluster analysis of all de-regulated genes in three ABU 83972 *in vivo* re-isolates CK12, KA25 and SR12 and one *in vitro* re-isolate 4.9 relative to their parent strain 83972. The strains were grown *in vitro* at 37 °C in pooled human urine. Each bar represents one gene and its expression level corresponds to the colour bar on the bottom left hand side. Numbers from 1 to 6 indicate six sub-clusters of commonly regulated genes in one re-isolate. The datasets for each strain are mean values of the expression ratio from at least three independent microarray experiments. Genes without statistically significant changes in their expression pattern (p -value >0.05) are shown in black.

Interestingly, in each strain distinct genes were affected. This illustrates the very unique environmental conditions faced by the different bacteria. Although the re-isolates SR12, KA25 and CK12 originate from the human colonization study, not many commonly de-regulated genes could be observed. However, a subgroup of genes from the subcluster 1 and 4 show similarity exclusively in between the *in vivo* re-isolates (Fig. 36). In contrast, only a few genes which were grouped into subcluster 4 were de-regulated in the *in vitro* re-isolate 4.9.

Transcriptome changes of in vitro re-isolate 4.9 relative to parent strain 83972

Interestingly, the two component system TorSR involved in the regulation of the carbon metabolism and anaerobic respiration (Jourlin *et al.*, 1997) was down-regulated in re-isolate 4.9. This regulatory system also controls the transcriptional regulation of the *gadAX* operon,

which was also down-regulated in strain 4.9 according to the array data. GadA, a glutamate decarboxylase, is part of the glutamate-dependent acid resistance system 2 (AR2) which confers resistance to extreme acid conditions. AR2 also protects the cell during anaerobic phosphate starvation when glutamate is available by preventing damage from weak acids produced from carbohydrate fermentation (Moreau, 2007). In addition to that, all genes of the regulon *gcl-hyi-glxR-ybbVW-allB-ybbY-glxK* involved in glyoxylate catabolism and the allantoin assimilation pathway turned out to be down-regulated. These reactions take place during anaerobic respiration.

Taken together, among hypothetical proteins and phage-related genes, most of the changes in the global gene regulation pattern of the *in vitro* re-isolate 4.9 are implicated in anaerobic respiration (Table 24 and Table 25).

Transcriptome changes of in vivo re-isolate SR12 relative to parent strain 83972

Genes with higher expression levels in the *in vivo* re-isolates were grouped into the sub-clusters 1 and 2. Most of them are exclusively up-regulated in strain SR12. As already shown in Fig. 35, the affected genes encode for the flagella apparatus and chemotaxis, or are involved in carbohydrate transport and metabolism, as well as energy production and conversion (Table 18).

Pentose and glucuronate interconversions as well as sialic acid, arabinose, mannose and xylose uptake and metabolism seem to be main pathways involved in extra energy delivery during growth in urine (Fig. 37). Most likely, up-regulation of these genes is directly connected to the nutrient availability during *in vivo* growth in the bladder. These sugars are taken up by a number of up-regulated uptake systems and degraded thus supplying the glycolysis with glyceraldehyde-3-phosphate.

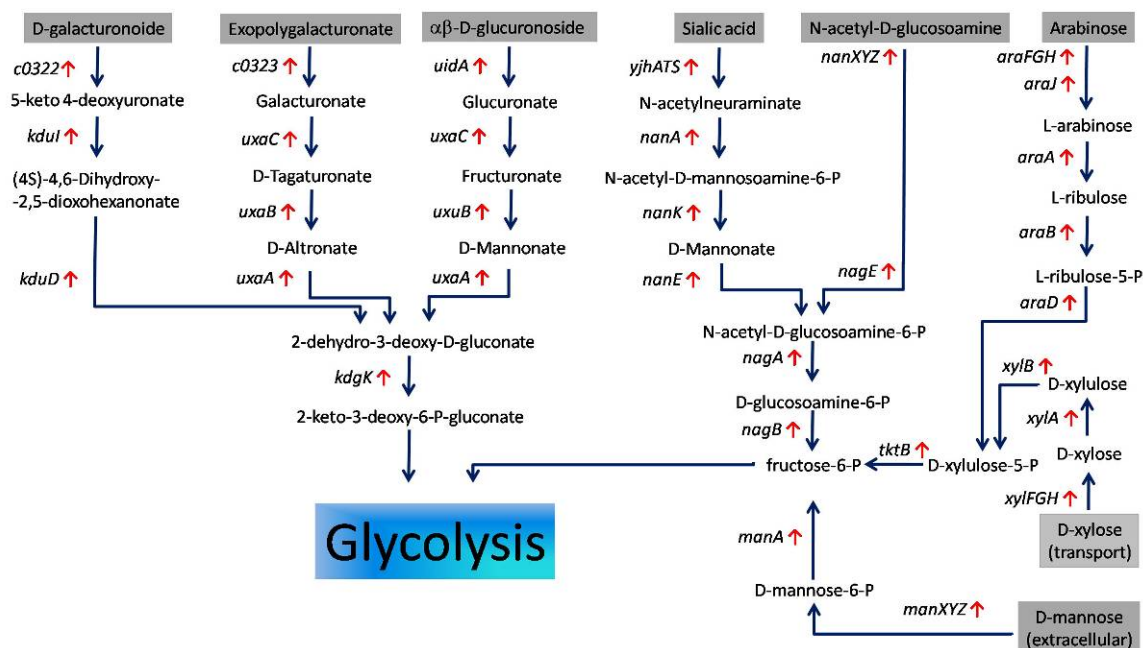


Fig. 37: Altered expression of sugar transport and degradation pathways in the *in vivo* re-isolate SR12 compared to strain 83972. Red arrows indicate up-regulated genes during *in vitro* growth in pooled human urine.

Moreover, a number of genes involved in the citrate cycle (TCA cycle) and glutamate metabolism were found to be affected in strain SR12 (Table 18 and Table 19). The two genes, *glnG* encoding the response regulator (NtrC, synonymous name GlnG) and *glnL* encoding the sensor kinase (NtrB, synonymous name GlnL) were down-regulated. NtrB functions as a membrane-associated protein kinase that phosphorylates NtrC in response to nitrogen- and carbon-limitation. This reflects adaptation to urine, which is a nitrogen-rich environment. This two component system regulates the expression of the *glnALG* and *glnHPQ* operons, which indeed were down-regulated according to the array results. In addition to that, purine degradation turned out to be down-regulated. Interestingly, D-serine uptake and deamination pathway to pyruvate were significantly up-regulated in re-isolate SR12 relative to parent strain 83972.

Transcriptome changes of in vivo re-isolates KA25 and CK12 relative to parent strain 83972

The hierarchical cluster analysis grouped most of the down-regulated genes together (subclusters 3-6; Fig. 36). Interestingly, major fractions of the genes with the same expression pattern were strain-specific. After functional classification, it turned out that most of the genes

encode for hypothetical, unclassified and unknown proteins. The second largest group of genes comprises those related to mobile elements like phages, transposons and plasmids (Table 21 and Table 23). The significance of this result might be questionable, since many of the de-regulated genes don't represent complete transcriptional units. Nevertheless, each re-isolate represents a unique gene expression pattern that is due to distinct environmental niches that bacteria have been growing in.

5.4.3. Common adaptive patterns in re-isolates

To identify general adaptation strategies to prolonged bacterial growth in urine, hierarchical cluster analysis was performed to group genes of at least two re-isolates that are commonly de-regulated. Altogether, 35 genes turned out to be similarly expressed in more than one re-isolate relative to strain 83972 (Fig. 38).

Four clusters of genes were formed according to similar changes of their expression pattern among at least two re-isolates. The clusters one and two represent genes which are similarly expressed in re-isolates CK12 and KA25. The last two clusters comprise commonly regulated genes of re-isolates SR12 and KA25.

The first cluster comprises nine genes that are less expressed in re-isolates CK12 and KA25 relative to the parent strain 83972. Except for the gene *glpC*, the remaining eight genes code for hypothetical proteins with predicted function. The meaning of this result is unclear as these nine genes represent single genes of polycistronic operons. Subcluster 2 consists of eight genes whose expression was similarly affected in strains CK12 and SR12. As already shown by phenotypic tests (Fig. 26), the *in vivo* re-isolates differed in their ability to express flagella. Although strain CK12 was as motile as the parent strain 83972, microarray data indicated that the expression of two genes, *flgB* and *tar*, which are involved in motility and chemotaxis, was down-regulated. In contrast, in strain SR12 these genes were up-regulated. This is consistent with the corresponding phenotype (section 5.3.5.).

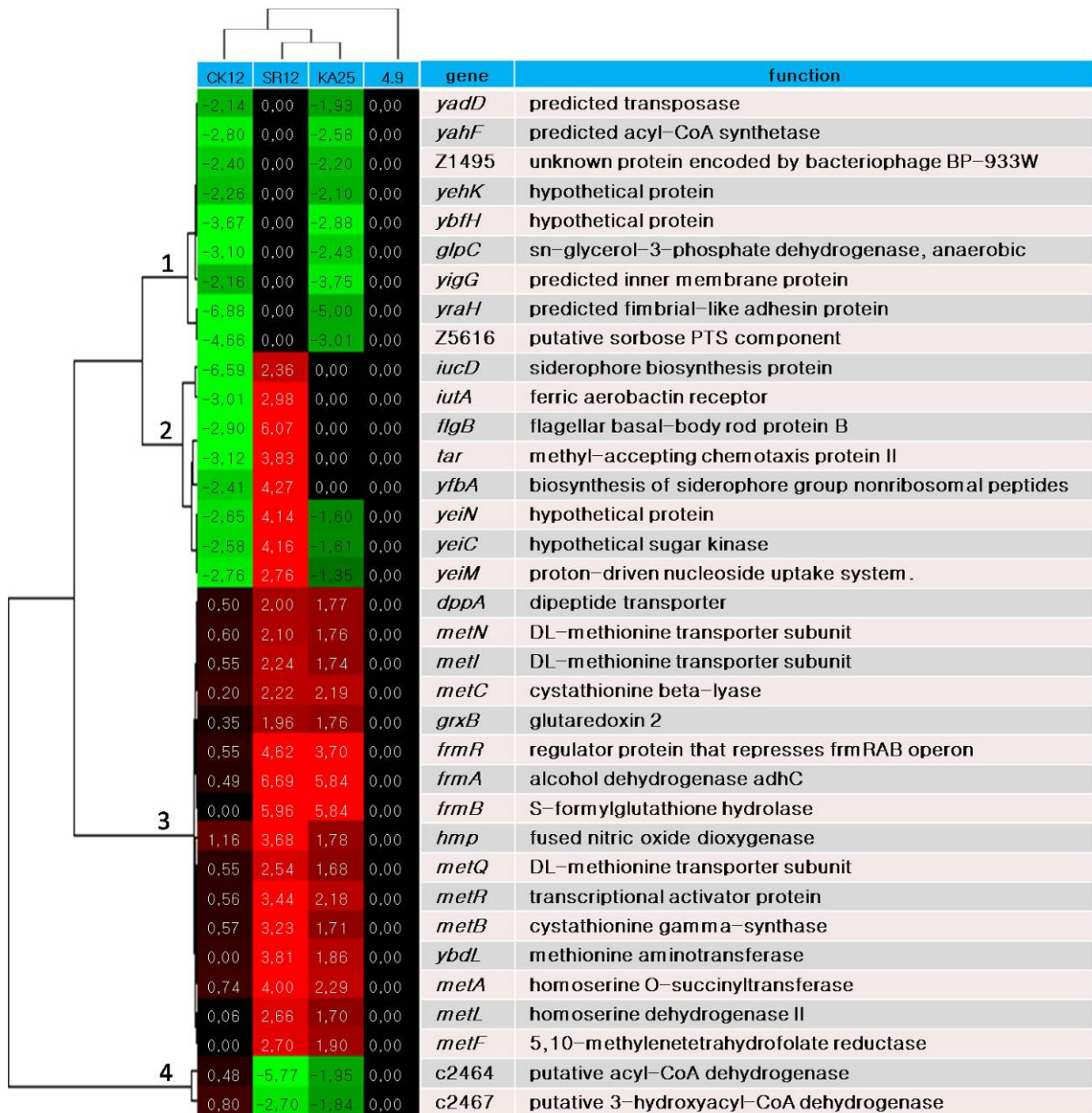


Fig. 38: Hierarchical cluster analysis of commonly de-regulated genes in at least two re-isolates of strain 83972 relative to their parent strain. Numbers from 1 to 4 indicate the four main subclusters of commonly de-regulated genes. Clustered values are mean values of the expression ratio from at least three independent microarray experiments. Results with a p-value >0.05 are indicated in black colour.

Moreover, together with *flgB* and *tar*, almost the entire determinants coding for the flagellar apparatus were significantly up-regulated in re-isolate SR12 (Table 18). Several genes of subcluster 2 belong to gene clusters, e.g. *yeiCNM* as well as *iucD*, *iutA* and *yfbA*.

The last two subclusters include 18 commonly de-regulated genes of re-isolates SR12 and KA25. While 16 genes were up-regulated, expression of the remaining two genes was

repressed relative to the parent strain 83972. Interestingly, in the group of up-regulated genes the whole *frmRAB* gene cluster could be found. The FrmA protein is a glutathione-dependent alcohol dehydrogenase that is, together with FrmB, involved in the metabolism of endogenously formed formaldehyde and detoxification of exogenous formaldehyde (Gutheil *et al.*, 1997). However, it was also shown that this alcohol dehydrogenase (also designated AdhC) is conserved from humans to bacteria and apart from the metabolic functions mentioned before is involved in the protection against nitrosative stress (Liu *et al.*, 2001). In addition to that, the gene *hmp* encoding for flavohemoglobin was grouped right next to the *frmRAB* operon. Multiple studies describe the implication of Hmp in protection against NO released upon bacterial infection (Crawford and Goldberg, 1998; Poole *et al.*, 1996). Moreover, many genes encoding proteins involved in glycine, serine, threonine and methionine transport and metabolism were found within the same subcluster (Fig. 38). The MetR protein was already shown to bind and modulate the *glyA-hmp* intergenic region. This results in induction of flavohemoglobin expression encoded by *hmp* gene (Membrillo-Hernandez *et al.*, 1998). Altogether, this supports the significance of the transcriptome data and functional relationship of genes as displayed in the cluster analysis.

In contrast to the previously described up-regulated genes, two genes coding for putative dehydrogenases were down-regulated in strains SR12 and KA25 relative to strain 83972 (subcluster 4; Fig. 38). Interestingly, both of them are located within a polyketide biosynthesis gene cluster (Nougayrede *et al.*, 2006).

5.4.4. Verification of microarray results by quantitative RT-PCR

Quantitative RT-PCR was performed to verify changes of transcript levels of selected genes as determined by DNA array hybridization. In general, the trend of de-regulation of gene expression as determined by microarray results could be confirmed by quantitative RT-PCR. Transcript levels of the genes *metR* and *hmp* were about two times higher in strain SR12 than in strain KA25, while in strains CK12 and 4.9 the differences were not significant (less than 2-fold) relative to strain 83972. The expression level obtained for the *tar* gene was 200-fold higher and 4-fold lower than in strains SR12 and CK12, respectively. A significant down-regulation could be observed for expression of *iutA* and *yeiC* in strain CK12 (15- and 12-fold), whereas in strain SR12 these genes were up-regulated 5- and 8-fold, respectively. The

transcript levels of the gene *frmA* encoding the glutathione-dependent alcohol dehydrogenase (AdhC) were analyzed in a larger number of *in vivo* re-isolates (Fig. 39 A). It turned out that *frmA* expression is up-regulated in other *in vivo* re-isolates as well. Moreover, *frmA* expression levels in strains isolated from the same patient were comparable, while they differed from patient to patient. The highest *frmA* transcript level could be observed in re-isolates from patient SR (120-fold higher than in the parent strain). In re-isolates from patients KA and POS, the up-regulation was on average 40-fold and 5-fold, respectively. It is important to mention, that the patient SR was colonized twice during the course of study (Table 11) and that re-isolate SR12 was obtained from an independent inoculation event compared to strains SR3 and SR6. Taken together, the significant up-regulation of the gene *frmA* could be observed in all re-isolates obtained from the patients KA, SR and POS, indicating that the adaptation of bacterial gene regulation might be patient-specific.

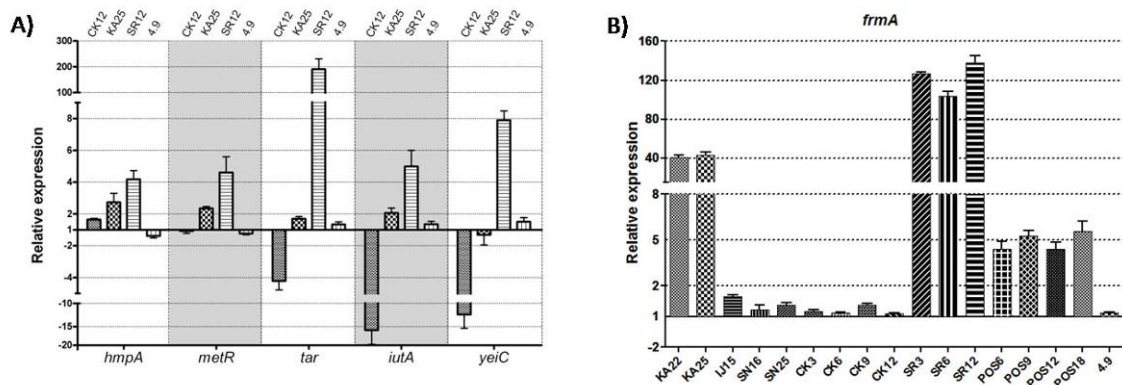


Fig. 39: Real Time-PCR-based quantification of transcript levels of selected genes in ABU re-isolates. Relative expression of *hmpA*, *metR*, *tar*, *iutA* and *yeiC* genes A) and of *frmA* B) in *in-vitro* re-isolate 4.9 and all *in vivo* re-isolates. In all cases, the gene expression of the re-isolates was normalized to that of parent strain 83972. All experiments were performed in triplicate. Gene expression was standardized using the *rnnB* gene as an internal control.

Taken together, to evaluate changes on the transcriptional level, microarray experiments were performed with three *in vivo* (CK12, SR12 and KA25) and one *in vitro* (4.9) re-isolates and compared to that of the parent strain 83972. Genes affected as determined by microarray hybridisation demonstrated remarkable differences among the investigated re-isolates. Each re-isolate represented a unique gene expression pattern, however, a small fraction of genes that were commonly expressed in *in vivo* re-isolates SR12 and KA25 was detected. Among hypothetical proteins and phage-related genes, most of the changes in the global gene regulation pattern of the *in vitro* re-isolate 4.9 were implicated in anaerobic respiration. TCA cycle, differed sugars and amino acids transport and metabolism were found to be up-regulated in re-isolate SR12 in response to prolonged growth in the bladder. Genes encoding for hypothetical, unclassified and unknown proteins as well phage and transposone related were the main fraction of those individually affected in strains CK12 and KA25. Whereas genes involved in protection against NO (*frmAB*, *hmpA*) released upon bacterial infection were commonly up-regulated in re-isolates SR12 and KA25 when compared to parent strain 83972. Moreover, the significant up-regulation of the gene *frmA* could be observed in all re-isolates obtained from the patients KA, SR and POS. Finally, many genes encoding proteins involved in glycine, serine, threonine and methionine transport and metabolism were found to be up-regulated in re-isolates SR12 and KA25 relative to parent strain 83972.

5.5. Changes in the cytoplasmic protein expression of the 83972 re-isolates

To analyze changes in protein expression of the re-isolates derived from the human colonization study, a 2D protein gel electrophoresis approach was used. As already described (section 4.3.), cytoplasmic proteins were extracted from bacteria grown *in vitro* at 37 °C in pooled human urine. The extracted proteins were separated on the basis of their isoelectric point (pH range 4 to 7), followed by a separation according to their molecular weight. Representative cytoplasmic protein profiles are shown in Fig. 40.

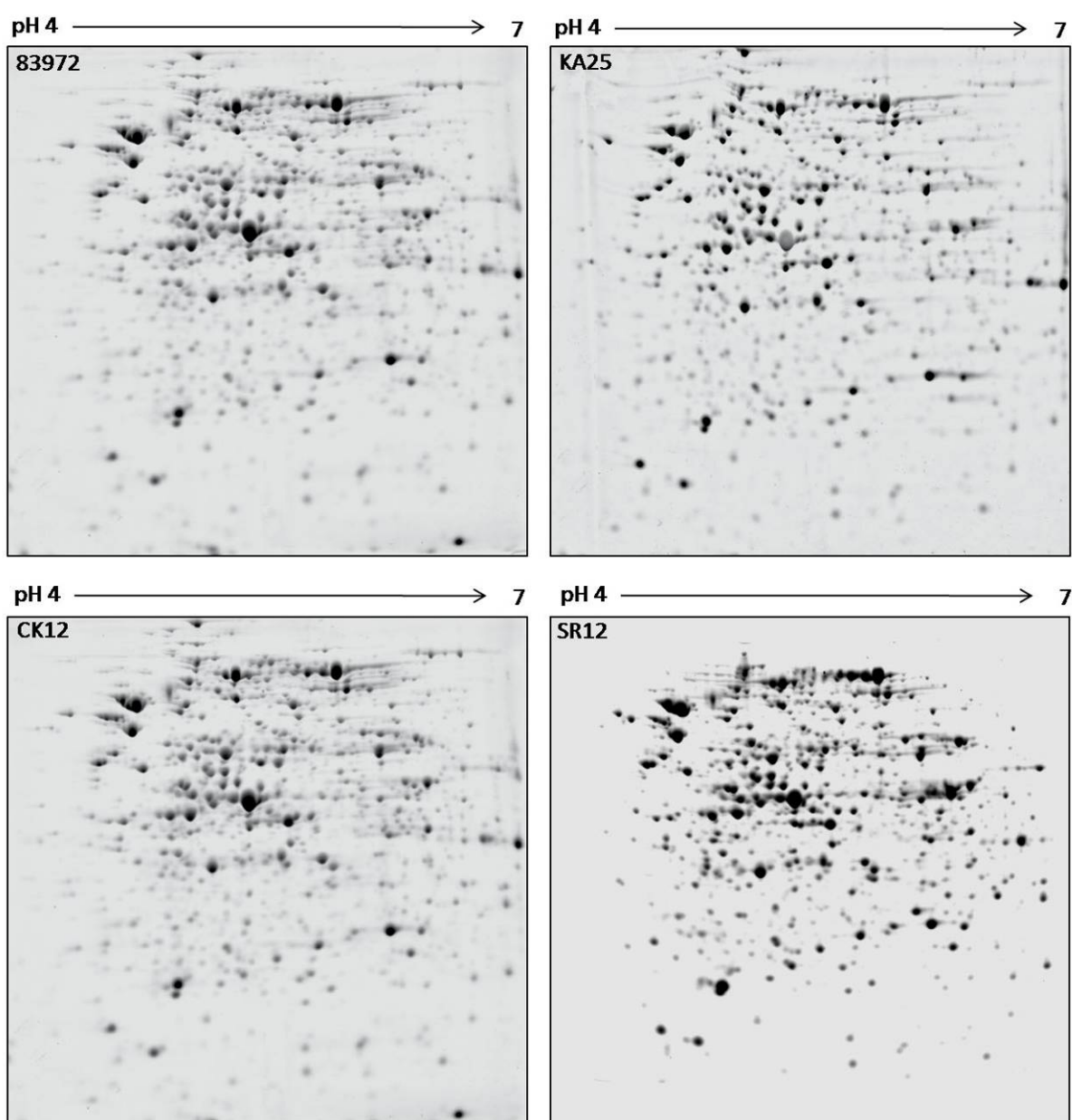


Fig. 40: Comparison of 2D cytoplasmic protein profiles from ABU strain 83972 and the *in vivo* re-isolates KA25, CK12 and SR12 upon growth *in vitro* at 37 °C in pooled human urine.

5.5.1. Cytoplasmic proteome changes of *in vivo* re-isolate KA25 relative to parent strain 83972

Altogether, 18 differently expressed proteins were identified (Fig. 41). In accordance with the gene expression profiles on the transcriptional level (section 5.4.1), the number of repressed proteins was higher than that of induced proteins (13 – down, 5 – up) when compared to the cytoplasmic proteome pattern of ancestor strain 83972. These 18 proteins were identified by MALDI-TOF Mass Spectrometry (Table 14). Interestingly, the most striking differences between strains KA25 and 83972 were observed for the proteins FrmA and FrmB which were detectable in higher amounts in re-isolate KA25 than in strain 83972 (Fig. 41). As already described (section 5.4.3), expression of the corresponding genes was strongly up-regulated in strains KA25 and SR12 relative to their parent strain 83972.

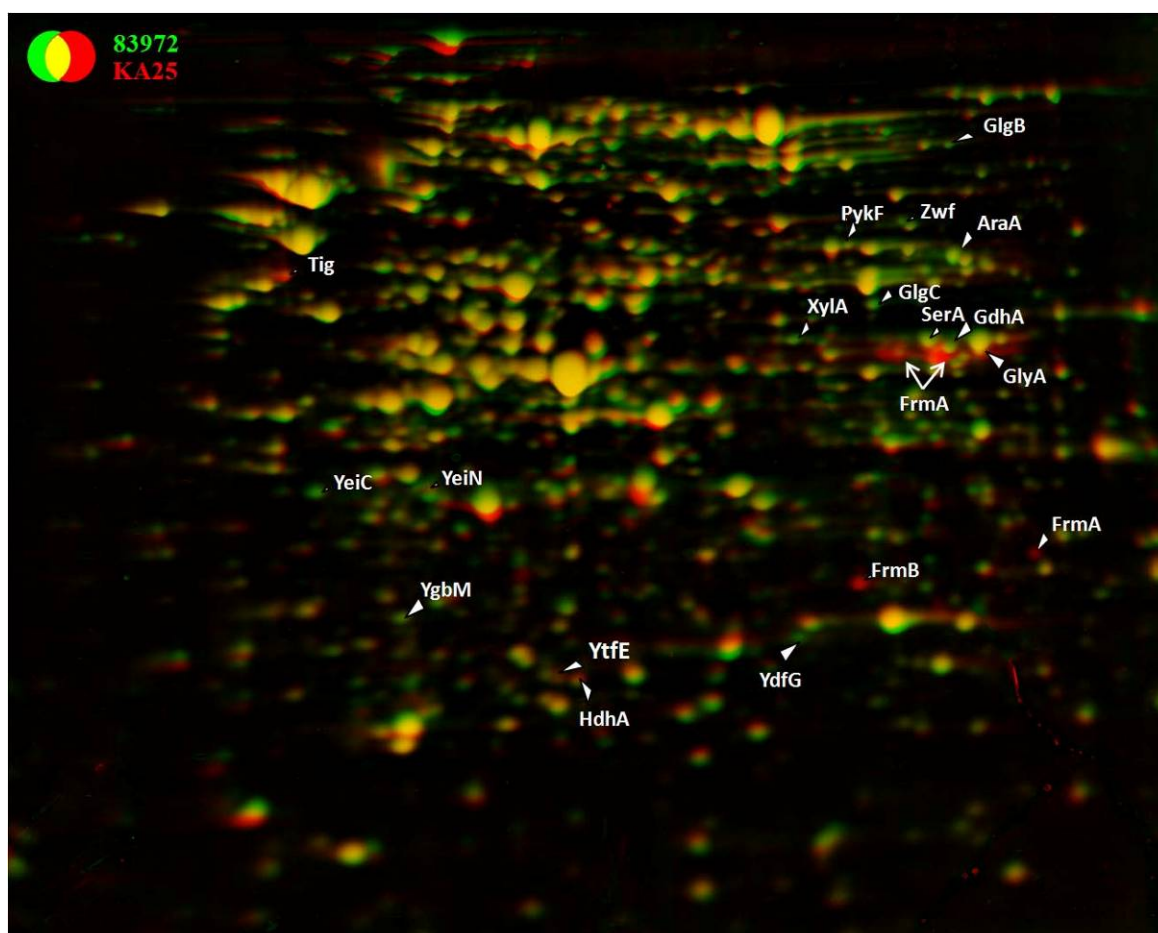


Fig. 41: Comparison of the cytoplasmic proteome of ABU strain 83972 and the *in vivo* re-isolate KA25. Red-channel, cytoplasmic proteins of re-isolate KA25; Green-channel, cytoplasmic proteins of strain 83972. Proteins with the same expression level are shown in yellow. On each gel 300 μ g of cytoplasmic proteins were separated and Coomassie-stained. Differently expressed proteins were identified by MALDI-TOF mass spectrometry.

Results

The isoelectric point and molecular weight of the FrmA is very close to those of SerA and GdhA (Table 14). The high amount of FrmA protein might be a reason for problems with GdhA identification in the re-isolate, where spot positions most likely overlap each other. The proteins YdfG and GlyA are involved in serine metabolism while FrmA and FrmB contribute to glutathione metabolism. GdhA is glutamate dehydrogenase that catalyzes the NADPH-dependent amination of alpha-ketoglutarate to L-glutamate. It has been reported that impaired metabolism of these amino acids might be due to oxidative and nitrosative stress (Jarboe *et al.*, 2008; Liu *et al.*, 2001). Another over-expressed protein, YtfE, is involved in the repair of damaged iron-sulfur clusters, again due to oxidative and nitrosative stress (Justino *et al.*, 2007).

Table 14: Differently expressed cytoplasmic proteins in the *in vivo* re-isolate KA25 and the ancestor strain 83972.

Protein	Function	Mw ^b	pI ^b	UniProt	Expression
FrmA	alcohol dehydrogenase AdhC	39358.99	5.85	P25437	↑ ^a
FrmB	S-formylglutathione hydrolase	31424.48	5.81	P51025	↑ ^a
Tig	trigger factor	48250.71	4.81	Q8FKA7	↑
GdhA	glutamate dehydrogenase	48581.37	5.98	P00370	?
SerA	D-3-phosphoglycerate dehydrogenase	44044.59	5.93	P0A9T1	↓
GlyA	serine hydroxymethyltransferase	45316.59	6.03	P0A826	↓
GlgB	1,4-alpha-glucan branching enzyme	84362.92	5.93	Q1R5J4	↓
GlgC	glucose-1-phosphate adenylyltransferase	50069.42	5.78	A1AGW3	↓
XylA	xylose isomerase	49742.01	5.75	P00944	↓
AraA	L-arabinose isomerase	56088.96	5.95	Q8FL89	↓
PykF	pyruvate kinase	50729.42	5.77	A2UN64	↓
Zwf	glucose-6-phosphate 1-dehydrogenase	55704.44	5.56	P0AC53	↓
YdfG	L-serine/L-allo-threonine dehydrogenase	27246.90	5.65	Q8FHD2	↓ ^a
HdhA	7-alpha-hydroxysteroid dehydrogenase	26763.58	5.38	Q0THK9	↑
YtfE	regulator of cell morphogenesis and NO signaling	24896.65	5.24	Q0T9H5	↑
YgbM	conserved protein	29216.99	5.09	Q46891	↓
YeiC	hypothetical sugar kinase	38130.41	4.99	Q1R9Q6	↓ ^a
YeiN	putative uncharacterized protein	33003.96	5.11	Q0TF55	↓ ^a

Arrows indicate changes of protein expression in re-isolate KA25 when compared to the strain 83972

^a – results consistent with microarray experiment

^b – Theoretical masses and isoelectric points were determined by using the ExPASy proteomics server UniProt Knowledgebase (<http://ca.expasy.org>).

The GlgB and GlgC proteins, involved in glycogen biosynthesis, were less abundant in the re-isolate. In addition, multiple proteins like XylA, AraA, Zwf, PykF which play an important role in the central metabolism were also not as much expressed as in the strain 83972. Interestingly, two proteins, YeiC and YeiN, which are up-regulated in human urine (Roos *et al.*, 2006b; Snyder *et al.*, 2004), were lesser expressed in re-isolate KA25. YeiC is a putative

sugar kinase from the ribokinase protein family catalysing degradation of pentose sugars. The second protein, YeiN, is not characterized yet. However, it shows more than 90 % homology to the indigoidine synthase A (IndA)-like protein from *Thermotoga maritima*. Indigoidine is a blue pigment that has been initially described in *Erwinia chrysanthemi* to be implicated in pathogenicity and protection from oxidative stress (Reverchon *et al.*, 2002). HahA catalyzes the dehydroxylation of bile acids (Yoshimoto *et al.*, 1991). By dehydroxylation, bile acids lose their detergent properties. An increased amount of HahA in re-isolate KA25 might have a positive effect when bacteria grow in the human bladder.

5.5.2. Cytoplasmic proteome changes of *in vivo* re-isolate SR12 relative to parent strain 83972

The main alterations of the SR12 cytoplasmic proteome relative to that of parent strain 83972 were very similar to that of strain KA25 (Fig. 42).

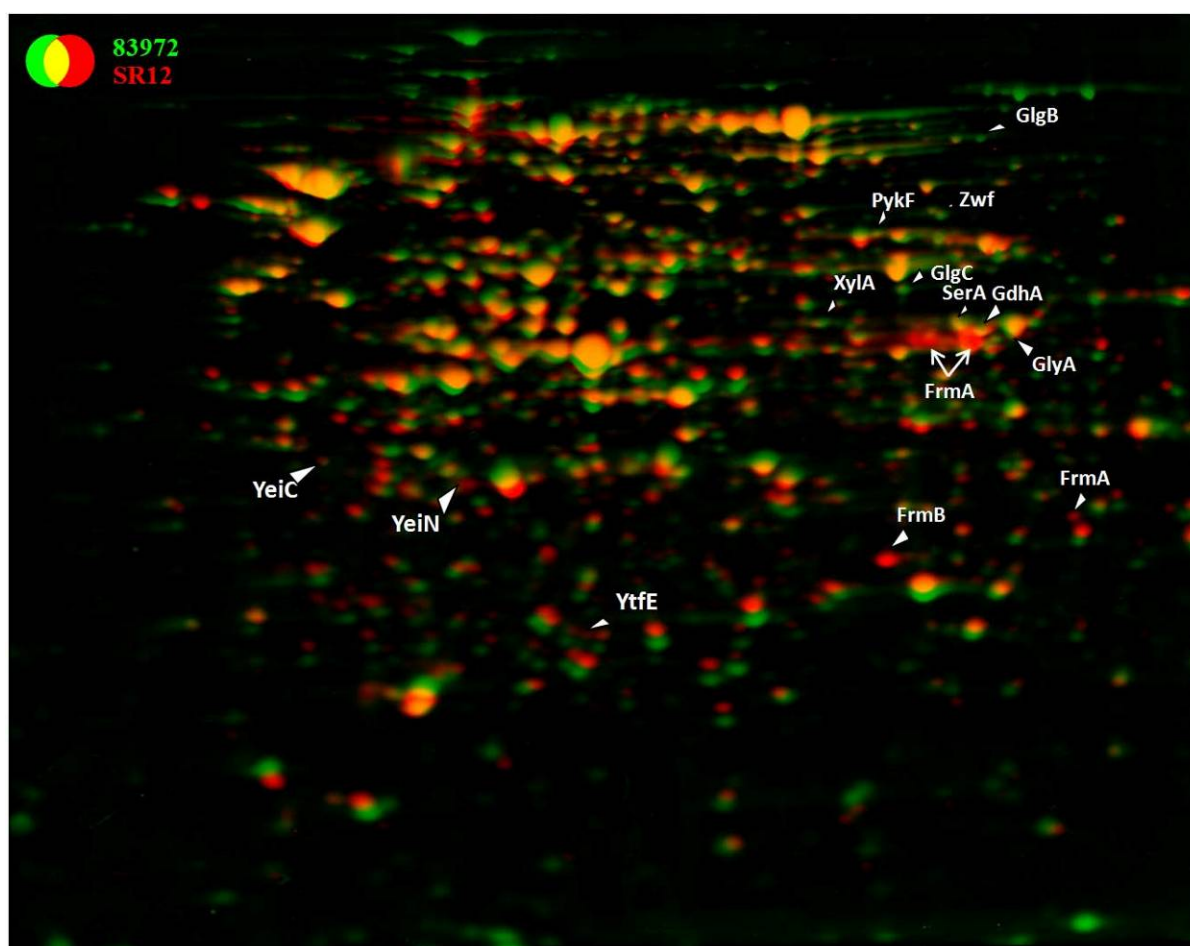


Fig. 42: Comparison of the cytoplasmic proteome of ABU strain 83972 and the *in vivo* re-isolate SR12. Red-channel, cytoplasmic proteins of re-isolate SR12; Green-channel, cytoplasmic proteins of strain 83972. Proteins with the same expression level are shown in yellow. On each gel 300 μ g of cytoplasmic proteins were separated and Coomassie-stained. Differently expressed proteins were identified by MALDI-TOF mass spectrometry.

Results

Several de-regulated proteins were identified by MALDI-TOF (Table 15). Interestingly, the most striking differences of the SR12 cytoplasmic proteome profiles were exactly the same as those described in re-isolate KA25. The proteins FrmA and FrmB were significantly higher expressed than in the ancestor strain 83972 (Fig. 42). However, the expression level for both proteins in the re-isolate SR12 was twice as much as in KA25 and 100-fold more than both in CK12 and 83972 (Fig. 43).

Table 15: Differently expressed cytoplasmic proteins in the *in vivo* re-isolate SR12 and the ancestor strain 83972.

Protein	Function	Mw ^b	pI ^b	UniProt	Expression
FrmA	alcohol dehydrogenase AdhC	39358.99	5.85	P25437	↑ ^a
FrmB	S-formylglutathione hydrolase	31424.48	5.81	P51025	↑ ^a
GdhA	glutamate dehydrogenase	48581.37	5.98	P00370	?
SerA	D-3-phosphoglycerate dehydrogenase	44044.59	5.93	P0A9T1	↓
GlyA	serine hydroxymethyltransferase	45316.59	6.03	P0A826	↓
GlgB	1,4-alpha-glucan branching enzyme	84362.92	5.93	Q1R5J4	↓
GlgC	glucose-1-phosphate adenylyltransferase	50069.42	5.78	A1AGW3	↓
PykF	pyruvate kinase	50729.42	5.77	A2UN64	↓
Zwf	glucose-6-phosphate 1-dehydrogenase	55704.44	5.56	P0AC53	↓
YtfE	regulator of cell morphogenesis and NO signaling	24896.65	5.24	Q0T9H5	↑
YeiC	hypothetical sugar kinase	38130.41	4.99	Q1R9Q6	↓ ^a
YeiN	putative uncharacterized protein	33003.96	5.11	Q0TFS5	↓ ^a

Arrows indicate expression changes of the protein in re-isolate SR12 when compared to the strain 83972

^a – results consistent with microarray experiment

^b – Theoretical masses and isoelectric points were determined by using the ExpASY proteomics server UniProt Knowledgebase (<http://ca.expasy.org>).

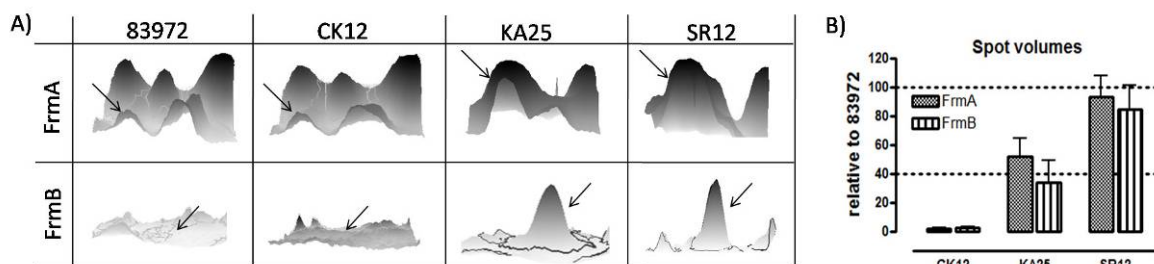


Fig. 43: Quantification of FrmA and FrmB protein expression in *in vivo* re-isolates of ABU strain 83972. **A)** 3-D representation of the selected proteins spots; **B)** Change of protein expression in the *in vivo* re-isolate relative to strain 83972 calculated from normalized spot volumes in triplicate experiments.

Moreover, the YtfE protein involved in NO signalling as well as the proteins SerA, GlyA, GlgB, GlgC, PykF and Zwf were similarly de-regulated as in strain KA25. Nevertheless, YeiC and YeiN were induced in re-isolate SR12 compared to that of re-isolate KA25.

5.5.3. Cytoplasmic proteome changes of *in vivo* re-isolate CK12 relative to parent strain 83972

The direct comparison of the intracellular proteomes of strain 83972 and re-isolate CK12 allowed the identification of several differently expressed proteins (Fig. 44). In total, eleven candidate spots were detected to differ from the protein profile of strain 83972 (Table 16). Only one protein which was exclusively found in the CK12 isolate was unidentifiable.

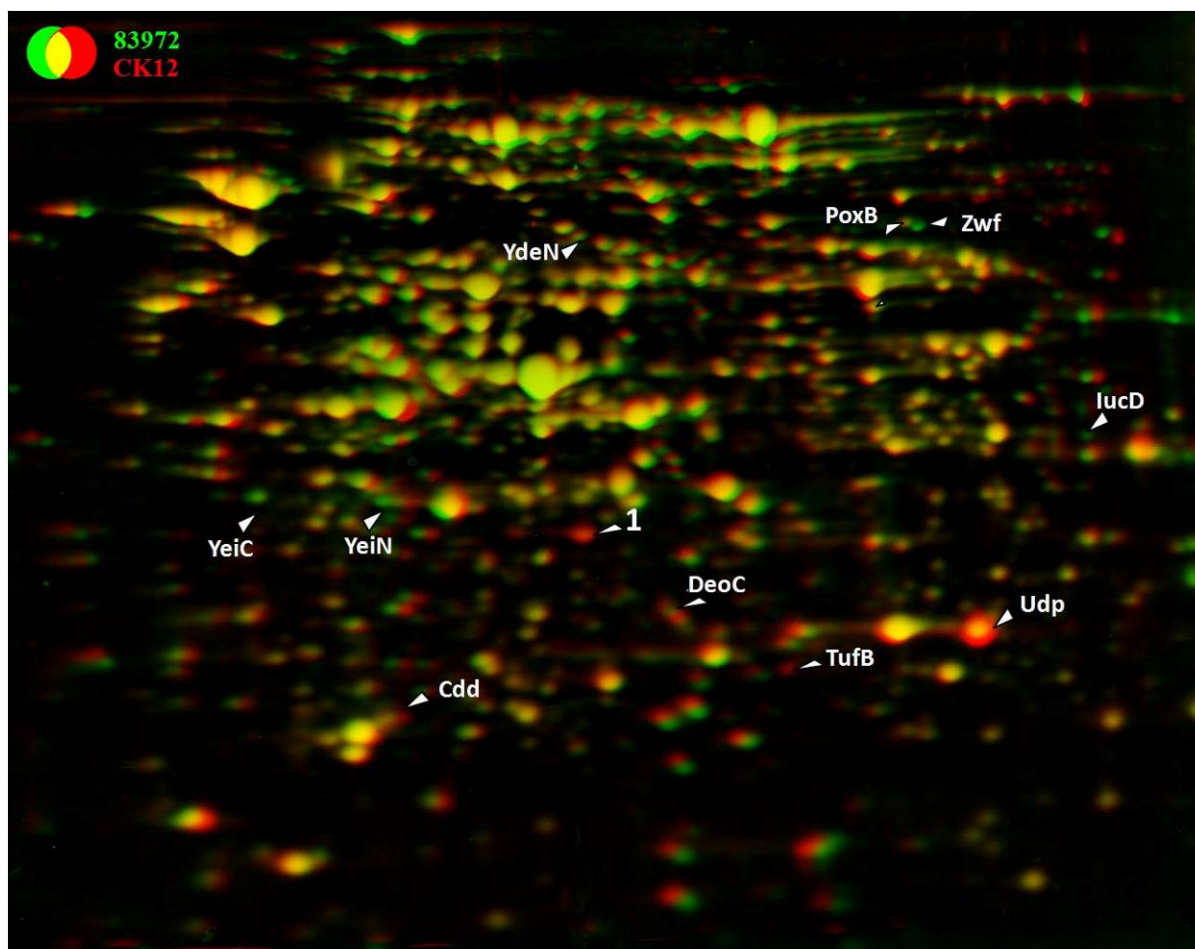


Fig. 44: Comparison of the cytoplasmic proteome of ABU strain 83972 and the *in vivo* re-isolate CK12. Red-channel, cytoplasmic proteins of re-isolate CK12; Green-channel, cytoplasmic proteins of strain 83972. Proteins with the same expression level are shown in yellow. On each gel 300 μ g of cytoplasmic proteins were separated and Coomassie-stained. Differently expressed proteins were identified by MALDI-TOF mass spectrometry.

Whereas the above mentioned proteomes of the re-isolates KA25 and SR12 were very similar to each other, the one of strain CK12 was more distinct. The most prominent features of KA25 and SR12, namely increased amounts of FrmA and FrmB, could not be detected in strain CK12. Also common patterns in expression of YtfE, SerA, GlyA, GlgB, GlgC, XylA,

PykF were not detectable in strain CK12. This might indicate that expression of genes encoding for these proteins is functionally dependent and co-regulated with the *frmRAB* operon by the same factors. Two proteins, YeiC and YeiN, were identified as commonly down-regulated in strains CK12 and KA25. Moreover, only Zwf turned out to be lesser expressed in all three *in vivo* re-isolates. One protein (Protein #1) which was exclusively expressed in re-isolate CK12 but not in the parent strain and other re-isolates could not be identified.

Table 16: Differently expressed cytoplasmic proteins in the *in vivo* re-isolate CK12 and the ancestor strain 83972.

Protein	Function	Mw ^b	pI ^b	UniProt KB	Expression
Udp	Uridine phosphorylase	27027.89	5.81	P12758	↑ ^a
TufB	Translation elongation factor Tu	43182.39	5.30	A2UNY4	↑
DeoC	Deoxyribose-phosphate aldolase	27733.80	5.50	P0A6L0	↑ ^a
Protein #1	Not identified	-	-	-	↑
IucD	L-lysine 6-monooxygenase	48653.49	6.44	Q3L7J2	↓ ^a
PoxB	Pyruvate dehydrogenase	62071.44	5.86	Q8FJE2	↓
Zwf	glucose-6-phosphate 1-dehydrogenase	55704.44	5.56	P0AC53	↓
YdeN	Putative sulfatase	62842.33	5.76	A1AB86	↓
Cdd	cytidine deaminase	31539.87	5.42	P0ABF6	↑ ^a
YeiC	hypothetical sugar kinase	38130.41	4.99	Q1R9Q6	↓ ^a
YeiN	putative uncharacterized protein	33003.96	5.11	Q0TFS5	↓ ^a

Arrows indicate expression changes of the protein in re-isolate CK12 when compared to the strain 83972

^a – results consistent with microarray experiment

^b – Theoretical masses and isoelectric points were determined by using the ExPASy proteomics server UniProt Knowledgebase (<http://ca.expasy.org>).

Interestingly, the uridine phosphorylase (Udp), cytidine deaminase (Cdd) and deoxyribose-phosphate aldolase (DeoC) proteins appeared also from the transcriptome data to be up-regulated. According to the protein profile, the Udp protein is one of the most significantly expressed proteins. Proteins Udp and Cdd are involved degradation of ribonucleosides (Fig. 45), while Cdd and DeoC contribute to the degradation of deoxyribonucleosides (Fig. 46).

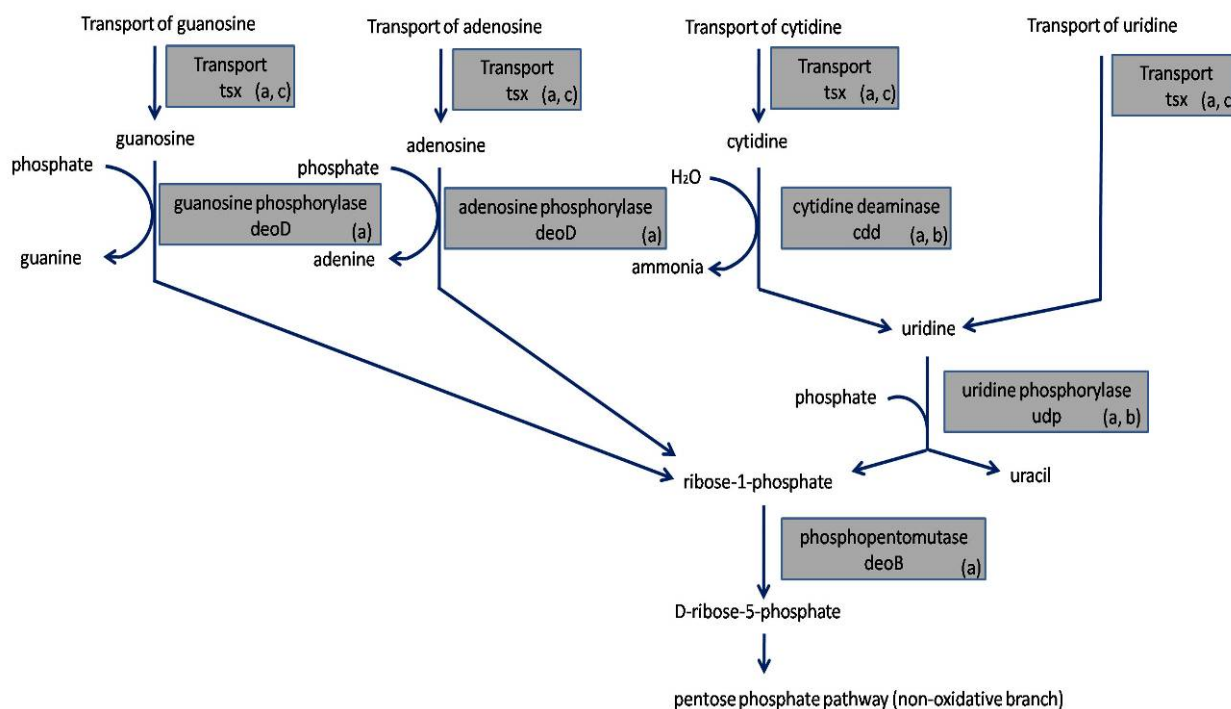


Fig. 45: Adaptation of the ribonucleoside degradation pathway in *in vivo* re-isolate CK12 of ABU strain 83972. The different steps of ribonucleoside uptake and degradation identified to be de-regulated in the different re-isolates are indicated: significantly up-regulated genes according to microarray experiments **a**); over-expressed proteins according to cytoplasmic proteome comparison **b**); over-expressed proteins according to outer membrane proteome comparison **c**).

According to the proteome comparison, only DeoC was found to be present in higher amounts, whereas microarray data indicated that the entire *deoCABD* operon was up-regulated. In addition, transcriptome comparison indicated that the *tsx* gene encoding for a protein involved in the transport of ribo- and deoxy-nucleosides across the outer membrane of *E. coli* was up-regulated in re-isolate CK12. This result was also confirmed by comparison of the outer membrane protein expression (section 5.6).

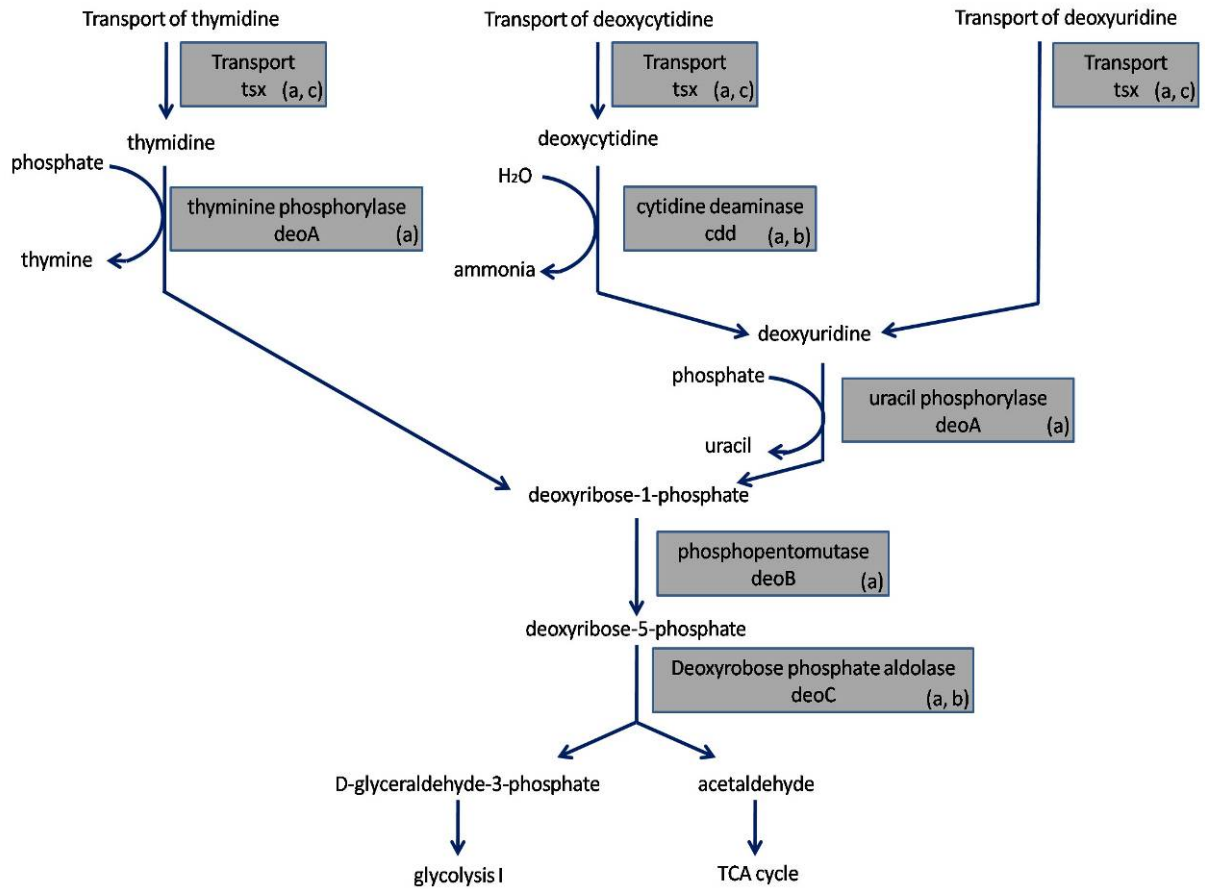


Fig. 46: Adaptation of the deoxy-ribonucleoside degradation pathway in *in vivo* re-isolate CK12 of ABU strain 83972. The different steps of deoxy-ribonucleoside uptake and degradation identified to be de-regulated in the different re-isolates are indicated: significantly up-regulated genes according to microarray experiments **a**); over-expressed proteins according to cytoplasmic proteome comparison **b**); over-expressed proteins according to outer membrane proteome comparison **c**).

Taken together, to analyze changes in cytoplasmic proteins expression of the re-isolates derived from the human colonization study, a 2D protein gel electrophoresis approach was applied. In all three re-isolates (KA25, SR12, CK12) a number of 18, 12 and 11 proteins, respectively, turned out to be de-regulated. Interestingly, cytoplasmic proteome profiles of isolates KA25 and SR12 were comparable. The most striking differences between those strains and 83972 were observed for the proteins FrmA and FrmB. These results are in a strict accordance with microarray data. The proteome of strain CK12 was more distinct. The most prominent features of KA25 and SR12, namely increased amounts of FrmA and FrmB, could not be detected in strain CK12. Instead, degradation of deoxy- and ribonucleosides was up-regulated in strain CK12 compared to SR12, KA25 and 83972.

5.6. Outer membrane proteome changes of the *in vivo* re-isolates of strain 83972.

Bacterial surface proteins have different main functions. They are involved in the uptake and transport of different substances into the cell, in adhesion, and in cell-to-cell communication. Microorganisms growing in the urinary tract encounter iron depletion. Thus they must have evolved multiple iron uptake mechanisms. Moreover, all proteins located on the bacterial surface are potential targets for antibodies of the human immune system.

To extend our knowledge about changes in the outer membrane proteome and adaptation of ABU strain 83972 during growth in the human bladder, the membrane protein fractions of this strains and its *in vivo* re-isolates were compared. As already described (section 4.3), following bacterial growth in pooled human urine, carbonate-insoluble proteins were separated by 2D gel electrophoresis. Protein spots differing between the parent strain 83972 and its derivatives were identified by MALDI-TOF mass spectrometry.

Complete solubilisation of the membrane proteins is critical for proteomic analysis of membrane fractions. Using the carbonate extraction method, 19 different membrane associated proteins were identified (Table 17). This represents 73 % of the 26 predicted outer membrane proteins of *E. coli* strain K-12 (Molloy *et al.*, 2000). However, many of the detected proteins (42 %) represented components of iron uptake systems which are not present in the strain K-12 strain MG1655.

Results

Table 17: Changes in the outer membrane subproteome of the *in vivo* re-isolates of strain 83972 following *in vitro* culture in pooled human urine. Expression of each protein in the re-isolates relative to that one of the strain 83972.

Protein	Function	UniProt	Mw ^b	pI ^b	Expression		
					KA25	KA12	SR12
OmpA	outer membrane protein A	Q8CW76	41054.22	6.24	=	=	=
OmpC	outer membrane protein C	Q8CVW1	39164.52	4.49	=	=	=
OmpX	outer membrane protein X	P0A917	16382.89	5.30	=	=	=
Tsx	nucleoside channel-forming protein	Q0TKN0	33624.03	5.18	=	↑	=
FadL	long-chain fatty acid transport protein	Q6KCX0	48910.28	4.80	=	=	=
Ag43	Antigen 43 precursor	Q6KD18	107303.94	5.74	=	=	=
TolC	outer membrane-associated protein	A1AFV8	54030.07	5.46	=	=	=
BtuB	vitamin B12 transporter	Q8CVJ0	66315.91	5.27	=	=	=
YeaT	membrane protein assembly factor	P0A941	88426.12	4.87	=	=	↓
Imp	LPS-assembly protein	Q0TLT4	87051.03	4.98	=	=	↓
Iha ^a	exogenous ferric siderophore receptor	O87518	73805.93	5.72	=	↓	↑
FecA ^a	iron(III) dicitrate transport protein	P13036	81707.21	5.36	=	↑	=
IroN ^a	siderophore receptor	Q9RQ19	79384.89	5.79	=	↑	↓
IutA ^a	ferric aerobactin receptor	Q6Q7N8	81048.36	5.49	=	↓	↑
ChuA ^a	heme/hemoglobin receptor	Q8FCK0	71100.46	5.02	=	=	=
FhuA ^a	ferrichrome-iron receptor	Q8CWD4	82835.04	5.33	=	=	↓
FhuE ^a	ferric-rhodotorulic acid transporter	Q0TIX2	74162.93	4.93	=	=	↓
FliC	flagellar filament structural protein	Q7DBI0	59951.79	4.70	=	=	↑
FepA ^a	ferrienterobactin receptor	A1A8L5	73660.65	5.20	=	↑	↑

The expression of each protein in the re-isolates relative to that of the strain 83972 has been indicated.

^{a)} Proteins involved in iron acquisition

^{b)} Theoretical masses and isoelectric points were determined using the ExPASy proteomics server UniProt Knowledgebase (<http://ca.expasy.org>).

The protein profiles of the three *in vivo* re-isolates were comparable. However, minor changes either in the composition or in the expression level could be detected. In general, protein separation was of a good quality and allowed precise alignment of the profiles from parent strain and its consecutive re-isolates (Fig. 47; Fig. 48; Fig. 49). Different protein isoforms could not always be perfectly aligned during *in silico* proteome comparison and are therefore either underlined or boxed as the same protein. All changes between the re-isolates and the wild type strain are summarised in Table 17.

While the outer membrane protein profiles of the strains KA25 and 83972 were very similar (Fig. 47), the outer membrane proteome of re-isolate CK12 exhibited minor changes (Fig. 48). The most prominent difference in the strain CK12 was the lack of the ferric aerobactin receptor protein IutA. Interestingly, the iron(III) dicitrate transport protein (FecA) was found to be located in almost the same position on the gel. Because of the almost identical

isoelectric points and molecular weights of these two proteins (Table 17), it is difficult to distinguish them when both proteins IutA and FecA are expressed together.

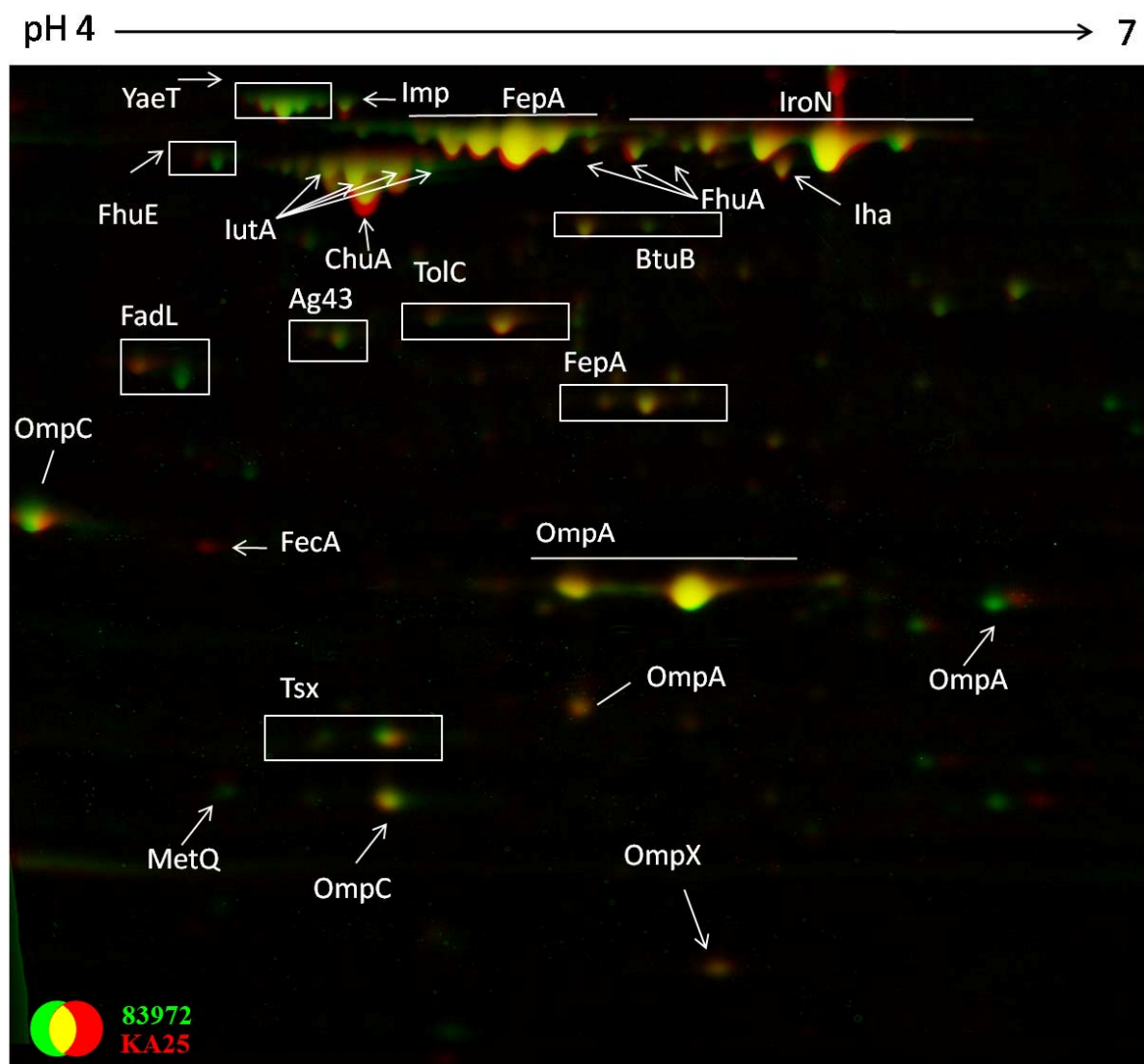


Fig. 47: Comparison of the outer membrane proteome of ABU strain 83972 and the *in vivo* re-isolate KA25. Red-channel, outer membrane proteins of re-isolate KA25; Green-channel, outer membrane proteins of strain 83972. Proteins with the same expression level are shown in yellow. On each gel 100 μ g of proteins were separated and Coomassie-stained. Differently expressed proteins were identified by MALDI-TOF mass spectrometry.

These results are consistent with the microarray data, indicating that the *iutA* gene was 2-fold down- and the *fecABCDE* operon was 2-fold up-regulated relative to parent strain 83972 (Table 21). Moreover, the protein profiles showed that the amount of Iha, the exogenous ferric siderophore receptor was significantly decreased in strain CK12, while another siderophore receptor, IroN, seemed to be present in higher amounts.

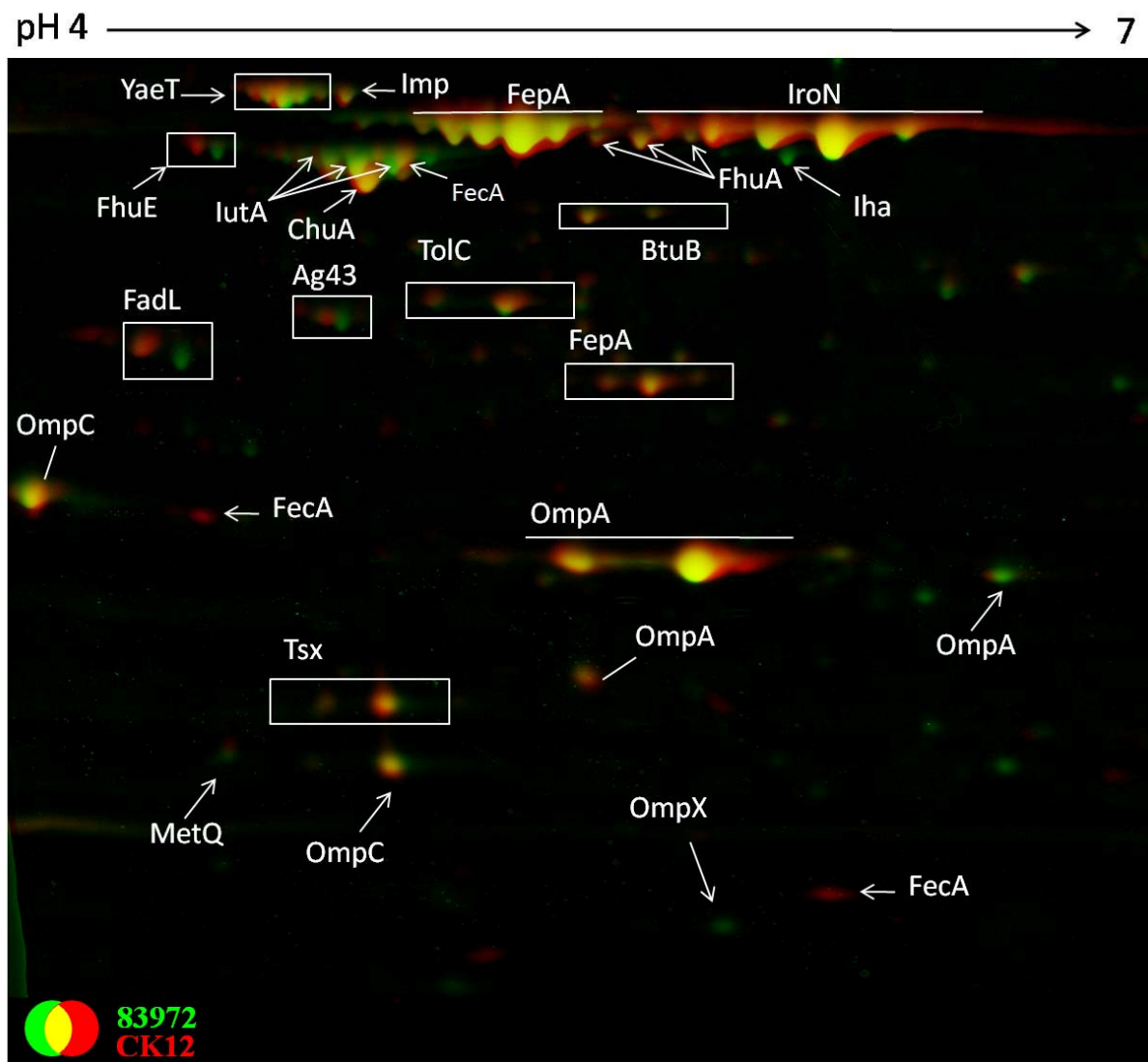


Fig. 48: Comparison of the outer membrane proteome of ABU strain 83972 and the *in vivo* re-isolate CK12. Red-channel, outer membrane proteins of re-isolate CK12; Green-channel, outer membrane proteins of strain 83972. Proteins with the same expression level are shown in yellow. On each gel 100 μ g of proteins were separated and Coomassie-stained. Differently expressed proteins were identified by MALDI-TOF mass spectrometry.

One more interesting protein that was found to be expressed in higher amounts in re-isolate CK12 than in strain 83972 is Tsx, the nucleoside-specific channel-forming protein. As already described in section 5.5.3, this protein facilitates the uptake of ribo- and deoxyribonucleosides from the environment. The *tsx* gene was 2-fold up-regulated in strain CK12 when compared to 83972. Moreover, other proteins involved in that uptake processes were identified to be present in higher amounts in the intracellular proteome of strain CK12 (Fig. 44).

Regarding strain SR12, some alterations in the outer membrane protein profile could also be detected (Fig. 49).

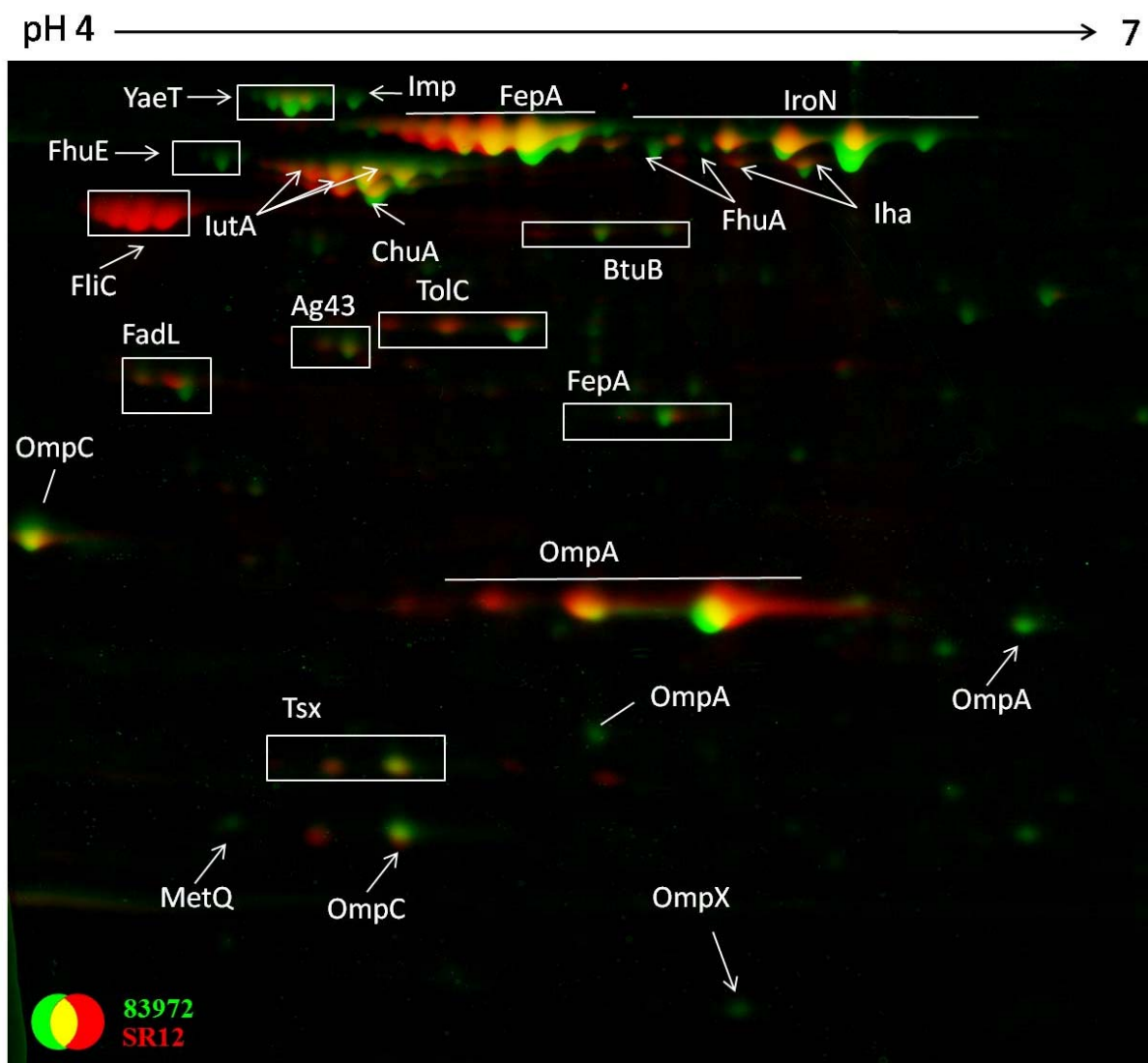


Fig. 49: Comparison of the outer membrane proteome of ABU strain 83972 and the *in vivo* re-isolate SR12. Red-channel, outer membrane proteins of re-isolate SR12; Green-channel, outer membrane proteins of strain 83972. Proteins with the same expression level are shown in yellow. On each gel 100 μ g of proteins were separated and Coomassie-stained. Differently expressed proteins were identified by MALDI-TOF mass spectrometry.

The most striking difference was the presence of multiple isomeric forms of the protein FliC. As already shown, this strain is motile (Fig. 26) and many genes of the flagella regulon were up-regulated when compared to the parent strain 83972 (Table 18).

In addition to FliC, the expression of different components of iron uptake systems was affected. First of all, the protein FhuE could not be detected and FhuA was much lesser

expressed than in strain 83972. In contrast to re-isolate CK12, the Iha protein was present in higher amounts and IroN was less prevalent than in the ancestor strain. Also the ferrienterobactin receptor FepA turned out to be present in higher amounts in the re-isolate SR12. However, many differences on the protein level were not as clear as for strain CK12 and KA25. This might be due to the expression of flagella and a thus significant fraction of the FliC protein in the protein preparation.

The fact that in all outer membrane protein proteomes of the three re-isolates and the parent strain 83972 some prototypic outer membrane proteins like OmpF, OmpW, YfiO and ZipA could not be detected indicates the limitation of 2D gel analysis of outer membrane proteins which can frequently not be resolved due to their high hydrophobicity. Gel-free analysis of outer membrane protein fractions may be a suitable alternative to get a more complete picture of the outer membrane proteome.

Taken together, to assess changes in the outer membrane proteome and adaptation of ABU strain 83972 during growth in the human bladder, the membrane protein fractions of this strain and its *in vivo* re-isolates were compared. Together, 19 different membrane associated proteins were identified. Many of the detected proteins (42 %) represented components of iron uptake systems. Outer membrane protein profiles of the strains KA25 and 83972 were very similar, however, the outer membrane proteome of re-isolate CK12 and SR12 exhibited already minor changes. In isolate CK12, nucleoside uptake system was up-regulated what clearly correlated with microarray data. In addition to that, the expression of different components of iron uptake systems was affected in isolates SR12 and CK12.

6. Discussion

Asymptomatic bacteriuria (ABU) probably represents the most frequent form of urinary tract infections. Up to 6 % of healthy individuals and up to 50 % of elderly patients are estimated to be colonized by ABU strains (Colgan *et al.*, 2006). Despite ABU isolates frequently reach cell densities of $>10^5$ bacteria/ml urine, colonization of the urogenital tract usually occurs in these cases without symptoms as the urogenital epithelia are rarely damaged and no inflammation is induced (Lindberg *et al.*, 1978; Wullt *et al.*, 2003). Several virulence-associated factors of uropathogenic *E. coli* that contribute to colonization of the urinary tract and symptomatic UTI have been well characterized. However, little is known about the virulence determinants of ABU isolates. Moreover, gene expression of asymptomatic isolates has not been studied in detail and there is no study concerning the host-driven bacterial evolution within the urinary tract, promoting bacteria to enter a commensal-like state.

In the first part of this work, a more general approach was used. To learn more about the characteristics of ABU isolates that may account for the ABU lifestyle, the genome content and phenotypic traits of eleven ABU isolates were studied in detail and compared to those of uropathogenic and non-pathogenic *E. coli* isolates. Later, the ABU model *E. coli* strain 83972 was used to analyze the genome flexibility and adaptive changes during human bladder colonisation.

6.1. Asymptomatic bacteriuria is caused by a heterogeneous group of *E. coli* isolates

Interestingly, ABU isolates represent a rather heterogeneous group of organisms with regard to their phylogenetic lineage and repertoire of typical virulence-associated genes of UPEC. Although the majority of strains tested belongs to the ECOR groups B2 and D to which UPEC can be usually affiliated, some isolates could be grouped to the ECOR groups A and B1. These lineages normally include non-pathogenic as well as intestinal pathogenic variants. Accordingly, and in contrast to the strains of ECOR group B2 and D, typical UPEC virulence-associated genes could not be detected in these ABU isolates and their pathoarray CGH barcode differs markedly from those ABU strains which seem to be more closely related to UPEC (Fig. 10; Table 7; Table 9)

The ABU isolates could be allocated to different phylogenetic lineages and different clonal groups. These results demonstrate that asymptomatic bacteriuria is not caused by one specialized clonal group of organisms. Instead, bacteria with different independent phylogenetic backgrounds are able to efficiently colonize the urinary tract without causing symptoms. Furthermore, comparison of the genome structure accessed by PFGE uncovered that even strains falling into the same ST differed markedly in the genome structure. It underlines the diversity and genome flexibility among strains causing ABU.

6.2. Impaired ability of ABU isolates to express typical UPEC virulence factors

As expected, the ABU strains of ECOR group B2 and D exhibited a pathoarray CGH barcode similar to those of archetypal UPEC variants which cause symptomatic UTI. This indicates that UPEC virulence-associated genes are present in the genomes of these ABU isolates. Their inability to cause symptomatic UTI cannot be attributed to the absence of such virulence-associated genes *per se*.

Therefore, comparison of the *foc* determinants of the F1C-fimbriae-negative ABU strains 83972 and 27 relative to F1C fimbriae-positive isolate 37 led to the discovery that one particular amino acid exchange in FocD (glutamine 472 → leucine) is responsible for the loss of the usher activity of FocD and thus the absence of functional F1C fimbriae in strains 83972 and 27 (Table 10). This glutamine residue is conserved among the related usher subunits FocD, FimD and SfaF (Fig. 15) and its exchange probably results in an altered conformation or stability of the usher protein thus impairing its function.

The accumulation of point mutations resulting in a loss of gene function is further corroborated by the DNA sequence comparison of *pap* determinants coding for P fimbriae. P fimbriae are considered as one of the most important virulence factors contributing to UTI (Plos *et al.*, 1995; Vaisanen *et al.*, 1981). Five out of eleven isolates tested were *pap*-positive (Table 9). Interestingly only one strain, ABU64, was able to express functional P fimbriae. The fact that P fimbriae trigger mucosal inflammatory responses to *Escherichia coli* in the human urinary tract (Bergsten *et al.*, 2005) may explain the frequency of P-fimbrial inactivation in ABU isolates.

The type 1 fimbriae-encoding gene cluster, besides its inactivation by point mutations in strains 5 and 57, seems to represent a rather unstable genomic region involved in partial chromosomal deletions resulting in loss of a central 4.2-kb part of the operon or in larger 29-kb deletions including adjacent DNA stretches. It is an interesting observation that in all cases of partial *fim* gene cluster deletion the *fimH* gene which is frequently used in generally accepted screening tests as a marker for the presence of the type 1 fimbrial gene cluster (Johnson and Stell, 2000), stays intact. Furthermore, it is tempting to speculate that also the loss of functional type 1 fimbriae may be correlated with the ABU lifestyle as it is non-functional in the majority of strains tested.

The comparison of other virulence-associated characteristics such as motility, LPS phenotype and biofilm formation further supports the finding that *E. coli* ABU isolates are not characterized by a common phenotypic appearance. Consequently, the establishment of asymptomatic bacteriuria not solely depends on a specific set of bacterial traits, but results from different bacterial colonization strategies. In this context, it has been recently suggested, that increased growth rates in urine enable ABU isolate 83972 to outcompete, e.g. uropathogenic *E. coli* isolates from symptomatic urinary tract infections (Roos *et al.*, 2006b). However, growth characteristics of examined eleven ABU isolates were very diverse, in a range from the non-pathogenic strain K-12 to that of 83972, underlying complexity of the ABU phenomena.

The detailed phenotypic and genotypic comparison demonstrated, that important virulence-associated determinants such as those coding for α -hemolysin (*hly*), type 1- fimbriae (*fim*), P-fimbriae (*pap*) and F1C-fimbriae (*foc*) have been frequently inactivated in ABU isolates by point mutations and (IS element-mediated) deletions. These findings are in accordance with results published recently by Klemm and co-workers who described the inactivation of fimbrial adhesin determinants in ABU model strain 83972 by point mutations and deletions (Klemm *et al.*, 2006; Roos *et al.*, 2006a). Our data suggest that, in addition to the bacterial traits, also host factors which allow urinary tract colonization by less specialized *E. coli* variants and even by those harbouring a functional *hly* and *pap* determinant contribute to the development of asymptomatic bacteriuria.

The loss of virulence factors has been shown to reduce the host response to infection in animal models and specifically, the loss of fimbriae decreases the innate host response and

bacterial clearance from the urinary tract. More than 80 % of UPEC strains express P fimbriae, 14-30 % of UPEC strains express F1C fimbriae (Pere *et al.*, 1987) and type 1 fimbrial expression is quite frequent. P fimbriae enhance the establishment of bacteriuria and trigger the innate defence by stimulating the production of cytokines, which orchestrate the subsequent recruitment of inflammatory cells. Type 1 fimbriae have a similar function in mice and have also been shown to enhance intracellular persistence in the mouse bladder mucosa, but these effects have not been reproduced in the human urinary tract (Bergsten *et al.*, 2005; Bergsten *et al.*, 2007; Hultgren *et al.*, 1985). The weak host response to ABU is therefore consistent with the loss of adherence and functional fimbriae. Our results thus suggest that the host response may drive co-evolution, and that virulence-associated genes with pro-inflammatory effects may be targeted for inactivation. In this way, ABU isolates may succeed in persisting without inducing a bactericidal inflammatory response.

Classical studies (Haldane, 1949) proposed that microbes evolve to increase their virulence. The theory was based mainly on the observation that virulence increases pathogen transmission between hosts thereby increasing the number of available multiplication sites for the microbe. Virulence for the urinary tract may in part fit this theory, but does not mainly serve to increase the number of infected hosts, but rather the number of sites in a given host. By expressing fimbriae and other virulence factors, UPEC establish a monoculture in the urinary tract, with less competition than in the complex and competitive intestinal microflora. Unfortunately, virulence is only partially successful, due to the brief time window between the establishment of bacteriuria and the activation of a host defence, which in most cases eliminates the infection. ABU is an interesting model to study the evolution of commensalism rather than virulence. The ABU strains, in contrast, avoid provoking a host response that leads to their elimination and instead, they establish long-term persistence. The loss of virulence may therefore be a preferred evolutionary strategy and there may be positive selection for variants, which are adapted for growth in the urinary tract. Advantages include a rich source of nutrients and the potential for transmission to new hosts. This is in contrast to acute pyelonephritis, which is associated with mortality, premature delivery and reduced fertility and thus with a potential loss of the ecologic niche. Our results clearly support the notion of reductive evolution as an attenuation mechanism converting virulent uropathogenic *E. coli* to asymptomatic carrier strains. While there was no common or specific set of genes that was inactivated or lost by all ABU isolates relative to virulent UPEC, the ECOR group B2 and D

isolates showed distinct mutations in virulence-associated genes rather than a large overall genome loss, which is consistent with an ongoing host-bacterial evolution.

6.3. Genome reduction and evolution of ST 73 ABU strains

This study suggests that ABU is caused by *E. coli* strains of different backgrounds, which share the ability to establish bacteriuria and to persist in the urinary tract, but the molecular details are poorly understood. Sequence type 73 represents an important and successful phylogenetic lineage within ECOR group B2, which also includes the prototypic UPEC strain *E. coli* CFT073 and the non-pathogenic *E. coli* strain Nissle 1917. The genomic and phenotypic diversity among members of ST73 reflects the genome plasticity of *E. coli*. Although four ABU strains as well as UPEC isolate CFT073 and non-pathogenic strain Nissle 1917 belong to the same ST, they differ in the presence of functional fimbrial determinants as well as in their LPS and hemolytic phenotype (Grozdanov *et al.*, 2002; Grozdanov *et al.*, 2004; Welch *et al.*, 2002). The DNA sequence diversity of their *fim*, *pap* and *foc* genes is consistent with the phenotypic heterogeneity within this group of identical or very closely related organisms. However, genome size assessment could show that differences in between isolates exist. Accordingly, the *E. coli* ST73 includes highly virulent uropathogenic, ABU as well as non-pathogenic variants, which may have arisen from a common ancestor by reductive evolution (Fig. 50). Our results confirm recent findings (Johnson *et al.*, 2006; Wirth *et al.*, 2006), that the current MLST schemes do not reliably predict the genotypes or phenotypes of individual isolates.

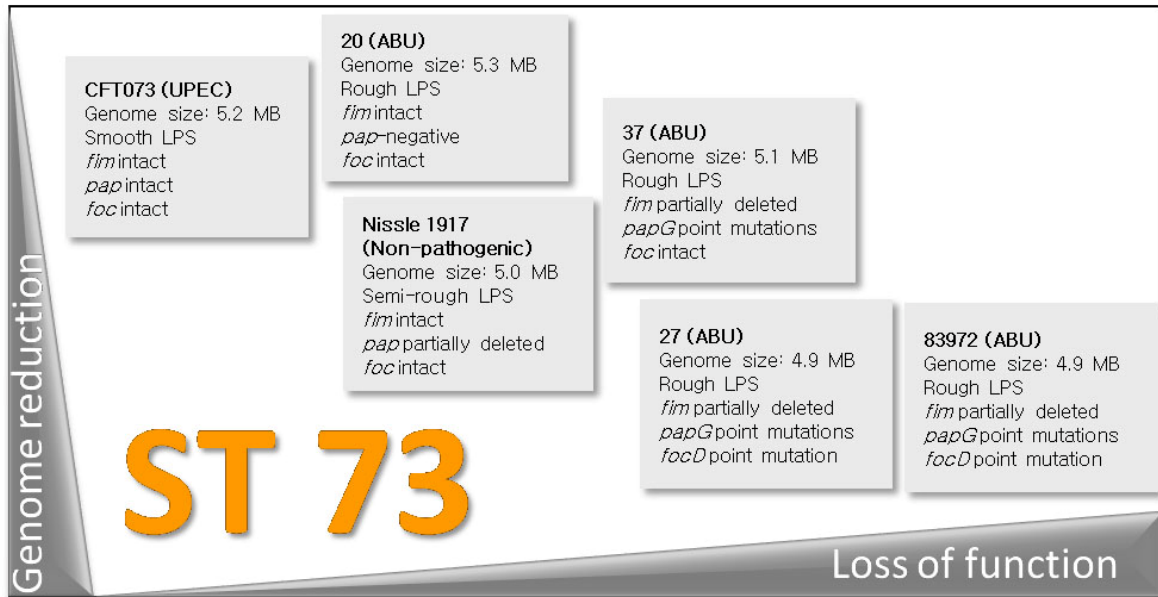


Fig. 50: Geno- and phenotypic diversity among closely related members of *E. coli* clonal group (ST 73). The high *E. coli* genome plasticity results in a marked phenotypic variability among individual members of the same sequence type, which thus includes pathogenic and non-pathogenic variants. Genome reduction/loss of function contributes to the evolution of these ABU variants from uropathogenic ancestors. ST, sequence type; *fim*, type 1 fimbrial determinant; *pap*, P fimbrial determinant; *papG*, P fimbrial adhesin encoding gene; *foc*, F1C fimbrial determinant; *focD*, F1C fimbrial usher encoding gene.

6.4. Host immune response during bacterial colonisation

ABU development is affected by the quality of the host response. In the murine UTI model, an ABU-like state is created when the innate immune response is disturbed. The innate response is controlled by TLR4 and mutations, which disturb TLR4 signalling, result in an asymptomatic carrier state resembling human ABU. The infected mice fail to recruit the inflammatory cells, which are crucial for bacterial clearance (Freundus *et al.*, 2001a; Freundus *et al.*, 2001b; Hagberg *et al.*, 1984) and as a result, bacteria persist in the urinary tract. In another study, the response of human epithelial cells, obtained from urinary tract surgery, to infection with either fimbriated or non-fimbriated bacteria was examined (Samuelsson *et al.*, 2004). It was shown that production of IL 6 and IL 8 correlated with bacterial fimbriation. Human uroepithelial cells possess the molecular machinery to respond to UPEC. It was speculated that differential expression of the membrane-bound receptors regulates its sensitivity to infection and allows discrimination between more-virulent (UPEC) and less-virulent (ABU) strains. Therefore, the combination of the expression of different bacterial

surface-associated molecules and the host ability to sense them is critical for the development of symptoms and bacterial clearance or the asymptomatic carrier state.

The lack of inflammation prevents the symptoms and tissue damage that are associated with symptomatic UTI in a fully responsive host. Recently, children with ABU were shown to express lower amounts of TLR4 than controls without a history of UTI and children with primary ABU had even lower levels than those who had an ABU recurrence after a prior symptomatic UTI episode (Ragnarsdottir *et al.*, 2007). The TLR4 variations add an essential variable to the understanding of ABU. Independently of the host genetics, a “commensal” ABU strain would not be expected to cause symptomatic UTI, but a more virulent strain might cause symptoms and an attenuating host response in patients with normal TLR4 expression, would eventually lead to ABU. Patients with low TLR4 levels would be expected to have a reduced innate response to infection, and would develop ABU also upon infection by more virulent. A good example for such strain is ABU 64, which in contrast to the other examined isolates was able to express many UPEC-associated virulence factors (Table 9).

Bacteria were reported to actively modulate host immune response (Klumpp *et al.*, 2001; Klumpp *et al.*, 2006). UPEC strain NU14 suppresses both TNF- α - and LPS-mediated NF- κ B activation and IL 6 secretion in urothelial cell cultures. Additionally, NU14 can inhibit IL 6 secretion induced by nonsuppressor strain K-12 strain from urothelial cells in a mixed culture. Furthermore, examination of a panel of clinical *E. coli* isolates, broadly representing different phylogenetic groups, revealed that 15 of 17 strains also possessed the ability to suppress cytokine secretion (Billips *et al.*, 2007). In addition, modulation of cytokine secretion was independent of the presence of type 1 fimbriae and 21 other known virulence factors. Another example how bacteria subvert host defences is expression of TIR (Toll/interlucien-1 receptor) domain containing proteins (Tcps). These proteins were found to be common in the virulent UPEC and were termed TcpC. TcpC acts by inhibiting Toll-like receptor (TLR) and myeloid differentiation factor 88 (MyD88) specific signalling, thus suppressing innate immunity and increasing virulence (Cirl *et al.*, 2008).

Asymptomatic bacteriuria, i.e. colonization of the urinary tract without causing significant host responses could be a combination of different strategies. First of all, it is patient-dependent, and as already mentioned, due to variations of the uroepithelial host receptors (Ragnarsdottir *et al.*, 2007; Samuelsson *et al.*, 2004). Secondly, as a result of this study

(Zdziarski *et al.*, 2008), bacteria might prevent recognition by their host and subsequent innate immune response activation due to point mutations in genes encoding for virulence factors. Finally, ABU isolates might actively modulate the immune system by expressing so far unknown molecules, which are independent from still functional or already deactivated virulence factors. A high diversity among ABU strains suggests that a successful ABU state is a sophisticated process and is a combination of above mentioned components. Therefore, future experiments should include sequencing of ABU genomes, looking for interkingdom crosstalk and a more detailed characterisation of ABU isolates regarding host response modulation.

6.5. Host-bacterium interactions

Already in 1989, Hansson and colleagues reported that long term carriage of bacteria in the urinary tract seemed to induce changes in bacterial surface antigens. However, at that time methods to analyse bacterial relatedness were not yet very well developed. Using multilocus enzyme electrophoresis and O antigen analysis they found that 10 out of 25 O-typeable strains converted to non-typeable while retaining the same electrophoretic type. It was suggested that the loss of surface antigens occurs during long term exposure of *E. coli* to the components of the urinary tract. This study was a consequence of the discovery that untreated asymptomatic bacteriuria in young school girls protected against invasion by other bacterial strains, often leading to symptomatic infections (Lindberg *et al.*, 1978; Savage *et al.*, 1975). Interestingly, in the next years one of the isolates, *E. coli* strain 83972, was used for deliberate patient colonisation (Andersson *et al.*, 1991; Sunden *et al.*, 2006). Thanks to the close collaboration with Catharina Svanborg and Björn Wullt (Lund), the consequences of host–bacterium interaction could be analyzed in more details.

6.5.1. Bacterial variability and host response

Consecutive re-isolates of strain 83972 derived from the patient colonisation study were analysed regarding their genome structure. It turned out that several bacterial clones have changed their restriction pattern indicative of DNA rearrangements, deletions or point mutations. One of the frequently observed DNA modifications are point mutations resulting in single nucleotide polymorphisms (SNPs). It is rather difficult to detect SNPs by the PFGE

approach, because it would then have to be located in the restriction site of the used enzyme. So far, only genome sequencing allows detection of unknown point mutations. However, in the genomics era with sequencing techniques becoming cheaper and faster, this might give us more insights into bacterial microevolution during host colonisation. Second, and most likely easier to detect by genomic fingerprints are DNA rearrangements mediated by mobile DNA elements. This includes IS element transposition, prophage insertions and excisions as well as acquisition of larger DNA stretches called genomic or pathogenicity islands (Dobrindt *et al.*, 2004; Hacker and Kaper, 2000).

When bacteria enter a new host, as it was also the case for strain 83972 during deliberate colonisation studies, they enter a new environment and must start to grow and reproduce. The growth rate, the same colonization success, depends on several factors. Among the most important are the availability of nutrients, physical conditions like urodynamics in the bladder (Wullt *et al.*, 1998), competitiveness against other microbes and antimicrobial host defences (Bergsten *et al.*, 2005; Wullt *et al.*, 2003). Even if the bacterium is able to initially multiply, due to its former life in the urinary bladder of a young girl for three years (Andersson *et al.*, 1991), its fitness is probably be suboptimal in the new niche. Optimal fitness has to be reached through a process of adaptation within this environment by modifications of pre-existing genes. Thus, point mutations, gene loss and acquisition, IS element-mediated transposition may contribute to improve bacterial fitness. The cycles of natural selection will be repeated until the bacterium reaches an optimal adaptation state in the bladder of a currently colonised patient.

Bacterial persistence in the urinary tract is not without an effect on the bladder physiology. Depending on the bacterial epitope, innate immune response is induced to a certain extent. Uropathogenic *E. coli* strains activate IL 6 and IL 8 chemokines. Activation is much stronger when bacteria express functional fimbriae, however, non-fimbriated isolates cause lower and delayed response (Samuelsson *et al.*, 2004). Likely, in most cases asymptomatic bacteriuria isolates belong to the second group of ‘activators’. The same bacterium might have distinct activating abilities, what could be seen among colonized patients with strain 83972 (Fig. 21 and Fig. 22), where the mean of IL 8 expression was very diverse, and in the strongest ‘responder’ was over 8-fold higher than in the lowest one. On the other hand, the level of immune response may vary due to patients susceptibility to UTI and theirs prevalence to a group of low- or high-responders (Svanborg *et al.*, 2006).

IL 6 may cause fever and triggers the acute phase response, while IL 8 recruits inflammatory cells to the site of infection (Hedges *et al.*, 1995). The most important are neutrophils (PMN), which play a pivotal role in host defence against microbial infection (Engel *et al.*, 2006; Haraoka *et al.*, 1999). In response to pathogens, neutrophils adhere to the endothelium and transmigrate into the infected tissue, where their activation induces the production of nitric oxide (NO) and release of granular enzymes that eliminate the intruding pathogen. Nitric oxide synthetase (iNOS) from PMNs is 43-fold up-regulated in patients with urinary tract infections when compared to healthy individuals (Wheeler *et al.*, 1997), what results in 30-50 times higher NO concentrations in urine (Lundberg *et al.*, 1996). Klemm and co-workers corroborated these results, finding genes involved in NO protection and metabolism to be induced in ABU strain 83972 upon intravesical growth *in vivo* (Roos and Klemm, 2006). Moreover, urine contains significant amounts of nitrate (Tsikas *et al.*, 1994) and anaerobic NO₃ metabolism results in the generation of additional nitric oxide. It is well documented, that nitrosating agents produce mutagenic lesions (Weiss, 2006). Therefore, regarding the frequent occurrence of mutations in the genomes of certain ABU isolates which are not mutators by themselves, it is tempting to speculate that prolonged growth in urine and exposure to immune response promotes the mutation rate thus being a driving force for the development of the ABU lifestyle and evolution within the urinary tract.

The current approach, where the same bacterium was subjected to interaction with multiple human hosts, further corroborates this hypothesis. Numerous changes in the genome structure of consecutive re-isolates derived from the human colonisation study imply the importance of interactions with the host during bacterial evolution. Furthermore, genome structure of re-isolates from the continuous flow culture, where strain 83972 was propagated without host contact, was not affected. However, two of four bacterial populations were propagated with addition of nitric oxide. Altogether, the results indicate that not only prolonged growth in urine and the presence of nitric oxide but also direct contact with the host tissues and selective pressure promote bacterial variability. Regarding the presence of nitric oxide in the continuous culture, it would need further investigation since it is difficult to stably provide the required concentration of this extremely instable compound. Moreover, the mutagenic effect of NO is rather due to the occurrence of point mutations than to bigger DNA rearrangements detectable by PFGE and final conclusions can be drawn after the analysis of the genome sequences of bacteria grown with and without contact with the human host.

Taken together, so far not well-characterized host factors play an important role in evolution of bacterial commensalism within the urinary tract. Point mutations and other DNA rearrangements, unless they are deleterious, contribute to adaptation and survival of asymptomatic *E. coli* in the urinary bladder environment. Without doubt, positive selection of clones which do not activate a strong immune response favours bacteria which are less aggressive to the host. Moreover, detection of the genomic regions subjected to host-driven mutagenesis might help to discover new potential drug targets.

6.5.2. Flagella expression / motility

Although *E. coli* strain 83972 has been characterized in many details regarding the expression of different fimbriae (Klemm *et al.*, 2006; Roos *et al.*, 2006a; Zdziarski *et al.*, 2008), not much is known about flagella expression by this strain. Both animal and human *in vivo* transcription studies indicate that motility is down-regulated during *E. coli* bladder colonisation (Roos and Klemm, 2006; Snyder *et al.*, 2004). However, flagellum-mediated motility/chemotaxis was proven to be not required but beneficial during colonization of the urinary tract by contribution to the fitness of the bacterium (Lane *et al.*, 2005). The parent strain 83972 used for both the human colonization study and the *in vitro* “2000 generation experiment” is very little motile. Whereas it was found that several *in vivo* re-isolates were characterized by different degrees of motility suggesting that its genetic determinants is intact and is subjected to active regulation. Moreover, bacteria grown *in vitro* in urine exhibited flagella up-regulation in a few cases, while none of the LB-grown re-isolates exhibited this phenotype.

The flagella was shown to stimulate IL 8 production (Zhou *et al.*, 2003). Therefore, in accordance with the model of ABU lifestyle where immune response activation is avoided, in most re-isolates some weak motility could be observed. Interestingly, close to the time points when most *in vivo* re-isolates with up-regulated flagella expression were found, host response was increased. Since in many cases only a few isolates from a certain time point were analysed, it is difficult to estimate how much of the bacterial population in the bladder is represented by the same phenotype. Because adhesion is not necessary for persistence of bacteria in the urinary tract (Andersson *et al.*, 1991), other fitness factors might be more important. Heterogeneous cultures with regard to motility, like in the microfermenters, may

be advantageous for the ABU strain as urodynamic defects of colonized patients support colonisation with non-virulent strain 83972 (Wullt *et al.*, 1998). A mixed bacterial population with a low percentage of motile individuals (minimal host response activation) could play an important role in bladder colonisation, especially at voiding time points. Because strain 83972 does not adhere to the bladder tissue, the time shortly after voiding might resemble initial steps of urinary tract colonisation, for which flagella was reported to be beneficial (Lane *et al.*, 2005). Therefore, future studies are needed to analyze the function and importance of this still not deactivated feature of strain 83972 for the establishment of asymptomatic bacteriuria.

6.5.3. Biofilm formation

Another suggested mechanism how bacteria colonise the urinary tract is biofilm formation. Whereas in nature bacteria often exist within biofilms (Costerton *et al.*, 1999), formation of this structures within the urinary tract is still questionable. Although biofilm formation on abiotic surfaces is well reported and of particular interest in medical field, not much is known about biofilm structures *in vivo* within the bladder. Intracellular bacterial communities (IBC) are considered as one of the biofilm forms and rather restricted to pathogenic bacteria expressing type 1 fimbriae and flagellum (Anderson *et al.*, 2004). Moreover, it has been reported that *in vitro* biofilm formation of a significant number of wild type *E. coli* isolates could not be correlated to any of the pathotypes and is dependent on the used medium (Reisner *et al.*, 2006). On the other hand, Klemm and co-workers reported that asymptomatic bacteria isolates form significantly more biofilm than other uropathogenic *E. coli* strains and propose it to be the favourable strategy for successful ABU lifestyle (Ferrieres *et al.*, 2007; Hancock *et al.*, 2007).

In contrast to that, our study did not reveal significant differences in biofilm formation of uropathogenic and ABU isolates. Moreover, the wild type strain 83972, being a relatively good biofilm former, did not preserve this phenotype after long term persistence within the bladder. Only one re-isolate was shown to be better and two other were nearly as good biofilm formers as their parent strain. However, this situation was observed only in human urine and already in laboratory medium M63 the differences could not be observed. This also further corroborates the results of Reisner and colleagues (2006). The transcriptome analysis of *in vivo* re-isolates confirmed *luxS* (*ygaG*), coding for protein involved in autoinducer 2 (AI-2) biosynthesis, to be up-regulated. AI-2 is a quorum sensing (QS) molecule that also

negatively controls biofilm formation (Surette *et al.*, 1999). While it has been proposed that asymptomatic bacteriuria isolates express more biofilm than symptomatic UPEC strains which is required for biofilm formation to colonise the bladder (Hancock and Klemm, 2007), our data show a reduction in this phenotype upon prolonged contact with the host. In agreement with that, biofilm formation of re-isolates derived from the ‘host free’ experiment was at least as good as that of the parent strain, sometimes even better.

As already mentioned, the gene *ygaG* is involved in methionine metabolism, which was reported to be induced upon nitrosative stress (Flatley *et al.*, 2005; Jarboe *et al.*, 2008). This condition might be encountered by bacteria either during denitrification or NO-mediated host defence. Biofilm forming bacteria are in a very close contact with the host tissue, what increase the possibility of activation of the host immune system, the IL 8 recruit inflammatory cells to the site of infection and toxic nitric oxide is released (Hedges *et al.*, 1995). As ABU isolates rather resemble commensal bacteria, an unnecessary immune system activation should be avoided. Interestingly, it was shown that NO causes dispersal of *Pseudomonas aeruginosa* and *Staphylococcus aureus* biofilms (Barraud *et al.*, 2006; Schlag *et al.*, 2007). Because NO concentrations in the bladder are rather high and further elevated when host defence is activated, it is expected that asymptomatic bacteria will not form much biofilm and rather live as planktonic cells. Furthermore, our results of the microfermenter experiments support this hypothesis, as they showed a significant reduction in biofilm formation after addition of nitric oxide to the medium.

6.5.4. Growth characteristics

Presumably, the fast growth and efficient utilization of resources available in urine belong to the most important factors enabling ABU isolates to inhabit the urinary tract. In healthy adults, normal urine production ranges from 1-2 litres per day and single micturition results in release of 200-400 ml of urine. Following micturition, about 1 ml of urine remains in the bladder and might function as a sufficient inoculum for repeated bladder colonization until the next voiding episode. When growth rate is high enough so that the number of proliferating bacteria exceeds the number of those which are lost due to micturition, surface-associated growth is not needed to persist within the bladder (Gordon and Riley, 1992). The early phase of colonisation is critical in successful establishment of bacteriuria, because at that time point the innate immune system might be able to clear the bacteria. Therefore, fast growth in the

early exponential phase in combination with low host defence activation might be a successful strategy to establish a permanent asymptomatic bacteriuria.

Indeed, the eleven tested ABU isolates exhibited good growth rates *in vitro* in human urine, however, varied from strain to strain. Moreover, the analysis of the re-isolates of strain 83972 from the human colonisation study implicated that, depending on the patient, nutrients availability and the quality of the host response, these strains might not take advantage of their growth potential. The results demonstrate, that multiple *in vivo* re-isolates exhibited slower growth rates than their parent strain and in many cases different re-isolates from the same patient exhibited similar growth rates. This further underlines the importance of the host background. Without doubt, the extent of the host response is one of the most important factors for the modulation of bacterial growth in the bladder. ABU isolate 83972 does also induce a human immune response to a certain extent (C. Svanborg, personal communication). If bacteria grow too fast, their number might exceed a threshold that is considered to be dangerous and they will thus be subsequently cleared. As a consequence, the host defence, in case of asymptomatic bacteriuria, might function as a negative feedback and regulate commensalism in the urinary tract.

6.6. Metabolic activity of ABU isolates

Another critical and limiting factor during bacterial growth in the bladder is nutrient availability. The metabolic variability in an individual and between different persons results in significant differences in the urine composition not only in between but also in the same host. Different reasons like genetic differences, age and lifestyle, nutrition, and exposure to specific chemicals result in a wide variety of urine compositions in individual patients (Rezzi *et al.*, 2007; Stella *et al.*, 2006). Changes in diet, day- and night-time, and different stages of hormonal cycle contribute to inter-individual fluctuations (Rezzi *et al.*, 2007).

Bacterial metabolic networks have to be adjusted to grow fast and optimally utilize nutrients present in the urine. This is achieved in many cases by transcriptional regulation of gene expression. Stable alterations in the expression of metabolic pathways, even after *in vitro* cultivation of re-isolates in urine, indicate that also stable DNA modifications (e.g. point mutations, insertions, deletion) contribute to this process. Transcriptome analysis of the

chosen re-isolates uncovered significant differences not only between *in vivo* and *in vitro* growth conditions, but also among *in vivo* re-isolates. Bacteria in individual hosts might approach slightly different strategies how to supply enough energy for fast proliferation. This has been very well demonstrated by the comparison of the transcriptomes of re-isolates SR12 and CK12.

Naturally occurring sugar acids such as galacturonate from pectin and gluconate and ketogluconate from muscle tissues are present in the food we eat (Peekhaus and Conway, 1998). The bladder urothelium is covered by a thick layer of protective glycoprotein and is rich in *N*-acetylglucosamine, *N*-acetylgalactosamine, sialic acid and lesser amounts of glucuronate and galacturonate. In line with that, the *in vivo* re-isolate SR12 possesses up-regulated pathways of uptake and metabolism many of these sugars. It has been already reported that during growth in urine *E. coli* induces expression of genes involved in uptake and utilization of the sugar acids galacturonate, glucuronate and galactonate (Roos *et al.*, 2006b). We found out, that the induction of these genes is not only de-regulated because of growth in urine but also depends on the patient and might be connected to the diet and physiological state.

Another example of an alternative nutritional strategy of strain 83972 during growth in the bladder is the degradation of ribo- and deoxyribonucleosides. This is apparent from the proteome and transcriptome comparison of *in vivo* re-isolate CK12 and its parent strain 83972. Nucleic acids are highly abundant in the urine when many epithelial cells undergo apoptosis and their DNA is degraded. Also bacterial lysis is a good source of freely available nucleic acids in the urine. In the re-isolate, the gene *udp* and its product uridine phosphorylase were found to be strongly up-regulated by transcriptome and cytoplasmic proteome comparison, respectively. This enzyme catalyses phosphorylation of uridine followed by the conversion to ribose and uracil. Uridine diphosphate serves as a glycosyl carrier in many important reactions like glucuronidation, where UDP-glucuronic acid (glucuronic acid linked via a glycosidic bond to uridine diphosphate) is an intermediate in the process (King *et al.*, 2000). In the animal body, glucuronic acid is often linked to the xenobiotic metabolism of substances such as drugs, pollutants, bilirubin, androgens, estrogens, mineralocorticoids, glucocorticoids, fatty acid derivatives, retinoids, and bile acids. The substances resulting from glucuronidation are known as glucuronides (or glucuronosides) and are typically much more water-soluble than the non-glucuronic acid-containing substance from which they were

originally synthesised. The human body uses glucuronidation to make a large variety of substances more water-soluble, and in this way, allow for their subsequent elimination from the body upon urination (King *et al.*, 2000). Most likely bacteria might be able to employ enzymes like Udp to use uridine as a carbon source via the pentose phosphate pathway.

One more example how bacteria utilize compounds from urine as a carbon source is D-serine metabolism. D-serine is excreted in human urine at concentrations ranging from 3.0 to 40 $\mu\text{g ml}^{-1}$ (Brückner *et al.*, 1994). An epidemiological study demonstrated that the *dsdA* gene encoding for the D-serine deaminase is more frequently present in uropathogenic than in faecal isolates (Roesch *et al.*, 2003). Indeed, the asymptomatic strain 83972 possesses the *dsdA* gene and, depending on the colonized host, might use it to certain extent. In case of re-isolate SR12, transcriptome analysis demonstrated that the genes *dsdA* and *dsdX* (encoding for D-serine transport) were significantly up-regulated compared to the parent strain 83972. Moreover, genes coding for proteins involved in L-serine metabolism were found to be down-regulated indicating that D-serine but not L-serine is used by *E. coli* strain SR12 as a carbon source. Interestingly, D-serine inhibits in higher concentrations growth of *E. coli* by blocking the L-serine and pantothenate biosynthesis (Cosloy and McFall, 1973). Therefore, up-regulation of D-serine catabolism by *E. coli* strains colonizing the urinary tract might have a dual function: nutrition and detoxification.

Recent findings further underline the importance of D-serine during urinary tract colonisation in addition to the nutritional aspect. *In vitro* transcriptome analysis of UPEC strain CF073 and its *dsdA* mutant during murine infection revealed that a set of genes coding for virulence factors including P- and F1C fimbriae as well as alpha-hemolysin were up-regulated in the mutant. Moreover the *dsdA* mutant was hyperflagellated and outcompetes the wild type strain in the murine urinary tract (Haugen *et al.*, 2007). *dsdA* expression is phase variable and this switch is linked to the expression of type 1 fimbriae and reciprocal to motility (Anfora *et al.*, 2007). Altogether, these findings underline the importance of serine homeostasis in the bacterial cell during growth in the urinary tract. According to this model, already inactivated virulence-associated genes in ABU strain 83972 would be further down-regulated due to up-regulation of *dsdA* expression. Furthermore, increased D-serine transport into the cell would explain the increased flagella expression in re-isolate SR12.

D-serine deamination results in pyruvate and ammonia (Roesch *et al.*, 2003) and the latter product can be used as a nitrogen source. In line with that, the transcriptome analysis of re-isolate SR12 revealed along with the up-regulation of genes required for D-serine catabolism, induction of many genes involved in nitrogen homeostasis (Fig. 51). There are two physiologically independent pathways of ammonium assimilation in *E. coli* with glutamate and glutamine as primary products (Reitzer, 2003). Glutamate synthesis from α -ketoglutarate and ammonia (via the GDH pathway) is employed under energy-limited (presumably nitrogen-rich) conditions, whereas glutamine synthesis (via the GS-GOGAT pathway) is used under energy-rich conditions and consumes ATP (Helling, 1994). According to transcriptome data, the first pathway is particularly used by strain SR12 since the expression of glutamate dehydrogenase and glutamine synthetase-encoding genes was found to be up-regulated and down-regulated, respectively (Fig. 51). In addition, expression of the two-component system GlnGL, which is involved in response to nitrogen limitation and which positively regulates glutamine synthesis (Reitzer, 2003), was also found to be down-regulated on the transcriptional level. Moreover, transcriptome profiling uncovered glutamine transport to be repressed in strain SR12 relative to parent strain 83972.

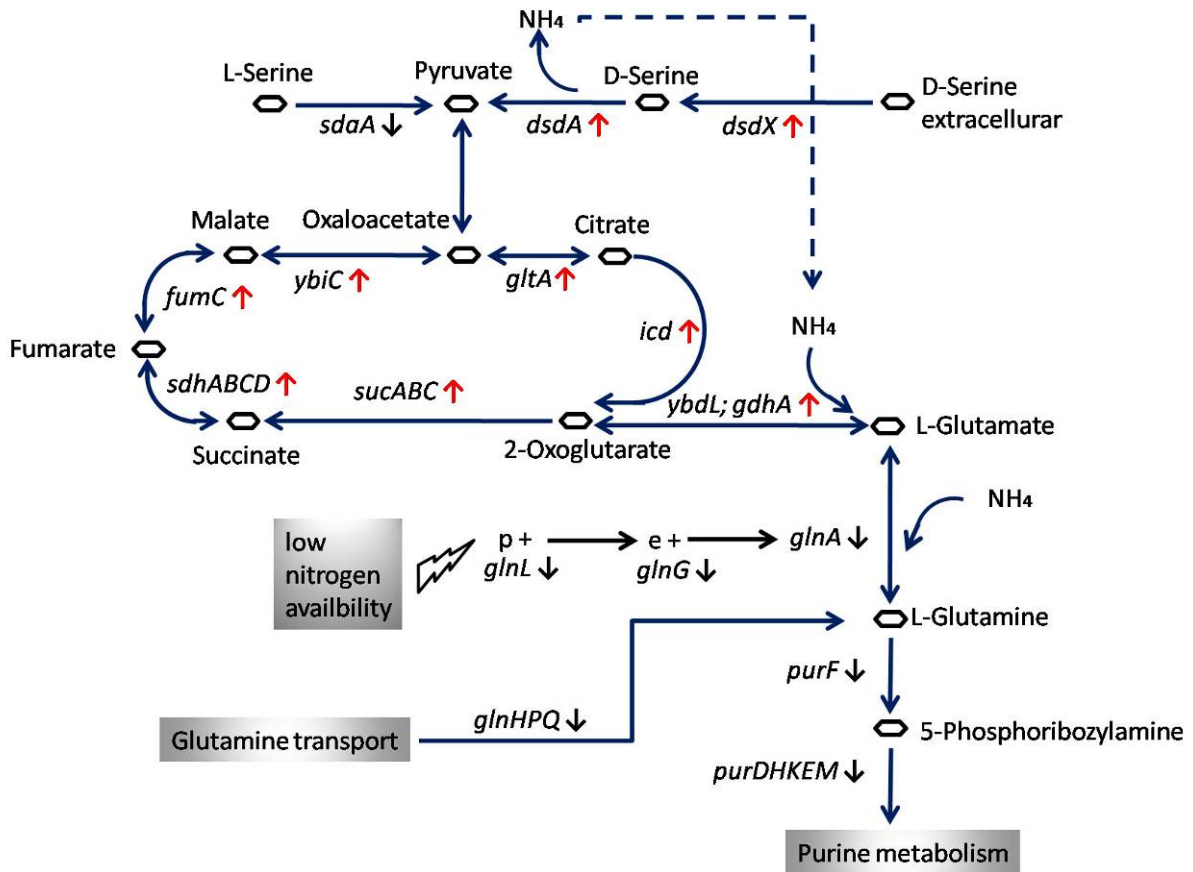


Fig. 51: Model of D-serine catabolism and nitrogen assimilation in strain SR12. Red arrows indicate up-regulated, black down-regulated genes in strain SR12 when compared to strain 83972.

Taken together, these data demonstrate that during growth in the urinary tract the *E. coli* metabolism and catabolism are efficiently adjusted to the specific nutrients supplied. Strain 83972 is able to take up and metabolize a number of sugars, sugar-derivatives and amino acids present in urine. Energy metabolism and nitrogen assimilation seem to be adjusted to the low energy and nitrogen-rich growth conditions in urine.

6.7. Outer membrane protein profile and iron uptake

For bacteria living within other organisms, the outer membrane is a critical barrier that directly interacts with the host components (Cullen *et al.*, 2004). Depending on the bacterial colonization strategy, either many cell surface-associated proteins including adhesins will be expressed or only a minimal protein set that facilitates the acquisition of nutrients and macromolecules from the respective niche. *E. coli* associated with asymptomatic bacteriuria would be expected to fall into the second group because outer membrane proteins are known

to induce host response and immunogenic reactions (Hagan and Mobley, 2007). To characterise the expression of cell surface-associated structures, ABU strain 83972 was analysed with regard to the outer membrane protein (OMP) profile.

2D gel electrophoresis (2D-GE) is a powerful tool to investigate the composition of protein fractions. Unfortunately, there are some drawbacks like protein solubility and their hydrophobic character. Another critical step is protein isolation (Molloy *et al.*, 2000), as, depending on the cell lysis strategy, most of the loosely surface-associated proteins such as fimbrial components are removed and the remaining fraction consists of mainly integral OMPs. As the determinants coding for typical UPEC adhesins like F1C, P, type 1 fimbriae are non-functional in strain 83972 (Klemm *et al.*, 2006; Roos *et al.*, 2006a), and due to the bacterial cell lysis using the French press, it was not expected to detect these adhesins by means of 2D-GE.

The three *in vivo* re-isolates (CK12, SR12 and KA25) and their parent strain 83972 exhibited very similar OMP profiles. Nevertheless, certain alterations in individual protein amounts were observed. Of the 18 detected proteins in parent strain 83972, eight proteins (FepA, FecA, FhuA, FhuE, ChuA, IutA, IroN and Iha) are known components of siderophore systems. Among the proteins which are not involved in iron uptake, OmpA and OmpC the major porins involved in diffusion and influx of nutrients into the periplasm (Garten *et al.*, 1975) were the most abundant ones. This data further corroborate our expectations that the strain 82972 is well adapted to growth in urine as an iron-limited medium. The expression of multiple iron uptake systems is therefore fundamental to efficiently grow in this niche (Andrews *et al.*, 2003; Baumler *et al.*, 1996; Torres and Payne, 1997).

E. coli surface-exposed proteins are frequently anchored in the outer membrane and serve as antigens for the human immune system. It is expected that individual patients differ markedly in their efficiency to express defence mechanisms against bacteria. To analyse the impact of prolonged host-pathogen interaction, the outer membrane protein profile of the *in vivo* re-isolates from individual patients were compared. The most abundant and rather constitutively expressed protein among the tested re-isolates was FepA, which is involved in transport of enterobactin-bound iron across the outer membrane (Sansom, 1999). The second most accumulated protein was IroN. In contrast to FepA, IroN amounts varied from strain to strain. Hagan and Mobley (2007) reported IroN to be immunogenic in mice. In the same study, the

proteins IutA, ChuA and Iha were mentioned to be antigenic in the murine model. We found out that IutA and Iha were differently expressed in the patients and that they were not expressed at all in re-isolate CK12. This shows that expression of multiple iron uptake systems in strain 83972 varies depending on the colonized host. Referring to the work of Hagan and Mobley (2007), many surface-associated proteins are immunogenic. Therefore, we propose that the quality of the host immune response plays an important role and directs the optimal expression of individual iron uptake systems under these conditions.

6.8. Host defence-driven bacterial gene expression

Changes in bacterial gene expression upon contact with the human host are intensely studied during the last years. This co-existence does also affect the host physiology. Even ABU isolates do induce host immune response, which involves chemokine production and neutrophil influx at the site of infection (Haraoka *et al.*, 1999; Samuelsson *et al.*, 2004). Neutrophils are known to produce and release significant amounts of nitric oxide (NO), which is, however, also produced by other mammalian cells (Bogdan, 2001). Therefore, NO functions not only as an antimicrobial agent but also has a pleiotropic effect in the human body (i.e. signalling function) (Bogdan, 2001). It is interesting to understand how eukaryotic cells switch off these signals or protect themselves from NO and NO-related molecules produced for defence purposes. Recently, it has been shown that in eukaryotes the glutathione-dependent formaldehyde dehydrogenase (GS-FDH or ADH III) is required to control intracellular levels of both S-nitrosoglutathione (GSNO) and S-nitrosothiols (SNOs) (Liu *et al.*, 2001). Moreover, the GS-FDH is conserved from humans to bacteria and the deletion the reductase-encoding gene in mice and yeast abolishes the GSNO-consuming activity and increases susceptibility to a nitrosative challenge.

E. coli harbours the *frmRAB* gene cluster coding for the glutathione-dependent formaldehyde dehydrogenase and the S-formylglutathione hydrolase that were primary ascribed to formaldehyde detoxification. FrmR is predicted to be a negative regulator of the *frmRAB* operon. In addition to FrmB, *E. coli* possesses a second S-formylglutathione hydrolase encoded by *yeiG*, which in contrast to FrmB is constitutively transcribed (Gonzalez *et al.*, 2006). Interestingly, the *in vitro* transcriptome analysis of the re-isolates from the human colonisation study revealed the *frmRAB* gene cluster to be de-regulated relative to the parent

strain. In two re-isolates (SR12 and KA25) these genes were found among the most strongly up-regulated genes when compared to their ancestor strain. Moreover, this observation was further corroborated on the protein level where FrmA and FrmB could be identified as the most up-regulated proteins in the cytoplasm when compared to strain 83972. These data indicate that the re-isolates SR12 and KA25 might have encountered during patient colonization conditions which demand either formaldehyde or nitric oxide detoxification.

Many extensive studies regarding NO response faced by pathogens have shown a diverse number of genes to be affected (Flatley *et al.*, 2005; Jarboe *et al.*, 2008; Poole *et al.*, 1996; Pullan *et al.*, 2007). The gene *hmpA* coding for the NO-inducible flavohaemoglobin was found to be up-regulated in many bacteria during NO detoxification. In our study, we further corroborate these results, and demonstrate that prolonged exposure to host defence factors and most likely elevated concentrations of nitric oxide in the bladder lead to the up-regulation of *hmpA* expression in *E. coli*.

The cytoplasmic protein profiles of the re-isolates SR12 and KA25 together with the transcriptome of re-isolate SR12 pinpointed a di-iron protein YtfE to be up-regulated when compared to the parent strain. Interestingly, growth *E. coli ytfE* mutants is impaired upon nitrosative stress and this effect was even stronger than for *hmpA* or *norV* mutants (Justino *et al.*, 2005). NorV is a protein with non-heme di-iron site involved in NO detoxification (Gardner *et al.*, 2002). Recent studies of the same working group revealed that YtfE is involved in iron-sulphur containing protein activity (Justino *et al.*, 2007). Furthermore, YtfE is required during anaerobic respiration under iron-limiting conditions and is hypothesized to be involved in the biosynthesis and repair of iron-sulphur clusters. Thus, the comparison of *in vivo* re-isolates and the parent strain 83972 revealed another gene, *ytfE*, which is indirectly involved in stress response and NO detoxification during human bladder colonization.

Chemostat-cultured *E. coli* exhibit distinct regulatory responses upon exposure to either NO or GSNO (Flatley *et al.*, 2005; Pullan *et al.*, 2007). While the genes *hmpA* and *ytfE* were described to be affected under both conditions, the Fnr and Fur regulon were exclusively down-regulated during exposure to NO. The GSNO-specific response includes methionine biosynthesis, multidrug transport (*mdtC*) and amino acid transport (*yhaO*) (Pullan *et al.*, 2007). Analysis of the transcriptome of *in vivo* re-isolates indicated that the strains SR12 and KA25 exhibited, with minor exceptions, an expression pattern that resembled that of GSNO-

exposed bacteria. While in strain SR12 none of the genes from Fnr and Fur regulon were de-regulated, in strain KA25 transcript levels of the *nrfHIEF* gene cluster were up-regulated. In addition, *norV* and *narV* transcript levels were down-regulated.

Interestingly, our study indicates for the first time that in *E. coli* methionine biosynthesis and protection against nitrosative stress might be linked to FrmA expression. As already mentioned above, FrmA (also designated as AdhC) belongs to the family of class III glutathione-dependent alcohol dehydrogenase and is reported to protect eukaryotic cells from antimicrobial nitric oxide (Hedberg *et al.*, 2003; Liu *et al.*, 2001). Kidd and colleagues (2007) discovered that the *adhC* gene in *Haemophilus influenzae* is required for defence against nitrosative stress. *Salmonella enterica* mutants in *adhC*, however, were not impaired in NO detoxification (Bang *et al.*, 2006). Up to date, nothing is known regarding the function of AdhC during urinary tract colonisation of *E. coli*, and therefore, a new model is proposed as follows (Fig. 52):

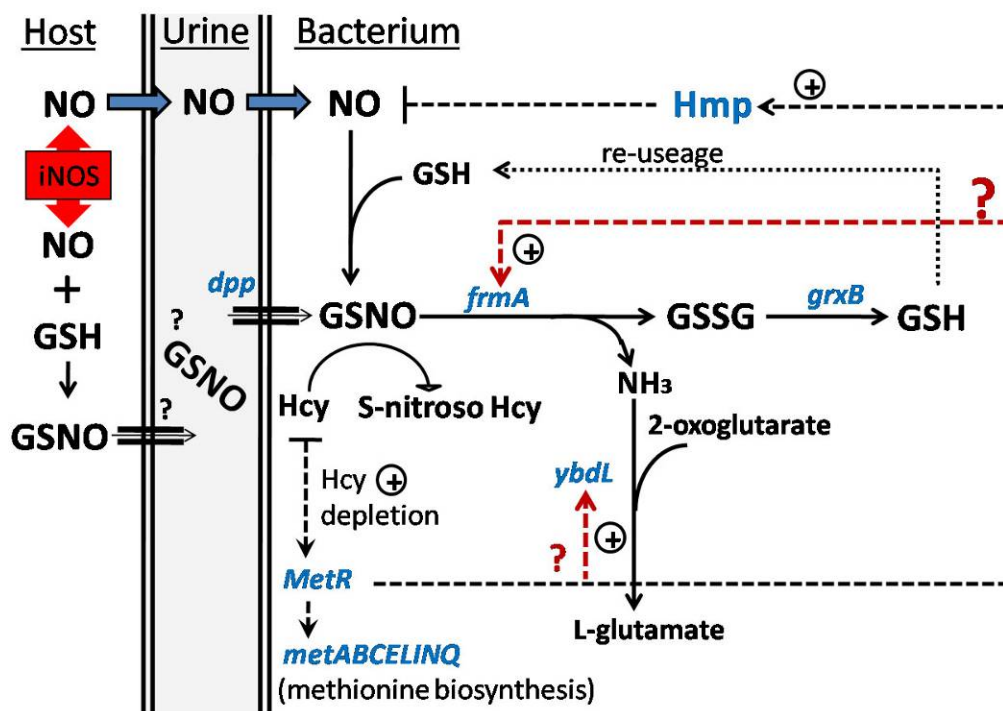


Fig. 52: Model of nitric oxide detoxification based on hierarchical cluster analysis of genes differently de-regulated in *in vivo* re-isolates SR12 and KA25 relative to their parent strain 83972. The different genes and proteins found to be up-regulated in the transcriptome and proteome profiles of strains SR12 and KA25 are indicated in blue. Black dotted lines show known regulatory responses. Red dotted lines with a question mark indicate proposed new functional relationships. NO – nitric oxide, iNOS - inducible nitric oxide synthase, GSH – glutathione, GSNO - S-nitrosoglutathione, GSSG – glutathione disulphide, Hcy - homocysteine.

It has been proven that NO and GSNO exhibit distinct chemical reactivities (Wink and Mitchell, 1998). NO is well soluble in water, diffuses easily through membranes and interacts with biomolecules within its immediate environment to form other reactive nitrogen species (RNS), such as GSNO and SNOs through interactions with glutathione (GSH) and thiols, respectively (Fang, 2004). GSNO has been shown to be dependent on the Dpp dipeptide ABC transporter (Abouhamad *et al.*, 1991). The transcriptome analysis of *in vivo* re-isolates SR12 and KA25 indicated, however, only one gene *dppA* from the entire *dppABCDF* operon to be up-regulated relative to strain 83972. Therefore, it is not clear whether in re-isolates SR12 and KA25 GSNO is only intracellularly formed by interaction of NO with GSH or whether it is also transported from the environment into the cell. The *ex vivo* character of the study increases the possibility of false-negative artefacts and future *in situ* experiments would be needed to address this question.

Current experimental approaches tend to distinguish NO from GSNO response mechanisms (Flatley *et al.*, 2005; Pullan *et al.*, 2007). However, there are some implications that both of them take place at the same time depending on the redox state of the cell (Fang, 2004). Either imported or intracellularly formed GSNO nitrosates homocysteine, thereby withdrawing an intermediate product from the methionine biosynthetic pathway (Flatley *et al.*, 2005). Homocysteine depletion results in free MetR, and this protein activates methionine biosynthesis and Hmp expression (Fig. 52). Hmp detoxifies nitric oxide. However, GSNO is still being formed and needs to be neutralized. Although, GSNO-induced gene expression has been analysed, it was not shown how this compound is metabolized by *E. coli*.

Ammonia and glutathione disulphide (GSSG) are the main products of the AdhC enzyme. The yield depends on the free GSH pool in the cell (Liu *et al.*, 2001), however, in the transcription profiles of *in vivo* re-isolates SR12 and KA25 the glutathione synthesis pathway was not affected. Interestingly, ammonium generated from the NO detoxification reaction might be incorporated to 2-oxoglutarate resulting in L-glutamate. This reaction is performed by methionine aminotransferase YbdL.

Not much is known about the molecular basis of regulation of *frmRAB* expression. So far, only one report describes that an amber suppressor tRNA inactivates the repressor FrmR resulting in de-repression of the *frmRAB* operon (Herring and Blattner, 2004). These authors also identified another seven genes to be de-regulated by the same mechanism. Among those

were *rbsDAC* coding for proteins involved in ribose metabolism. However, the whole transcriptional unit consists of the *rbsDACBKR* genes. In our study only *rbsB* was significantly up-regulated, while the other genes were not de-regulated. Performed hierarchical cluster analysis of deregulated genes in strains SR12 and KA25 implies a functional relatedness of the *metR*, *frmRAB*, *hmp* and probably *ybdL* genes. Therefore, future studies are needed in order to uncover molecular mechanisms of *frmA* expression in *E. coli*.

The expression level of this alcohol dehydrogenase in *E. coli* seems to be host-dependent. All analysed re-isolates from the same patient exhibited similar *frmA* transcript levels which varied from patient to patient. Interestingly, independent inoculation events of patient SR pinpointed that up-regulation of *frmRAB* transcription was not an accidental event and was not inherited to the next bacterial generations but occurred upon exposure to the specific conditions existing in the bladder of patient SR.

6.9. Implications and Outlook

In this study, several aspects of asymptomatic bacteriuria were investigated. First of all, it was found that strains with different phylogenetic backgrounds have the ability to establish asymptomatic bacteriuria. Among those were strains that resembled rather commensal-like isolates as well as degenerated UPEC strains with inactivated virulence factors. It was also shown that ABU isolates belong frequently to a certain phylogenetic lineage (ST73), that also includes pathogenic and commensal strains. Furthermore, this study showed that the host plays an important role in bacterial micro-evolution. Future efforts might consider the detailed analysis based on complete genome sequences of several such closely related organisms and the identification of DNA regions that undergo modification upon exposure host defence mechanisms. This, in combination with drug development, might help to improve the quality of life of people frequently suffering from urinary tract infections.

Another, very important implication of the presented study is the impact of host variability in the establishment of asymptomatic bacteriuria. It was documented that bacterial gene expression depends on the host background and is permanently regulated what allows the bacterium to persist in the bladder. Depending on the patient, *E. coli* strain 83972 was able to

take up and metabolize diverse carbon sources, thus being able to colonize this usually sterile niche and to avoid colonization by uropathogens causing symptomatic urinary tract infection.

ABU strain 83972 was carefully characterized regarding many virulence and fitness factors, however, flagella has never been considered as an important factor during the establishment of asymptomatic bacteriuria. We were able to show that flagella are still functional and are expressed in several *in vivo* re-isolates. This supports its possible function during ABU. Thereby mutant analysis would be needed to define the importance of this still remaining intact bacterial surface-associated organelle.

It has never been shown that host defence might trigger bacterial evolution. Here, due to the carefully designed study, we were able to show that *in vivo* growth in the human bladder but not *in vitro* growth in human urine triggered genomic changes in *E. coli*. Using single strains re-isolated from different host backgrounds bacterial co-evolution was captured. Future analyses should include the comparison of genome sequences of the parent strain and its consecutive *in vivo* re-isolates.

Finally, the direct exposure of strain 83972 to host defence factors led to discovery that similar strategies of antimicrobial nitric oxide detoxification take place, both in humans and *E. coli* grown in the urinary tract. It has already been shown for *Haemophilus influenza* that AdhC is required for defence against nitrosative stress (Kidd *et al.*, 2007) and this protein is conserved among many organisms (Liu *et al.*, 2001), but it was never documented that uropathogenic or ABU *E. coli* isolates take advantage of it to detoxify reactive nitrogen species. Recently, Richardson *et al.* (2008) proved that *Staphylococcus aureus*, one of the most successful human pathogens, evades the antimicrobial activity of nitric oxide by expressing an NO-inducible L-lactate dehydrogenase (Ldh1), implicating the role of adaptive metabolism in microbial defence mechanisms. Therefore, much effort is needed to further assess the molecular basis of regulation of *adhC* expression by uropathogenic bacteria and its role during bladder colonisation.

In summary, the presented work on the characterisation of asymptomatic bacteriuria *E. coli* isolates also addresses important aspects of commensalism, host-driven bacterial evolution and the impact of individual host responses during bladder colonisation.

7. References

- Abouhamad, W.N., Manson, M., Gibson, M.M., and Higgins, C.F. (1991) Peptide transport and chemotaxis in *Escherichia coli* and *Salmonella typhimurium*: characterization of the dipeptide permease (Dpp) and the dipeptide-binding protein. *Mol Microbiol* **5**: 1035-1047.
- Agace, W., Hedges, S., Andersson, U., Andersson, J., Ceska, M., and Svanborg, C. (1993a) Selective cytokine production by epithelial cells following exposure to *Escherichia coli*. *Infect Immun* **61**: 602-609.
- Agace, W.W., Hedges, S.R., Ceska, M., and Svanborg, C. (1993b) Interleukin-8 and the neutrophil response to mucosal gram-negative infection. *J Clin Invest* **92**: 780-785.
- Akaike, T. (2001) Role of free radicals in viral pathogenesis and mutation. *Rev Med Virol* **11**: 87-101.
- Aktories, K. (1997) Rho proteins: targets for bacterial toxins. *Trends Microbiol* **5**: 282-288.
- Amor, K., Heinrichs, D.E., Fridrich, E., Ziebell, K., Johnson, R.P., and Whitfield, C. (2000) Distribution of core oligosaccharide types in lipopolysaccharides from *Escherichia coli*. *Infect Immun* **68**: 1116-1124.
- Anderson, G.G., Palermo, J.J., Schilling, J.D., Roth, R., Heuser, J., and Hultgren, S.J. (2003) Intracellular bacterial biofilm-like pods in urinary tract infections. *Science* **301**: 105-107.
- Anderson, G.G., Dodson, K.W., Hooton, T.M., and Hultgren, S.J. (2004) Intracellular bacterial communities of uropathogenic *Escherichia coli* in urinary tract pathogenesis. *Trends Microbiol* **12**: 424-430.
- Andersson, P., Engberg, I., Lidin-Janson, G., Lincoln, K., Hull, R., Hull, S., and Svanborg, C. (1991) Persistence of *Escherichia coli* bacteriuria is not determined by bacterial adherence. *Infect Immun* **59**: 2915-2921.
- Andrews, S.C., Robinson, A.K., and Rodriguez-Quinones, F. (2003) Bacterial iron homeostasis. *FEMS Microbiol Rev* **27**: 215-237.
- Anfora, A.T., Haugen, B.J., Roesch, P., Redford, P., and Welch, R.A. (2007) Roles of serine accumulation and catabolism in the colonization of the murine urinary tract by *Escherichia coli* CFT073. *Infect Immun* **75**: 5298-5304.
- Arber, W. (1993) Evolution of prokaryotic genomes. *Gene* **135**: 49-56.
- Bang, I.S., Liu, L., Vazquez-Torres, A., Crouch, M.L., Stamler, J.S., and Fang, F.C. (2006) Maintenance of nitric oxide and redox homeostasis by the salmonella flavohemoglobin hmp. *J Biol Chem* **281**: 28039-28047.
- Barraud, N., Hassett, D.J., Hwang, S.H., Rice, S.A., Kjelleberg, S., and Webb, J.S. (2006) Involvement of nitric oxide in biofilm dispersal of *Pseudomonas aeruginosa*. *J Bacteriol* **188**: 7344-7353.
- Barua, S., Yamashino, T., Hasegawa, T., Yokoyama, K., Torii, K., and Ohta, M. (2002) Involvement of surface polysaccharides in the organic acid resistance of Shiga Toxin-producing *Escherichia coli* O157:H7. *Mol Microbiol* **43**: 629-640.
- Baumler, A.J., Tsolis, R.M., van der Velden, A.W., Stojiljkovic, I., Anic, S., and Heffron, F. (1996) Identification of a new iron regulated locus of *Salmonella typhi*. *Gene* **183**: 207-213.
- Berger, H., Hacker, J., Juarez, A., Hughes, C., and Goebel, W. (1982) Cloning of the chromosomal determinants encoding hemolysin production and mannose-resistant hemagglutination in *Escherichia coli*. *J Bacteriol* **152**: 1241-1247.

- Bergsten, G., Samuelsson, M., Wullt, B., Leijonhufvud, I., Fischer, H., and Svanborg, C. (2004) PapG-dependent adherence breaks mucosal inertia and triggers the innate host response. *J Infect Dis* **189**: 1734-1742.
- Bergsten, G., Wullt, B., and Svanborg, C. (2005) Escherichia coli, fimbriae, bacterial persistence and host response induction in the human urinary tract. *Int J Med Microbiol* **295**: 487-502.
- Bergsten, G., Wullt, B., Schembri, M.A., Leijonhufvud, I., and Svanborg, C. (2007) Do type 1 fimbriae promote inflammation in the human urinary tract? *Cell Microbiol*.
- Beutler, B. (2000) Tlr4: central component of the sole mammalian LPS sensor. *Curr Opin Immunol* **12**: 20-26.
- Billips, B.K., Forrestal, S.G., Rycyk, M.T., Johnson, J.R., Klumpp, D.J., and Schaeffer, A.J. (2007) Modulation of host innate immune response in the bladder by uropathogenic Escherichia coli. *Infect Immun* **75**: 5353-5360.
- Birch, A., Hausler, A., Ruttener, C., and Hutter, R. (1991) Chromosomal deletion and rearrangement in Streptomyces glaucescens. *J Bacteriol* **173**: 3531-3538.
- Blattner, F.R., Plunkett, G., 3rd, Bloch, C.A., Perna, N.T., Burland, V., Riley, M., Collado-Vides, J., Glasner, J.D., Rode, C.K., Mayhew, G.F., Gregor, J., Davis, N.W., Kirkpatrick, H.A., Goeden, M.A., Rose, D.J., Mau, B., and Shao, Y. (1997) The complete genome sequence of Escherichia coli K-12. *Science* **277**: 1453-1474.
- Blum, G., Ott, M., Lischewski, A., Ritter, A., Imrich, H., Tschape, H., and Hacker, J. (1994) Excision of large DNA regions termed pathogenicity islands from tRNA-specific loci in the chromosome of an Escherichia coli wild-type pathogen. *Infect Immun* **62**: 606-614.
- Bogdan, C. (2001) Nitric oxide and the immune response. *Nat Immunol* **2**: 907-916.
- Brückner, H., Haasmann, S., and Friedrich, A. (1994) Quantification of D-amino acids in human urine using GC-MS and HPLC. *Amino Acids* **6**: 205-211.
- Brzuszkiewicz, E., Bruggemann, H., Liesegang, H., Emmerth, M., Olschlager, T., Nagy, G., Albermann, K., Wagner, C., Buchrieser, C., Emody, L., Gottschalk, G., Hacker, J., and Dobrindt, U. (2006) How to become a uropathogen: comparative genomic analysis of extraintestinal pathogenic Escherichia coli strains. *Proc Natl Acad Sci U S A* **103**: 12879-12884.
- Cavaliere, S.J., Bohach, G.A., and Snyder, I.S. (1984) Escherichia coli alpha-hemolysin: characteristics and probable role in pathogenicity. *Microbiol Rev* **48**: 326-343.
- Cirl, C., Wieser, A., Yadav, M., Duerr, S., Schubert, S., Fischer, H., Stappert, D., Wantia, N., Rodriguez, N., Wagner, H., Svanborg, C., and Miethke, T. (2008) Subversion of Toll-like receptor signaling by a unique family of bacterial Toll/interleukin-1 receptor domain-containing proteins. *Nat Med* **14**: 399-406.
- Clermont, O., Bonacorsi, S., and Bingen, E. (2000a) Rapid and simple determination of the Escherichia coli phylogenetic group. *Appl Environ Microbiol* **66**: 4555-4558.
- Clermont, O., Bonacorsi, S., and Bingen, E. (2000b) Rapid and Simple Determination of the Escherichia coli Phylogenetic Group. Vol. 66, pp. 4555-4558.
- Coban, A.Y., and Durupinar, B. (2003) The effect of nitric oxide combined with fluoroquinolones against Salmonella enterica serovar Typhimurium in vitro. *Mem Inst Oswaldo Cruz* **98**: 419-423.
- Colgan, R., Nicolle, L.E., McGlone, A., and Hooton, T.M. (2006) Asymptomatic bacteriuria in adults. *Am Fam Physician* **74**: 985-990.
- Comayras, C., Tasca, C., Peres, S.Y., Ducommun, B., Oswald, E., and De Rycke, J. (1997) Escherichia coli cytolethal distending toxin blocks the HeLa cell cycle at the G2/M transition by preventing cdc2 protein kinase dephosphorylation and activation. *Infect Immun* **65**: 5088-5095.

- Connell, H., Poulsen, L.K., and Klemm, P. (2000) Expression of type 1 and P fimbriae in situ and localisation of a uropathogenic *Escherichia coli* strain in the murine bladder and kidney. *Int J Med Microbiol* **290**: 587-597.
- Coolsaet, B.L., Griffiths, D.J., van Mastrigt, R., and Duyl, W.A. (1980) Urodynamic investigation of the wide ureter. *J Urol* **124**: 666-672.
- Cooper, V.S., and Lenski, R.E. (2000) The population genetics of ecological specialization in evolving *Escherichia coli* populations. *Nature* **407**: 736-739.
- Cosloy, S.D., and McFall, E. (1973) Metabolism of D-serine in *Escherichia coli* K-12: mechanism of growth inhibition. *J Bacteriol* **114**: 685-694.
- Costerton, J.W., Stewart, P.S., and Greenberg, E.P. (1999) Bacterial biofilms: a common cause of persistent infections. *Science* **284**: 1318-1322.
- Crawford, M.J., and Goldberg, D.E. (1998) Regulation of the *Salmonella typhimurium* flavohemoglobin gene. A new pathway for bacterial gene expression in response to nitric oxide. *J Biol Chem* **273**: 34028-34032.
- Cullen, P.A., Haake, D.A., and Adler, B. (2004) Outer membrane proteins of pathogenic spirochetes. *FEMS Microbiol Rev* **28**: 291-318.
- Darouiche, R.O., Donovan, W.H., Del Terzo, M., Thornby, J.I., Rudy, D.C., and Hull, R.A. (2001) Pilot trial of bacterial interference for preventing urinary tract infection. *Urology* **58**: 339-344.
- Darwin, C. (1872) Origin of Species. *Senate Sixth Edition*.
- Datsenko, K.A., and Wanner, B.L. (2000) One-step inactivation of chromosomal genes in *Escherichia coli* K-12 using PCR products. *Proc Natl Acad Sci U S A* **97**: 6640-6645.
- de Visser, J.A., and Lenski, R.E. (2002) Long-term experimental evolution in *Escherichia coli*. XI. Rejection of non-transitive interactions as cause of declining rate of adaptation. *BMC Evol Biol* **2**: 19.
- Der Vartanian, M., Jaffeux, B., Contrepolis, M., Chavarot, M., Girardeau, J.P., Bertin, Y., and Martin, C. (1992) Role of aerobactin in systemic spread of an opportunistic strain of *Escherichia coli* from the intestinal tract of gnotobiotic lambs. *Infect Immun* **60**: 2800-2807.
- DeRisi, J.L., Iyer, V.R., and Brown, P.O. (1997) Exploring the metabolic and genetic control of gene expression on a genomic scale. *Science* **278**: 680-686.
- Dobrindt, U., Blum-Oehler, G., Hartsch, T., Gottschalk, G., Ron, E.Z., Fünfstück, R., and Hacker, J. (2001) S-Fimbria-encoding determinant *sfa(I)* is located on pathogenicity island III(536) of uropathogenic *Escherichia coli* strain 536. *Infect Immun* **69**: 4248-4256.
- Dobrindt, U., Agerer, F., Michaelis, K., Janka, A., Buchrieser, C., Samuelson, M., Svanborg, C., Gottschalk, G., Karch, H., and Hacker, J. (2003) Analysis of genome plasticity in pathogenic and commensal *Escherichia coli* isolates by use of DNA arrays. *J Bacteriol* **185**: 1831-1840.
- Dobrindt, U., Hochhut, B., Hentschel, U., and Hacker, J. (2004) Genomic islands in pathogenic and environmental microorganisms. *Nat Rev Microbiol* **2**: 414-424.
- Edén, C., Janson, G., and Lindberg, U. (1979) Adhesiveness to urinary tract epithelial cells of fecal and urinary *Escherichia coli* isolates from patients with symptomatic urinary tract infections or asymptomatic bacteriuria of varying duration. *J Urol* **122**: 185-188.
- Eisen, M.B., Spellman, P.T., Brown, P.O., and Botstein, D. (1998) Cluster analysis and display of genome-wide expression patterns. *Proc Natl Acad Sci U S A* **95**: 14863-14868.
- Emody, L., Kerényi, M., and Nagy, G. (2003) Virulence factors of uropathogenic *Escherichia coli*. *Int J Antimicrob Agents* **22 Suppl 2**: 29-33.

- Engel, D., Dobrindt, U., Tittel, A., Peters, P., Maurer, J., Gutgemann, I., Kaissling, B., Kuziel, W., Jung, S., and Kurts, C. (2006) Tumor necrosis factor alpha- and inducible nitric oxide synthase-producing dendritic cells are rapidly recruited to the bladder in urinary tract infection but are dispensable for bacterial clearance. *Infect Immun* **74**: 6100-6107.
- Fang, F.C., and Vazquez-Torres, A. (2002) Nitric oxide production by human macrophages: there's NO doubt about it. *Am J Physiol Lung Cell Mol Physiol* **282**: L941-943.
- Fang, F.C. (2004) Antimicrobial reactive oxygen and nitrogen species: concepts and controversies. *Nat Rev Microbiol* **2**: 820-832.
- Ferrieres, L., Hancock, V., and Klemm, P. (2007) Biofilm exclusion of uropathogenic bacteria by selected asymptomatic bacteriuria *Escherichia coli* strains. *Microbiology* **153**: 1711-1719.
- Fischer, H., Yamamoto, M., Akira, S., Beutler, B., and Svanborg, C. (2006) Mechanism of pathogen-specific TLR4 activation in the mucosa: fimbriae, recognition receptors and adaptor protein selection. *Eur J Immunol* **36**: 267-277.
- Flatley, J., Barrett, J., Pullan, S.T., Hughes, M.N., Green, J., and Poole, R.K. (2005) Transcriptional responses of *Escherichia coli* to S-nitrosoglutathione under defined chemostat conditions reveal major changes in methionine biosynthesis. *J Biol Chem* **280**: 10065-10072.
- Foxman, B. (2002) Epidemiology of urinary tract infections: incidence, morbidity, and economic costs. *Am J Med* **113 Suppl 1A**: 5S-13S.
- Foxman, B., Manning, S.D., Tallman, P., Bauer, R., Zhang, L., Koopman, J.S., Gillespie, B., Sobel, J.D., and Marrs, C.F. (2002) Uropathogenic *Escherichia coli* are more likely than commensal *E. coli* to be shared between heterosexual sex partners. *Am J Epidemiol* **156**: 1133-1140.
- Freudeus, B., Godaly, G., Hang, L., Karpman, D., and Svanborg, C. (2001a) Interleukin-8 receptor deficiency confers susceptibility to acute pyelonephritis. *J Infect Dis* **183 Suppl 1**: S56-60.
- Freudeus, B., Wachtler, C., Hedlund, M., Fischer, H., Samuelsson, P., Svensson, M., and Svanborg, C. (2001b) *Escherichia coli* P fimbriae utilize the Toll-like receptor 4 pathway for cell activation. *Mol Microbiol* **40**: 37-51.
- Gardner, A.M., Helmick, R.A., and Gardner, P.R. (2002) Flavorubredoxin, an inducible catalyst for nitric oxide reduction and detoxification in *Escherichia coli*. *J Biol Chem* **277**: 8172-8177.
- Garten, W., Hindennach, I., and Henning, U. (1975) The major proteins of the *Escherichia coli* outer cell envelope membrane. Characterization of proteins II* and III, comparison of all proteins. *Eur J Biochem* **59**: 215-221.
- Giron, J.A., Torres, A.G., Freer, E., and Kaper, J.B. (2002) The flagella of enteropathogenic *Escherichia coli* mediate adherence to epithelial cells. *Mol Microbiol* **44**: 361-379.
- Godaly, G., Proudfoot, A.E., Offord, R.E., Svanborg, C., and Agace, W.W. (1997) Role of epithelial interleukin-8 (IL-8) and neutrophil IL-8 receptor A in *Escherichia coli*-induced transuroepithelial neutrophil migration. *Infect Immun* **65**: 3451-3456.
- Gonzalez, C.F., Proudfoot, M., Brown, G., Korniyenko, Y., Mori, H., Savchenko, A.V., and Yakunin, A.F. (2006) Molecular basis of formaldehyde detoxification. Characterization of two S-formylglutathione hydrolases from *Escherichia coli*, FrmB and YeiG. *J Biol Chem* **281**: 14514-14522.
- Gordon, D.M., and Riley, M.A. (1992) A theoretical and experimental analysis of bacterial growth in the bladder. *Mol Microbiol* **6**: 555-562.
- Griebing, T.L. (2005) Urologic diseases in america project: trends in resource use for urinary tract infections in men. *J Urol* **173**: 1288-1294.

- Grozdanov, L., Zähringer, U., Blum-Oehler, G., Brade, L., Henne, A., Knirel, Y.A., Schombel, U., Schulze, J., Sonnenborn, U., Gottschalk, G., Hacker, J., Rietschel, E.T., and Dobrindt, U. (2002) A single nucleotide exchange in the *wzy* gene is responsible for the semirough O6 lipopolysaccharide phenotype and serum sensitivity of *Escherichia coli* strain Nissle 1917. *J Bacteriol* **184**: 5912-5925.
- Grozdanov, L., Raasch, C., Schulze, J., Sonnenborn, U., Gottschalk, G., Hacker, J., and Dobrindt, U. (2004) Analysis of the genome structure of the nonpathogenic probiotic *Escherichia coli* strain Nissle 1917. *J Bacteriol* **186**: 5432-5441.
- Gutheil, W.G., Kasimoglu, E., and Nicholson, P.C. (1997) Induction of glutathione-dependent formaldehyde dehydrogenase activity in *Escherichia coli* and *Haemophilus influenzae*. *Biochem Biophys Res Commun* **238**: 693-696.
- Hacker, J., Blum-Oehler, G., Muhldorfer, I., and Tschape, H. (1997) Pathogenicity islands of virulent bacteria: structure, function and impact on microbial evolution. *Mol Microbiol* **23**: 1089-1097.
- Hacker, J., and Kaper, J.B. (2000) Pathogenicity islands and the evolution of microbes. *Annu Rev Microbiol* **54**: 641-679.
- Hacker, J., and Carniel, E. (2001) Ecological fitness, genomic islands and bacterial pathogenicity. A Darwinian view of the evolution of microbes. *EMBO Rep* **2**: 376-381.
- Hacker, J., Hentschel, U., and Dobrindt, U. (2003) Prokaryotic chromosomes and disease. *Science* **301**: 790-793.
- Hagan, E.C., and Mobley, H.L. (2007) Uropathogenic *Escherichia coli* outer membrane antigens expressed during urinary tract infection. *Infect Immun* **75**: 3941-3949.
- Hagberg, L., Hull, R., Hull, S., Falkow, S., Freter, R., and Svanborg Eden, C. (1983) Contribution of adhesion to bacterial persistence in the mouse urinary tract. *Infect Immun* **40**: 265-272.
- Hagberg, L., Hull, R., Hull, S., McGhee, J.R., Michalek, S.M., and Svanborg Eden, C. (1984) Difference in susceptibility to gram-negative urinary tract infection between C3H/HeJ and C3H/HeN mice. *Infect Immun* **46**: 839-844.
- Haldane, J.B.S. (1949) Disease and evolution. In *Ric. Sci.* Vol. 19, pp. 2-11.
- Hancock, V., Ferrieres, L., and Klemm, P. (2007) Biofilm formation by asymptomatic and virulent urinary tract infectious *Escherichia coli* strains. *FEMS Microbiol Lett* **267**: 30-37.
- Hancock, V., and Klemm, P. (2007) Global gene expression profiling of asymptomatic bacteriuria *Escherichia coli* during biofilm growth in human urine. *Infect Immun* **75**: 966-976.
- Hang, L., Haraoka, M., Agace, W.W., Leffler, H., Burdick, M., Strieter, R., and Svanborg, C. (1999) Macrophage inflammatory protein-2 is required for neutrophil passage across the epithelial barrier of the infected urinary tract. *J Immunol* **162**: 3037-3044.
- Hansson, S., Caugant, D., Jodal, U., and Svanborg-Eden, C. (1989a) Untreated asymptomatic bacteriuria in girls: I--Stability of urinary isolates. *Bmj* **298**: 853-855.
- Hansson, S., Jodal, U., Noren, L., and Bjure, J. (1989b) Untreated bacteriuria in asymptomatic girls with renal scarring. *Pediatrics* **84**: 964-968.
- Haraoka, M., Hang, L., Frendeus, B., Godaly, G., Burdick, M., Strieter, R., and Svanborg, C. (1999) Neutrophil recruitment and resistance to urinary tract infection. *J Infect Dis* **180**: 1220-1229.
- Haugen, B.J., Pellett, S., Redford, P., Hamilton, H.L., Roesch, P.L., and Welch, R.A. (2007) In vivo gene expression analysis identifies genes required for enhanced colonization of the mouse urinary tract by uropathogenic *Escherichia coli* strain CFT073 *dsdA*. *Infect Immun* **75**: 278-289.

- Hedberg, J.J., Griffiths, W.J., Nilsson, S.J., and Hoog, J.O. (2003) Reduction of S-nitrosoglutathione by human alcohol dehydrogenase 3 is an irreversible reaction as analysed by electrospray mass spectrometry. *Eur J Biochem* **270**: 1249-1256.
- Hedges, S.R., Agace, W.W., and Svanborg, C. (1995) Epithelial cytokine responses and mucosal cytokine networks. *Trends Microbiol* **3**: 266-270.
- Helling, R.B. (1994) Why does *Escherichia coli* have two primary pathways for synthesis of glutamate? *J Bacteriol* **176**: 4664-4668.
- Hengge-Aronis, R. (1999) Interplay of global regulators and cell physiology in the general stress response of *Escherichia coli*. *Curr Opin Microbiol* **2**: 148-152.
- Herring, C.D., and Blattner, F.R. (2004) Global transcriptional effects of a suppressor tRNA and the inactivation of the regulator *frmR*. *J Bacteriol* **186**: 6714-6720.
- Herzer, P.J., Inouye, S., Inouye, M., and Whittam, T.S. (1990) Phylogenetic distribution of branched RNA-linked multicopy single-stranded DNA among natural isolates of *Escherichia coli*. *J Bacteriol* **172**: 6175-6181.
- Hughes, M.N. (1999) Relationships between nitric oxide, nitroxyl ion, nitrosonium cation and peroxyxynitrite. *Biochim Biophys Acta* **1411**: 263-272.
- Hull, R., Rudy, D., Donovan, W., Svanborg, C., Wieser, I., Stewart, C., and Darouiche, R. (2000) Urinary tract infection prophylaxis using *Escherichia coli* 83972 in spinal cord injured patients. *J Urol* **163**: 872-877.
- Hultgren, S.J., Porter, T.N., Schaeffer, A.J., and Duncan, J.L. (1985) Role of type 1 pili and effects of phase variation on lower urinary tract infections produced by *Escherichia coli*. *Infect Immun* **50**: 370-377.
- Jacques, M. (1996) Role of lipo-oligosaccharides and lipopolysaccharides in bacterial adherence. *Trends Microbiol* **4**: 408-409.
- Jarboe, L.R., Hyduke, D.R., Tran, L.M., Chou, K.J., and Liao, J.C. (2008) Determination of the *Escherichia coli* S-nitrosoglutathione response network using integrated biochemical and systems analysis. *J Biol Chem* **283**: 5148-5157.
- Johnson, J.R. (1991) Virulence factors in *Escherichia coli* urinary tract infection. *Clin Microbiol Rev* **4**: 80-128.
- Johnson, J.R., and Stell, A.L. (2000) Extended virulence genotypes of *Escherichia coli* strains from patients with urosepsis in relation to phylogeny and host compromise. *J Infect Dis* **181**: 261-272.
- Johnson, J.R., Owens, K.L., Clabots, C.R., Weissman, S.J., and Cannon, S.B. (2006) Phylogenetic relationships among clonal groups of extraintestinal pathogenic *Escherichia coli* as assessed by multi-locus sequence analysis. *Microbes Infect* **8**: 1702-1713.
- Jourlin, C., Ansaldi, M., and Mejean, V. (1997) Transphosphorylation of the TorR response regulator requires the three phosphorylation sites of the TorS unorthodox sensor in *Escherichia coli*. *J Mol Biol* **267**: 770-777.
- Justino, M.C., Vicente, J.B., Teixeira, M., and Saraiva, L.M. (2005) New genes implicated in the protection of anaerobically grown *Escherichia coli* against nitric oxide. *J Biol Chem* **280**: 2636-2643.
- Justino, M.C., Almeida, C.C., Teixeira, M., and Saraiva, L.M. (2007) *Escherichia coli* di-iron YtfE protein is necessary for the repair of stress-damaged iron-sulfur clusters. *J Biol Chem* **282**: 10352-10359.
- Kaper, J.B., Nataro, J.P., and Mobley, H.L. (2004) Pathogenic *Escherichia coli*. *Nat Rev Microbiol* **2**: 123-140.
- Kidd, S.P., Jiang, D., Jennings, M.P., and McEwan, A.G. (2007) Glutathione-dependent alcohol dehydrogenase AdhC is required for defense against nitrosative stress in *Haemophilus influenzae*. *Infect Immun* **75**: 4506-4513.

- Kim, K.S. (2002) Strategy of *Escherichia coli* for crossing the blood-brain barrier. *J Infect Dis* **186 Suppl 2**: S220-224.
- King, C.D., Rios, G.R., Green, M.D., and Tephly, T.R. (2000) UDP-glucuronosyltransferases. *Curr Drug Metab* **1**: 143-161.
- Klemm, P., Roos, V., Ulett, G.C., Svanborg, C., and Schembri, M.A. (2006) Molecular characterization of the *Escherichia coli* asymptomatic bacteriuria strain 83972: the taming of a pathogen. *Infect Immun* **74**: 781-785.
- Klumpp, D.J., Weiser, A.C., Sengupta, S., Forrester, S.G., Butler, R.A., and Schaeffer, A.J. (2001) Uropathogenic *Escherichia coli* potentiates type 1 pilus-induced apoptosis by suppressing NF-kappaB. *Infect Immun* **69**: 6689-6695.
- Klumpp, D.J., Rycyk, M.T., Chen, M.C., Thumbikat, P., Sengupta, S., and Schaeffer, A.J. (2006) Uropathogenic *Escherichia coli* induces extrinsic and intrinsic cascades to initiate urothelial apoptosis. *Infect Immun* **74**: 5106-5113.
- Korona, R., Nakatsu, C.H., Forney, L.J., and Lenski, R.E. (1994) Evidence for multiple adaptive peaks from populations of bacteria evolving in a structured habitat. *Proc Natl Acad Sci U S A* **91**: 9037-9041.
- Lane, M.C., Lockett, V., Monterosso, G., Lamphier, D., Weinert, J., Hebel, J.R., Johnson, D.E., and Mobley, H.L. (2005) Role of motility in the colonization of uropathogenic *Escherichia coli* in the urinary tract. *Infect Immun* **73**: 7644-7656.
- Lane, M.C., Alteri, C.J., Smith, S.N., and Mobley, H.L. (2007) Expression of flagella is coincident with uropathogenic *Escherichia coli* ascension to the upper urinary tract. *Proc Natl Acad Sci U S A* **104**: 16669-16674.
- Leathart, J.B., and Gally, D.L. (1998) Regulation of type 1 fimbrial expression in uropathogenic *Escherichia coli*: heterogeneity of expression through sequence changes in the fim switch region. *Mol Microbiol* **28**: 371-381.
- Lenski, R., Rose, M., Simpson, S., and Tadler, S. (1991) Long-Term Experimental Evolution in *Escherichia coli*. I. Adaptation and Divergence During 2,000 Generations. *The American Naturalist* **138**: 1315-1341.
- Lenski, R.E., and Travisano, M. (1994) Dynamics of adaptation and diversification: a 10,000-generation experiment with bacterial populations. *Proc Natl Acad Sci U S A* **91**: 6808-6814.
- Lindberg, U., Hanson, L.A., Jodal, U., Lidin-Janson, G., Lincoln, K., and Olling, S. (1975) Asymptomatic bacteriuria in schoolgirls. II. Differences in *Escherichia coli* causing asymptomatic bacteriuria. *Acta Paediatr Scand* **64**: 432-436.
- Lindberg, U., and Winberg, J. (1976) [Asymptomatic bacteriuria]. *Lakartidningen* **73**: 1617-1618.
- Lindberg, U., Claesson, I., Hanson, L.A., and Jodal, U. (1978) Asymptomatic bacteriuria in schoolgirls. VIII. Clinical course during a 3-year follow-up. *J Pediatr* **92**: 194-199.
- Liu, L., Hausladen, A., Zeng, M., Que, L., Heitman, J., and Stamler, J.S. (2001) A metabolic enzyme for S-nitrosothiol conserved from bacteria to humans. *Nature* **410**: 490-494.
- Luck, S.N., Turner, S.A., Rajakumar, K., Sakellaris, H., and Adler, B. (2001) Ferric dicitrate transport system (Fec) of *Shigella flexneri* 2a YSH6000 is encoded on a novel pathogenicity island carrying multiple antibiotic resistance genes. *Infect Immun* **69**: 6012-6021.
- Lundberg, J.O., Ehren, I., Jansson, O., Adolfsson, J., Lundberg, J.M., Weitzberg, E., Alving, K., and Wiklund, N.P. (1996) Elevated nitric oxide in the urinary bladder in infectious and noninfectious cystitis. *Urology* **48**: 700-702.
- Mahillon, J., and Chandler, M. (1998) Insertion sequences. *Microbiol Mol Biol Rev* **62**: 725-774.

- Membrillo-Hernandez, J., Coopamah, M.D., Channa, A., Hughes, M.N., and Poole, R.K. (1998) A novel mechanism for upregulation of the *Escherichia coli* K-12 hmp (flavo-haemoglobin) gene by the 'NO releaser', S-nitrosoglutathione: nitrosation of homocysteine and modulation of MetR binding to the glyA-hmp intergenic region. *Mol Microbiol* **29**: 1101-1112.
- Mobley, H.L., Green, D.M., Trifillis, A.L., Johnson, D.E., Chippendale, G.R., Lockatell, C.V., Jones, B.D., and Warren, J.W. (1990) Pyelonephritogenic *Escherichia coli* and killing of cultured human renal proximal tubular epithelial cells: role of hemolysin in some strains. *Infect Immun* **58**: 1281-1289.
- Mobley, H.L., Island, M.D., and Massad, G. (1994) Virulence determinants of uropathogenic *Escherichia coli* and *Proteus mirabilis*. *Kidney Int Suppl* **47**: S129-136.
- Mobley, H.L., Belas, R., Lockatell, V., Chippendale, G., Trifillis, A.L., Johnson, D.E., and Warren, J.W. (1996) Construction of a flagellum-negative mutant of *Proteus mirabilis*: effect on internalization by human renal epithelial cells and virulence in a mouse model of ascending urinary tract infection. *Infect Immun* **64**: 5332-5340.
- Molloy, M.P., Herbert, B.R., Slade, M.B., Rabilloud, T., Nouwens, A.S., Williams, K.L., and Gooley, A.A. (2000) Proteomic analysis of the *Escherichia coli* outer membrane. *Eur J Biochem* **267**: 2871-2881.
- Moreau, P.L. (2007) The lysine decarboxylase CadA protects *Escherichia coli* starved of phosphate against fermentation acids. *J Bacteriol* **189**: 2249-2261.
- Musser, J.M. (1995) Antimicrobial agent resistance in mycobacteria: molecular genetic insights. *Clin Microbiol Rev* **8**: 496-514.
- Nicolle, L.E. (2006) Asymptomatic bacteriuria: review and discussion of the IDSA guidelines. *Int J Antimicrob Agents* **28 Suppl 1**: S42-48.
- Nicolle, L.E., Zhanel, G.G., and Harding, G.K. (2006) Microbiological outcomes in women with diabetes and untreated asymptomatic bacteriuria. *World J Urol* **24**: 61-65.
- Nougayrede, J.P., Homburg, S., Taieb, F., Boury, M., Brzuszkiewicz, E., Gottschalk, G., Buchrieser, C., Hacker, J., Dobrindt, U., and Oswald, E. (2006) *Escherichia coli* induces DNA double-strand breaks in eukaryotic cells. *Science* **313**: 848-851.
- Nougayrède, J.P., Homburg, S., Taieb, F., Boury, M., Brzuszkiewicz, E., Gottschalk, G., Buchrieser, C., Hacker, J., Dobrindt, U., and Oswald, E. (2006) *Escherichia coli* induces DNA double-strand breaks in eukaryotic cells. *Science* **313**: 848-851.
- Olsen, A., Arnqvist, A., Hammar, M., and Normark, S. (1993) Environmental regulation of curli production in *Escherichia coli*. *Infect Agents Dis* **2**: 272-274.
- Orskov, I., Orskov, F., Jann, B., and Jann, K. (1977) Serology, chemistry, and genetics of O and K antigens of *Escherichia coli*. *Bacteriol Rev* **41**: 667-710.
- Peekhaus, N., and Conway, T. (1998) What's for dinner? Entner-Doudoroff metabolism in *Escherichia coli*. *J Bacteriol* **180**: 3495-3502.
- Pere, A., Nowicki, B., Saxen, H., Siitonen, A., and Korhonen, T.K. (1987) Expression of P, type-1, and type-1C fimbriae of *Escherichia coli* in the urine of patients with acute urinary tract infection. *J Infect Dis* **156**: 567-574.
- Perez-Amador, M.A., Lidder, P., Johnson, M.A., Landgraf, J., Wisman, E., and Green, P.J. (2001) New molecular phenotypes in the dst mutants of *Arabidopsis* revealed by DNA microarray analysis. *Plant Cell* **13**: 2703-2717.
- Picard, B., Garcia, J.S., Gouriou, S., Duriez, P., Brahimi, N., Bingen, E., Elion, J., and Denamur, E. (1999) The link between phylogeny and virulence in *Escherichia coli* extraintestinal infection. *Infect Immun* **67**: 546-553.
- Plos, K., Lomberg, H., Hull, S., Johansson, I., and Svanborg, C. (1991) *Escherichia coli* in patients with renal scarring: genotype and phenotype of Gal alpha 1-4Gal beta-, Forssman- and mannose-specific adhesins. *Pediatr Infect Dis J* **10**: 15-19.

- Plos, K., Connell, H., Jodal, U., Marklund, B.I., Marild, S., Wettergren, B., and Svanborg, C. (1995) Intestinal carriage of P fimbriated *Escherichia coli* and the susceptibility to urinary tract infection in young children. *J Infect Dis* **171**: 625-631.
- Poock, S.R., Leach, E.R., Moir, J.W., Cole, J.A., and Richardson, D.J. (2002) Respiratory detoxification of nitric oxide by the cytochrome c nitrite reductase of *Escherichia coli*. *J Biol Chem* **277**: 23664-23669.
- Poole, R.K., Anjum, M.F., Membrillo-Hernandez, J., Kim, S.O., Hughes, M.N., and Stewart, V. (1996) Nitric oxide, nitrite, and Fnr regulation of hmp (flavo-hemoglobin) gene expression in *Escherichia coli* K-12. *J Bacteriol* **178**: 5487-5492.
- Poole, R.K. (2005) Nitric oxide and nitrosative stress tolerance in bacteria. *Biochem Soc Trans* **33**: 176-180.
- Porat, R., Mosseri, R., Kaplan, E., Johns, M.A., and Shibolet, S. (1992) Distribution of polysaccharide side chains of lipopolysaccharide determine resistance of *Escherichia coli* to the bactericidal activity of serum. *J Infect Dis* **165**: 953-956.
- Pullan, S.T., Gidley, M.D., Jones, R.A., Barrett, J., Stevanin, T.M., Read, R.C., Green, J., and Poole, R.K. (2007) Nitric oxide in chemostat-cultured *Escherichia coli* is sensed by Fnr and other global regulators: unaltered methionine biosynthesis indicates lack of S nitrosation. *J Bacteriol* **189**: 1845-1855.
- Ragnarsdottir, B., Samuelsson, M., Gustafsson, M.C., Leijonhufvud, I., Karpman, D., and Svanborg, C. (2007) Reduced toll-like receptor 4 expression in children with asymptomatic bacteriuria. *J Infect Dis* **196**: 475-484.
- Raz, R. (2003) Asymptomatic bacteriuria. Clinical significance and management. *Int J Antimicrob Agents* **22 Suppl 2**: 45-47.
- Reeves, P. (1995) Role of O-antigen variation in the immune response. *Trends Microbiol* **3**: 381-386.
- Reisner, A., Krogfelt, K.A., Klein, B.M., Zechner, E.L., and Molin, S. (2006) In vitro biofilm formation of commensal and pathogenic *Escherichia coli* strains: impact of environmental and genetic factors. *J Bacteriol* **188**: 3572-3581.
- Reitzer, L. (2003) Nitrogen assimilation and global regulation in *Escherichia coli*. *Annu Rev Microbiol* **57**: 155-176.
- Reverchon, S., Rouanet, C., Expert, D., and Nasser, W. (2002) Characterization of indigoidine biosynthetic genes in *Erwinia chrysanthemi* and role of this blue pigment in pathogenicity. *J Bacteriol* **184**: 654-665.
- Rezzi, S., Ramadan, Z., Fay, L.B., and Kochhar, S. (2007) Nutritional metabonomics: applications and perspectives. *J Proteome Res* **6**: 513-525.
- Roesch, P.L., Redford, P., Batchelet, S., Moritz, R.L., Pellett, S., Haugen, B.J., Blattner, F.R., and Welch, R.A. (2003) Uropathogenic *Escherichia coli* use d-serine deaminase to modulate infection of the murine urinary tract. *Mol Microbiol* **49**: 55-67.
- Ronald, A. (2002) The etiology of urinary tract infection: traditional and emerging pathogens. *Am J Med* **113 Suppl 1A**: 14S-19S.
- Roos, V., and Klemm, P. (2006) Global gene expression profiling of the asymptomatic bacteriuria *Escherichia coli* strain 83972 in the human urinary tract. *Infect Immun* **74**: 3565-3575.
- Roos, V., Schembri, M.A., Ulett, G.C., and Klemm, P. (2006a) Asymptomatic bacteriuria *Escherichia coli* strain 83972 carries mutations in the foc locus and is unable to express F1C fimbriae. *Microbiology* **152**: 1799-1806.
- Roos, V., Ulett, G.C., Schembri, M.A., and Klemm, P. (2006b) The asymptomatic bacteriuria *Escherichia coli* strain 83972 outcompetes uropathogenic *E. coli* strains in human urine. *Infect Immun* **74**: 615-624.

- Rozen, D.E., de Visser, J.A., and Gerrish, P.J. (2002) Fitness effects of fixed beneficial mutations in microbial populations. *Curr Biol* **12**: 1040-1045.
- Russo, T.A., and Johnson, J.R. (2000) Proposal for a new inclusive designation for extraintestinal pathogenic isolates of *Escherichia coli*: ExPEC. *J Infect Dis* **181**: 1753-1754.
- Sakai, A., Nakanishi, M., Yoshiyama, K., and Maki, H. (2006) Impact of reactive oxygen species on spontaneous mutagenesis in *Escherichia coli*. *Genes Cells* **11**: 767-778.
- Sambrook, J., Fritsch, E., and Maniatis, T. (1989) *Molecular cloning. A Laboratory Manual*. 2nd ed.
- Samuelsson, P., Hang, L., Wullt, B., Irjala, H., and Svanborg, C. (2004) Toll-like receptor 4 expression and cytokine responses in the human urinary tract mucosa. *Infect Immun* **72**: 3179-3186.
- Sansom, M.S. (1999) Membrane proteins: A tale of barrels and corks. *Curr Biol* **9**: R254-257.
- Sauer, F.G., Mulvey, M.A., Schilling, J.D., Martinez, J.J., and Hultgren, S.J. (2000) Bacterial pili: molecular mechanisms of pathogenesis. *Curr Opin Microbiol* **3**: 65-72.
- Savage, D.C., Howie, G., Adler, K., and Wilson, M.I. (1975) Controlled trial of therapy in covert bacteriuria of childhood. *Lancet* **1**: 358-361.
- Schilling, J.D., Mulvey, M.A., and Hultgren, S.J. (2001) Structure and function of *Escherichia coli* type 1 pili: new insight into the pathogenesis of urinary tract infections. *J Infect Dis* **183 Suppl 1**: S36-40.
- Schlag, S., Nerz, C., Birkenstock, T.A., Altenberend, F., and Gotz, F. (2007) Inhibition of staphylococcal biofilm formation by nitrite. *J Bacteriol* **189**: 7911-7919.
- Shaikh, N., Morone, N.E., Lopez, J., Chianese, J., Sangvai, S., D'Amico, F., Hoberman, A., and Wald, E.R. (2007) Does this child have a urinary tract infection? *Jama* **298**: 2895-2904.
- Shapiro, R., and Pohl, S.H. (1968) The reaction of ribonucleosides with nitrous acid. Side products and kinetics. *Biochemistry* **7**: 448-455.
- Smyth, C.J., Marron, M.B., Twohig, J.M., and Smith, S.G. (1996) Fimbrial adhesins: similarities and variations in structure and biogenesis. *FEMS Immunol Med Microbiol* **16**: 127-139.
- Snyder, J.A., Haugen, B.J., Buckles, E.L., Lockatell, C.V., Johnson, D.E., Donnenberg, M.S., Welch, R.A., and Mobley, H.L. (2004) Transcriptome of uropathogenic *Escherichia coli* during urinary tract infection. *Infect Immun* **72**: 6373-6381.
- Sokurenko, E.V., Hasty, D.L., and Dykhuizen, D.E. (1999) Pathoadaptive mutations: gene loss and variation in bacterial pathogens. *Trends Microbiol* **7**: 191-195.
- Stamm, W.E., and Hooton, T.M. (1993) Management of urinary tract infections in adults. *N Engl J Med* **329**: 1328-1334.
- Stella, C., Beckwith-Hall, B., Cloarec, O., Holmes, E., Lindon, J.C., Powell, J., van der Ouderaa, F., Bingham, S., Cross, A.J., and Nicholson, J.K. (2006) Susceptibility of human metabolic phenotypes to dietary modulation. *J Proteome Res* **5**: 2780-2788.
- Struelens, M.J., Denis, O., and Rodriguez-Villalobos, H. (2004) Microbiology of nosocomial infections: progress and challenges. *Microbes Infect* **6**: 1043-1048.
- Sunden, F., Hakansson, L., Ljunggren, E., and Wullt, B. (2006) Bacterial interference--is deliberate colonization with *Escherichia coli* 83972 an alternative treatment for patients with recurrent urinary tract infection? *Int J Antimicrob Agents* **28 Suppl 1**: S26-29.
- Surette, M.G., Miller, M.B., and Bassler, B.L. (1999) Quorum sensing in *Escherichia coli*, *Salmonella typhimurium*, and *Vibrio harveyi*: a new family of genes responsible for autoinducer production. *Proc Natl Acad Sci U S A* **96**: 1639-1644.

- Suzuki, T., Ide, H., Yamada, M., Endo, N., Kanaori, K., Tajima, K., Morii, T., and Makino, K. (2000) Formation of 2'-deoxyoxanosine from 2'-deoxyguanosine and nitrous acid: mechanism and intermediates. *Nucleic Acids Res* **28**: 544-551.
- Svanborg-Eden, C., Hagberg, L., Hull, R., Hull, S., Magnusson, K.E., and Ohman, L. (1987) Bacterial virulence versus host resistance in the urinary tracts of mice. *Infect Immun* **55**: 1224-1232.
- Svanborg, C., Frendeus, B., Godaly, G., Hang, L., Hedlund, M., and Wachtler, C. (2001) Toll-like receptor signaling and chemokine receptor expression influence the severity of urinary tract infection. *J Infect Dis* **183 Suppl 1**: S61-65.
- Svanborg, C., Bergsten, G., Fischer, H., Godaly, G., Gustafsson, M., Karpman, D., Lundstedt, A.C., Ragnarsdottir, B., Svensson, M., and Wullt, B. (2006) Uropathogenic *Escherichia coli* as a model of host-parasite interaction. *Curr Opin Microbiol* **9**: 33-39.
- Svensson, M., Lindstedt, R., Radin, N.S., and Svanborg, C. (1994) Epithelial glucosphingolipid expression as a determinant of bacterial adherence and cytokine production. *Infect Immun* **62**: 4404-4410.
- Torres, A.G., and Payne, S.M. (1997) Haem iron-transport system in enterohaemorrhagic *Escherichia coli* O157:H7. *Mol Microbiol* **23**: 825-833.
- Trautner, B., Hull, R., and Darouiche, R. (2003) *Escherichia coli* 83972 inhibits catheter adherence by a broad spectrum of uropathogens. *Urology* **61**: 1059-1062.
- Tsai, C.M., and Frasch, C.E. (1982) A sensitive silver stain for detecting lipopolysaccharides in polyacrylamide gels. *Anal Biochem* **119**: 115-119.
- Tsikakos, D., Boger, R.H., Bode-Boger, S.M., Gutzki, F.M., and Frolich, J.C. (1994) Quantification of nitrite and nitrate in human urine and plasma as pentafluorobenzyl derivatives by gas chromatography-mass spectrometry using their ¹⁵N-labelled analogs. *J Chromatogr B Biomed Appl* **661**: 185-191.
- Vaisanen, V., Elo, J., Tallgren, L.G., Siitonen, A., Makela, P.H., Svanborg-Eden, C., Kallenius, G., Svenson, S.B., Hultberg, H., and Korhonen, T. (1981) Mannose-resistant haemagglutination and P antigen recognition are characteristic of *Escherichia coli* causing primary pyelonephritis. *Lancet* **2**: 1366-1369.
- Victorin, K. (1994) Review of the genotoxicity of nitrogen oxides. *Mutat Res* **317**: 43-55.
- Warren, J.W., Tenney, J.H., Hoopes, J.M., Muncie, H.L., and Anthony, W.C. (1982) A prospective microbiologic study of bacteriuria in patients with chronic indwelling urethral catheters. *J Infect Dis* **146**: 719-723.
- Weiss, B. (2006) Evidence for mutagenesis by nitric oxide during nitrate metabolism in *Escherichia coli*. *J Bacteriol* **188**: 829-833.
- Welch, R.A., Burland, V., Plunkett, G., 3rd, Redford, P., Roesch, P., Rasko, D., Buckles, E.L., Liou, S.R., Boutin, A., Hackett, J., Stroud, D., Mayhew, G.F., Rose, D.J., Zhou, S., Schwartz, D.C., Perna, N.T., Mobley, H.L., Sonnenberg, M.S., and Blattner, F.R. (2002) Extensive mosaic structure revealed by the complete genome sequence of uropathogenic *Escherichia coli*. *Proc Natl Acad Sci U S A* **99**: 17020-17024.
- Wheeler, M.A., Smith, S.D., Garcia-Cardena, G., Nathan, C.F., Weiss, R.M., and Sessa, W.C. (1997) Bacterial infection induces nitric oxide synthase in human neutrophils. *J Clin Invest* **99**: 110-116.
- Wildsmith, S.E., and Elcock, F.J. (2001) Microarrays under the microscope. *Mol Pathol* **54**: 8-16.
- Wink, D.A., Kasprzak, K.S., Maragos, C.M., Elespuru, R.K., Misra, M., Dunams, T.M., Cebula, T.A., Koch, W.H., Andrews, A.W., Allen, J.S., and et al. (1991) DNA deaminating ability and genotoxicity of nitric oxide and its progenitors. *Science* **254**: 1001-1003.

- Wink, D.A., and Mitchell, J.B. (1998) Chemical biology of nitric oxide: Insights into regulatory, cytotoxic, and cytoprotective mechanisms of nitric oxide. *Free Radic Biol Med* **25**: 434-456.
- Wirth, T., Falush, D., Lan, R., Colles, F., Mensa, P., Wieler, L.H., Karch, H., Reeves, P.R., Maiden, M.C., Ochman, H., and Achtman, M. (2006) Sex and virulence in *Escherichia coli*: an evolutionary perspective. *Mol Microbiol* **60**: 1136-1151.
- Wullt, B., Connell, H., Rollano, P., Mansson, W., Colleen, S., and Svanborg, C. (1998) Urodynamic factors influence the duration of *Escherichia coli* bacteriuria in deliberately colonized cases. *J Urol* **159**: 2057-2062.
- Wullt, B., Bergsten, G., Samuelsson, M., and Svanborg, C. (2002) The role of P fimbriae for *Escherichia coli* establishment and mucosal inflammation in the human urinary tract. *Int J Antimicrob Agents* **19**: 522-538.
- Wullt, B., Bergsten, G., Fischer, H., Godaly, G., Karpman, D., Leijonhufvud, I., Lundstedt, A.C., Samuelsson, P., Samuelsson, M., Svensson, M.L., and Svanborg, C. (2003) The host response to urinary tract infection. *Infect Dis Clin North Am* **17**: 279-301.
- Wyckoff, E.E., Duncan, D., Torres, A.G., Mills, M., Maase, K., and Payne, S.M. (1998) Structure of the *Shigella dysenteriae* haem transport locus and its phylogenetic distribution in enteric bacteria. *Mol Microbiol* **28**: 1139-1152.
- Yang, R.B., Mark, M.R., Gurney, A.L., and Godowski, P.J. (1999) Signaling events induced by lipopolysaccharide-activated toll-like receptor 2. *J Immunol* **163**: 639-643.
- Yoshimoto, T., Higashi, H., Kanatani, A., Lin, X.S., Nagai, H., Oyama, H., Kurazono, K., and Tsuru, D. (1991) Cloning and sequencing of the 7 alpha-hydroxysteroid dehydrogenase gene from *Escherichia coli* HB101 and characterization of the expressed enzyme. *J Bacteriol* **173**: 2173-2179.
- Zdziarski, J., Svanborg, C., Wullt, B., Hacker, J., and Dobrindt, U. (2008) Molecular basis of commensalism in the urinary tract: low virulence or virulence attenuation? *Infect Immun* **76**: 695-703.
- Zhou, X., Giron, J.A., Torres, A.G., Crawford, J.A., Negrete, E., Vogel, S.N., and Kaper, J.B. (2003) Flagellin of enteropathogenic *Escherichia coli* stimulates interleukin-8 production in T84 cells. *Infect Immun* **71**: 2120-2129.
- Ziebuhr, W., Ohlsen, K., Karch, H., Korhonen, T., and Hacker, J. (1999) Evolution of bacterial pathogenesis. *Cell Mol Life Sci* **56**: 719-728.
- Zogaj, X., Nimtz, M., Rohde, M., Bokranz, W., and Romling, U. (2001) The multicellular morphotypes of *Salmonella typhimurium* and *Escherichia coli* produce cellulose as the second component of the extracellular matrix. *Mol Microbiol* **39**: 1452-1463.
- Zorc, J.J., Kiddoo, D.A., and Shaw, K.N. (2005) Diagnosis and management of pediatric urinary tract infections. *Clin Microbiol Rev* **18**: 417-422.

8. Appendix

8.1. Legends to figures and tables

Table 1: Prevalence of asymptomatic bacteriuria in selected populations	17
Table 2: Bacterial strains used in this study	33
Table 3: Plasmids used in this study.	34
Table 4: Oligonucleotides used in this study.....	34
Table 5: Antibiotic substances used in this study.....	39
Table 6: Parameters of the ArrayVision pre-set protocols (Wizard) used for reading intensity values.	60
Table 7: Genotypic characterization of asymptomatic bacteriuria <i>E. coli</i> strains by comparative genomic hybridization.....	82
Table 8: Genome size of ABU <i>E. coli</i> isolates.....	86
Table 9: Geno- and phenotypic characterization of selected virulence traits of asymptomatic bacteriuria <i>E. coli</i> strains.....	90
Table 10: Identification of the Gln472 → Leu substitution critical for FocD function	91
Table 11: Geno- and phenotypic characterization of <i>in vivo</i> re-isolates of ABU strain 83972.....	106
Table 12: Motility of <i>in vitro</i> 83972 re-isolates on urine soft agar plates.	112
Table 13: Total number of de-regulated genes in the <i>in vivo</i> and <i>in vitro</i> re-isolates of ABU strain 83972.....	115
Table 14: Differently expressed cytoplasmic proteins in the <i>in vivo</i> re-isolate KA25 and the ancestor strain 83972.	127
Table 15: Differently expressed cytoplasmic proteins in the <i>in vivo</i> re-isolate SR12 and the ancestor strain 83972.	129
Table 16: Differently expressed cytoplasmic proteins in the <i>in vivo</i> re-isolate CK12 and the ancestor strain 83972.	131
Table 17: Changes in the outer membrane subproteome of the <i>in vivo</i> re-isolates of strain 83972 following <i>in vitro</i> culture in pooled human urine.....	136
Table 18: Genes with up-regulated expression in <i>in vivo</i> re-isolate SR12.....	181
Table 19/1: Genes with down-regulated expression in <i>in vivo</i> re-isolate SR12.....	184
Table 20/1: Genes with up-regulated expression in <i>in vivo</i> re-isolate CK12.....	186
Table 21/1: Genes with down-regulated expression in <i>in vivo</i> re-isolate CK12.....	187
Table 22: Genes with up-regulated expression in <i>in vivo</i> re-isolate KA25.....	190
Table 23/1: Genes with down-regulated expression in <i>in vivo</i> re-isolate KA25.....	190
Table 24: Genes with up-regulated expression in <i>in vitro</i> re-isolate 4.9.....	193
Table 25: Genes with down-regulated expression in re-isolate <i>in vitro</i> 4.9.....	194
Fig. 1: Pathogenesis of urinary tract infection caused by uropathogenic <i>E. coli</i>	19
Fig. 2: Phenotypic comparison of <i>E. coli</i> strains CFT073, Nissle 1917 and 83972.....	25
Fig. 3.: Bacterial genome plasticity.....	29
Fig. 4: DNA markers used for electrophoresis.....	39
Fig. 5: Triplex PCR profiles specific for the four <i>E. coli</i> phylogenetic groups.....	47
Fig. 6: Agarose gel showing PCR products from the multiplex virulence factor-PCR assay	48
Fig. 7: Strategy for inactivation of chromosomal genes using PCR products.....	55
Fig. 8: Schematic construction of the single flow culture unit.....	79
Fig. 9: Four-chamber microfermenter setup.....	79
Fig. 10: Analysis of the genome content of ABU <i>E. coli</i> isolates.....	83

Fig. 11: Genomic fingerprints of asymptomatic bacteriuria <i>E. coli</i> isolates.	85
Fig. 12: Assessment of the genome size of asymptomatic bacteriuria <i>E. coli</i> isolates by PFGE.....	86
Fig. 13: Genetic structure of the <i>fim</i> determinant and adjacent KpLE2 phage-like chromosomal region in asymptomatic bacteriuria <i>E. coli</i> isolates.....	88
Fig. 14: Allelic variation of the FimH type 1 fimbrial adhesins among asymptomatic bacteriuria <i>E. coli</i> isolates.....	89
Fig. 15 Amino acid alignment of FocD, SfaF and FimD fimbrial ushers.....	91
Fig. 16: Inactivation of the <i>hly</i> determinant in strains 27 and 83972.....	92
Fig. 17: Analysis of the LPS phenotype among asymptomatic bacteriuria <i>E. coli</i> isolates.....	93
Fig. 18: Analysis of biofilm formation of asymptomatic bacteriuria <i>E. coli</i> isolates in urine.....	93
Fig. 19: Growth characteristics of <i>E. coli</i> isolates in pooled human urine.....	94
Fig. 20: Schematic representation of the experimental design of patients colonisation study.....	96
Fig. 21: Mean of host response parameters in urine samples collected from patients during the time of colonization with strain 83972.	97
Fig. 22: Levels of IL 8 and PMNs at each sampling time point.....	98
Fig. 23: Genetic organization of the <i>fim</i> loci in <i>E. coli</i> K-12 and <i>E. coli</i> 83972.....	99
Fig. 24: Verification of the patient re-isolates of <i>E. coli</i> strain 83972.....	99
Fig. 25 Genomic fingerprints of <i>in vivo</i> re-isolates of strain 83972 from different human patients... ..	100
Fig. 26: Motility of <i>in vivo</i> re-isolates of strain 83972 on urine soft agar plates incubated overnight at 37 °C.....	102
Fig. 27: Growth characteristics of <i>in vivo</i> re-isolates of strain 83972 and their parent strain in pooled human urine.....	103
Fig. 28: Competitiveness in urine of <i>in vivo</i> re-isolates of <i>E. coli</i> 83972 against their parent strain derivative 83972 <i>cat</i>	104
Fig. 29: Analysis of biofilm formation of <i>in vivo</i> re-isolates of ABU strain 83972 at 37 °C.....	105
Fig. 30: Growth dynamics of <i>E. coli</i> strain 83972 during continuous culture experiments.....	108
Fig. 31: Biofilm formation of ABU strain 83972 in continuous cultures.....	109
Fig. 32: Comparison of the genome structure of <i>in vitro</i> re-isolates of <i>E. coli</i> strain 83972.....	111
Fig. 33: Growth characteristics of <i>in vitro</i> re-isolates of strain 83972.....	113
Fig. 34: Analysis of biofilm formation of <i>in vitro</i> re-isolates of ABU strain 83972.....	114
Fig. 35: Functional grouping of the de-regulated genes in <i>in vivo</i> and <i>in vitro</i> re-isolates of ABU strain 83972 upon <i>in vitro</i> growth in pooled human urine.....	116
Fig. 36: Hierarchical cluster analysis of all de-regulated genes in three ABU 83972 <i>in vivo</i> re-isolates CK12, KA25 and SR12 and one <i>in vitro</i> re-isolate 4.9 relative to their parent strain 83972.....	117
Fig. 37: Altered expression of sugar transport and degradation pathways in the <i>in vivo</i> re-isolate SR12 compared to strain 83972.	119
Fig. 38: Hierarchical cluster analysis of commonly de-regulated genes in at least two re-isolates of strain 83972 relative to their parent strain.....	121
Fig. 39: Real Time-PCR-based quantification of transcript levels of selected genes in ABU re-isolates.....	123
Fig. 40: Comparison of 2D cytoplasmic protein profiles from ABU strain 83972 and the <i>in vivo</i> re-isolates KA25, CK12 and SR12 upon growth <i>in vitro</i> at 37 °C in pooled human urine.....	125
Fig. 41: Comparison of the cytoplasmic proteome of ABU strain 83972 and the <i>in vivo</i> re-isolate KA25.....	126
Fig. 42: Comparison of the cytoplasmic proteome of ABU strain 83972 and the <i>in vivo</i> re-isolate SR12.....	128
Fig. 43: Quantification of FrmA and FrmB protein expression in <i>in vivo</i> re-isolates of ABU strain 83972.....	129
Fig. 44: Comparison of the cytoplasmic proteome of ABU strain 83972 and the <i>in vivo</i> re-isolate CK12.....	130
Fig. 45: Adaptation of the ribonucleoside degradation pathway in <i>in vivo</i> re-isolate CK12 of ABU strain 83972.....	132

Fig. 46: Adaptation of the deoxy-ribonucleoside degradation pathway in *in vivo* re-isolate CK12 of ABU strain 83972..... 133

Fig. 47: Comparison of the outer membrane proteome of ABU strain 83972 and the *in vivo* re-isolate KA25 137

Fig. 48: Comparison of the outer membrane proteome of ABU strain 83972 and the *in vivo* re-isolate CK12 138

Fig. 49: Comparison of the outer membrane proteome of ABU strain 83972 and the *in vivo* re-isolate SR12 139

Fig. 50: Geno- and phenotypic diversity among closely related members of *E. coli* clonal group (ST 73)..... 146

Fig. 51: Model of D-serine catabolism and nitrogen assimilation in strain SR12..... 158

Fig. 52: Model of nitric oxide detoxification based on hierarchical cluster analysis of genes differently de-regulated in *in vivo* re-isolates SR12 and KA25 relative to their parent strain 83972 162

8.2. Expression profiling data

Data derived from expression profiling of three ABU 83972 *in vivo* re-isolates CK12, KA25 and SR12 and one *in vitro* re-isolate 4.9, sorted according to their level of expression.

Table 18/1: Genes with up-regulated expression in *in vivo* re-isolate SR12

gene	function	ratio	p-value
<i>fliC</i>	flagellin	8,66	0.001087
<i>frmA</i>	formaldehyde dehydrogenase, glutathione-dependent	6,42	0.003399
<i>fliM</i>	flagellar motor switch protein M	6,11	0.004536
<i>flgC</i>	flagellar basal-body rod protein C	6,10	0.050710
<i>flgB</i>	flagellar basal-body rod protein B	6,07	0.000233
<i>frmB</i>	predicted esterase	5,96	0.001933
<i>ygbK</i>	hypothetical protein	5,82	0.018833
<i>ygbK</i>	hypothetical protein	5,82	0.018833
<i>ydeN</i>	putative sulfatase <i>ydeN</i> precursor	5,71	0.009626
<i>ygbL</i>	hypothetical aldolase class II protein	5,64	0.018983
<i>fliI</i>	flagellum-specific ATP synthase	5,57	0.035347
<i>cheA</i>	fused chemotactic sensory histidine kinase	5,35	0.001679
<i>cheW</i>	purine-binding chemotaxis protein	5,34	0.001610
<i>fliL</i>	flagellar basal body-associated protein FliL	5,11	0.011405
<i>mglB</i>	transport of small molecules	5,03	0.029173
<i>araA</i>	L-arabinose isomerase	5,00	0.007611
<i>fliJ</i>	flagellar biosynthesis chaperone	4,96	0.012779
<i>fliZ</i>	FliZ protein	4,94	0.001242
<i>cheR</i>	protein-glutamate methyltransferase	4,90	0.029924
<i>yjHT</i>	hypothetical protein	4,76	0.017080
<i>frmR</i>	regulator protein that represses <i>frmRAB</i> operon	4,62	0.001138
<i>fliA</i>	flagellar biosynthesis sigma factor	4,58	0.001469
<i>motB</i>	flagellar motor protein MotB	4,49	0.000610
<i>ygbJ</i>	6-phosphogluconate dehydrogenase	4,43	0.021442
<i>fliD</i>	flagellar capping protein	4,42	0.001895
<i>ygbN</i>	gluconate:H ⁺ symporter, GntP family	4,38	0.042368
<i>rbsB</i>	D-ribose transporter subunit	4,38	0.011056
<i>yahK</i>	hypothetical zinc-type alcohol dehydrogenase	4,33	0.007739
<i>yeiC</i>	hypothetical sugar kinase	4,27	0.014557
<i>flgD</i>	flagellar basal body rod modification protein D	4,23	0.043625
<i>ybdL</i>	putative aminotransferase	4,23	0.001618
<i>yhjH</i>	EAL domain containing protein involved in flagellar function	4,18	0.037394
<i>flgF</i>	flagellar component of cell-proximal portion of basal-body rod	4,18	0.009644
<i>flgE</i>	flagellar hook protein E	4,16	0.012716
<i>yeiN</i>	hypothetical protein	4,14	0.017059
<i>dsdA</i>	D-serine dehydratase	4,07	0.063889
<i>lacA</i>	galactoside O-acetyltransferase	4,06	0.020097
<i>araD</i>	L-ribulose-5-phosphate 4-epimerase	4,04	0.006646
<i>araF</i>	L-arabinose transporter subunit	4,03	0.016067
<i>metA</i>	homoserine O-succinyltransferase	4,00	0.005343
<i>cheZ</i>	chemotaxis regulator, protein phosphatase for CheY	3,91	0.001710
<i>fliF</i>	flagellar M-ring protein	3,88	0.018288
<i>Tar</i>	methyl-accepting chemotaxis protein II	3,83	0.015660
c0318	putative sugar-phosphate isomerase	3,80	0.040402
<i>fadH</i>	2,4-dienoyl-CoA reductase	3,78	0.005511
<i>araG</i>	fused L-arabinose transporter	3,78	0.051022
<i>uidC</i>	predicted outer membrane porin protein	3,76	0.044296
<i>hmp</i>	fused nitric oxide dioxygenase/dihydropteridine reductase 2	3,68	0.000649
c1273	antigen 43 precursor	3,68	0.044683

Appendix

Table 18/2: Genes with up-regulated expression in *in vivo* re-isolate SR12

gene	function	ratio	p-value
<i>yjhS</i>	hypothetical protein	3,62	0.014845
<i>araB</i>	ribulokinase	3,62	0.018031
<i>metR</i>	DNA-binding transcriptional activator, homocysteine-binding	3,61	0.005323
<i>araE</i>	arabinose transporter	3,49	0.029326
<i>ydeU</i>	conserved protein, predicted pseudogene	3,47	0.003416
<i>flgN</i>	export chaperone for FlgK and FlgL	3,45	0.000976
<i>flgA</i>	flagellar basal body P-ring biosynthesis protein A	3,44	0.020545
<i>ygbM</i>	hypothetical protein	3,29	0.012104
<i>ybdH</i>	predicted oxidoreductase	3,26	0.004944
<i>malE</i>	maltose ABC transporter periplasmic protein	3,25	0.008623
<i>yhcH</i>	hypothetical protein	3,25	0.023108
<i>metB</i>	cystathionine gamma-synthase	3,23	0.005708
<i>fliG</i>	flagellar motor switch protein G	3,22	0.055549
<i>uxaB</i>	tagaturonate reductase	3,22	0.013546
<i>dsdX</i>	predicted transporter	3,22	0.069039
<i>lacZ</i>	Beta-galactosidase	3,21	0.022748
<i>pin</i>	putative DNA-invertase	3,18	0.049643
<i>nanK</i>	N-acetylmannosamine kinase	3,13	0.048044
<i>ygeA</i>	predicted racemase	3,13	0.010206
UTI89_P090	hypothetical protein	3,12	0.028604
<i>wrbA</i>	TrpR binding protein WrbA	3,04	0.007790
UTI89_C5097	hypothetical protein	3,04	0.008516
<i>tsr</i>	methyl-accepting chemotaxis protein I	3,01	0.001132
<i>iutA</i>	TonB-dependent ferric aerobactin receptor	2,98	0.010673
<i>cheB</i>	chemotaxis-specific methylesterase	2,95	0.005914
<i>flgM</i>	anti-sigma factor for FlhA (sigma 28)	2,94	0.010655
<i>uxaC</i>	glucuronate isomerase	2,90	0.018853
<i>hisP</i>	histidine/lysine/arginine/ornithine transporter subunit	2,87	0.035457
<i>yeeS</i>	CP4-44 prophage; predicted DNA repair protein	2,82	0.043772
<i>tktB</i>	transketolase II	2,80	0.009529
<i>yeiM</i>	proton-driven nucleoside uptake system.	2,76	0.081431
<i>xyIG</i>	fused D-xylose transporter	2,75	0.028536
<i>metF</i>	5,10-methylenetetrahydrofolate reductase	2,75	0.006491
<i>kduI</i>	5-keto-4-deoxyuronate isomerase	2,75	0.067555
<i>flhD</i>	transcriptional activator FlhD	2,73	0.012422
c2347	hypothetical protein	2,72	0.005504
<i>yjhI</i>	predicted DNA-binding transcriptional regulator	2,71	0.079398
<i>ompF</i>	outer membrane porin 1a (Ia;b;F)	2,70	0.004687
<i>araJ</i>	predicted transporter	2,69	0.008024
<i>uidB</i>	glucuronide transporter	2,67	0.023007
<i>metL</i>	bifunctional aspartate kinase II/homoserine dehydrogenase II	2,66	0.005303
<i>manZ</i>	mannose-specific enzyme IID component of PTS	2,63	0.043059
<i>nagE</i>	fused N-acetyl glucosamine specific PTS enzyme	2,59	0.029942
<i>manX</i>	fused mannose-specific PTS enzymes: IIA	2,58	0.064599
<i>metQ</i>	DL-methionine transporter subunit	2,54	0.005116
UTI89_C1735	hypothetical protein	2,53	0.036384
<i>uxaA</i>	altronate hydrolase	2,52	0.049642
<i>sucB</i>	dihydrolipoamide acetyltransferase	2,51	0.043394
<i>nanT</i>	transport; Murein sacculus, peptidoglycan	2,48	0.041061
Z3657	hypothetical protein	2,48	0.017646
<i>flhC</i>	DNA-binding transcriptional dual regulator with FlhD	2,46	0.026071
UTI89_C2987	bacteriophage V small terminase subunit	2,45	0.042589
<i>usp</i>	putative colicin	2,44	0.013607
<i>manY</i>	mannose-specific enzyme IIC component of PTS	2,42	0.051885
<i>phoH</i>	phosphate starvation-inducible	2,39	0.059384

Appendix

Table 18/3: Genes with up-regulated expression in *in vivo* re-isolate SR12

gene	function	ratio	p-value
ECP_4566	hypothetical transposase-like protein	2,39	0.039221
<i>yjhA</i>	N-acetylnuraminic acid outer membrane channel protein	2,37	0.049790
<i>iucD</i>	IucD protein	2,36	0.006012
<i>ycgR</i>	protein involved in flagellar function	2,36	0.015452
<i>nagA</i>	N-acetylglucosamine-6-phosphate deacetylase	2,35	0.000159
<i>nagB</i>	glucosamine-6-phosphate deaminase	2,35	0.021069
<i>xylH</i>	D-xylose transporter subunit	2,33	0.044072
<i>yidA</i>	hypothetical protein	2,33	0.007749
<i>yjhG</i>	KpLE2 phage-like element; predicted dehydratase	2,32	0.071624
<i>xylB</i>	xylulokinase	2,31	0.042449
<i>nanE</i>	predicted N-acetylmannosamine-6-P epimerase	2,30	0.017900
<i>fumC</i>	fumarate hydratase	2,29	0.028713
<i>mdh</i>	malate dehydrogenase	2,28	0.008209
<i>sdhB</i>	succinate dehydrogenase, FeS subunit	2,28	0.046384
<i>sucD</i>	succinyl-CoA synthetase subunit alpha	2,28	0.048211
<i>ytfE</i>	predicted regulator of cell morphogenesis	2,26	0.034695
<i>uxuA</i>	mannonate dehydratase	2,26	0.022885
<i>metI</i>	DL-methionine transporter subunit	2,24	0.014490
c0323	putative exopolysaccharide lyase	2,22	0.044032
<i>manA</i>	mannose-6-phosphate isomerase	2,22	0.023647
<i>pfkB</i>	6-phosphofructokinase II	2,22	0.010508
<i>nanA</i>	N-acetylneuraminic acid lyase subunit	2,20	0.032583
<i>xylF</i>	D-xylose transporter subunit	2,19	0.015392
<i>ybiC</i>	predicted dehydrogenase	2,18	0.049839
<i>clpB</i>	ATP-dependent Clp protease	2,18	0.042639
<i>sdhA</i>	succinate dehydrogenase flavoprotein subunit	2,18	0.037097
<i>yjdI</i>	hypothetical protein	2,17	0.030119
<i>sdhC</i>	succinate dehydrogenase cytochrome	2,16	0.033638
<i>yrdA</i>	hypothetical protein	2,15	0.008492
<i>metC</i>	cystathionine beta-lyase	2,15	0.015372
<i>sdhD</i>	succinate dehydrogenase cytochrome	2,15	0.027522
<i>uidA</i>	beta-D-glucuronidase	2,12	0.070442
<i>kdgK</i>	2-dehydro-3-deoxygluconokinase	2,11	0.044214
<i>fbaB</i>	fructose-bisphosphate aldolase	2,11	0.031618
c1464	putative factor; DNA packaging, phage assembly	2,10	0.041981
<i>metN</i>	DL-methionine transporter subunit	2,10	0.012049
<i>sucA</i>	alpha-ketoglutarate decarboxylase	2,09	0.036161
<i>glpQ</i>	periplasmic glycerophosphodiester phosphodiesterase	2,09	0.056232
<i>yjdA</i>	conserved protein	2,07	0.047900
<i>oppA</i>	oligopeptide transporter subunit	2,06	0.010796
<i>yeaR</i>	hypothetical protein	2,06	0.010792
<i>flgH</i>	flagellar L-ring protein precursor H	2,05	0.059368
<i>sucC</i>	succinyl-CoA synthetase subunit beta	2,04	0.041434
<i>yeaG</i>	serine protein kinase	2,03	0.020852
<i>ybjP</i>	predicted lipoprotein	2,02	0.019312
<i>sodA</i>	superoxide dismutase	1,99	0.002197
<i>mbhA</i>	flagellar motor protein	1,99	0.006426
<i>icdA</i>	isocitrate dehydrogenase	1,98	0.001180
<i>sufA</i>	iron-sulfur cluster assembly scaffold protein	1,97	0.005700
<i>grxB</i>	glutaredoxin 2 (Grx2)	1,96	0.010410
<i>gdhA</i>	glutamate dehydrogenase	1,96	0.007256
c0322	putative oligogalacturonide transporter	1,93	0.066034

Appendix

Table 18/4: Genes with up-regulated expression in *in vivo* re-isolate SR12

gene	function	ratio	p-value
<i>yhaO</i>	predicted transporter	1,90	0.024590
<i>uxuB</i>	D-mannonate oxidoreductase, NAD-binding	1,90	0.014400
<i>xylA</i>	xylose isomerase	1,86	0.066314
<i>tas</i>	predicted oxidoreductase	1,85	0.009933
<i>rna</i>	ribonuclease I	1,84	0.022282
<i>metE</i>	homocysteine methyltransferase	1,84	0.015186
<i>gltA</i>	citrate synthase	1,83	0.031147
<i>ycjU</i>	predicted beta-phosphoglucomutase	1,79	0.016836
<i>yidA</i>	predicted hydrolase	1,79	0.025859
<i>iroB</i>	putative glucosyltransferase	1,78	0.015239
<i>flhA</i>	flagellar biosynthesis protein A	1,77	0.057666
<i>kduD</i>	2-deoxy-D-gluconate 3-dehydrogenase	1,76	0.012391
<i>fliT</i>	predicted chaperone	1,73	0.031235
<i>ptsH</i>	phosphohistidinoprotein-hexose phosphotransferase	1,73	0.001322
<i>luxS</i>	S-ribosylhomocysteinase	1,72	0.012512
<i>pepN</i>	aminopeptidase N	1,60	0.016456

Table 19/1: Genes with down-regulated expression in *in vivo* re-isolate SR12

gene	function	ratio	p-value
c2464	putative acyl-CoA dehydrogenase	-5,77	0.001178
<i>yajF</i>	inositol phosphate metabolism: fructokinase	-5,20	0.031784
<i>yjiH</i>	conserved inner membrane protein	-4,96	0.036361
<i>yqcB</i>	tRNA pseudouridine synthase	-4,58	0.007510
<i>ybbK</i>	predicted protease, membrane anchored	-4,53	0.075384
<i>glnG</i>	fused DNA-binding response regulator	-4,51	0.024150
<i>malQ</i>	4-alpha-glucanotransferase (amylomaltase)	-4,32	0.011202
<i>yphC</i>	predicted Zn-dependent dehydrogenase	-4,11	0.047909
c2474	transposase	-4,05	0.043321
c1191	conserved hypothetical protein	-3,93	0.013694
Z1355	unknown protein	-3,81	0.070836
<i>yraL</i>	predicted methyltransferase	-3,68	0.023138
<i>frwD</i>	predicted enzyme IIB component of PTS	-3,63	0.008823
Z2106	unknown protein encoded within prophage CP-9330	-3,63	0.059160
<i>ygcF</i>	hypothetical protein	-3,62	0.046793
<i>ldcC</i>	lysine degradation: lysine decarboxylase, constitutive	-3,61	0.018342
<i>ssb</i>	single-strand DNA-binding protein	-3,49	0.049279
Z1778	unknown protein encoded by prophage CP-933N	-3,47	0.024673
Z3957	hypothetical protein	-3,43	0.009223
<i>corA</i>	magnesium/nickel/cobalt transporter	-3,28	0.013879
<i>rnfE</i>	NADH-ubiquinone oxidoreductase	-3,17	0.039392
<i>ydgG</i>	predicted inner membrane protein	-3,07	0.087474
<i>yeaN</i>	predicted transporter	-3,05	0.056488
<i>sidI</i>	putative capsid morphogenesis protein encoded in CP-933I	-2,95	0.002663
<i>pqiB</i>	paraquat-inducible protein B	-2,89	0.022660
<i>obgE</i>	GTPase involved in cell partitioning and DNA repair	-2,89	0.075132
<i>yneF</i>	predicted diguanylate cyclase	-2,84	0.020621
<i>ybiR</i>	predicted transporter	-2,83	0.051678

Appendix

Table 19/2: Genes with down-regulated expression in *in vivo* re-isolate SR12

gene	function	ratio	p-value
<i>hypF</i>	carbamoyl phosphate phosphatase	-2,82	0.067106
<i>yfhK</i>	predicted sensory kinase in two-component system	-2,82	0.035332
<i>ygiQ</i>	hypothetical protein	-2,82	0.000802
<i>purE</i>	phosphoribosylaminoimidazole carboxylase catalytic subunit	-2,81	0.048854
<i>glnL</i>	sensory histidine kinase in two-component regulatory system	-2,79	0.017928
<i>artJ</i>	arginine transporter subunit	-2,78	0.046050
c3633	hypothetical protein	-2,76	0.034726
c2437	putative pesticin receptor precursor	-2,73	0.049984
<i>paaH</i>	putative 3-hydroxyacyl-CoA dehydrogenase	-2,70	0.049050
c0349	putative transposase within prophage	-2,68	0.041583
c1189	putative 3-oxoacyl-[ACP] synthase;	-2,68	0.027324
<i>cysP</i>	thiosulfate-binding protein precursor	-2,67	0.029340
<i>yfeZ</i>	predicted inner membrane protein	-2,66	0.006973
<i>aroH</i>	3-deoxy-D-arabino-heptulosonate-7-phosphate synthase	-2,61	0.038728
<i>yhiN</i>	predicted oxidoreductase with FAD/NAD(P)-binding domain	-2,60	0.060571
c1536	putative factor; Integration, recombination	-2,60	0.027013
<i>glnA</i>	glutamine synthetase	-2,58	0.071730
<i>phnL</i>	carbon-phosphorus lyase complex subunit	-2,54	0.078754
<i>moaE</i>	molybdopterin synthase, large subunit	-2,54	0.055856
<i>proW</i>	glycine betaine transporter subunit	-2,53	0.002783
<i>recE</i>	exodeoxyribonuclease VIII	-2,52	0.058425
<i>purF</i>	purine metabolism: Amidophosphoribosyltransferase	-2,51	0.056675
<i>yadL</i>	predicted fimbrial-like adhesin protein	-2,50	0.052720
c1259	hypothetical protein	-2,50	0.000268
<i>ybjK</i>	predicted DNA-binding transcriptional regulator	-2,50	0.015125
<i>trmE</i>	tRNA modification GTPase	-2,48	0.006793
<i>pyrE</i>	pyrimidine metabolism: orotate phosphoribosyltransferase	-2,44	0.034673
<i>pgpA</i>	phosphatidylglycerophosphatase A	-2,44	0.007819
<i>eutB</i>	ethanolamine ammonia-lyase, large subunit, heavy chain	-2,42	0.034046
<i>yicM</i>	purine ribonucleoside exporter; predicted transporter	-2,41	0.007540
<i>mtlD</i>	mannitol-1-phosphate 5-dehydrogenase	-2,40	0.041884
<i>purD</i>	phosphoribosylamine--glycine ligase	-2,40	0.044766
<i>dinD</i>	DNA-damage-inducible protein	-2,39	0.057304
<i>glnP</i>	glutamine ABC transporter permease protein	-2,38	0.002374
<i>glnH</i>	glutamine ABC transporter periplasmic protein	-2,35	0.022858
<i>rcsC</i>	hybrid sensory kinase in two-component regulatory system	-2,34	0.031004
c3749	conserved hypothetical protein	-2,33	0.022805
ECP_3783	putative F17-like fimbrial adhesin subunit	-2,32	0.048605
<i>ynjA</i>	hypothetical protein	-2,31	0.030621
<i>yjaA</i>	hypothetical protein	-2,30	0.002432
<i>rep</i>	DNA helicase and single-stranded DNA-dependent ATPase	-2,30	0.067267
<i>ydhA</i>	predicted lipoprotein	-2,29	0.033131
<i>sppA</i>	protease IV (signal peptide peptidase)	-2,28	0.045503
<i>yfiM</i>	hypothetical protein	-2,27	0.009797
<i>yhbE</i>	conserved inner membrane protein	-2,27	0.016936
Z3312 Z2347	putative superoxide dismutase copper-zinc superoxide dismutase	-2,26	0.011764
<i>frlC</i>	predicted isomerase	-2,26	0.027871
<i>ptr</i>	protease III	-2,25	0.048972
Z2391	unknown protein encoded within prophage CP-933R	-2,24	0.028815
<i>rnhB</i>	ribonuclease HIII	-2,23	0.012138
<i>glnQ</i>	glutamine ABC transporter ATP-binding protein	-2,22	0.001290
<i>trkD</i>	potassium transporter	-2,22	0.054158

Appendix

Table 19/3: Genes with down-regulated expression in *in vivo* re-isolate SR12

gene	function	ratio	p-value
<i>hycH</i>	protein required for maturation of hydrogenase 3	-2,20	0.069761
<i>Z5294</i>	hypothetical protein	-2,20	0.016938
<i>trkA</i>	potassium transporter peripheral membrane component	-2,19	0.063783
<i>c1523</i>	unknown protein encoded by bacteriophage	-2,16	0.047474
<i>rluB</i>	23S rRNA pseudouridylate synthase	-2,16	0.006805
<i>rseC</i>	RseC protein involved in reduction of the SoxR iron-sulfur cluster	-2,15	0.041879
<i>c3411</i>	N-acetylmuramoyl-L-alanine amidase <i>amiC</i> precursor	-2,14	0.055017
<i>yedC</i>	predicted DNA-binding transcriptional regulator	-2,14	0.074342
<i>yhhY</i>	hypothetical protein	-2,12	0.033298
<i>purH</i>	bifunctional phosphoribosylaminoimidazolecarboxamide	-2,11	0.066982
<i>purM</i>	phosphoribosylaminoimidazole synthetase	-2,07	0.007227
<i>ygjG</i>	probable ornithine aminotransferase	-2,03	0.074282
<i>cysG</i>	siroheme synthase 1,3-dimethyluroporphyriongen III dehydrogenase	-2,02	0.010059
<i>purK</i>	phosphoribosylaminoimidazole carboxylase	-2,02	0.018088
<i>ydaN</i>	zinc transporter	-2,02	0.029881
<i>Z0721</i>	hypothetical protein	-2,01	0.021130
<i>yjeS</i>	predicted Fe-S electron transport protein	-1,96	0.057172
<i>plsC</i>	1-acyl-sn-glycerol-3-phosphate acyltransferase	-1,95	0.021872
<i>atpI</i>	F0F1 ATP synthase subunit I	-1,94	0.051568
<i>ECs1396</i>	<i>AidA-I</i>	-1,94	0.002474
<i>folC</i>	bifunctional folylpolyglutamate synthase	-1,94	0.020833
<i>ynjB</i>	putative thiamine transport system	-1,93	0.012330
<i>ygeD</i>	predicted inner membrane protein	-1,93	0.002465
<i>sdaA</i>	L-serine deaminase I	-1,92	0.036107
<i>hcaB</i>	2,3-dihydroxy-2,3-dihydrophenylpropionate dehydrogenase	-1,90	0.067728
<i>yhjQ</i>	cell division protein	-1,88	0.148903
<i>thiL</i>	thiamine monophosphate kinase	-1,84	0.006680
<i>hcaT</i>	predicted 3-phenylpropionic transporter	-1,81	0.024023
<i>yceP</i>	hypothetical protein	-1,77	0.048521
<i>proV</i>	glycine betaine transporter subunit	-1,77	0.044664
<i>yecS</i>	predicted transporter subunit	-1,75	0.056760

Table 20/1: Genes with up-regulated expression in *in vivo* re-isolate CK12

gene	function	ratio	p-value
<i>cdd</i>	cytidine deaminase	3,50	0.004303
<i>udp</i>	uridine phosphorylase	3,47	0.001118
<i>ycjU</i>	putative beta-phosphoglucomutase	2,58	0.006752
<i>Z3115</i>	putative endonuclease encoded within prophage CP-933U	2,52	0.001105
<i>orn</i>	oligoribonuclease	2,40	0.001225
<i>yhfC</i>	hypothetical protein	2,39	0.007638
<i>deoB</i>	phosphopentomutase	2,31	0.003412
<i>yjgB</i>	predicted alcohol dehydrogenase, Zn-dependent and NAD(P)-binding	2,30	0.001156
<i>yhfC</i>	hypothetical protein	2,28	0.004610
<i>deoA</i>	thymidine phosphorylase	2,25	0.019214
<i>argA</i>	N-acetylglutamate synthase	2,23	0.020099
<i>c5039</i>	putative lactate dehydrogenase	2,22	0.001756
<i>yrdA</i>	hypothetical protein	2,20	0.004322

Appendix

Table 20/2: Genes with up-regulated expression in *in vivo* re-isolate CK12

gene	function	ratio	p-value
<i>edd</i>	phosphogluconate dehydratase	2,19	0.071959
<i>uidB</i>	glucuronide transporter	2,16	0.075343
<i>uidC</i>	predicted outer membrane porin protein	2,16	0.060678
<i>tsx</i>	nucleoside channel, receptor of phage T6 and colicin K	2,16	0.007529
<i>grxA</i>	glutaredoxin 1, redox coenzyme for ribonucleotide reductase (RNR1a)	2,14	0.031578
<i>c1464</i>	putative factor; DNA packaging, phage assembly	2,13	0.039219
<i>eda</i>	keto-hydroxyglutarate-aldolase/keto-deoxy- phosphogluconate aldolase	2,12	0.073465
<i>rnk</i>	nucleoside diphosphate kinase regulator	2,12	0.010185
<i>yhcM</i>	conserved protein with nucleoside triphosphate hydrolase domain	2,11	0.011270
<i>deoD</i>	purine nucleoside phosphorylase	2,11	0.001030
<i>deoC</i>	deoxyribose-phosphate aldolase	2,08	0.021257
<i>uidA</i>	beta-D-glucuronidase	2,08	0.060042
<i>Z0893</i>	putative methylaspartate ammonia-lyase	2,08	0.000045
<i>fecC</i>	KpLE2 phage-like element; iron-dicitrate transporter subunit	2,07	0.011613
<i>fecE</i>	KpLE2 phage-like element; iron-dicitrate transporter subunit	2,06	0.000662
<i>fecA</i>	KpLE2 phage-like element; ferric citrate outer membrane transporter	2,05	0.001410
<i>fecD</i>	KpLE2 phage-like element; iron-dicitrate transporter subunit	2,05	0.005962
<i>ada</i>	Ada transcriptional dual regulator	2,04	0.000854
<i>fecR</i>	transmembrane signal transducer for ferric citrate transport	2,02	0.005792
<i>fecI</i>	KpLE2 phage-like element; RNA polymerase, sigma 19 factor	2,01	0.000175
<i>ECP_2994</i>	hypothetical protein	1,92	0.004457
<i>fadH</i>	2,4-dienoyl-CoA reductase (NADPH2)	1,91	0.001996
<i>hmp</i>	fused nitric oxide dioxygenase/dihydropteridine reductase 2	1,16	0.020434

Table 21/1: Genes with down-regulated expression in *in vivo* re-isolate CK12

gene	function	ratio	p-value
<i>sat</i>	hypothetical protein Acreted auto transpoter toxin	-7,15	0.010209
<i>yraH</i>	predicted fimbrial-like adhesin protein	-6,88	0.069727
<i>iucD</i>	siderophore biosynthesis protein	-6,59	0.007250
<i>iucA</i>	siderophore biosynthesis protein	-6,56	0.019315
<i>c3604</i>	hypothetical protein	-5,74	0.015268
<i>insM</i>	transposase	-5,40	0.083988
<i>Z1486</i>	BP-933W unknown protein encoded by bacteriophage	-5,38	0.081437
<i>yhfL</i>	hypothetical protein	-5,12	0.023448
<i>c1400</i>	IS, phage, Tn; Phage-related functions and prophages	-5,04	0.056116
<i>yjFY</i>	hypothetical protein	-4,89	0.009967
<i>ypdH</i>	predicted enzyme IIB component of PTS	-4,79	0.027572
<i>ybhM</i>	hypothetical protein	-4,64	0.020526
<i>c4657</i>	hypothetical protein	-4,39	0.026301
<i>c3201</i>	hypothetical protein	-4,27	0.036751
<i>Z3926 Z3108</i>	unknown protein encoded by prophageprophage	-4,19	0.046835
<i>relE</i>	Qin prophage; toxin of the RelE-RelB toxin-antitoxin system	-4,16	0.054855
<i>c3389</i>	hypothetical protein	-3,98	0.048469
<i>torY</i>	TMAO reductase III (TorYZ), cytochrome c-type subunit	-3,87	0.020031
<i>ybfH</i>	hypothetical protein	-3,67	0.049534
<i>Z2801</i>	hypothetical protein	-3,63	0.046724
<i>Z2973</i>	CP-933T unknown protein encoded by prophage	-3,59	0.098665

Appendix

Table 21/2: Genes with down-regulated expression in *in vivo* re-isolate CK12

gene	function	ratio	p-value
<i>ydfD</i>	Qin prophage; predicted protein	-3,47	0.010126
Z3072	CP-933U unknown protein encoded within prophage	-3,37	0.068793
Z4824	hypothetical protein	-3,36	0.052374
<i>ydaV</i>	Rac prophage; predicted DNA replication protein	-3,36	0.072324
<i>yjgK</i>	hypothetical protein	-3,34	0.057853
Z5898	hypothetical protein	-3,34	0.050561
<i>yidI</i>	predicted inner membrane protein	-3,30	0.013888
<i>ydfO</i>	Qin prophage; predicted protein	-3,29	0.098399
<i>ydfQ</i>	Qin prophage; predicted lysozyme	-3,29	0.044827
Z3358	CP-933V putative repressor protein CI of prophage	-3,27	0.062914
<i>ulaA</i>	ascorbate-specific PTS system enzyme IIC	-3,25	0.051875
<i>yiaL</i>	hypothetical protein	-3,18	0.026400
<i>tar</i>	methyl-accepting chemotaxis protein II	-3,12	0.033779
Z5080	hypothetical protein	-3,10	0.044743
<i>ydjK</i>	hypothetical metabolite transport protein <i>ydjK</i>	-3,10	0.027336
<i>glpC</i>	sn-glycerol-3-phosphate dehydrogenase anaerobic	-3,10	0.038206
Z0959	CP-933K unknown protein encoded by prophage	-3,09	0.010552
<i>ybfL</i>	predicted transposase (pseudogene)	-3,07	0.084518
Z1562 Z1124	unknown in IS1N unknown in IS1N	-3,05	0.041266
Z0326	CP-933I unknown protein encoded in prophage	-3,05	0.083180
<i>yohC</i>	predicted inner membrane protein	-3,02	0.050355
<i>insH-5</i>	Rac prophage; IS5 transposase and trans-activator	-3,02	0.021055
<i>iutA</i>	ferric siderophore receptor	-3,01	0.032643
Z1573 Z1135	unknown in IS600 unknown in IS600	-3,01	0.016242
<i>fadA</i>	putative fatty acyl chain dehydrase	-3,00	0.029667
<i>ssuA</i>	alkanesulfonate transporter subunit	-2,95	0.009536
<i>ybfB</i>	predicted inner membrane protein	-2,93	0.058313
<i>appY</i>	DLP12 prophage; DNA-binding transcriptional activator	-2,91	0.041079
Z2386	CP-933R unknown protein encoded within prophage	-2,91	0.060377
<i>bglH</i>	carbohydrate-specific outer membrane porin, cryptic	-2,90	0.014760
<i>flgB</i>	flagellar basal-body rod protein B	-2,90	0.014984
<i>bcsA</i>	cellulose synthase, catalytic subunit	-2,90	0.012511
Z1816	CP-933N unknown protein encoded by prophage	-2,88	0.073381
<i>yafL</i>	predicted lipoprotein and C40 family peptidase	-2,86	0.021730
<i>yehD</i>	putative fimbrial-like protein	-2,85	0.019012
<i>ninE</i>	DLP12 prophage; conserved protein	-2,82	0.017317
<i>wcaB</i>	putative colanic acid biosynthesis acetyltransferase <i>wcaB</i>	-2,81	0.055450
Z1570 Z1131	unknown protein	-2,78	0.024227
<i>mhpF</i>	acetaldehyde dehydrogenase	-2,77	0.030248
<i>yjfX</i>	hypothetical protein	-2,76	0.035052
<i>ygiU</i>	hypothetical protein	-2,76	0.010228
<i>yeiM</i>	proton-driven nucleoside uptake system.	-2,76	0.002513
Z1824	CP-933N unknown protein encoded by prophage	-2,75	0.071609
Z1919	CP-933X unknown protein encoded by prophage	-2,74	0.034168
<i>yfbJ</i>	hypothetical protein	-2,73	0.048817
<i>phnD</i>	phosphonate/organophosphate ester transporter subunit	-2,69	0.025084
<i>yjgG_2</i>	hypothetical protein	-2,69	0.030505
<i>yqeG</i>	predicted transporter	-2,67	0.021998
c3637	transport; Murein sacculus, peptidoglycan	-2,66	0.056576
<i>yeiN</i>	hypothetical protein	-2,65	0.002642
<i>bcsZ</i>	endo-1,4-D-glucanase	-2,65	0.010404

Appendix

Table 21/3: Genes with down-regulated expression in *in vivo* re-isolate CK12

gene	function	ratio	p Value
<i>yjcF</i>	hypothetical protein	-2,65	0.019733
Z1850	CP-933C unknown protein encoded by prophage	-2,63	0.076467
<i>php</i>	predicted hydrolase	-2,62	0.036454
<i>yIbF</i>	hypothetical protein	-2,61	0.039153
<i>yphG</i>	hypothetical protein	-2,61	0.046571
c4829	putative dehydrogenase (zinc binding)	-2,60	0.027570
<i>yieK</i>	hypothetical protein	-2,59	0.039619
<i>yeiC</i>	hypothetical sugar kinase	-2,58	0.005908
<i>ybbC</i>	hypothetical protein	-2,57	0.030611
c2401	hypothetical protein	-2,56	0.018391
<i>yegJ</i>	hypothetical protein	-2,56	0.020791
<i>hsdR</i>	endonuclease R	-2,55	0.079482
Z1453	BP-933W unknown protein encoded by bacteriophage	-2,52	0.041217
<i>yffW</i>	CP4-57 prophage; predicted inner membrane protein	-2,46	0.043008
<i>ydfP</i>	Qin prophage; conserved protein	-2,46	0.016802
<i>yjgH</i>	predicted mRNA endoribonuclease	-2,45	0.089219
<i>ygfO</i>	predicted transporter	-2,42	0.013830
<i>YtfJ</i>	protein YtfJ precursor	-2,42	0.017480
<i>ydhV</i>	predicted oxidoreductase	-2,41	0.032830
<i>yfbA</i>	biosynthesis of siderophore group nonribosomal peptides	-2,41	0.000590
Z1495	BP-933W unknown protein encoded by bacteriophage	-2,40	0.048208
UTI89_C1724	phage hypothetical protein	-2,40	0.010787
Z4330	putative transposase	-2,38	0.014206
<i>tynA</i>	tyramine oxidase, copper-requiring	-2,38	0.025944
<i>ynbA</i>	predicted inner membrane protein	-2,37	0.014359
c0331	putative ribokinase	-2,37	0.018014
Z6022	putative integrase fragment	-2,35	0.018006
<i>yicO</i>	predicted xanthine/uracil permase	-2,33	0.040070
Z3370	CP-933V unknown protein encoded within prophage	-2,31	0.082537
<i>yobD</i>	hypothetical protein	-2,31	0.015870
<i>yieL</i>	predicted xylanase	-2,26	0.046419
<i>ybeR</i>	hypothetical protein	-2,26	0.025934
c4739	Conserved hypothetical protein	-2,25	0.049342
<i>yffL</i>	CP4-57 prophage; predicted protein	-2,25	0.053677
<i>mhpE</i>	4-hydroxy-2-ketovaleate aldolase	-2,20	0.036397
c4987	transcriptional regulator of sorbose uptake and utilization genes	-2,19	0.043012
c3172	putative head-tail joining protein of prophage	-2,19	0.076821
Z6065	CP-933P unknown protein encoded by cryptic prophage	-2,18	0.013040
Z1431	BP-933W unknown protein encoded by bacteriophage	-2,17	0.008425
<i>yadD</i>	predicted transposase	-2,14	0.023019
<i>mcrA</i>	5-methylcytosine-specific restriction endonuclease B	-2,14	0.008450
c1444	IS, phage, Tn; Phage-related functions and prophages	-2,13	0.039544
Z1329	CP-933M unknown protein encoded by cryptic prophage	-2,11	0.014498
c4565	predicted GTPase	-2,10	0.033993
<i>frvX</i>	predicted endo-1,4-beta-glucanase	-2,08	0.010087
Z2969	CP-933T unknown protein encoded by prophage	-2,08	0.056358
<i>agaC</i>	N-acetylgalactosamine-specific enzyme IIC component of PTS	-2,07	0.017913
<i>narZ</i>	nitrate reductase 2 (NRZ), alpha subunit	-2,06	0.041511
<i>agaB</i>	N-acetylgalactosamine-specific enzyme IIB component of PTS	-2,04	0.015102
<i>ycjP</i>	predicted sugar transporter subunit	-2,02	0.026653
<i>ydaG</i>	Rac prophage; predicted protein	-2,01	0.034160
<i>bgIF</i>	fused beta-glucoside-specific PTS enzymes: IIA	-2,01	0.030471

Appendix

Table 22: Genes with up-regulated expression in *in vivo* re-isolate KA25

gene	function	ratio	p-value
<i>frmA</i>	formaldehyde dehydrogenase, glutathione-dependent	5,84	0,001181
<i>frmB</i>	S-formylglutathione hydrolase	5,84	0,004392
<i>c0447</i>	hypothetical protein	4,90	0.006958
<i>marR</i>	DNA-binding transcriptional repressor of multiple antibiotic resistance	4,42	0.000711
<i>marA</i>	DNA-binding transcriptional dual activator of multiple antibiotic resistance	3,82	0.004549
<i>frmR</i>	regulator protein that represses frmRAB operon	3,70	0.051727
<i>marB</i>	hypothetical protein	2,31	0.326488
<i>metA</i>	homoserine O-succinyltransferase	2,29	0.047671
<i>malY</i>	cystathionine beta-lyase	2,19	0.054391
<i>metR</i>	transcriptional activator protein	2,18	0.041275
<i>cynS</i>	cyanate hydratase	2,14	0.017838
<i>nrdH</i>	glutaredoxin-like protein	2,13	0.049231
<i>fadH</i>	2,4-dienoyl-CoA reductase	2,12	0.003304
<i>nrdF</i>	ribonucleotide-diphosphate reductase beta subunit	2,11	0.042626
<i>nrdI</i>	hypothetical protein	2,11	0.041807
ECP_0113	putative colicin	2,09	0.013642
<i>sgaE</i>	L-ribose-5-phosphate 4-epimerase	2,09	0.046163
<i>fbaA</i>	fructose biphosphate aldolase	2,06	0.044267
<i>nrdE</i>	ribonucleotide-diphosphate reductase alpha subunit	2,06	0.043463
<i>metK</i>	S-adenosylmethionine synthetase	2,02	0.012050
<i>yrdA</i>	hypothetical protein	1,96	0.002033
<i>metF</i>	5,10-methylenetetrahydrofolate reductase	1,92	0.075932
<i>metC</i>	cystathionine beta-lyase	1,87	0.277647
<i>ybdL</i>	methionine aminotransferase	1,86	0.031802
<i>metA</i>	homoserine O-succinyltransferase	1,86	0.047671
<i>hmp</i>	fused nitric oxide dioxygenase/dihydropteridine reductase 2	1,78	0.061747
<i>dppA</i>	dipeptide transporter	1,77	0.021682
<i>grxB</i>	glutaredoxin 2 (Grx2)	1,76	0.047155
<i>metN</i>	DL-methionine transporter subunit	1,76	0.028322
<i>metI</i>	DL-methionine transporter subunit	1,74	0.067068
<i>ygaG</i>	S-ribosylhomocysteinase	1,71	0.006830
<i>metE</i>	5-methyltetrahydropteroyltriglutamate- homocysteine methyltransferase	1,71	0.032650
<i>metB</i>	cystathionine gamma-synthase	1,71	0.024972
<i>metL</i>	bifunctional aspartate kinase II/homoserine dehydrogenase II	1,70	0.047098
<i>c1464</i>	putative factor; DNA packaging, phage assembly	1,70	0.009964
<i>metQ</i>	DL-methionine transporter subunit	1,68	0.073134

Table 23/1: Genes with down-regulated expression in *in vivo* re-isolate KA25

gene	function	ratio	p-value
<i>atoE</i>	short chain fatty acid transporter	-5,72	0.069676
<i>frwD</i>	predicted enzyme IIB component of PTS	-5,21	0.037958
Z5693	sensor protein - putative histidine kinase	-4,78	0.026828
<i>c1813</i>	hypothetical protein	-4,27	0.047535
<i>paaX</i>	transcriptional repressor of phenylacetic acid degradation	-4,16	0.013937
Z1421	hypothetical protein	-4,11	0.020400
<i>tdcR</i>	threonine dehydratase operon activator protein	-3,89	0.009255
<i>c1959</i>	putative conserved protein	-3,79	0.003945

Appendix

Table 23/2: Genes with down-regulated expression in *in vivo* re-isolate KA25

gene	function	ratio	p-value
<i>ydhY</i>	predicted 4Fe-4S ferridoxin-type protein	-3,61	0.049761
<i>yahE</i>	hypothetical protein	-3,52	0.031234
Z1501	unknown protein encoded by bacteriophage BP-933W	-3,50	0.026269
<i>yjfK</i>	CP4-57 prophage; conserved protein	-3,45	0.002304
<i>yafX</i>	hypothetical protein	-3,44	0.025325
<i>yraJ</i>	predicted outer membrane protein	-3,43	0.027466
c0747	hypothetical protein	-3,42	0.001023
Z5885	putative resolvase	-3,40	0.042101
<i>ypjC</i>	hypothetical protein	-3,23	0.017948
<i>ycjN</i>	predicted sugar transporter subunit	-3,23	0.025068
<i>insE</i>	IS3 element protein InsE	-3,22	0.034835
Z2077	unknown protein encoded by prophage CP-933O	-3,21	0.016962
<i>yicO</i>	predicted xanthine/uracil permase	-3,20	0.005699
<i>kdpA</i>	potassium-transporting ATPase A chain	-3,20	0.004882
<i>ydfD</i>	Qin prophage; predicted protein	-3,20	0.017029
<i>yqeH</i>	conserved protein with bipartite regulator domain	-3,18	0.031296
<i>yahF</i>	hypothetical protein	-3,17	0.003520
<i>yafW</i>	antitoxin of the YkfI-YafW toxin-antitoxin system	-3,11	0.040936
c1172	conserved hypothetical protein	-3,09	0.004755
<i>yjfS</i>	CP4-57 prophage; predicted protein	-3,06	0.012578
<i>yjgH</i>	predicted mRNA endoribonuclease	-3,03	0.013229
c4984	putative sorbose PTS component	-3,01	0.023392
<i>ydaY</i>	Rac prophage; predicted protein	-3,01	0.026192
<i>ybbQ</i>	2-hydroxy-3-oxopropionate reductase	-2,96	0.025660
<i>ykgH</i>	predicted inner membrane protein	-2,96	0.032885
Z3342	unknown protein encoded within prophage CP-933V	-2,96	0.020549
Z1821	unknown protein encoded by prophage CP-933N	-2,95	0.038216
c4729	hypothetical protein	-2,89	0.009362
<i>glvC</i>	arbutin specific enzyme IIC component of PTS	-2,88	0.054861
<i>norV</i>	anaerobic nitric oxide reductase flavorubredoxin	-2,86	0.053927
<i>htrE</i>	predicted outer membrane usher protein	-2,84	0.051282
<i>ybeW</i>	chaperone protein <i>hscC</i> (Hsc62)	-2,83	0.023761
<i>yffL</i>	CPZ-55 prophage; predicted protein	-2,83	0.029761
<i>lit</i>	e14 prophage; cell death peptidase, inhibitor of T4 late gene expression	-2,80	0.034710
c1095	hypothetical protein	-2,78	0.002111
c2258	hypothetical protein	-2,73	0.044759
Z2978	putative replication protein for prophage CP-933T	-2,71	0.010364
<i>ygfO</i>	predicted transporter	-2,70	0.012161
Z2121	unknown protein encoded within prophage CP-933O	-2,69	0.044869
<i>ydhV</i>	predicted oxidoreductase	-2,68	0.011086
<i>ygcU</i>	predicted FAD containing dehydrogenase	-2,66	0.002279
<i>yaiT</i>	hypothetical protein	-2,65	0.009854
<i>yfdP</i>	CPS-53 (KpLE1) prophage; predicted protein	-2,63	0.019085
<i>yieK</i>	hypothetical protein	-2,63	0.005401
<i>glvB</i>	arbutin specific enzyme IIB component of PTS	-2,62	0.005063
c4897	hypothetical protein	-2,62	0.021606
<i>yjcE</i>	putative Na(+)/H(+) exchanger yjcE	-2,60	0.026146
<i>yahF</i>	predicted acyl-CoA synthetase	-2,58	0.082086
<i>ykgI</i>	hypothetical protein	-2,58	0.029082
<i>insK</i>	IS150 conserved protein InsB	-2,56	0.055649
<i>idnK</i>	D-gluconate kinase, thermosensitive	-2,55	0.034975

Appendix

Table 23/3: Genes with down-regulated expression in *in vivo* re-isolate KA25

gene	function	ratio	p-value
<i>ygfT</i>	fused predicted oxidoreductase: Fe-S	-2,54	0.044237
<i>phnK</i>	phosphonates transport ATP-binding protein phnK	-2,54	0.007417
<i>ybhD</i>	DNA-binding transcriptional regulator - LysR family	-2,54	0.021056
<i>frvB</i>	fused predicted PTS enzymes: IIB component/IIC component	-2,54	0.086101
c2503	transposase	-2,53	0.042108
<i>ymfE</i>	e14 prophage; predicted inner membrane protein	-2,53	0.038029
<i>ynbA</i>	predicted inner membrane protein	-2,53	0.038768
<i>wbdN</i>	glycosyl transferase	-2,50	0.040363
<i>yceO</i>	hypothetical protein	-2,48	0.025275
c0964	phage baseplate assembly protein	-2,48	0.043643
<i>glvG</i>	predicted 6-phospho-beta-glucosidase pseudogene)	-2,46	0.086063
c4525	putative chormophorylate of CpcA	-2,45	0.010128
<i>yehC</i>	putative chaperone protein	-2,45	0.029486
c2493	putative carbohydrate kinase	-2,44	0.034352
<i>yieL</i>	predicted xylanase	-2,44	0.007328
<i>eutK</i>	predicted carboxysome structural protein	-2,44	0.055061
<i>glpC</i>	sn-glycerol-3-phosphate dehydrogenase anaerobic	-2,43	0.093060
UTI89_C2647	head assembly protein	-2,43	0.010744
<i>gspG</i>	pseudopilin, cryptic, general secretion pathway	-2,42	0.020474
<i>ureG_2 ureG</i>	putative urease accessory protein G	-2,40	0.021704
<i>yhiP</i>	predicted transporter	-2,39	0.020535
<i>ydfW</i>	Qin prophage; predicted protein	-2,39	0.008525
c0698	hypothetical protein	-2,39	0.034227
<i>ybgO</i>	predicted fimbrial-like adhesin protein	-2,37	0.011815
Z2040	unknown protein encoded by prophage CP-933O	-2,35	0.030302
Z3058	putative outer membrane protein	-2,35	0.009608
Z1500	unknown protein encoded by bacteriophage BP-933W	-2,35	0.034217
<i>yodB</i>	predicted cytochrome	-2,34	0.036985
<i>ydiL</i>	hypothetical protein	-2,33	0.042198
<i>narV</i>	nitrate reductase Z	-2,32	0.019065
<i>yegR</i>	hypothetical protein	-2,32	0.011040
<i>ydjE</i>	predicted transporter	-2,32	0.044413
<i>ybcW</i>	DLP12 prophage; predicted protein	-2,31	0.003310
<i>yddH</i>	hypothetical protein	-2,30	0.020230
<i>ybeR</i>	hypothetical protein	-2,29	0.005551
c1184	hypothetical protein	-2,29	0.022967
<i>aufG</i>	hypothetical protein	-2,28	0.006313
<i>yhcE</i>	hypothetical protein	-2,28	0.016783
<i>yubQ</i>	hypothetical protein	-2,27	0.000349
<i>rfaI</i>	(glucosyl)lipopolysaccharide- alpha-1,3-D-galactosyltransferase	-2,27	0.007590
<i>yafM</i>	hypothetical protein	-2,26	0.022216
c3499	putative conserved protein	-2,24	0.038772
<i>racR</i>	Rac prophage; predicted DNA-binding transcriptional regulator	-2,23	0.042552
Z2344	putative tail fiber protein encoded by prophage CP-933R	-2,22	0.028875
<i>yhhA</i>	hypothetical protein	-2,21	0.014581
<i>yqeA</i>	predicted amino acid kinase	-2,21	0.025598
<i>yghT</i>	predicted protein with nucleoside triphosphate hydrolase domain	-2,21	0.057804
c3660	unknown protein encoded by ISEc8	-2,19	0.023859
Z1444	putative serine/threonine kinase encoded by bacteriophage BP-933W	-2,18	0.027910
<i>ygeX</i>	diaminopropionate ammonia-lyase	-2,17	0.062904
<i>ydiR</i>	predicted electron transfer flavoprotein, FAD-binding	-2,17	0.032109

Appendix

Table 23/4: Genes with down-regulated expression in *in vivo* re-isolate KA25

gene	function	ratio	p-value
Z3322	putative major tail subunit encoded within prophage CP-933V	-2,16	0.006953
<i>mhpD</i>	2-keto-4-pentenoate hydratase	-2,14	0.035327
<i>yeeV</i>	hypothetical protein	-2,13	0.017854
<i>kdgK</i>	2-dehydro-3-deoxygluconokinase	-2,13	0.083520
<i>ycdE</i>	4-oxalocrotonate tautomerase	-2,11	0.031150
<i>ydaF</i>	Rac prophage; predicted protein	-2,11	0.008177
<i>yehA</i>	predicted fimbrial-like adhesin protein	-2,10	0.052195
c0290	hypothetical protein	-2,09	0.004755
<i>ynjE</i>	predicted thiosulfate sulfur transferase	-2,09	0.047851
<i>yfcU</i>	putative outer membrane protein	-2,09	0.045233
Z3127	unknown protein encoded within prophage CP-933U	-2,08	0.004435
<i>acs</i>	acetyl-coenzyme A synthetase	-2,08	0.007537
<i>ybgQ</i>	predicted outer membrane protein	-2,01	0.024281
Z1547	putative acyl-carrier protein	-2,00	0.013033
Z2086	similar to division inhibition protein DicB within CP-933O	-2,00	0.018529
<i>sorE</i>	putative L-sorbose-1-P-reductase	-1,98	0.029065
c3712	fatty acyl-CoA synthetase	-1,95	0.018098
c2464	putative acyl-CoA dehydrogenase	-1,95	0.047393
<i>ypdG</i>	predicted enzyme IIC component of PTS	-1,94	0.061740
<i>eutE</i>	predicted aldehyde dehydrogenase, ethanolamine utilization protein	-1,94	0.020202
<i>yadD</i>	predicted transposase	-1,93	0.005070
c2467	putative 3-hydroxyacyl-CoA dehydrogenase	-1,84	0.079293
<i>yeiC</i>	hypothetical sugar kinase <i>yeiC</i>	-1,61	0.030658
<i>yeiN</i>	hypothetical protein	-1,57	0.047133
<i>yeiM</i>	hypothetical transport protein	-1,35	0.036098

Table 24: Genes with up-regulated expression in *in vitro* re-isolate 4.9

gene	function	ratio	p-value
ECP_2993	hypothetical protein	2,35	0.036780
c1465	DNA packaging, phage assembly (Phage or Prophage Related)	2,22	0.009548
<i>pin</i>	pin; putative DNA-invertase	2,12	0.003612
Z3115	putative endonuclease encoded within prophage CP-933U	2,09	0.009268
ECs0762	3-methylaspartate ammonia-lyase	1,91	0.014568
UTI89_C5097	hypothetical protein	1,90	0.041377

Appendix

Table 25: Genes with down-regulated expression in re-isolate *in vitro* 4.9

gene	function	ratio	p-value
<i>gadA</i>	glutamate decarboxylase A, PLP-dependent	-5,64	0.017564
<i>yoeA</i>	CP4-44 prophage region predicted hemin or colicin receptor	-4,16	0.022580
<i>ykgJ</i>	predicted ferredoxin	-4,05	0.046764
Z1636 Z1196	hypothetical protein hypothetical protein	-3,70	0.041643
<i>yfcO</i>	hypothetical protein	-3,68	0.033515
c0746	hypothetical protein	-3,56	0.023946
<i>allB</i>	allantoinase	-3,40	0.046806
<i>torS</i>	TorSR Two-Component Signal Transduction System	-3,40	0.047458
<i>glxR</i>	tartronate semialdehyde reductase, NADH-dependent	-3,29	0.040806
<i>yibV</i>	hypothetical protein	-3,20	0.015941
<i>prpE</i>	predicted propionyl-CoA synthetase with ATPase domain	-3,08	0.027409
ECs1517	hypothetical protein	-3,06	0.014989
<i>guaD</i>	guanine deaminase	-3,03	0.019563
<i>ureD</i>	urease accessory protein	-3,00	0.038031
<i>ybbV</i>	hypothetical protein	-3,00	0.024055
<i>ybbV</i>	hypothetical protein	-3,00	0.024055
<i>yffO</i>	CPZ-55 prophage; predicted protein	-2,83	0.015731
c1939	hypothetical protein	-2,71	0.006216
ECs4865	hypothetical protein	-2,62	0.015320
c1648	conserved hypothetical protein	-2,60	0.012009
<i>csgF</i>	predicted transport protein	-2,59	0.049578
Z1889	putative capsid protein of prophage CP-933X	-2,59	0.003177
<i>torR</i>	DNA-binding response regulator in two-component regulatory	-2,54	0.040652
<i>yfiM</i>	CP4-57 prophage; predicted protein	-2,42	0.012904
Z3104 Z6051	putative endolysin of prophage	-2,37	0.013701
ECs4985	putative tail protein	-2,28	0.043664
<i>ybbY</i>	predicted uracil/xanthine transporter	-2,25	0.047911
<i>gadX</i>	DNA-binding transcriptional dual regulator	-2,22	0.016524
<i>gcl</i>	glyoxylate carboligase	-2,22	0.058052
<i>eutA</i>	reactivating factor for ethanolamine ammonia lyase	-2,20	0.005029
<i>ybbW</i>	predicted allantoin transporter	-2,12	0.050637
<i>idnO</i>	gluconate 5-dehydrogenase	-2,12	0.016528
<i>hyi</i>	hydroxypyruvate isomerase	-2,11	0.043272
Z2165	hypothetical protein	-2,11	0.016805
Z1845	putative single stranded DNA-binding protein of prophage CP-933C	-2,11	0.048769
<i>tdcD</i>	Propionate kinase	-2,10	0.038733
<i>yjaI</i>	hypothetical protein	-2,10	0.034414
<i>yehR</i>	hypothetical protein	-2,09	0.032722
<i>ycjM</i>	predicted glucosyltransferase	-2,06	0.026288
Z3269	hypothetical protein	-2,06	0.032001
<i>intT</i>	integrase for prophage CP-933T	-2,05	0.011732
<i>sgaE</i>	probable sugar isomerase	-2,03	0.038324
<i>glxK</i>	glycerate kinase II	-2,02	0.028274

8.3. Curriculum Vitae

Personal Data

Name: Jarosław Maciej Zdziarski
Address: Leiblstr. 6, 97070 Würzburg
Date of birth: 06.01.1980
Place of birth: Góra, Poland

Education:

2004-2008 PhD thesis at the University of Würzburg in the Institute for Molecular Infection Biology
Member:

- International Graduate School of Würzburg
Graduate School of Life Sciences
- Network of Excellence EuroPathoGenomics (EPG)

1999-2004 MSc. in Biotechnology at University of Technique and Agriculture in Bydgoszcz, Poland.
MSc. Thesis: *'The analysis of the homology of the tyrosinase gene between different mushroom strains using PCR method'*.

1995-1999 Secondary school in Kutno, Poland.
Main subjects: Biology, Geography, Chemistry, Physics, and Ecology

Würzburg, July 2008

8.4. Publications

Publications

Zdziarski, J., Svanborg, C., Wullt, B., Hacker, J., and Dobrindt, U. (2008) Molecular basis of commensalism in the urinary tract: low virulence or virulence attenuation? *Infect Immun* **76**: 695-703.

Bielaszewska, M., Dobrindt, U., Gartner, J., Gallitz, I., Hacker, J., Karch, H., Muller, D., Schubert, S., Alexander Schmidt, M., Sorsa, L.J., and **Zdziarski, J.** (2007) Aspects of genome plasticity in pathogenic *Escherichia coli*. *Int J Med Microbiol* **297**: 625-639.

Presentations

Zdziarski, J., Dobrindt, D., Svanborg, C., and Hacker, J. (2006) Geno- and phenotypic analysis of asymptomatic bacteriuria *Escherichia coli* isolates. Jahrestagung der Deutschen Gesellschaft für Hygiene und Mikrobiologie (DGHM), Würzburg. Poster presentation

Zdziarski, J., Hacker, J., Svanborg, C., and Dobrindt, U. (2007) Geno- and phenotypic analysis of asymptomatic bacteriuria *Escherichia coli* isolates. Vereinigung für Allgemeine und Angewandte Mikrobiologie (VAAM), Göttingen. Poster presentation

Zdziarski, J., Hacker, J., Svanborg, C., and Dobrindt, U. (2007) Diversity makes a difference – genome plasticity and its consequences for the evolution of asymptomatic bacteriuria strains. Leopoldina, Staffelstein. Poster presentation

Zdziarski, J. (2008) Asymptomatic Bacteriuria (ABU) - An Adaptive Challenge for *Escherichia Coli* within the Urinary Tract. 3rd Student's Meeting EuroPathoGenomics, Graduate Academy, Innsbruck, Austria. Oral presentation.

8.5. Abbreviations

µg	microgram	kb	kilo bases
µl	microliter	kDa	kilo Dalton
µM	micromolar	Km	kanamycin
µm	micrometer	l	liter
2D-GE	2 dimensional gel electrophoresis	LB	lysogeny broth
A	adenine	LPS	lipopolysaccharide acid
a.a.	amino acid	M	molar
ABU	asymptomatic bacteruria	mA	milliampere
Ap	ampicillin	mg	milligram
APS	ammonium persulfate	min	minute
bp	base pairs	ml	milliliter
BSA	bovine serum albumin	mm	millimeter
C	cytosine	mM	millimolar
CFU	colony forming unit	ng	nanogramm
Cm	chloramphenicol	NO	nitric oxide
DEPC	diethyl pyrocarbinat	nt	nucleotides
DNA	desoxyribonucleic acid	OD	optical density
DNase	desoxyribonuclease	ORF	open reading frame
EAEC	enteroaggregative <i>E. coli</i>	PAI	pathogenicity island
EDTA	ethylendiamintertraacetat	PBS	phosphate buffered saline
EHEC	enterohemorrhagic <i>E. coli</i>	PCR	polymerase chain reaction
EIEC	enteroinvasive <i>E. coli</i>	PFGE	pulls field gel electrophoresis
EPEC	enteropathogenic <i>E. coli</i>	PMN	polymorphonuclear cell
et al.	et altera (and others)	RNA	ribonucleic acid
ETEC	enterotoxigenic <i>E. coli</i>	RNase	ribonuclease
EtOH	ethanol	RNS	reactive nitrogen species
ExPEC	extraintestinal pathogenic <i>E. coli</i>	rpm	rounds per minute
Fig.	figure	RT	reverse transcription
Fim	type 1 fimbriae	RT-PCR	reverse transcription PCR
FRT	Flp recognition target	SD	standard deviation
g	gram	SDS	sodium dodecyl sulfat
G	guanine	sec	second
GEI	genomic island	SNOs	S-nitrosothiols
GSH	glutathione	SNP	single nucleotide polymorphism
GSNO	S-nitrosoglutathione	β-ME	beta-mercaptoethanol
h	hour	T	thymine
i.e.	id est (this means)	TAE	Tris-acetate-EDTA
IL 6	Interleukin 6	TLR4	toll like receptor 4
IL 8	Interleukin 8	U	unit
iNOS	inducible nitric oxide synthase	UPEC	uropathogenic <i>E.coli</i>
IPEC	intestinal pathogenic <i>E. coli</i>	UTI	urinary tract infection
IS	insertion sequence element	wt	wild typ